ESCONDIDA REACH

ESCONDIDA TO SAN ANTONIO

HYDRAULIC MODELING ANALYSIS

1962-2006

MIDDLE RIO GRANDE,

NEW MEXICO

SEPTEMBER 2011

PREPARED FOR:

US BUREAU OF RECLAMATION

ALBUQUERQUE, NEW MEXICO

PREPARED BY:

AMANDA K. LARSEN

SEEMA C. SHAH-FAIRBANK

DR. PIERRE JULIEN

COLORADO STATE UNIVERSITY

ENGINEERING RESEARCH CENTER

DEPARTMENT OF CIVIL ENGINEERING

FORT COLLINS, COLORADO 80523

ABSTRACT

HYDRAULIC MODELING ANALYSIS OF THE MIDDLE RIO GRANDE - ESCONDIDA REACH, NEW MEXICO

Human influence on the Middle Rio Grande has resulted in major changes throughout the Middle Rio Grande region in central New Mexico, including problems with erosion and sedimentation. Hydraulic modeling analyses have been performed on the Middle Rio Grande to determine changes in channel morphology and other important parameters. Important changes occurring in the Escondida reach between 1918 and 2005 were analyzed for this study.

The Escondida reach covers 17.7 miles from the Escondida Bridge to the US Highway 380 Bridge. Spatial and temporal trends in channel geometry, discharge, and sediment have been analyzed. In addition, historic bedform data were analyzed and potential equilibrium conditions were predicted. This study will help facilitate better management of restoration, irrigation, and flood protection efforts.

Aerial photographs, GIS active channel planforms, cross-section surveys, hydraulic model analysis and channel classification methods were used to analyze spatial and temporal trends in channel geometry and morphology. Narrowing of the channel was observed from GIS active channel planforms between 1918 and 2005, with the upstream section of the channel showing the greatest narrowing. Fluctuations were observed in nearly all channel geometry properties. These fluctuations may be caused by a complex response to past channel changes. In addition, the mean bed grain diameter increased slightly from about 0.15 mm to 0.31 mm between 1962 and 2002.

Field observations of bedforms were compiled and compared to the bedforms predicted by van Rijn and by Simons and Richardson. Both methods produced acceptable results, but a large amount of scatter was observed in the data. Wide variability across a single cross section may be the source of the scatter.

Analyses of trends in sediment and water discharge shows a dry period between 1949 and 1979, a wet period between 1979 and 2000, and a dry period between 2000 and 2005. By contrast, the mean daily suspended sediment discharge remained nearly constant. Difference mass curves showed aggradation and degradation that approximately correlated with changes in mean bed elevation.

A variety of approaches were used to predict future equilibrium width and slope conditions. The approaches used include hydraulic geometry equations, hyperbolic and exponential regressions, stable channel geometry, and sediment transport relationships. Several methods predicted an equilibrium width around 300 ft, and Julien-Wargadalam and SAM analysis predicted equilibrium slopes between 0.00065 and 0.00139. Both the equilibrium slope and width predictions seem to provide reasonable estimates of future conditions.

TABLE OF CONTENTS

ABSTRACT ii
TABLE OF CONTENTS iii
LIST OF FIGURES v
LIST OF TABLES vi
1. Introduction 1
2. Site Description and Background 5
2.1. Subreach Definition 9
2.2. Available Data 10
2.2.1. Water and Suspended Sediment Data 10
2.2.2. Bed Material 12
2.2.3. Tributary and Arroyo Information 13
2.2.4. Survey Lines and Dates 13
2.3. Channel Forming Discharge 16
2.3.1. Effective Flow 16
2.3.2. Recurrence Interval 17
2.3.3. Bankfull Measurements 19
3. Channel Classification 20
3.1. Channel Planform Methods 20
3.1.1. Slope-Discharge methods 20
3.1.2. Channel Morphology methods 21
3.2. Channel Planform Results 24
3.3. Sinuosity 29
3.3.1. Methods 29
3.3.2. Results 29
3.4. Longitudinal Profile 32
3.4.1. Methods 32
3.4.2. Results 32
3.5. Channel Geometry 38
3.5.1. Methods 38
3.5.2. Results 39
3.6. Bend Migration 41
3.6.1. Methods 41
3.6.2. Results 42
3.7. Material Analysis 46
3.7.1. Methods 46
3.7.2. Results 47
4. Suspended Sediment and Water 49
4.1. Methods 49
4.2. Results 49
4.2.1. Single Mass Curves 49
4.2.2. Double Mass Curves 51
4.2.3. Difference Mass Curve 53
5. Floodplain Analysis 55
5.1. Methods 55

5.2. Results 55
6. Bedform Analysis 57
6.1. Methods 57
6.2. Results 59
7. Equilibrium State Predictors 63
7.1. Hydraulic Geometry 63
7.1.1. Methods 63
7.1.2. Results 67
7.2. Width Regression Model 70
7.2.1. Methods 70
7.2.2. Results 73
7.3. Sediment Transport 76
7.3.1. Methods 76
7.3.2. Results 77
7.4. SAM 79
7.4.1. Methods 79
7.4.2. Results 80
8. Discussion 81
8.1. Historic trends and current conditions in the Escondida reach 81
8.2. Channel response models 85
8.2.1. Schumm's (1969) river metamorphosis model 85
8.2.2. Lane's (1955) balance 87
8.3. Potential future equilibrium conditions 89
8.3.1. Equilibrium Width 89
8.3.2. Equilibrium Slope 90
9. Summary 92
10. References 94
Appendix A – Socorro Line Survey Plots 98
Appendix B – Aerial Photography Information 115
Appendix C – HEC-RAS Model Output 117
Appendix D – Bed Material Grain Size Distributions 153
Appendix E – Bedforms 158
Appendix F – BORAMEP 170
Appendix G – HEC-RAS Sediment Transport Application Limits 179

LIST OF FIGURES

Figure 1.1 Location Map and Topographic Map of the Escondida Reach 3
Figure 2.1 2005 Aerial Photo of Subreach 1 6
Figure 2.2 2005 Aerial Photo of Subreach 2 7
Figure 2.3 2005 Aerial Photo of Subreach 3 8
Figure 2.4 Subreach Definitions and Agg/Deg Location 9
Figure 2.5 Hydrograph for San Acacia and San Marcial Gauges 11
Figure 2.6 Annual Suspended Sediment Yield at San Acacia and San Marcial Gauges..... 11
Figure 2.7 Socorro Range Line Locations 15
Figure 2.8 Annual peak flow at San Acacia gauge 17
Figure 2.9 Annual peak flow at San Marcial gauge 18
Figure 2.10 Comparisons of Annual Peak Flows 18
Figure 3.1 Rosgen Channel Classification Key (Rosgen 1996) 22
Figure 3.2 Chang's Stream Classification Method Diagram (Chang 1979) 23
Figure 3.3 Historical planforms 25
Figure 3.4 Sinuosity 30
Figure 3.5 Change in thalweg elevation by SO-line 33
Figure 3.6 Thalweg elevation profile 34
Figure 3.7 Reach averaged mean bed elevation 34
Figure 3.8 Change in mean bed elevations 36
Figure 3.9 Energy grade line slope 37
Figure 3.10 Water surface elevation slope 38
Figure 3.11 Channel Geometry Properties 40
Figure 3.12 Bend migration at Agg/Deg 1326 43
Figure 3.13 Bend migration at Agg/Deg 1378-1386 44
Figure 3.14 Bend migration at Agg/Deg 1419-1426 45
Figure 3.15 Grain size classification (Julien 1998) 46
Figure 3.16 Bed material mean grain size 47
Figure 3.17 Bed material particle size distributions 48
Figure 4.1 Water Discharge Single Mass Curve 50
Figure 4.2 Suspended Sediment Discharge Single Mass Curve 51
Figure 4.3 Suspended Sediment Concentration Double Mass Curve 52
Figure 4.4 Suspended Sediment Difference Mass Curve 53
Figure 5.1 Top width vs. discharge for Agg/Deg 1406-1418 55
Figure 5.2 Top width vs. discharge for Agg/Deg 1456-1476 56
Figure 6.1 Bedform classification by Simons and Richardson (from Julien 1998) 57
Figure 6.2 Bedform classification by van Rijn (1984, from Julien 1998) 58
Figure 6.3 Observed ripples plotted on graphs from Simons and Richardson (L) and van Rijn (R) (after Julien 1998) 59
Figure 6.4 Observed dunes plotted on graph from Simons and Richardson (L) and van Rijn (R) (after Julein 1998) 60
Figure 6.5 Observed transition bedforms plotted on graph from Simons and Richardson (L) and van Rijn (R) (after Julein 1998) 60
Figure 6.6 Observed antidunes/plane bed plotted on graph from Simons and Richardson (L) and van Rijn (R) (after Julien 1998) 61
Figure 6.7 Typical cross-section with bedforms 62
Figure 7.1 Variation of wetted perimeter P with discharge Q and type of channel (after Simons and Albertson 1963) 64
Figure 7.2 Variation of average width W with wetted perimeter P (after Simons and Albertson 1963) 64

Figure 7.3 Escondida empirical width-discharge relationships 69
Figure 7.4 Hyperbolic and exponential regressions – subreach 1 73
Figure 7.5 Hyperbolic and exponential regressions – subreach 2 73
Figure 7.6 Hyperbolic and exponential regressions – subreach 3 74
Figure 7.7 Hyperbolic and exponential regressions – total reach 74
Figure 7.8 Total load rating curves from BORAMEP and Psands 78
Figure 7.9 Results from SAM for 2002 conditions at Q = 5000 cfs 80
Figure 8.1 Lane's balance(1955) 87

LIST OF TABLES

Table 2.1 Available Daily Discharge Data 10
Table 2.2 Available Suspended Sediment Data 12
Table 2.3 Available Bed Material Data at SO-Lines 12
Table 2.4 Socorro Range Line Survey Dates 14
Table 2.5 GeoTool Inputs 16
Table 2.6 Recurrence Interval 19
Table 3.1 Channel Classification Inputs 26
Table 3.2 Channel Classification Results 27
Table 3.3 Change in Valley Length 29
Table 3.4 Sinuosity Changes 30
Table 3.5 – Summary of Hydraulic Parameters 41
Table 3.6 Bed Migration 42
Table 3.7 Bed material type 47
Table 4.1 Water Discharge 50
Table 4.2 Suspended Sediment Discharge 51
Table 4.3 Suspended Sediment Concentration 52
Table 7.1 Hydraulic geometry calculation inputs 66
Table 7.2 Escondida empirical width-discharge inputs 67
Table 7.3 Predicted equilibrium widths from hydraulic geometry equations 68
Table 7.4 Equilibrium slope predictions with Q = 5000 cfs 69
Table 7.5 Escondida empirical width-discharge results 70
Table 7.6 Hyperbolic and exponential regression input 72
Table 7.7 Hyperbolic regression equations and predicted widths 75
Table 7.8 Exponential regression equations and predicted widths 76
Table 7.9 Total load and bed load calculations 77
Table 7.10 Equilibrium slope determined from transport capacity equations 78
Table 7.11 Current conditions and equilibrium slope and width from SAM 80
Table 8.1 Channel geometry changes 82
Table 8.2 Schumm's (1969) channel metamorphosis model 86
Table 8.3 Observed channel changes at Q = 5000 cfs 86
Table 8.4 Observed Changes in Lane Balance Parameters and the Corresponding Trigger Variable 89

1. Introduction

Since the arrival of the first humans along the Middle Rio Grande River over 10,000 years ago, their activities have had a significant impact on the river as well as on the natural areas surrounding the river. Early Puebloan inhabitants cleared areas of the Bosque to make way for farmland. Later Spanish settlers introduced grazing livestock to the area and continued to clear native riparian forests for both farming and new settlements to accommodate their ever-increasing population. In addition to introducing livestock to the area, Spanish settlers also introduced many exotic plant species that invaded the habitat of native plants. These human impacts, coupled with natural events such as droughts, lead to changes in vegetation types as well as increased soil erosion along much of the Middle Rio Grande (Scurlock 1998).

By the beginning of the 20th century, significant changes had occurred in the Middle Rio Grande Valley. Increased mining, logging, and grazing had destroyed much of the vegetation, resulting in dramatic erosion and a subsequent increase in the sediment load in the River (Scurlock 1998). The increased erosion and sediment load had caused a loss of about 13 percent of the capacity of Elephant Butte Reservoir by the mid 1930's (Clark 1987). The increased sediment load also lead to severe aggradation along the River. Between 1880 and 1924, the bed of the river rose 9 feet at San Marcial (Scurlock 1998).

To combat the many problems facing the River, the Middle Rio Grande Conservancy District (MRGCD) was formed in 1923. The purpose of the MRGCD was to "provide flood protection from the Rio Grande, and make the surrounding area hospitable for urbanization and agriculture." Between 1923 and 1935 one storage dam and four diversion dams, as well as 817 miles of drainage and irrigation channels had been constructed by the MRGCD (MRGCD 2006).

The MRGCD's efforts were an initial success. However, the floods of 1941 and 1942 damaged many of the early MRGCD levees, irrigation and drainage systems. Following the Congressional Flood Control Acts in 1948 and 1950, the Bureau of Reclamation and the Army Corps of Engineers repaired and updated the structures originally installed by the MRGCD. New levees and the Cochiti Dam were also constructed to combat flooding and sedimentation problems along the river (MRGCD 2006).

The cumulative effect of centuries of human influence on the Middle Rio Grande caused a dramatic change in the habitat of many native species leading to a decrease in their presence along the river. Dams constructed for flood control purposes have regulated the flow of the river, virtually eliminating the seasonal flooding essential to the reproduction of the Rio Grande silvery minnow and many native trees such as the cottonwood (Bogan et al. 2006, Earick 1999). As a result, aging cottonwoods are being replaced by Russian olive and tamarisk, and the Rio Grande silvery minnow, once found from Espanola, NM to the Gulf of Mexico, is now present in only five percent of its former range (Earick 1999, MRGESACP 2006a). In some years, about ninety-five percent of the Rio Grande silvery minnow population is concentrated in the San Acacia

reach (below the San Acacia diversion dam) of the Middle Rio Grande (MGRCD v. Norton 2002). In addition, habitat reduction has also threatened the southwestern willow flycatcher. In 1994 and 1995 the Rio Grande silvery minnow and the southwestern willow flycatcher, respectively, were placed on the endangered species list in response to their dwindling numbers (MRGESACP 2006b, MRGCD v. Norton 2002).

Today, the Rio Grande runs, as it always has, through a valley caused not by the river, but by the Rio Grande Rift. The rift is formed by the earth's tectonic forces slowly pulling and stretching the Earth's crust, while at the same time, pushing up rock on either side of the rift. Over time, the aggrading nature of the Middle Rio Grande has helped fill the rift by depositing as much as 20,000 feet of sediment in some areas and about 5,000 feet in the Socorro area (Earick 1999, Hawley 1978). Another of the Earth's geological phenomenon is also changing the face of the Middle Rio Grande Valley. The Socorro Magma Body, centered about 12.5 miles upstream of the study reach, is causing an uplift of the valley (Larsen and Reilinger 1983, Ouchi 1983). The center was estimated to have risen at a rate of 1.3 to 2.3 mm/yr between 1951 and 1980. The uplift is causing an increase in slope downstream of the center and a decrease in the slope upstream of the center (Reclamation 2003).

The section of the Middle Rio Grande examined in detail in this report is frequently called the Escondida Reach and stretches 17.7 miles from the upstream extent at the Escondida Bridge to the downstream extent at the US Highway 380 Bridge near San Antonio. Figure 1.1 shows a topographic map of the study reach. Historically, this section of the river has been an aggrading, sand-bed channel showing some areas with a braided planform. However, narrowing of the channel has occurred both before and after the channelization projects completed in the 1950's (Porter and Massong 2004).

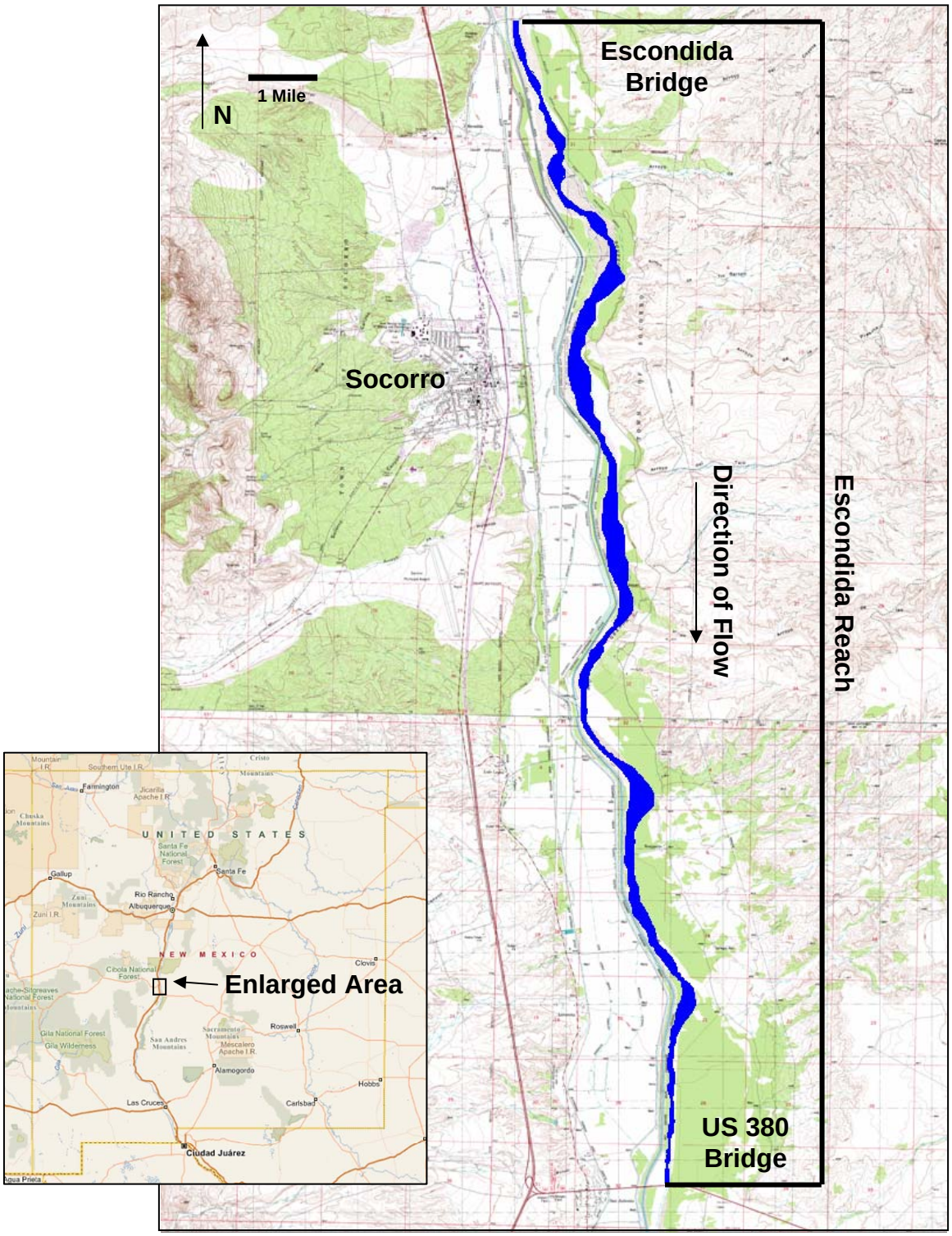

Figure 1.1 Location Map and Topographic Map of the Escondida Reach

The objectives of this study of the Escondida Reach include:

- Identifying spatial and temporal trends in channel geometry and morphology. Visual observations of aerial photographs and GIS active channel planforms, cross-section surveys, hydraulic modeling using HEC-RAS, and channel classification methods will be used to identify trends. In addition, changes in bed material were observed from cross-section data.

- Determining the ability of bedform prediction equations to match bedform observations. Field observations of bedforms will be compared with the bedforms predicted by van Rijn (1984) and Simons & Richardson (from Julien 1998).

- Analyzing trends in water and sediment discharge. Mass curves developed from USGS gauge data are used to show changes in the relevant parameters.

- Providing estimates of potential equilibrium slope and width conditions. Potential future conditions are estimated using hydraulic geometry equations, hyperbolic and exponential regressions, stable channel geometry, and sediment transport relationships.

The information presented in this report is divided into ten sections. An introduction to the Escondida reach and the Middle Rio Grande, along with the purpose and objectives of the study, is included in Section 1. Section 2 covers the site description, historical background of the study area, subreach definition, information about available data, and the determination of the channel forming discharge. In Section 3, the geomorphic and river characteristics are discussed. Suspended sediment and water history are the focus of Section 4. Analysis of the active floodplain is in Section 5, and a bedform analysis can be found in Section 6. Section 7 includes an investigation of equilibrium based on hydraulic geometry and sediment transport predictors for the study reach. A discussion of the results of the analysis and a summary of the reports are found in Sections 8 and 9 respectively. Finally, a list of cited references is located in Section 10. Appendices A-E include tables and plots relevant to the morphological assessment of the reach, including hydraulic model output, bed material gradations, and bedform classification. Appendices F and G include model output and other information used in the equilibrium predictor methods.

2. Site Description and Background

The Middle Rio Grande covers about 170 miles of central New Mexico from Cochiti Dam to Elephant Butte Reservoir (Tetra Tech, Inc. 2002). The river has been greatly influenced by humans beginning as early as 10,000 years ago (Scurlock 1998). More recently, the Middle Rio Grande Conservancy District, the Bureau of Reclamation and the Army Corps of Engineers have undertaken numerous projects along the Middle Rio Grande to combat floods and sedimentation problems (MRGCD 2006). The human influences on the river have caused significant habitat loss to native plant and animal species and have prompted detailed study of the Middle Rio Grande.

The 17.7-mile-long Escondida Reach is the subject of this report. The upstream extent of the reach is the Escondida Bridge (River Mile 104.8) north-west of the town of Escondida, NM (Figure 2.1). The downstream extent is the US Highway 380 Bridge (River Mile 87.1) located directly west of the town of San Antonio, NM (Figure 2.3). Historically, this reach has been an aggrading, sand-bed channel with a primarily braided planform, but the channel has narrowed due to human influences and natural processes (Porter and Massong 2004). Figures 2.1 through 2.3 show 2005 aerial photographs of the study reach. These figures show an abundance of arroyos entering the river in subreach 1 and the very straight, narrow planform of subreach 3. The river runs nearly parallel to the low-flow conveyance channel located on the west bank of the river, indicating that the levees protecting the conveyance channel may be influencing the path of the river.

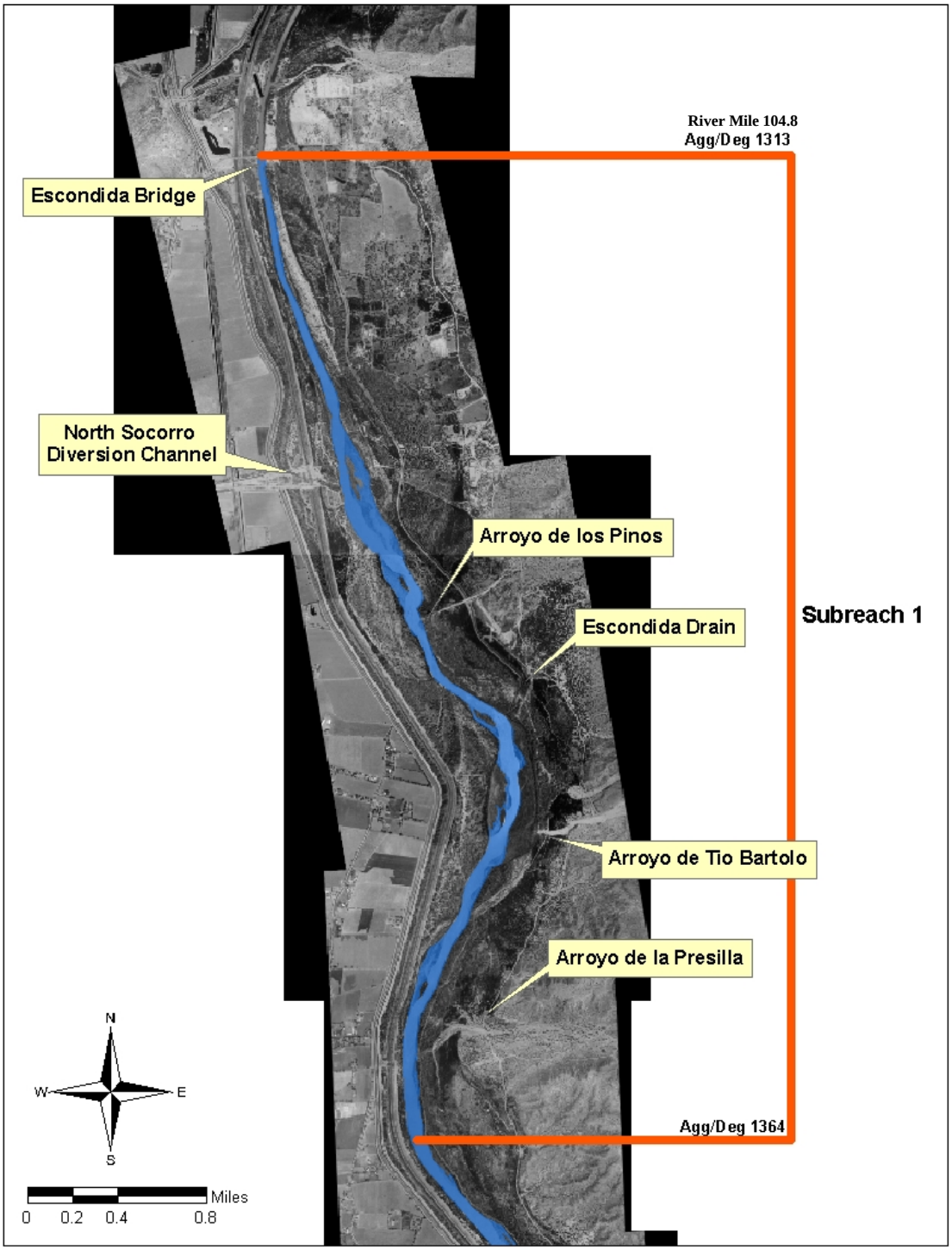

Figure 2.1 2005 Aerial Photo of Subreach 1

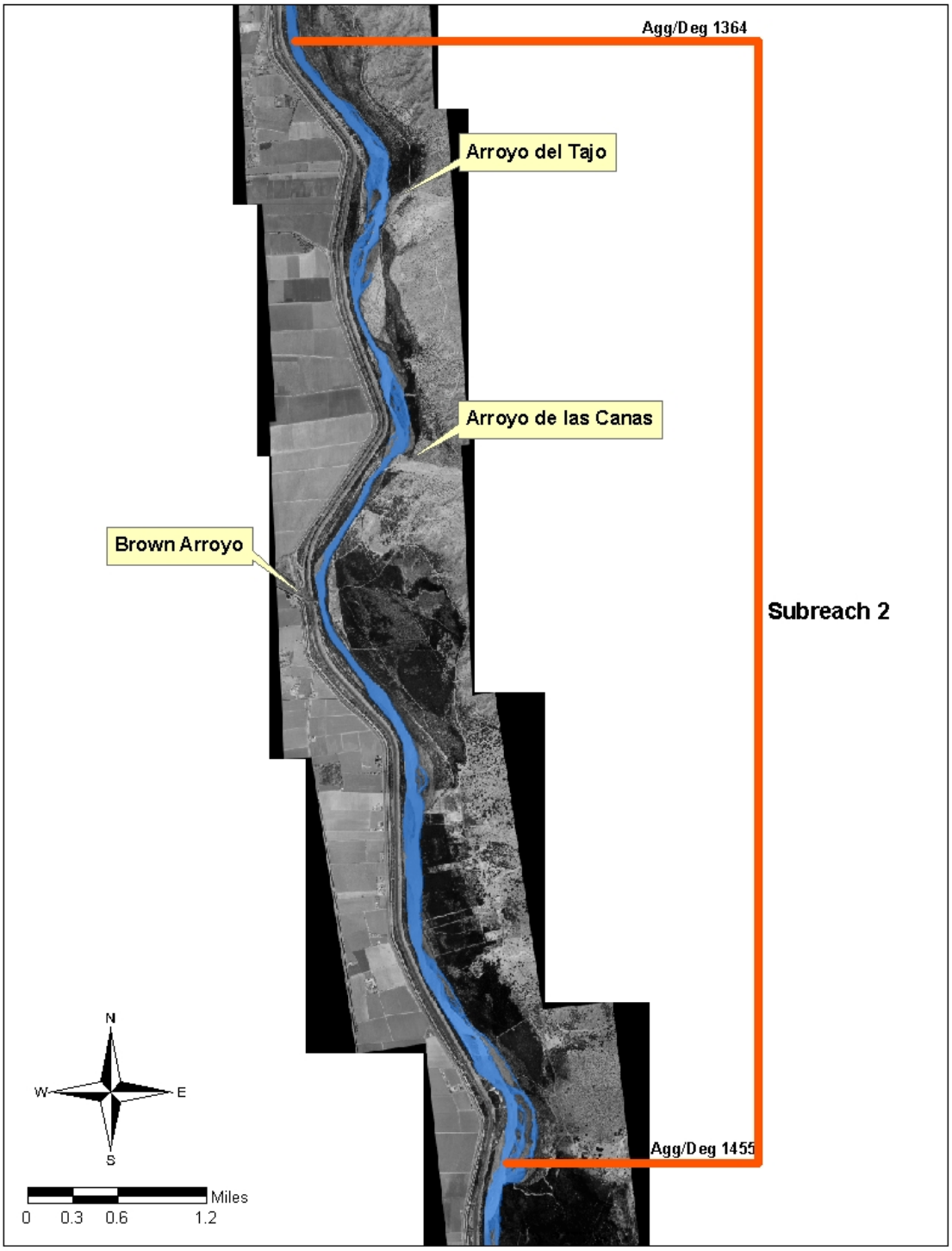

Figure 2.2 2005 Aerial Photo of Subreach 2

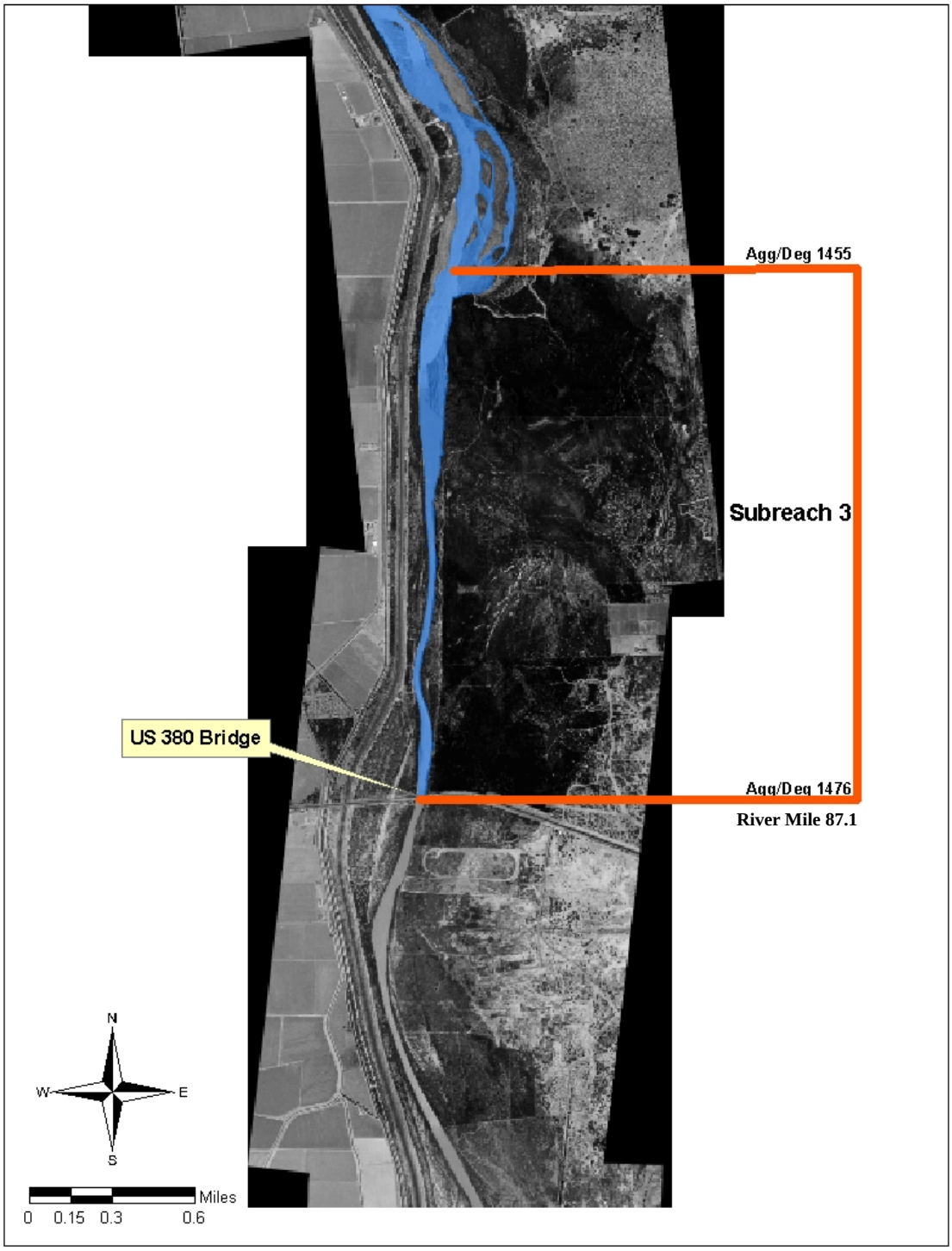

Figure 2.3 2005 Aerial Photo of Subreach 3

2.1. Subreach Definition

In an effort to better assess the historic changes in the Escondida reach, as well as to make better predictions of possible future conditions, the reach was divided into three subreaches. The subreach definitions were determined by initial assessments of the channel width and planform from GIS aerial photos. In addition, aggradation and degradation based on the minimum channel elevations also helped determine the final delineations. The location of the subreach delineations can be seen in Figure 2.4.

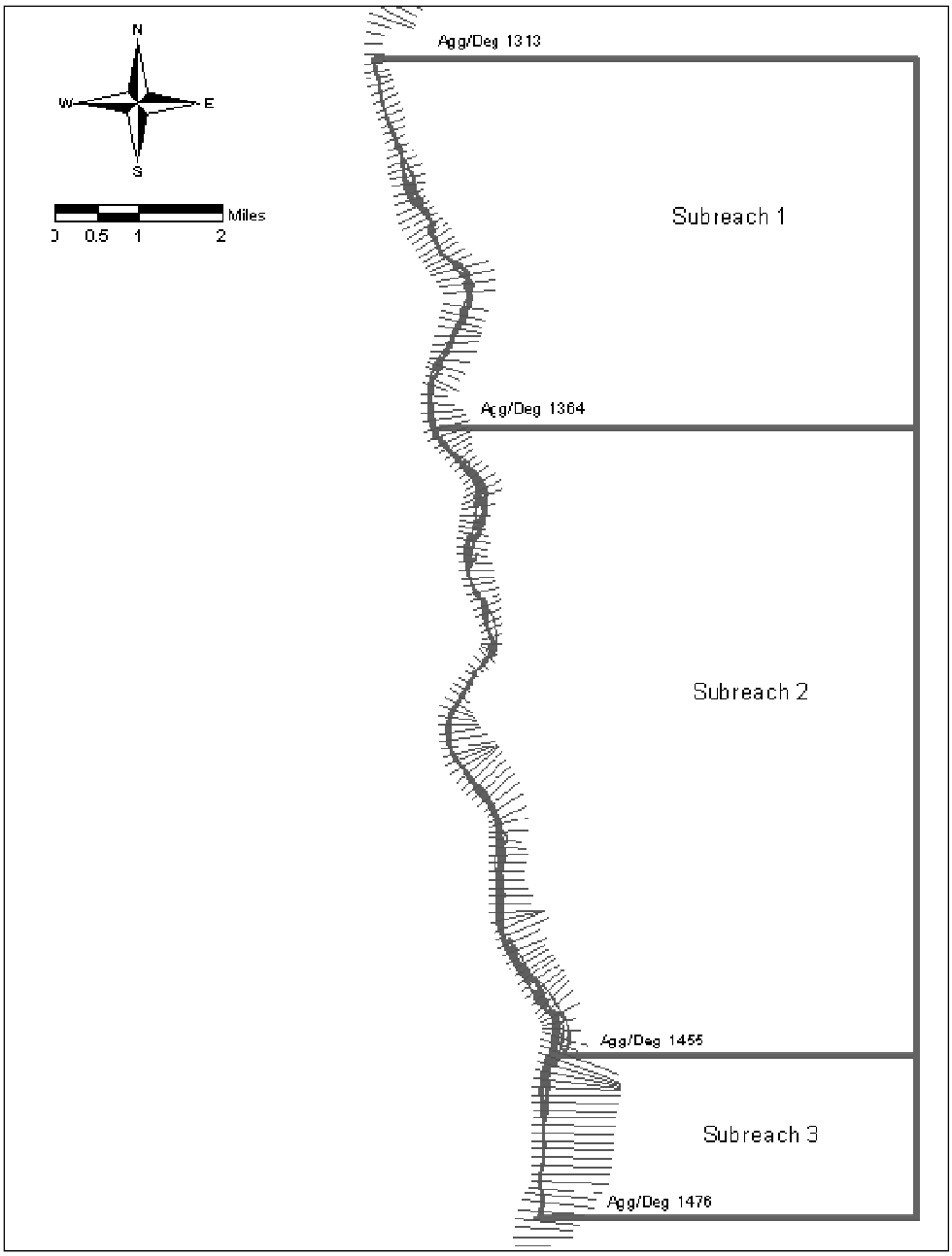

Figure 2.4 Subreach Definitions and Agg/Deg Location

Subreach 1 stretches from the Escondida Bridge to Agg/Deg line 1346, located between Arroyo de la Presilla and Arroyo del Tajo. Subreach 2 stretches from Agg/Deg line 1364 to Agg/Deg 1455. Finally, Subreach 3 stretches from Agg/Deg 1455 to the US Highway 380 Bridge.

2.2. Available Data

The data used in this study was retrieved from a number of different agencies including Reclamation, the United States Geological Survey (USGS), the National Oceanic and Atmospheric Administration (NOAA), and the Middle Rio Grande database complied at Colorado State University for Reclamation.

2.2.1. Water and Suspended Sediment Data

Historical mean daily discharge data was obtained from two USGS gauges; the San Acacia gauge (08354900), located approximately 11 miles upstream of the study reach, and the San Marcial gauge (08358400), located approximately 18 miles downstream of the study reach. The dates of available discharge data from the USGS website (http://waterdata.usgs.gov/nm/nwis/rt) are shown in Table 2.1.

Table 2.1 Available Daily Discharge Data

USGS Gauging Station	Dates
RG Floodway at San Acacia	1958-current
RG Floodway at San Marcial	1949-2006

Two additional gauges are located within the study reach, one at the upstream boundary (Escondida Bridge) and the second at the downstream boundary (San Antonio Bridge). These two gauges only have recent real-time discharge data, not the historical data necessary for this study. An example hydrograph for the San Acacia and San Marcial gauges is shown in Figure 2.5. This hydrograph has a peak near the bankfull discharge of 5000 cfs described later in Section 2.3. The first, longer peak seen between April and June is a result of snowmelt in the Rio Grande headwaters. The second, shorter peak seen in August is the result of an intense summer thunderstorm characteristic of the Middle Rio Grande Valley.

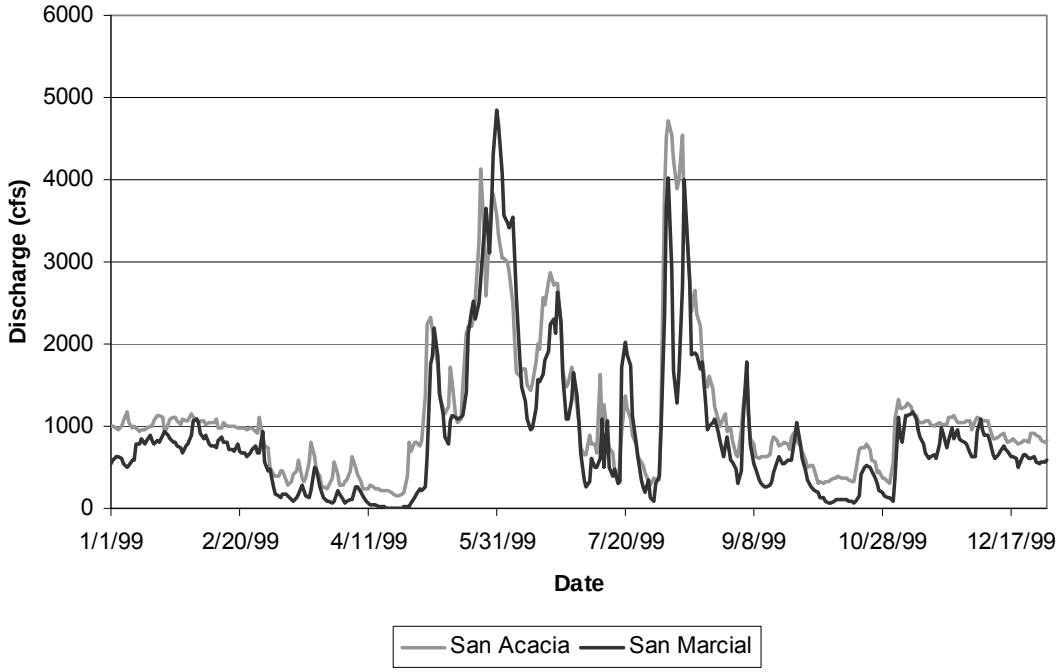

Figure 2.5 Hydrograph for San Acacia and San Marcial Gauges

In addition, daily-suspended sediment data was also available at the San Acacia and San Marcial gauges. Figure 2.6 shows the annual suspended sediment load at each gauge. A blank year indicates that complete sediment data was not available for that year.

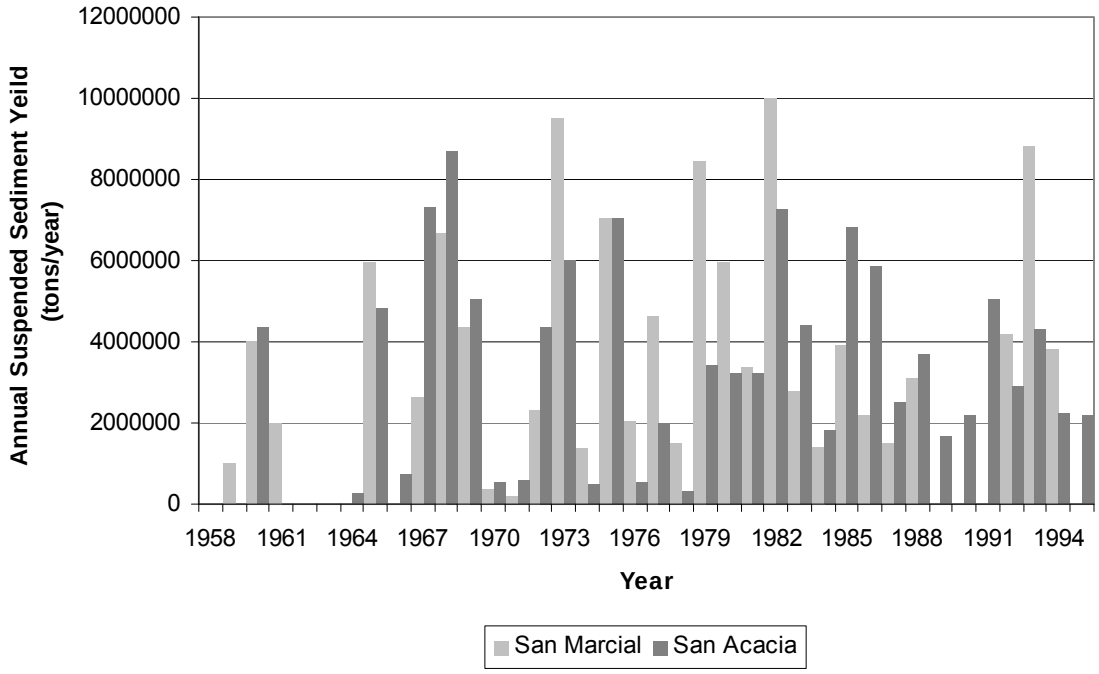

Figure 2.6 Annual Suspended Sediment Yield at San Acacia and San Marcial Gauges

Continuous suspended sediment data was not always available for all parameters at all gauges. Table 2.2 gives the dates of continuous, viable data at each gauge. Additional sediment data from 1955 to 2005 was provided by Reclamation (2011). This data set contained yearly suspended sediment totals, while Table 2.2 provides daily suspended sediment load that were obtained from the USGS sediment website (http://co.water.usgs.gov/sediment/).

Table 2.2 Available Suspended Sediment Data

USGS Gauging Station	Dates
RG at San Marcial	Oct. 1956 - July 1962
	Sep. 1962 - Aug. 1966
	Oct. 1966 - Sep. 1989
	Oct. 1991 - Sep. 1995
RG at San Acacia	Jan 1959 - Sep. 1959
	Jan 1960 - Sep. 1961
	July 1961
	April 1962 - July 1962
	Aug 1962 - Sep. 1962
	March 1963 - Sep. 1996

2.2.2. Bed Material

Bed material data was collected at Socorro range lines (SO-lines) by Reclamation from 1990-2005 (see Figure 2.8). The surveys include grain-size distributions for each sample. The dates and locations of the material collected are displayed in Table 2.3.

Table 2.3 Available Bed Material Data at SO-Lines

Years	SO Line Number									
	1313	1316	1346	1371	1380	1401	1414	1437.9	1450	1470.5
1990								x	x	x
1991					x	x			x	x
1992							x	x		x
1993							x	x		x
1994							x	x		x
1995							x	x		x
1996		x		x			x	x	x	x
1997		x	x	x			x	x	x	x
1998							x	x		x
1999	x	x	x	x			x	x		x
2002							x			
2005							x			x

Additional bed material data was also obtained from the USGS gauging stations at San Acacia and San Marcial. Data were sporadically available from 1966-2004 at the San Acacia gauge and from 1968-2004 at the San Marcial gauge.

The information from the gauging stations was only used in analysis when appropriate bed material data were not available from the SO-line surveys.

2.2.3. Tributary and Arroyo Information

Eight small tributaries enter the Middle Rio Grande in the Escondida reach. The majority of these tributaries are arroyos. The arroyos entering the river include the Arroyo de los Pinos, Arroyo de Tio Bartolo, Arroyo de la Presilla, Arroyo de Tajo, Arroyo de las Canas, and Brown Arroyo. In addition, the Escondida Drain and the North Socorro diversion channel also outfall in the Escondida reach. The location of the tributaries can be seen on the aerial photographs in Figures 2.1 through 2.3.

The role of arroyos in the Middle Rio Grande River is as a primary source of sediment. These arroyos contribute most of the gravel-sized material present in the reach. The sediment contribution occurs mostly during high-intensity summer thunderstorms (Reclamation 2003). The sediment (material) contributed by each tributary varies. For example, the Arroyo de las Canas typically contributes gravel-sized material, while the North Socorro diversion channel contributes mostly sand-sized material (Porter and Massong 2004).

2.2.4. Survey Lines and Dates

Cross-section information were collected by Reclamation using two methods. Agg/Deg lines were surveyed using aerial photography and do not provide detailed information about the channel in any location covered by water at the time of the survey. The average bed elevation was estimated using HEC-RAS and the discharge on the date of the aerial photography. These data sets provide topographic data on parts of the floodplain, not covered by the detailed on-ground surveys. Agg/Deg lines 1313-1476 were used in the hydraulic analysis (see Figure 2.4). This includes one cross-section upstream of the study reach and one cross-section downstream of the study reach. Because the extent of the Agg/Deg lines used does not exactly match the limits of study, the length of the reach used for hydraulic analysis is slightly longer than the actual study reach. Agg/Deg lines are spaced about 500 feet apart and were surveyed in 1962, 1972, 1985, 1992, and 2002.

SO range lines were surveyed by Reclamation beginning in 1987. These surveys provide detailed information about the channel cross-section that is not available from the aerial photographs. Thirty-three SO-lines are located in the reach. Figure 2.7 shows the location of the SO-lines and Table 3.4 shows the dates of available survey data at each SO-line. The SA and SO numbers correspond to the Agg/Deg lines numbers. Appendix A contains cross-section plots of the SO-line data.

Table 2.4 Socorro Range Line Survey Dates

SO - Line	Year														
	1987	1989	1990	1991	1992	1993	1994	1995	1996	1997	1998	1999	2002	2004	2005
1313								X		X		X		X	
1314								X		X		X		X	X
1316								X		X		X			
1320					X			X		X		X			X
1327									X	X		X	X		X
1339					X					X		X	X		X
1342.5												X			
1346					X				X	X		X	X		X
1349												X			
1352												X			X
1360					X				X	X		X	X		X
1371					X					X		X	X		X
1380			X		X				X	X		X	X		X
1392															X
1394			X		X					X		X	X		X
1396.5												X			
1398												X			
1401			X		X				X	X		X	X		X
1410			X		X	X	X	X	X	X		X	X		X
1414			X		X	X	X	X	X	X		X	X		X
1420			X		X	X	X	X	X	X		X	X		X
1428			X		X	X		X	X	X		X	X		X
1437.9	X	X	X	X	X	X		X	X	X		X			X
1443			X		X	X		X	X	X		X	X		X
1450	X	X	X	X	X	X		X	X	X		X	X		X
1456			X		X	X		X	X	X		X	X		X
1462			X		X	X		X	X	X		X	X		X
1464.5												X			
1469.5		X													
1470.5		X	X	X	X	X	X	X	X	X	X	X	X		X
1471.2		X													
1472	X	X													

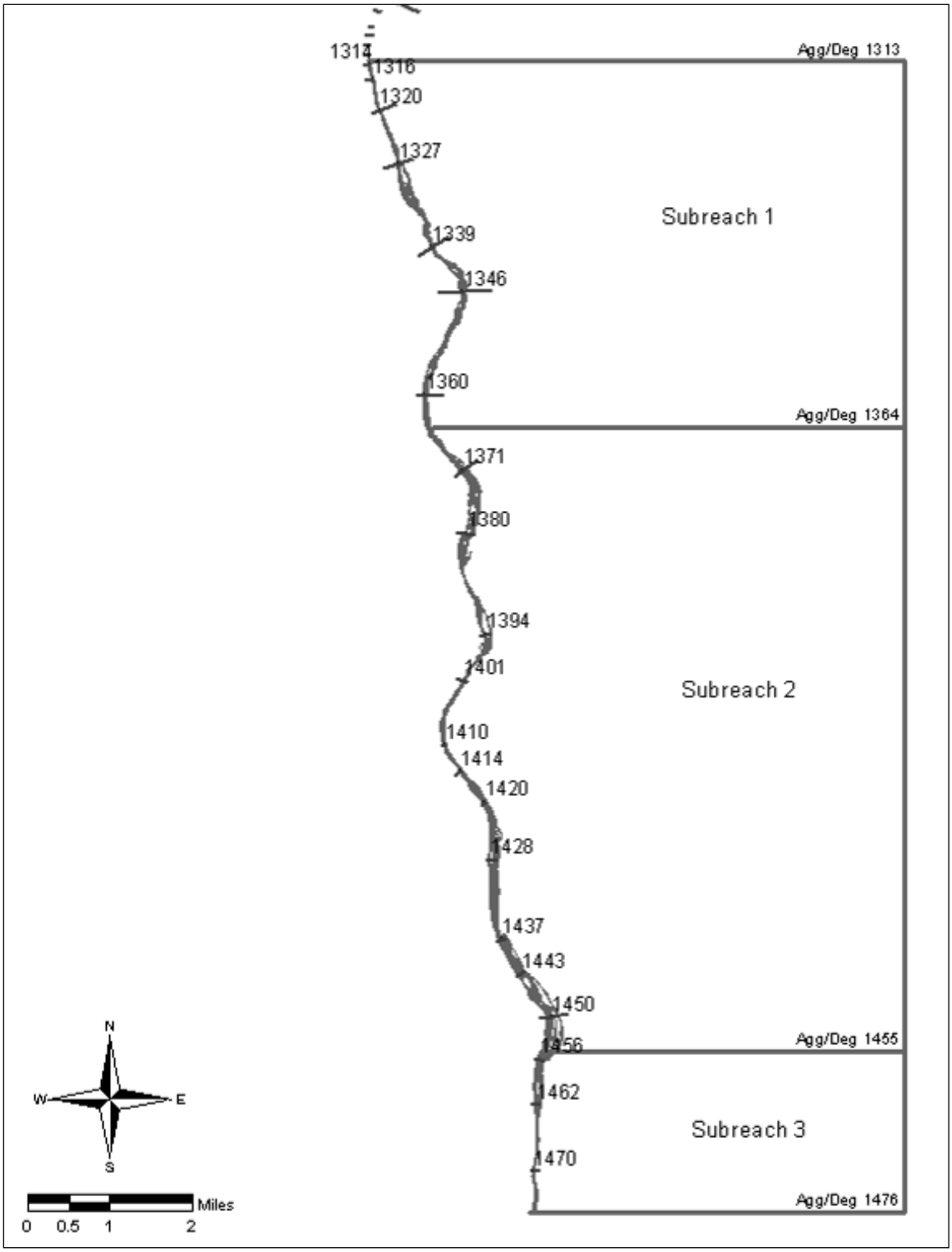

Figure 2.7 Socorro Range Line Locations

2.3. Channel Forming Discharge

2.3.1. Effective Flow

The effective flow in the channel was determined using GeoTool (Raff et al. 2004). This program uses discharge data and sediment data to determine the discharge at which the majority of the sediment in the channel is transported. The program was run twice. One run used the daily discharge data collected at the San Acacia gauge; the second run used the daily discharge data from the San Marcial gauge. Both sets of data were determined to have a lognormal distribution. Slope and width information was obtained from HEC-RAS runs using discharges near the expected effective flow. The bed material diameter information was taken from bed material data collected at the SO-lines throughout the reach.

Yang's sand equation was used to calculate the sediment transport rate. Of the methods available, Yang's sand equation is most applicable based on available input data. The energy slope was estimated from HEC-RAS runs in the same manner as the slope and width information. Temperature and bed material data were obtained from SO-line surveys.

An empirical relationship between discharge and hydraulic radius was developed by running HEC-RAS at a wide range of flows and using regression analysis to determine the relationship. The final input data for the effective flow calculations are shown Table 2.5.

Table 2.5 GeoTool Inputs

Input Parameters	
Slope (ft/ft)	0.00079
d_{50} (mm)	0.25
d_{84} (mm)	0.62
Characteristic Width (ft)	1044
Yang's Sand Method	
Energy Slope (ft/ft)	0.0093
d_{50}(mm)	0.25
Temp (°F)	60
Effective Width (ft)	1044
Regression Equation	$R_h = 0.11Q^{0.37}$
Manning's n	0.022

The GeoTool analysis resulted in effective discharges ranging from about 3000 cfs to 5000 cfs depending upon the number of bins specified, for data to be sorted into. The distribution of flows were divided into a number of “bins”, which span from the minimum discharge to the maximum discharge. The distribution of these bins can be either arithmetically or logarithmically distributed (henceforth called the “type” of binning). The number and type of bins substantially affects the determination of the effective discharge (Raff et al. 2004). The ideal number of bins is the largest number of bins with a minimum number of empty bins (Brown 2006). The effective discharge corresponding to the ideal number of bins was determined to be 4600 cfs for both the San Acacia and San Marcial gauges.

2.3.2. Recurrence Interval

The 2, 5, 7, and 10 year flows were calculated from the annual peak flow information obtained from the San Acacia and San Marcial gauges, which are based on mean daily data. Figure 2.8 and 2.9 show the annual peak flows at San Acacia and San Marcial. Figure 2.10 displays a comparison of the peak flows at the two gauges.

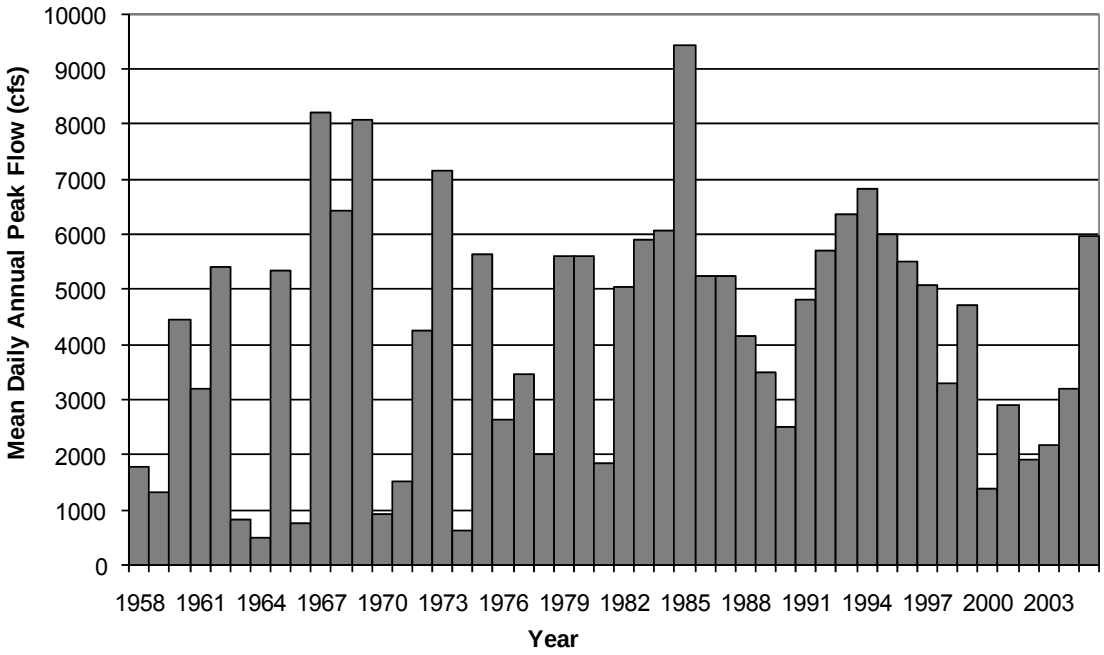

Figure 2.8 Annual peak flow at San Acacia gauge

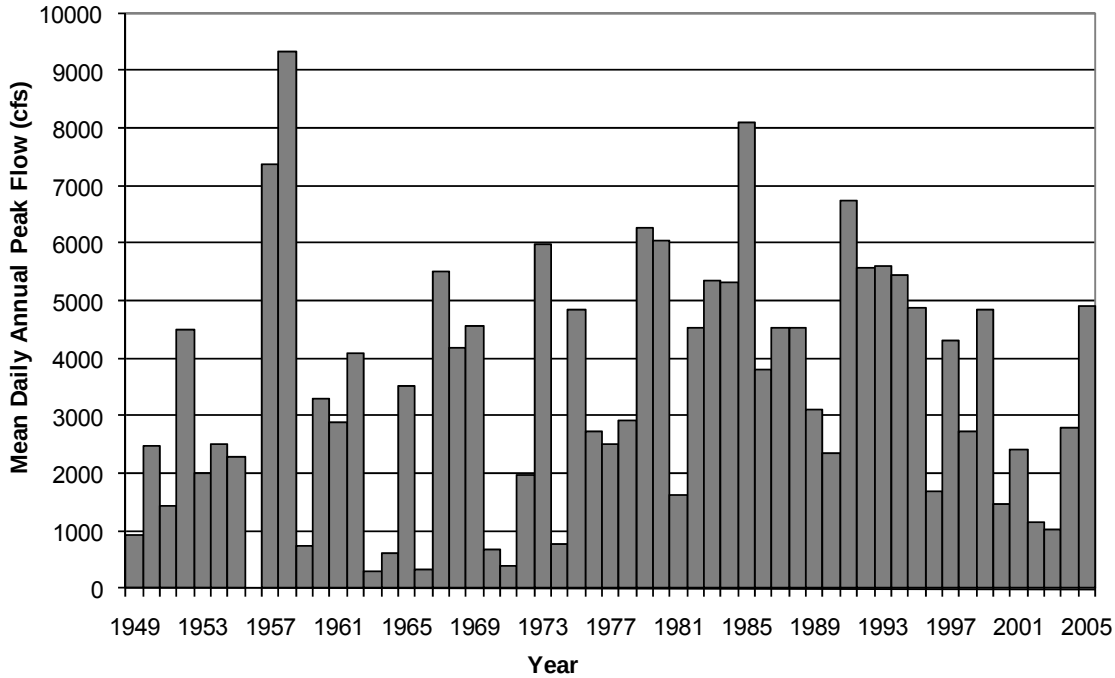

Figure 2.9 Annual peak flow at San Marcial gauge

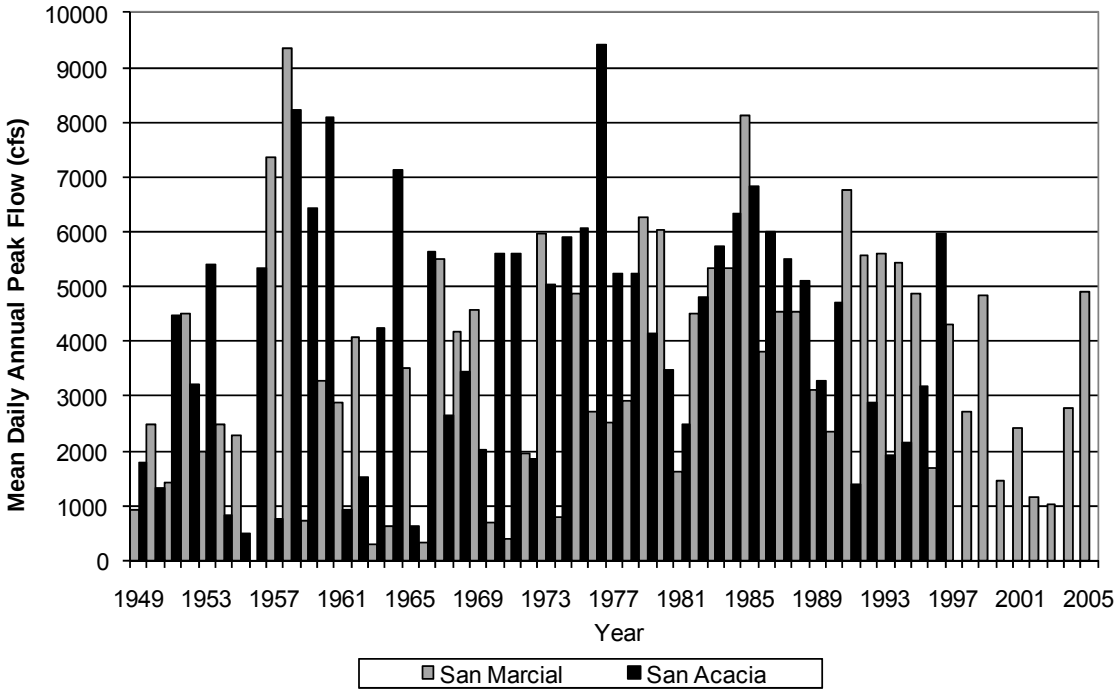

Figure 2.10 Comparisons of Annual Peak Flows

The recurrence intervals calculated from the peak flow and corresponding discharges can be seen in Table 2.6.

Table 2.6 Recurrence Interval

Recurrence Interval (years)	Discharge (cfs)	
	SA	SM
10	6,846	6,095
7	6,350	5,584
5	5,984	5,384
2	4,587	3,100

Based on the recurrence interval analysis, the effective discharge is in the approximate range of a 2-year storm event.

2.3.3. Bankfull Measurements

Bankfull flow was not calculated directly for the Escondida reach, but a near-bankfull discharge of 5000 cfs was observed by Reclamation in August, 1999 in the San Acacia reach located just upstream of the Escondida reach. In addition, calculations performed by Reclamation in the San Acacia reach estimated the bankfull discharge of 5000 cfs with a recurrence interval between 1.5 and 2.5 years (Reclamation 2003). The recurrence interval calculated by Reclamation corresponds well with the recurrence interval calculated above.

The two reaches (San Acacia and Escondida) are located immediately adjacent to one another. Therefore, their recurrence intervals match well to what the observed bank full was estimated to be, by Reclamation. In addition, the effective discharge calculation performed using Geo Tool also falls within the bankfull estimate. Thus, the 5000 cfs bankfull discharge determined by Reclamation was used in the hydraulic analysis of the Escondida reach.

3. Channel Classification

3.1. Channel Planform Methods

A number of quantitative channel classification methods were investigated to determine the methods most applicable to the Escondida reach. The channel was classified based on slope-discharge relationships, channel morphology methods and the stream power relationships. In addition, a qualitative classification of the channel was also made based on GIS evaluation of aerial photographs.

The channel was classified based on slope-discharge relationships developed by Leopold and Wolman (1957), Lane (from Richardson, et. al 2001), Henderson (1966), and Schumm and Khan (1972). Channel morphology methods developed by Rosgen (1996) and Parker (1976) were also used, along with stream power relationships developed by Nanson and Croke (1992) and Chang (1979).

Two additional methods were also investigated, but found to be not applicable to the Escondida reach. These methods were Ackers and Charlton (1970, Ackers 1982), and van den Berg (1995). Ackers and Charlton (from Ackers 1982) was developed for gravel-bed rivers and van den Berg (1995) was developed for channels with a sinuosity greater than 1.3.

3.1.1. Slope-Discharge methods

Leopold and Wolman (1957) determined a critical slope value, based on discharge, which separates braided from meandering planforms. The following equation shows the slope-discharge relationship:

$$S = 0.6Q^{-0.44}$$

Where S is the critical slope and Q is the channel discharge (cfs). Channels with slopes greater than the critical slope will have a braided planform, while channels with slopes less than the critical slope will have a meandering planform. Straight channels may fall on either side of the critical slope. Leopold and Wolman identified channels with a sinuosity greater than 1.5 as meandering and channels with a sinuosity less than 1.5 as straight. Using the slope-discharge relationship and the critical sinuosity value, channels can be divided into straight, meandering, braided, or straight/braided channels.

Lane (from Richardson et. al 2001) developed a slope-discharge threshold value, κ, calculated by this equation:

$$\kappa = SQ^{0.25}$$

Where S is the channel slope and Q is the channel discharge (cfs). The classification of the stream is based on the value of κ as shown below:

Meandering:	$\kappa \leq 0.0017$
Intermediate:	$0.010 > \kappa > 0.0017$
Braided:	$\kappa \geq 0.010$

These threshold values assume the use of English units. Values of κ are also available for SI units.

Henderson (1966) developed a slope-discharge method that also accounts for the median bed size by plotting the critical slope as defined by Leopold and Wolman against the median bed size. The following equation resulted:

$$S = 0.64{d_s}^{1.14}Q^{-0.44}$$

Where S is the critical slope, d_s is the median grain size (ft), and Q is the discharge (cfs). For slope values that plot close to this line, the channel planform is expected to be straight or meandering. Braided channels plot well above this line.

Schumm and Khan (1972) developed empirical relationships between valley slope and channel planform based on flume experiments. Thresholds were determined for each channel classification as follows:

Straight:	$S_v < 0.0026$
Meandering Thalwag:	$0.0026 < S_v < 0.016$
Braided:	$0.016 < S_v$

3.1.2. Channel Morphology methods

Rosgen (1996) developed a channel classification method based on entrenchment ratio, width/depth ratio, sinuosity, slope, and bed material. Using these channel characteristics, Rosgen developed eight major classifications and a number of sub-classifications. Figure 3.1, shows Rosgen's method for stream classification.

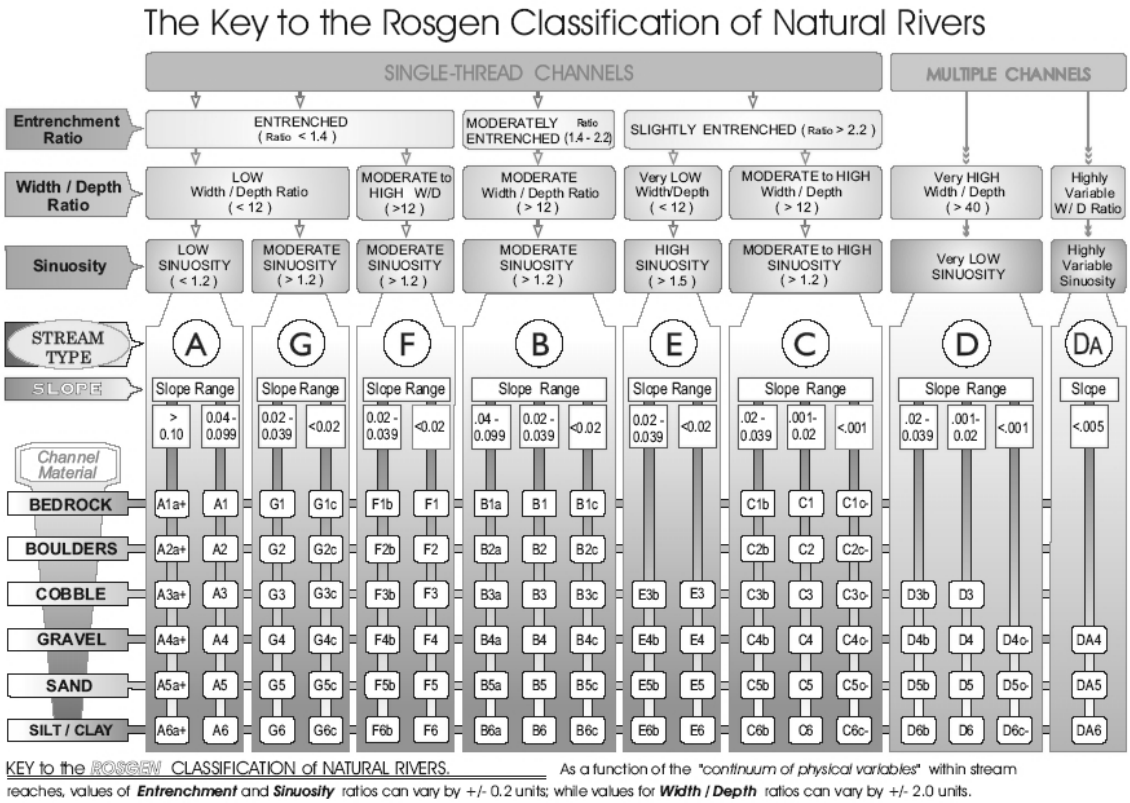

Figure 3.1 Rosgen Channel Classification Key (Rosgen 1996)

Parker (1976) considered the relationship between slope, Froude number, and width to depth ratio. Experiments in laboratory flumes and observations of natural channels lead to the following channel planform classifications:

Meandering:	$S/Fr << W/h$
Transitional:	$S/Fr \sim W/h$
Braided:	$S/Fr >> W/h$

Where S is the channel slope, Fr is the Froude number, and W/h represents the width to depth ratio.

3.1.3 Stream Power methods

Nanson and Croke (1992) used specific stream power and sediment characteristics to differentiate between types of channel planforms. The equation used to determine specific stream power is as follows:

$$\omega = \frac{\gamma S}{W}$$

Where ω is specific stream power (W/m^2), γ is the specific weight of water (N/m^3), S is channel slope, and W is channel width (m). Three main classes and twelve sub-classes where developed by Nanson and Croke. Three classifications of

interest in this reach, along with the corresponding specific stream power and expected sediment type, are shown below:

Braided-river floodplains (braided):
ω = 50-300
gravels, sand, and occasional silt
Meandering river, lateral migration floodplains (meandering):
ω = 10-60
gravels, sands, and silts
Laterally stable, single-channel floodplains (straight):
ω <10
silts and clays

Chang (1979) used data from numerous rivers and canals to develop channel classifications based on stream power. The classifications are presented in terms of valley slope and discharge. Figure 3.2, below, shows the four classification regions defined by Chang for sand streams.

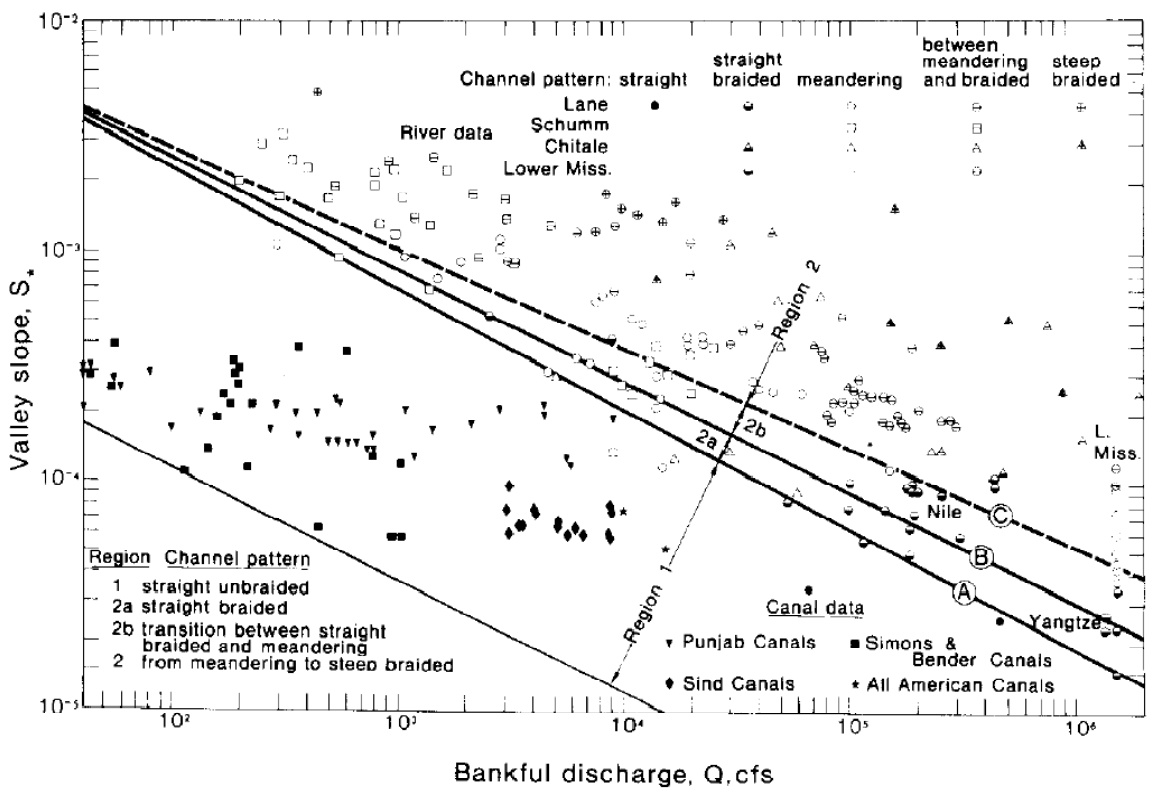

Figure 3.2 Chang's Stream Classification Method Diagram (Chang 1979)

Chang found that at low valley slopes, rivers will have a straight planform. With constant discharge, an increase in valley slope will cause the channel to transform to a braided or meandering planform.

3.2. Channel Planform Results

Visual, qualitative characterization of the channel was performed using channel planforms delineated from aerial photographs using GIS in 1918, 1935, 1949, 1962, 1972, 2001, 2002, 2004, and 2005. See Appendix B for information about the aerial photographs. Aerial photographs for 1985 were not available, so a planform delineation was obtained from the Reclamation database. Figure 3.3 show the historical planforms for the Escondida reach.

Based on visual observations, the historical channel was wide and mildly sinuous, but recent planforms show a relatively straight, narrow channel. Some planforms indicate a tendency toward areas of braiding, especially at low flow. The upstream and downstream extents of the reach have seen the most dramatic shift toward a very straight, non-braided channel. This change may be due to the flow being forced into a confined area under the bridges at the upstream and downstream extents of the reach.

Two of the largest shifts can be seen at the upstream and downstream extents of the reach. Between 1935 and 1949, the channel was shortened slightly on the downstream end of the reach. The bridge at this location was moved upstream. In addition, between 1949 and 1962, the upstream extent of the channel was moved considerably. These channel shifts were not caused by natural channel migration, but by bridge and levee construction.

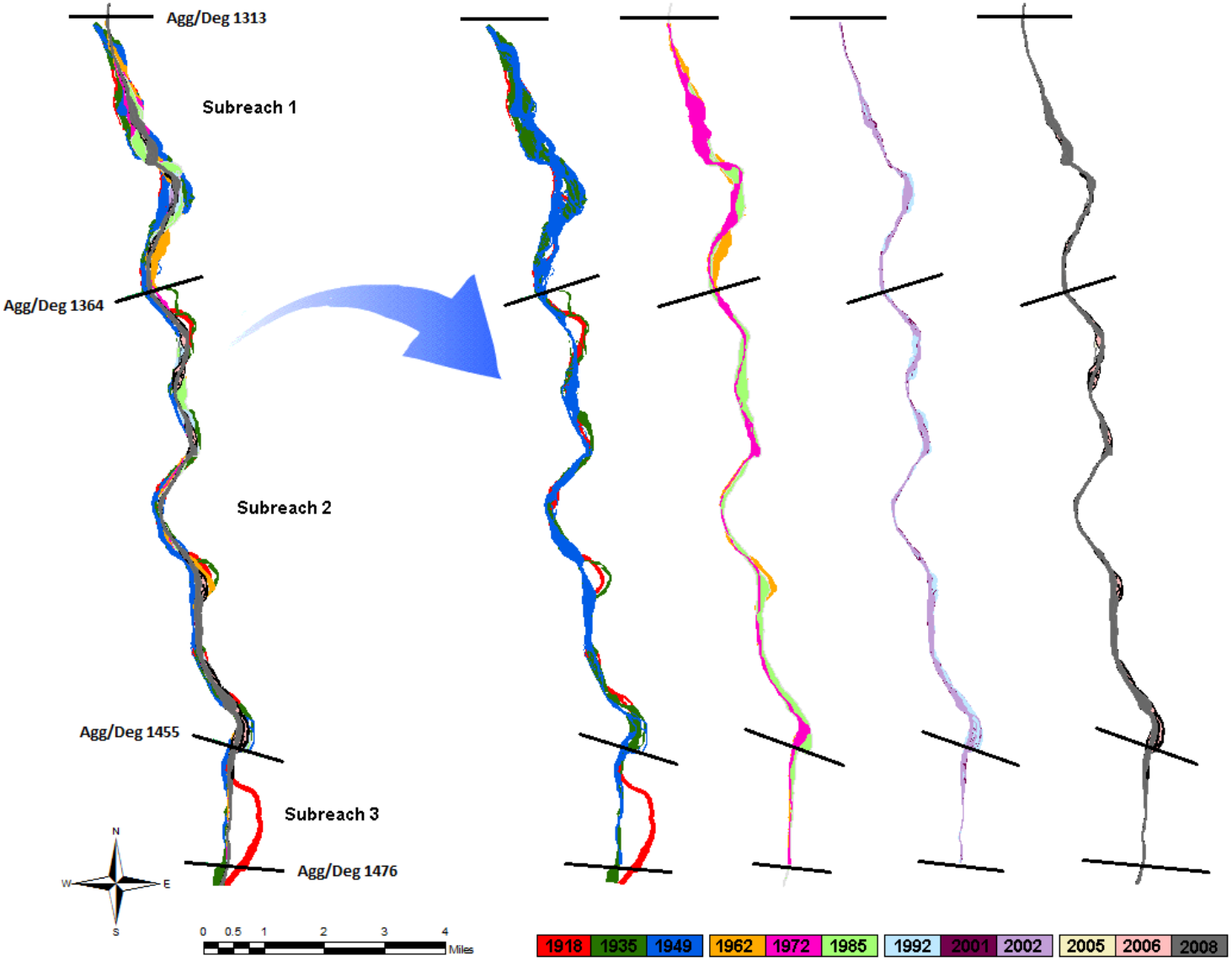

Figure 3.3 Historical planforms

To obtain the values needed in the quantitative channel classification methods, a HEC-RAS model of the reach was run at the bankfull discharge of 5000 cfs. The model was run in years that Agg/Deg survey information was available. Because the channel bed is not clearly defined in the Agg/Deg surveys, available SO survey line information was added to the models to increase detail. Measurements of the channel and valley lengths were obtained from aerial photos in GIS. Table 3.1 shows the input values obtained from HEC-RAS and GIS. Channel characteristics were averaged for each subreach and the overall reach using weighted averages based on half the distance to the next upstream and downstream cross-sections.

Table 3.1 Channel Classification Inputs

	Q (cfs)	Channel Slope (ft/ft)	Valley Slope (ft/ft)	d_{50} (mm)	Bankfull Width (ft)	Flood Prone Width (ft)	Depth (ft)	Fr	EG Slope (ft/ft)
1962									
1	5,000	0.00094	0.0010	0.15	1417	2387	1.54	0.39	0.0011
2	5,000	0.00078	0.0009	0.15	774	2344	2.37	0.42	0.0008
3	5,000	0.00055	0.0006	0.15	3234	5247	2.82	0.33	0.0010
Overall	5,000	0.00080	0.0009	0.15	1291	2713	2.16	0.39	0.0009
1972									
1	5,000	0.00089	0.0010	0.11	1416	2113	1.86	0.39	0.0010
2	5,000	0.00080	0.0009	0.11	1296	2077	2.51	0.43	0.0008
3	5,000	0.00070	0.0007	0.11	3156	5500	2.86	0.36	0.0009
Overall	5,000	0.00082	0.0009	0.11	1572	2503	2.34	0.40	0.0009
1985									
1	5,000	0.00082	0.0009	0.15	1417	2393	2.51	0.40	0.0012
2	5,000	0.00086	0.0009	0.13	774	2407	1.96	0.42	0.0010
3	5,000	0.00052	0.0005	0.10	3239	5535	2.75	0.28	0.0004
Overall	5,000	0.00081	0.0009	0.13	1295	2781	2.24	0.40	0.0010
1992									
1	5,000	0.00076	0.0008	0.22	468	2082	3.41	0.41	0.0009
2	5,000	0.00081	0.0009	0.27	881	2593	2.23	0.43	0.0010
3	5,000	0.00072	0.0007	0.25	1287	5203	3.20	0.39	0.0007
Overall	5,000	0.00078	0.0009	0.23	796	2739	2.74	0.42	0.0009
2002									
1	5,000	0.00078	0.0009	0.37	505	1775	3.04	0.46	0.0010
2	5,000	0.00077	0.0009	0.30	1024	2518	2.15	0.42	0.0009
3	5,000	0.00076	0.0008	0.24	2000	4867	2.37	0.36	0.0006
Overall	5,000	0.00077	0.0009	0.31	982	2572	2.46	0.42	0.0009

The channel classification for each subreach and the overall reach in the five sets of data analyzed are in Table 3.2. The table shows that none of the methods shows a distinct change in the channel planform over time. The channel morphology methods by Parker (1976) and Rosgen (1996) are the only methods that show variation over time and/or between the subreaches in a given

Table 3.2 Channel Classification Results

	D_{50} type	Slope-discharge				Channel Morphology		Stream Power	
		Leopold and Wolman	Lane	Henderson	Schumm & Khan	Rosgen	Parker	Nanson & Croke	Chang
1962									
1	Fine Sand	Straight	Intermediate	Braided	Straight	B5c	Braiding / Transitional	Straight	Meandering to Steep Braided
2	Fine Sand	Straight	Intermediate	Braided	Straight	C5c	Meandering / Transitional	Straight	Meandering to Steep Braided
3	Fine Sand	Straight	Intermediate	Braided	Straight	B5c	Braiding / Transitional	Straight	Meandering to Steep Braided
Total	Fine Sand	Straight	Intermediate	Braided	Straight	B5c	Braiding / Transitional	Straight	Meandering to Steep Braided
1972									
1	Very Fine Sand	Straight	Intermediate	Braided	Straight	B5c	Braiding / Transitional	Straight	Meandering to Steep Braided
2	Very Fine Sand	Straight	Intermediate	Braided	Straight	B5c	Meandering / Transitional	Straight	Meandering to Steep Braided
3	Very Fine Sand	Straight	Intermediate	Braided	Straight	B5c	Braiding / Transitional	Straight	Meandering to Steep Braided
Total	Very Fine Sand	Straight	Intermediate	Braided	Straight	B5c	Braiding / Transitional	Straight	Meandering to Steep Braided
1985									
1	Fine Sand	Straight	Intermediate	Braided	Straight	B5c	Braiding / Transitional	Straight	Meandering to Steep Braided
2	Fine Sand	Straight	Intermediate	Braided	Straight	C5c	Meandering / Transitional	Straight	Meandering to Steep Braided
3	Very Fine Sand	Straight	Intermediate	Braided	Straight	B5c	Braiding / Transitional	Straight	Meandering to Steep Braided
Total	Fine Sand	Straight	Intermediate	Braided	Straight	B5c	Braiding / Transitional	Straight	Meandering to Steep Braided
1992									
1	Fine Sand	Straight	Intermediate	Braided	Straight	C5c	Meandering / Transitional	Straight	Meandering to Steep Braided
2	Medium Sand	Straight	Intermediate	Braided	Straight	C5c	Meandering / Transitional	Straight	Meandering to Steep Braided
3	Fine Sand	Straight	Intermediate	Braided	Straight	C5c	Meandering / Transitional	Straight	Meandering to Steep Braided
Total	Fine Sand	Straight	Intermediate	Braided	Straight	C5c	Meandering / Transitional	Straight	Meandering to Steep Braided
2002									
1	Medium Sand	Straight	Intermediate	Braided	Straight	C5c	Meandering / Transitional	Straight	Meandering to Steep Braided
2	Medium Sand	Straight	Intermediate	Braided	Straight	C5c	Meandering / Transitional	Straight	Meandering to Steep Braided
3	Fine Sand	Straight	Intermediate	Braided	Straight	C5c	Braiding / Transitional	Straight	Meandering to Steep Braided
Total	Medium Sand	Straight	Intermediate	Braided	Straight	C5c	Meandering / Transitional	Straight	Meandering to Steep Braided

year. Leopold and Wolman (1957), Schumm and Khan (1972), and Nanson and Croke (1992) all indicated a straight planform for all subreaches in all years, which is true because the sinuosity in all cases is below 1.5. However, this generalization does not clearly explain the river's condition in this reach. Lane (from Richardson et. al, 2001) and Parker (1976) both classify the channel as in a transitional state between meandering and braided. Parker (1976) indicates an overall tendency toward braiding from 1962-1985 and a tendency toward meandering in 1992 and 2002. Rosgen (1996) classifies the channel as B5c from 1962 to 1985 and as C5c from 1992 to 2002. The B5c classification indicates a channel that is moderately entrenched, with a slope of less than 0.02 and a large width to depth ratio. The C5c classification is similar to the B5c classification except that C5c channels are only slightly entrenched and have well developed floodplains. Henderson (1966) shows a braided classification for all years and subreaches, while Chang (1979) gives a meandering or steep braided classification.

When compared with the observations from the aerial photographs, the methods that indicate a straight or braided channel classification provide the best representation of the actual channel characteristics. Braiding is only seen at low flows, the straight classification given by Leopold and Wolman (1957), Schumm and Khan (1972), and Nanson and Croke (1992) is the most accurate for the bankfull discharge of 5000 cfs. This is predicted by the channel classification methods from 1962 to 2002. The Rosgen's (1996) classifications is based on specific characteristics (i.e. entrenchment ratio, width to depth ratio, sinuosity, slope and channel material), thus this method also results in a reasonable description of the study reach. Based on the Rosgen classification the channel is best described as a C5c or B5c. However, the actual sinuosity in the reach is less than 1.2. Based on the C5c or B5c classification the sinuosity should be greater than 1.2, this is the only discrepancy in the Rosgen classification.

3.3. Sinuosity

3.3.1. Methods

The sinuosity of the Escondida reach, as well as the sinuosity of the three sub-reaches, was measured in GIS from aerial photographs of the reach. The valley length was measured for the entire reach and for each subreach as the straight-line distance between the upstream and downstream extents of the reach at the centerline between lateral constraints. The channel length was measured by estimating the location of the river thalweg based on the aerial photographs and planform delineations. The channel length was divided by the valley length to calculate the sinuosity.

Some difficulty was encountered when estimating the river thalweg due to varying quality of aerial photographs. In addition, aerial photographs were unavailable for 1985, however Reclamation's provided channel planform delineations. The delineation was used to estimate the channel and valley lengths for that year. The upstream and downstream extents of the Escondida reach were both relocated during the period of study. The downstream extent was relocated between 1935 and 1949 by 3%, and the upstream extent was relocated between 1949 and 1962 by 0.03%. The relocation is associated with the bridges moving. This resulted in a valley length that was not identical for all years measured, however this does not change the answer significantly. Table 3.3 shows the valley length and the years

Table 3.3 Change in Valley Length

Year	Valley Length (ft)
1935	76,582
1949	74,206
1962	74,229

3.3.2. Results

As seen in Table 3.4, the overall sinuosity decreased from 1.19 to 1.09 between 1918 and 2005. Sinuosity in all subreaches decreased between 1918 and 1949, and sinuosity decreased only a small amount during the period of levee construction and initial channelization between 1949 and 1962. Although the trend was toward a decreasing sinuosity, there were increases in the total channel sinuosity in 1972, 1992, and 2002. Figure 3.4 shows how the sinuosity changed in each subreach and in the entire reach over time.

Table 3.4 Sinuosity Changes

	1918	1935	1949	1962	1972	1985	1992	2001	2002	2005
Subreach 1	1.13	1.15	1.12	1.10	1.16	1.10	1.09	1.09	1.10	1.09
Subreach 2	1.21	1.14	1.12	1.12	1.11	1.09	1.13	1.12	1.12	1.10
Subreach 3	1.22	1.06	1.04	1.01	1.01	1.02	1.02	1.03	1.04	1.02
Total	1.19	1.13	1.11	1.10	1.12	1.08	1.10	1.10	1.11	1.09

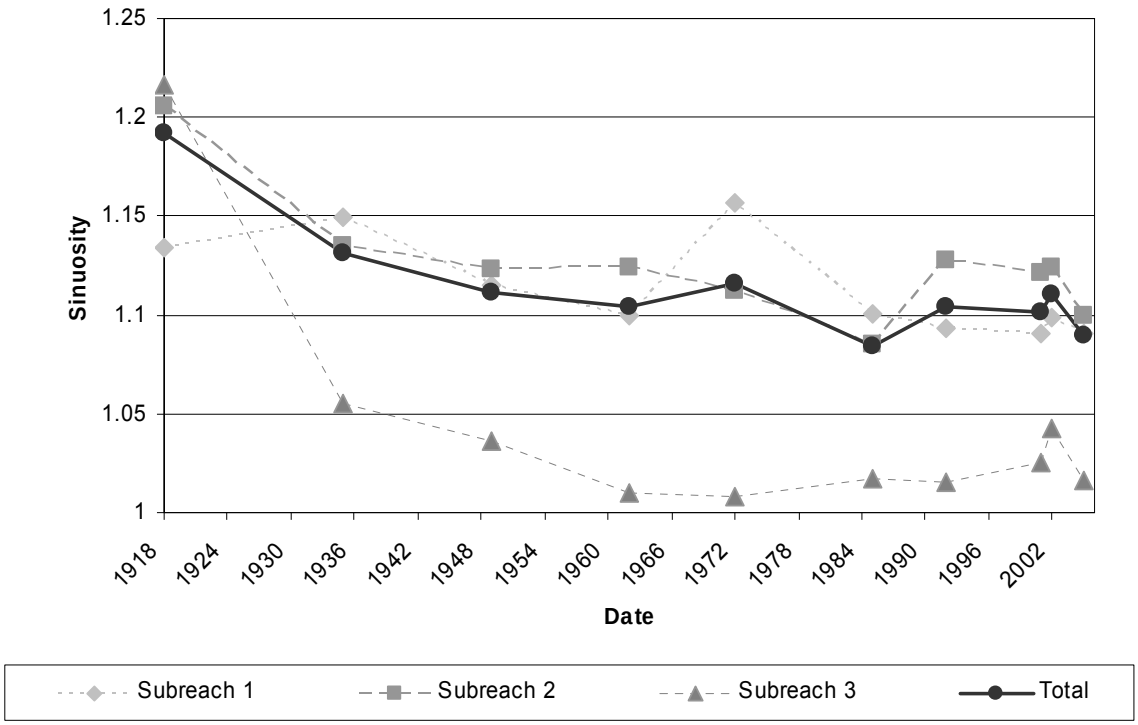

Figure 3.4 Sinuosity

Subreach 3 showed a decrease between 1918 and 1935. The sinuosity of this reach continued a steady decrease until 1985 when the sinuosity began to increase. This increase lasted until 2002, when sinuosity decreased again to its current value. Subreach 2 also began with a trend toward decreasing sinuosity. The sinuosity of subreach 2 followed that of subreach three with the exception of a slight increase seen in 1962. The sinuosity of subreach 1 alternated between increasing and decreasing more than the other reaches. An increase in sinuosity was seen between 1918 and 1935, followed by a decreasing trend that continued until 1962. The increase between 1962 and 1972 was followed by a steady decrease in sinuosity until 2002. In 2002, as in the other reaches, the sinuosity increased, only to decrease again in 2005.

In 1918, the sinuosity of subreach 3 was slightly higher than the other reaches, but following 1935, it remained far less sinuous than the other reaches.

Subreach 1 and subreach 2 tended to have sinuosity values close to each other and close to the overall sinuosity. This may be due to the straightening seen at the downstream extent of the reach extending far into subreach 3. Although relocation and straightening occurred at the upstream extent, it had less of an effect on the sinuosity of subreach 1 because it is much longer than subreach 3.

3.4. Longitudinal Profile

3.4.1. Methods

Thalweg Elevation
The thalweg elevation was calculated as the lowest point in the channel based on the SO-line surveys. Because the SO-line surveys offer more detailed cross section information, they were used instead of the Agg/Deg surveys. SO-line data were only available from 1987-2005.

Mean Bed Elevation
Trends in mean bed elevation were evaluated using the Agg/Deg survey data provided by Reclamation. Reclamation's Technical Service Center in Denver adjusted the cross section data by modifying the instream channel portion by lowering the bed elevation iteratively to minimize the error difference between the observed wetted width from the aerial photography and the HEC-RAS model. The method used to generate the Agg/Deg surveys from aerial photographs results in determination of the mean bed elevation. This elevation was used to show the changes in mean bed elevation through time. Because the SO-lines usually fall at the same location as the Agg/Deg lines, only the Agg/Deg lines were used to analyze the mean bed elevation. The change in mean bed elevation at each cross-section was evaluated, along with the changes in the average mean bed elevation by subreach. The averages calculated for the subreaches are based on weighted averages derived from half the distance between next upstream and downstream Agg/Deg line.

Energy Grade Slope
The energy grade line (EGL) slope for the reach was obtained from HEC-RAS models run at the bankfull discharge of 5000 cfs. The average EGL slope for each subreach and the entire reach was calculated in the same manner as the average mean bed elevation.

Water Surface Slope
The water surface slope between cross-sections was calculated from the water surface elevation at each cross section determined by HEC-RAS and distance between cross-sections. Because the water surface slope was computed as a property of the area between two cross-sections rather than a property of the cross-section itself, the weighting scheme used to calculate the subreach averages was based on the distance to the next downstream cross section.

3.4.2. Results

Thalwag Elevation
Figure 3.5 shows the change of the thalweg elevation at each SO-line over time. Only SO-lines with enough years of sample data to provide useful information about trends were plotted. The cross-sections in subreach 1, SO-lines 1313

through 1360 decrease as much as 5 feet and then increase several feet. In subreach 2, SO-lines 1380 through 1414 have a steadily decreasing trend with an overall degradation of around 5 feet. Then the thalweg elevation in subreach 2, SO-lines 1420 through 1450, alternates between increasing and decreasing with nearly every sample, resulting in little long-term change. In subreach 3, only a temporal change can be observed since only SO 1470.5 had available data. The general trend in subreach 3 is one of an initial degradation of about 5 feet over 7 years, followed by a generally increasing trend for the next 5 years. Two of the data points in cross-section 1470.5 indicate one-year aggradation and degradation of more than 10 feet. This can be associated with the channel filling with sediment and a pilot channel being carved. In addition, the data sampled in 2005 indicate an increase of 10 to 15 feet in just one year. There is a datum shift of 2.4 feet, but this does not explain the 10 plus feet of aggradation. It could be possible that significant deposition of sediment occurred throughout the Escondida Reach in 2005, however this was not observed in the San Acacia Reach directly upstream. Thus the data from 2005 was not considered in the above discussion, because the discrepancy could not be verified.

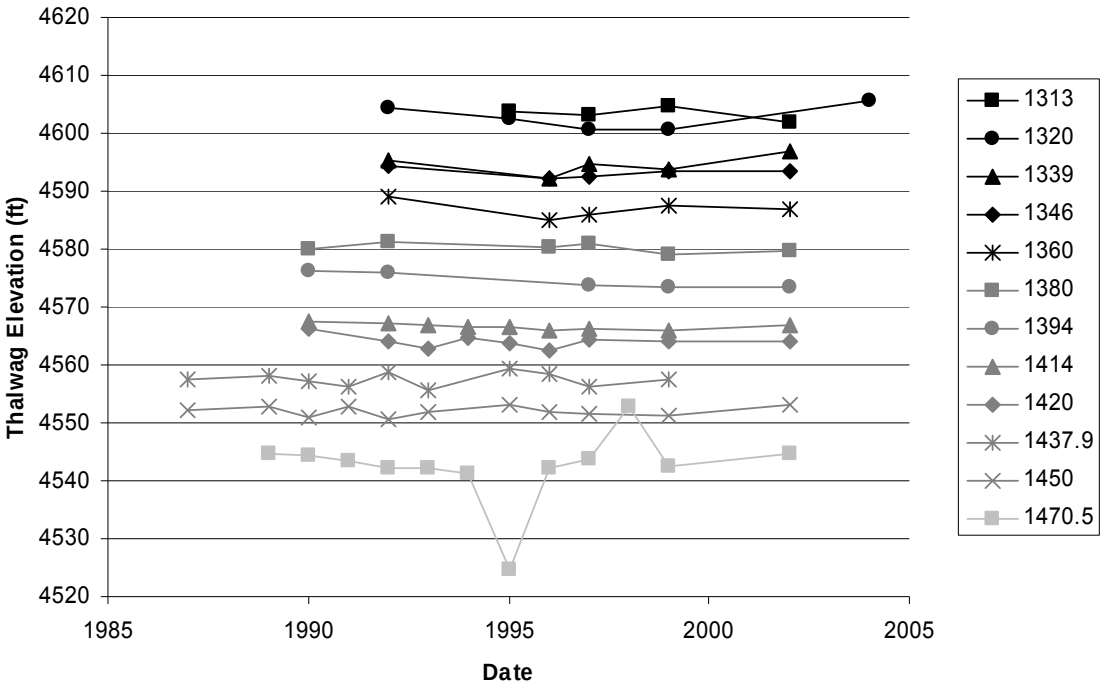

Figure 3.5 Change in thalweg elevation by SO-line

Figure 3.8 shows the thalweg elevation profile of the entire reach. Because the 2005 indicates an unreasonable amount of aggradation, it was not considered in the analysis of thalweg elevation trends. Subreach 3 has had the most change in since 1987, while subreach 2 seems to have been the most stable in recent years. Subreach 1 has seen some recent degradation of the thalweg elevation, but the changes are not as large as those seen in subreach 3.

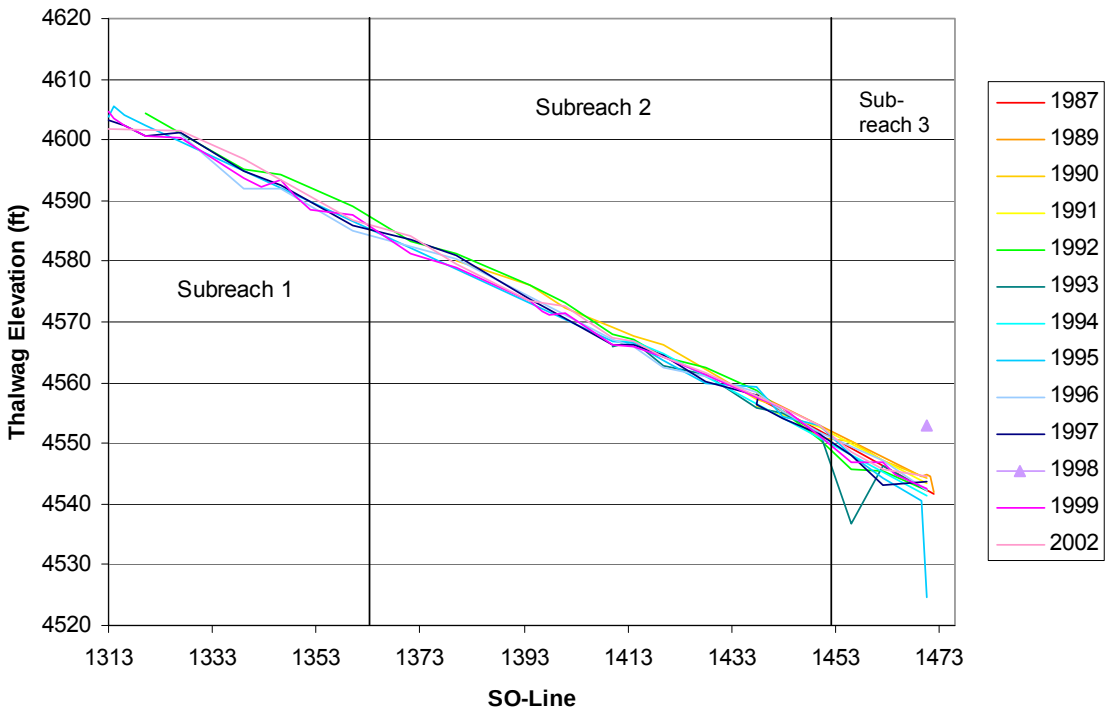

Figure 3.6 Thalweg elevation profile

<u>Mean Bed Elevation</u>

Changes in mean bed elevation based on Agg/Deg lines are shown over time in Figure 3.7 for each subreach and for the entire reach.

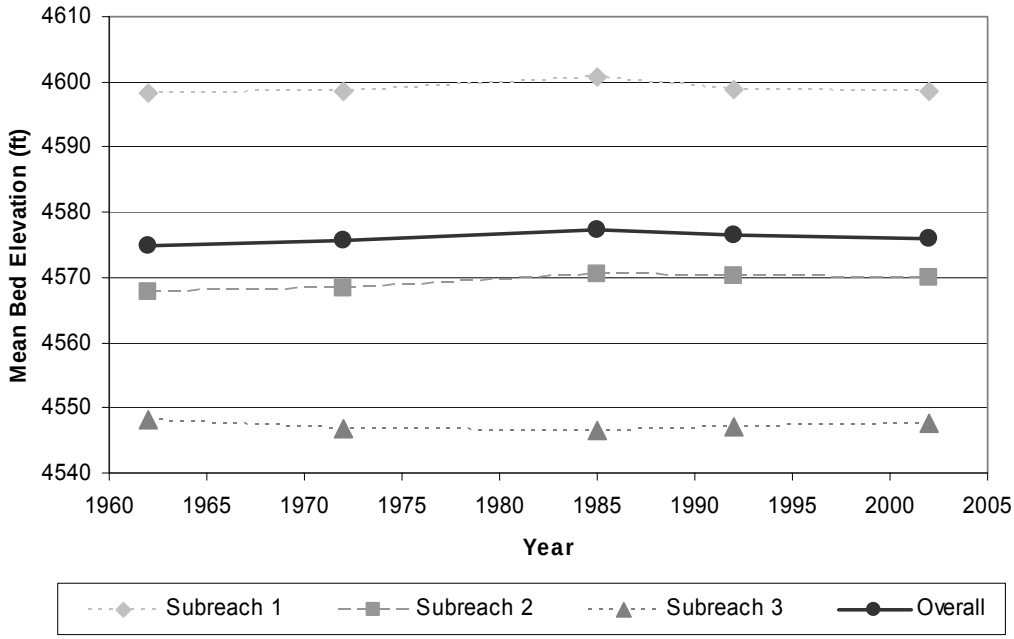

Figure 3.7 Reach averaged mean bed elevation

Subreach 1 and subreach 2 show an average increase of about 2 feet between 1962 and 1985. The mean bed elevation in these two subreaches then decreases between 1985 and 2002. Subreach 3 follows an opposite trend of first decreasing and then increasing. This is attributed to the river naturally adjusting itself due to the affects of channelization.

The change in mean bed elevation at each Agg/Deg line can be seen in Figure 3.8. Between 1962 to 1972, the reach fluctuated between aggradation and degradation spatially. In subreach 1 the river tends to aggrade, while in subreach 3 the river degrades. Subreach 2 shows some degradation but primarily aggradation. Between 1972 to 1992, the river has a tendency to degrade on both ends of the reach while the center of the reach shows aggradation. Between 1992 to 2002, there is spatial fluctuation. The overall river degrades however there are few cross sections where aggradation is observed. The overall change from 1962 to 2002 is similar to the pattern from 1972 to 1992. .

.

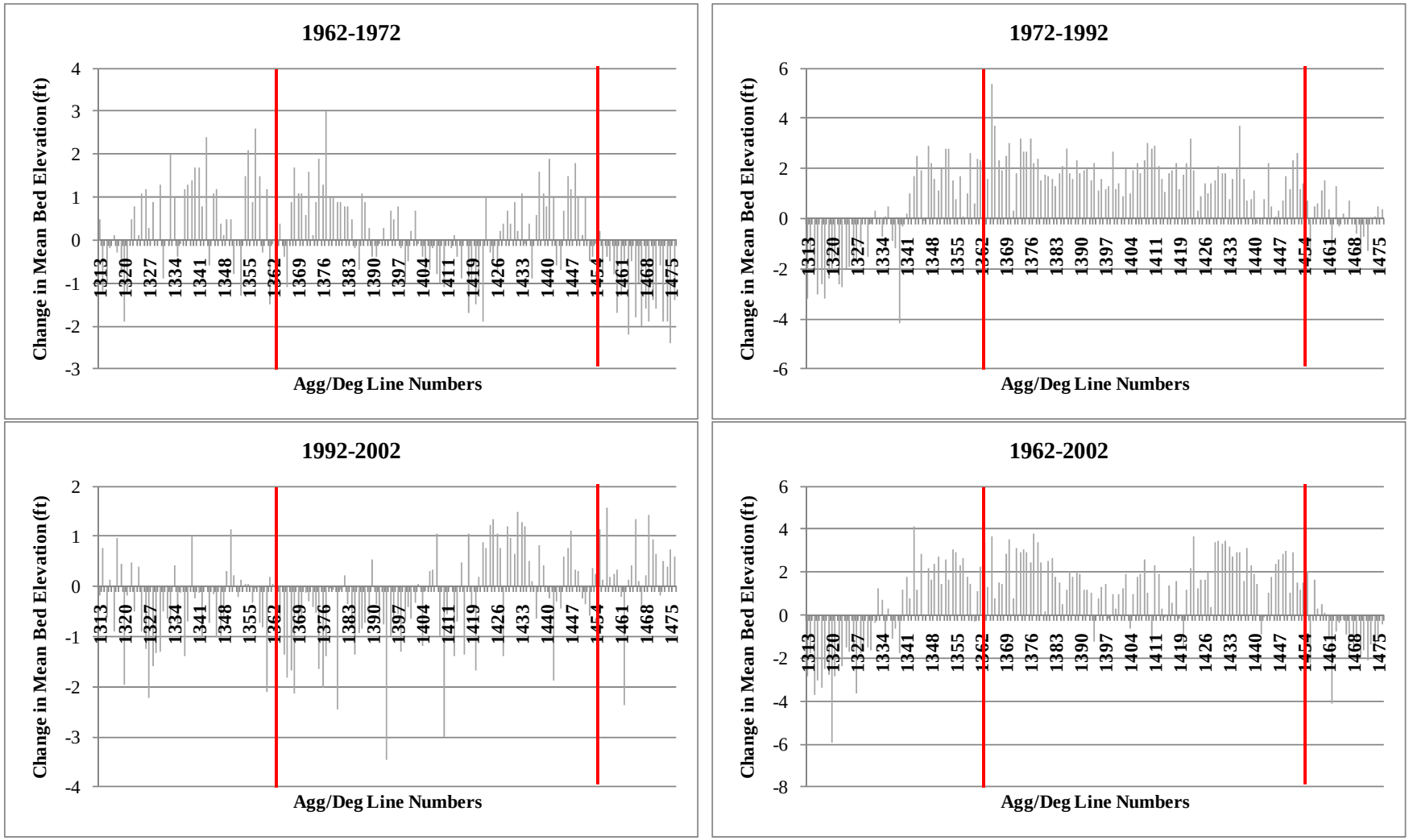

Figure 3.8 Change in mean bed elevations

Energy Grade Slope

Figure 3.9 shows the change in EGL slope with time for each subreach and the entire reach.

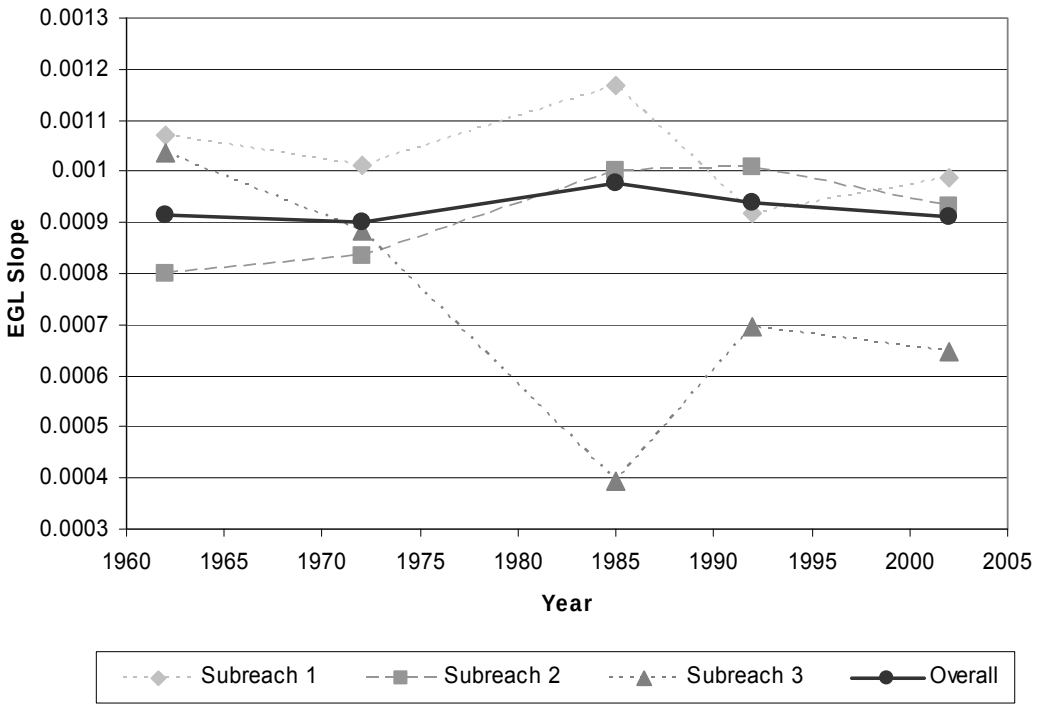

Figure 3.9 Energy grade line slope

In 1962 and 1972, the ELG slope for all three subreaches was within 0.0003 ft/ft of one another. In 1985, however, the EGL slope of subreach 3 decreased significantly, but subreaches one and two increased at approximately the same rate. By 2002, subreach 1 and subreach 2 had similar EGL slopes, while the EGL slope for subreach 3 was still far lower.

Water Surface Slope

The average water surface slope by subreach and for the entire reach is shown Figure 3.10.

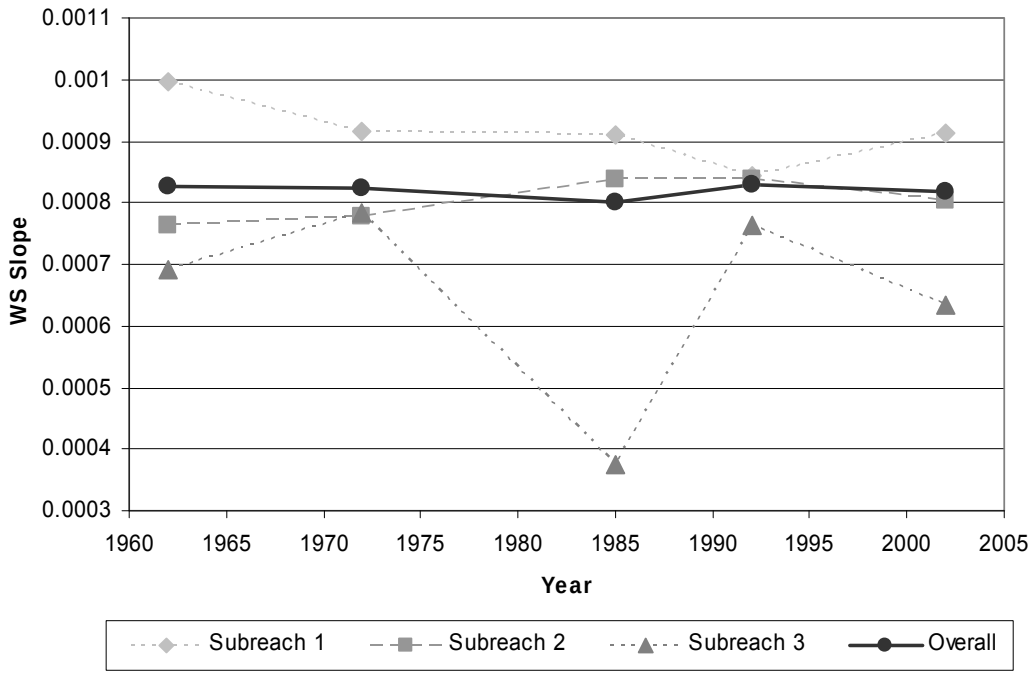

Figure 3.10 Water surface elevation slope

The water surface slope of subreach 1 showed a decreasing trend from 1962 to 1992 with an increase occurring between 1992 and 2002. Subreach 2 showed an opposite trend with an increase in water surface slope between 1962 and 1985, little change between 1985 and 1992, and a decrease between 1992 and 2002. The water surface slope of subreach 3 was highly variable. This reach showed an increase from 1962 to 1972 followed by a dramatic decrease in 1985. In 1992, the water surface slope increased again to near 1972 levels before falling again in 2002.

3.5. Channel Geometry

3.5.1. Methods

Trends in geometric properties where analyzed from HEC-RAS model runs using the bankfull discharge of 5000 cfs. The HEC-RAS geometry files where available from Reclamation for 1962, 1972, 1985, 1992, and 2002. Each model used 162 cross-sections at a spacing of approximately 500 feet. A Manning's n value of 0.02-0.024 was used for the main channel and a Manning's value of 0.1 was used for the overbank area. Manning's n values, bank station and levee locations, and downstream reach lengths where originally determined by Reclamation. Each geometry file was evaluated and compared to GIS aerial

photography for the corresponding year. Adjustments to the bank stations, levee locations, and reach lengths where made based on engineering judgment to best represent the actual channel conditions.

Channel geometry parameters calculated at each cross section by HEC-RAS include:

Cross-Sectional Area	A
Top Width	W
Wetted Perimeter	P_w
Hydraulic Depth	D
Velocity	V
Froude Number	Fr

The numerical results from the HEC-RAS output can been found in Appendix C. The above geometric parameters and other properties available from HEC-RAS where used to calculate two additional channel geometry properties. These properties include:

Max Depth D_{max} = Water Surface Elevation - Minimum Channel Elevation
Width/Depth Ratio W/D = Top width / Hydraulic Depth

The average values of the eight channel properties where calculated using the weighted averages based on half the distance to the next upstream and downstream cross-sections. This weighted average was also used earlier on the Energy Grade Line (EGL) slope calculations.

3.5.2. Results

Figure 3.12 and Table 3.5 shows the trends in the average cross-sectional area, top width, wetted perimeter, hydraulic depth, maximum depth, channel velocity, Froude number, and width/depth ratio in each subreach and in the overall reach.

Top width, cross-sectional area, and wetted perimeter all follow similar trends. The cross-sectional area and wetted perimeter show nearly identical trends. This is reasonable because the two parameters are a function of the width and depth. The top width and wetted perimeter not only have similar trends; they also have similar magnitudes. This indicates that the channel is very wide compared to the depth.

The trends in the width to depth ratio indicate a general trend toward a deeper, narrower channel until 1992, and a slightly wider, shallower channel in 2002. In addition, the high values of the width to depth ratio further reinforce the idea that the channel is very wide compared to its depth.

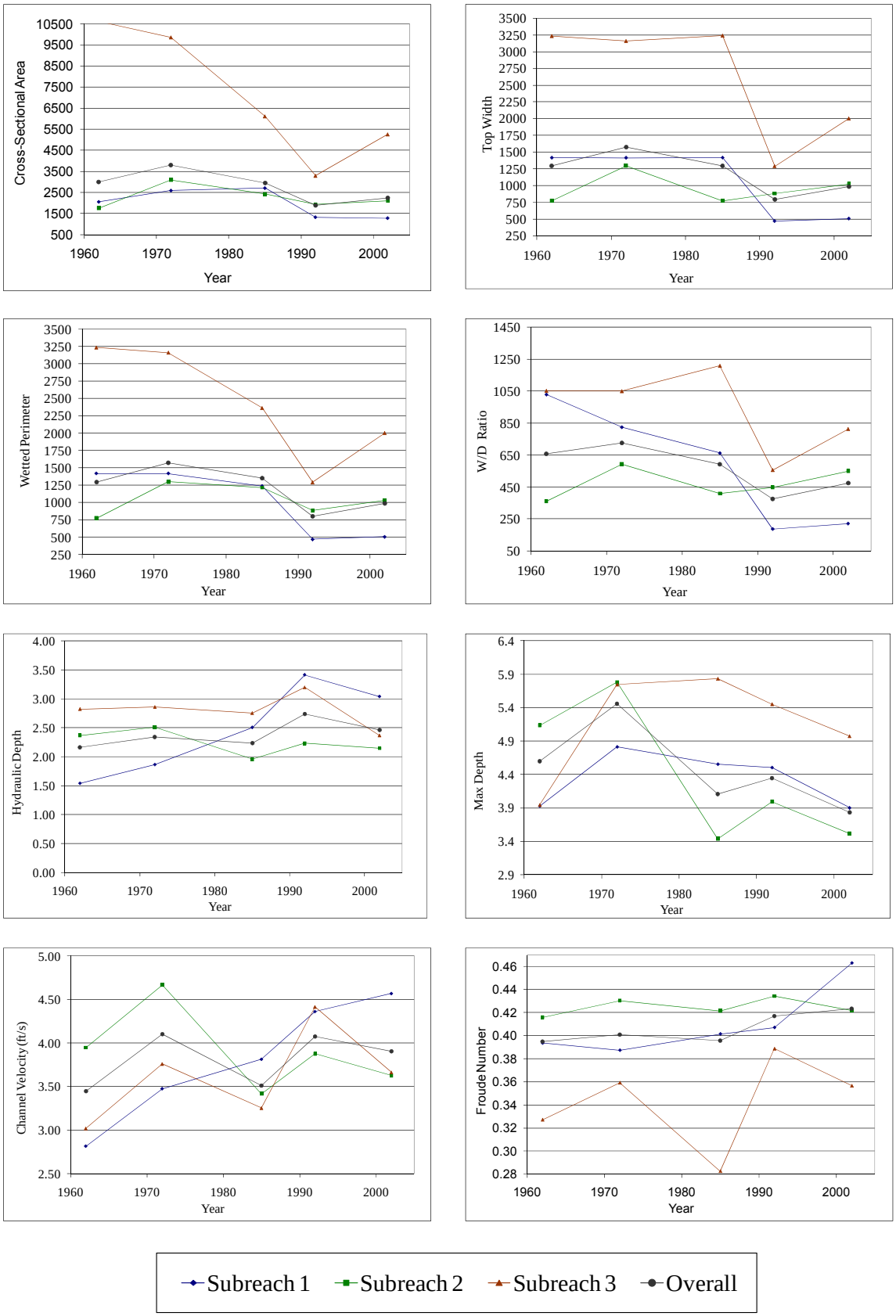

Figure 3.11 Channel Geometry Properties

Table 3.5 – Summary of Hydraulic Parameters

	Subreach	Area	Top Width	Wetted Perimeter	Hydraulic Depth	Max Depth	W/D	Velocity	Froude Number
1962-1972	1	(539.89)	1.05	0.34	(0.32)	(0.89)	204.74	(0.66)	0.01
	2	(1344.39)	(521.94)	(522.64)	(0.14)	(0.64)	(232.49)	(0.72)	(0.01)
	3	749.19	75.26	74.05	(0.03)	(1.80)	1.64	(0.74)	(0.03)
	Total	(804.88)	(280.77)	(281.53)	(0.17)	(0.86)	(68.98)	(0.65)	(0.01)
1972-1992	1	1273.84	948.22	946.20	(1.55)	0.31	637.72	(0.89)	(0.02)
	2	1171.73	415.51	413.13	0.28	1.78	145.00	0.79	(0.00)
	3	6570.81	1871.56	1868.75	(0.34)	0.29	495.15	(0.65)	(0.03)
	Total	1894.21	776.20	773.90	(0.40)	0.29	351.75	0.03	(0.02)
1992-2002	1	43.68	(37.49)	(36.15)	0.37	0.60	(33.86)	(0.21)	(0.06)
	2	(184.95)	(143.62)	(141.73)	0.09	0.48	(101.82)	0.25	0.01
	3	(1966.83)	(713.07)	(711.00)	0.83	0.48	(257.18)	0.75	0.03
	Total	(355.04)	(185.98)	(184.27)	0.28	0.52	(98.96)	0.17	(0.01)
1962-2002	1	777.64	911.78	910.40	(1.50)	0.03	808.61	(1.75)	(0.07)
	2	(357.61)	(250.05)	(251.24)	0.22	1.62	(189.32)	0.32	(0.01)
	3	5353.17	1233.75	1231.80	0.46	(1.03)	239.61	(0.64)	(0.03)
	Total	734.30	309.45	308.10	(0.29)	0.77	183.81	(0.45)	(0.03)

The hydraulic depth and the maximum depth are also closely related. The hydraulic depth is the depth of a rectangular channel which, when divided by the top width of the channel, gives the cross-sectional area of the channel. The maximum depth is the maximum depth found in the channel. The overall trend for both parameters is very similar. Both parameters show an increase in 1992, followed by a decrease in 2002. This correlates well with the decrease in width in 1992 and the subsequent increase in 2002, because as the channel becomes deeper, it must also narrow to maintain continuity.

The trends in velocity are generally opposite the trends observed in the width to depth ratio. This suggests that as the channel becomes narrower, the velocity in the channel increases. The opposite correlation can also be true. An increased channel velocity may scour the channel bed causing increased depth and decreased width.

The average Froude number in the channel in all subreaches and in all years is well below one, indicating that the flow in the channel is generally in the sub-critical regime. This is expected because supercritical flow would be very difficult to maintain in a mild slope, sand-bed channel. In addition, the general trends seen in the channel velocity are similar to those seen in the Froude number.

3.6. Bend Migration

3.6.1. Methods

General observations of the bend migration in the reach where performed using aerial photographs and channel planform delineations in GIS. Areas of movement where identified visually. The changes at the locations of movement where then measured and further analyzed using GIS.

3.6.2. Results

Observations made of recent bed migration indicate that since 1992, very little movement has occurred in the reach. However, observation of bend migrations since 1962 indicates that movement occurred between 1962 and 1992. Table 3.6 shows the locations of significant movement for each time period analyzed. The magnitude and direction of the movement is also included.

Table 3.6 Bed Migration

Year	Agg/Deg Number	Movement	
		Magnitude (ft)	Direction
1985-1992			
	1326-1332	330	R
	1333	120	L
	1352	100	R
	1376	220	L
	1471	150	R
1972-1985			
	1326	200	L
	1363	240	R
	1397-1405	300	L
	1413	120	L
	1421	100	R
	1467	100	L
1962-1972			
	1326	390	R
	1343	295	L
	1347	335	R
	1355	215	R
	1375	250	L
	1378-1386	590	R
	1419-1426	850	R

A few locations showed either very large movement in a single observation period or continued movement over several observation periods. Figure 3.12 shows the progressive channel location near Agg/Deg 1326, Figure 3.13 shows the 590 foot movement observed between Agg/Deg 1378 and Agg/Deg 1386 between 1962 and 1972, and Figure 3.14 shows the 850 foot migration of Agg/Deg 1419-1426 between 1962 and 1972.

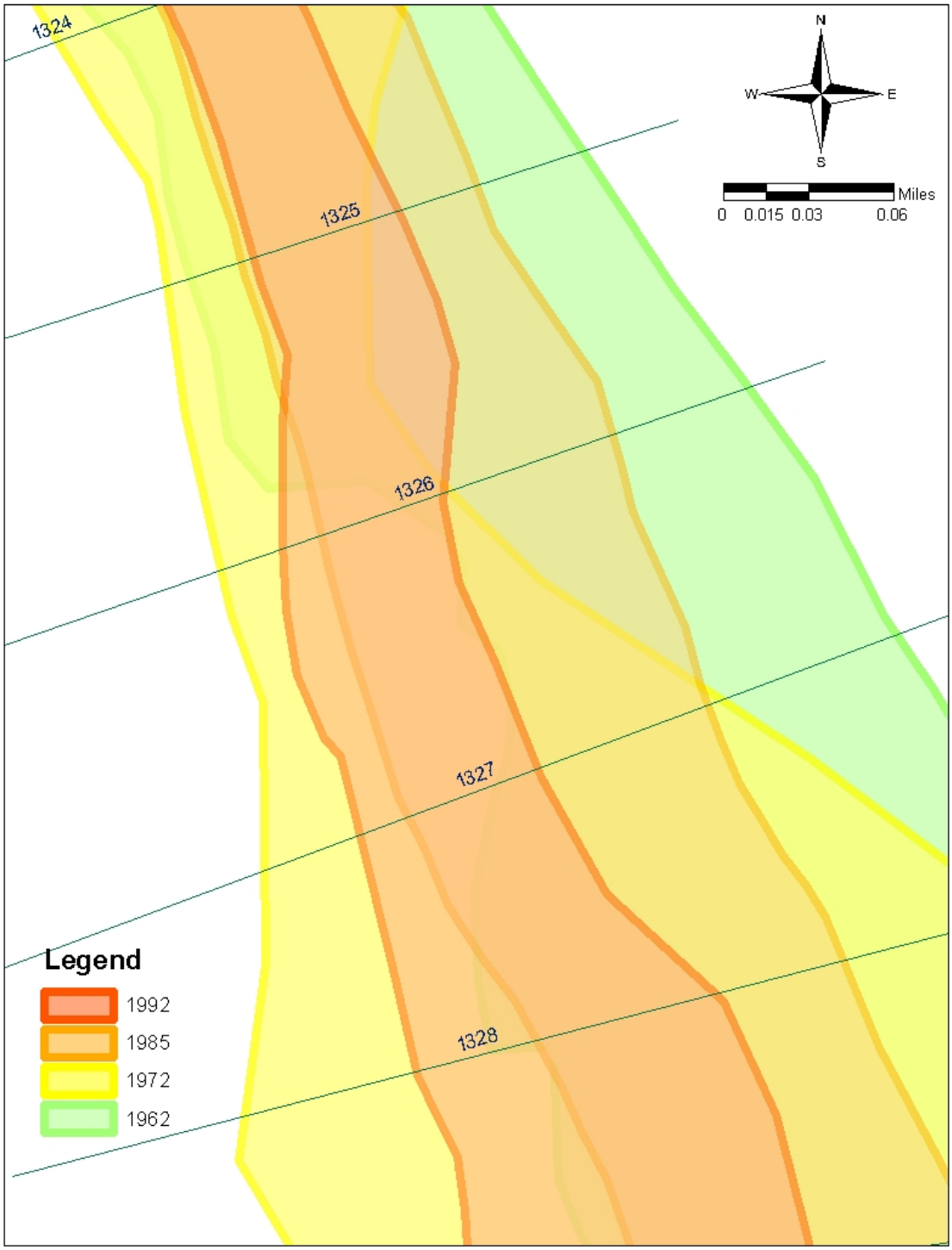

Figure 3.12 Bend migration at Agg/Deg 1326

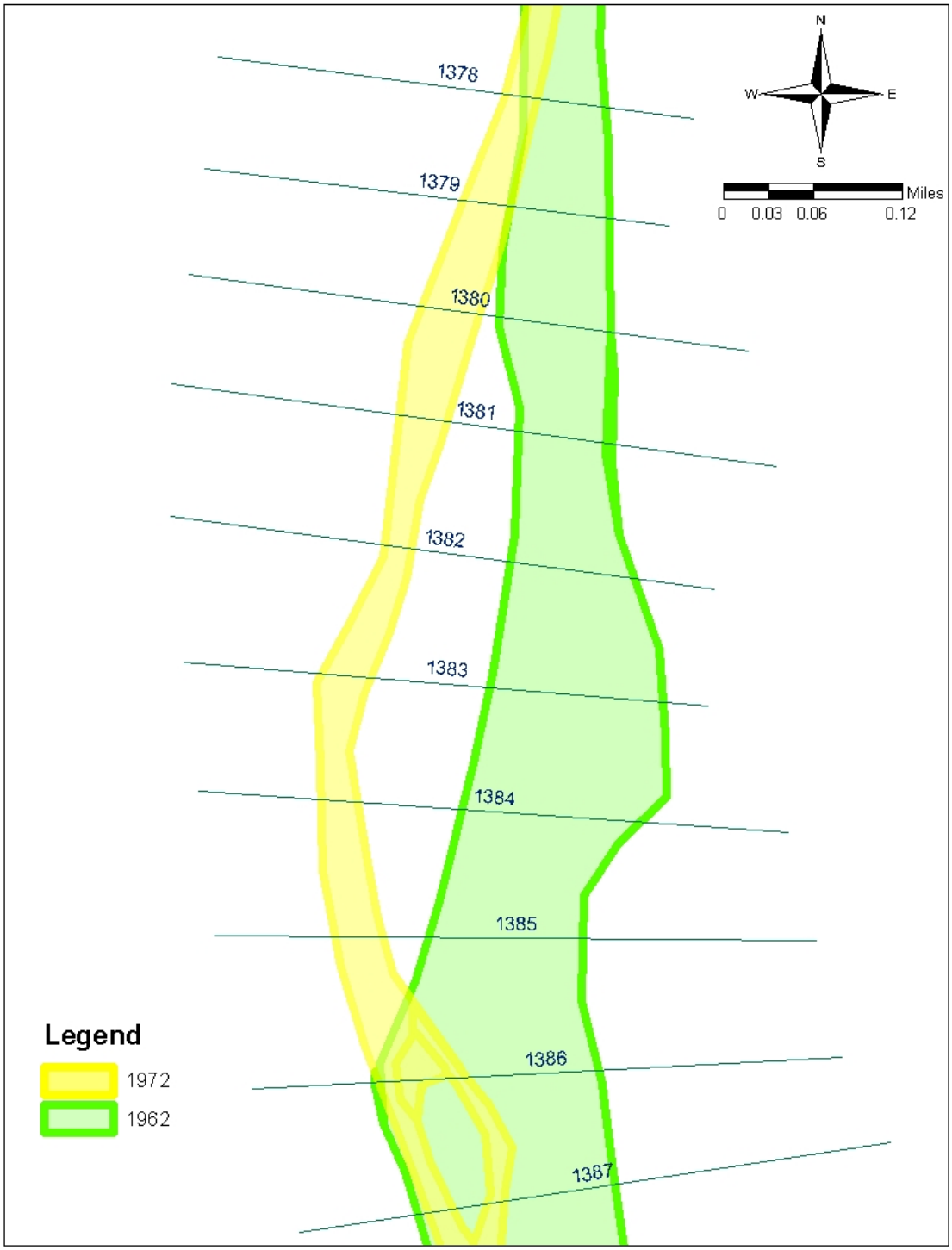

Figure 3.13 Bend migration at Agg/Deg 1378-1386

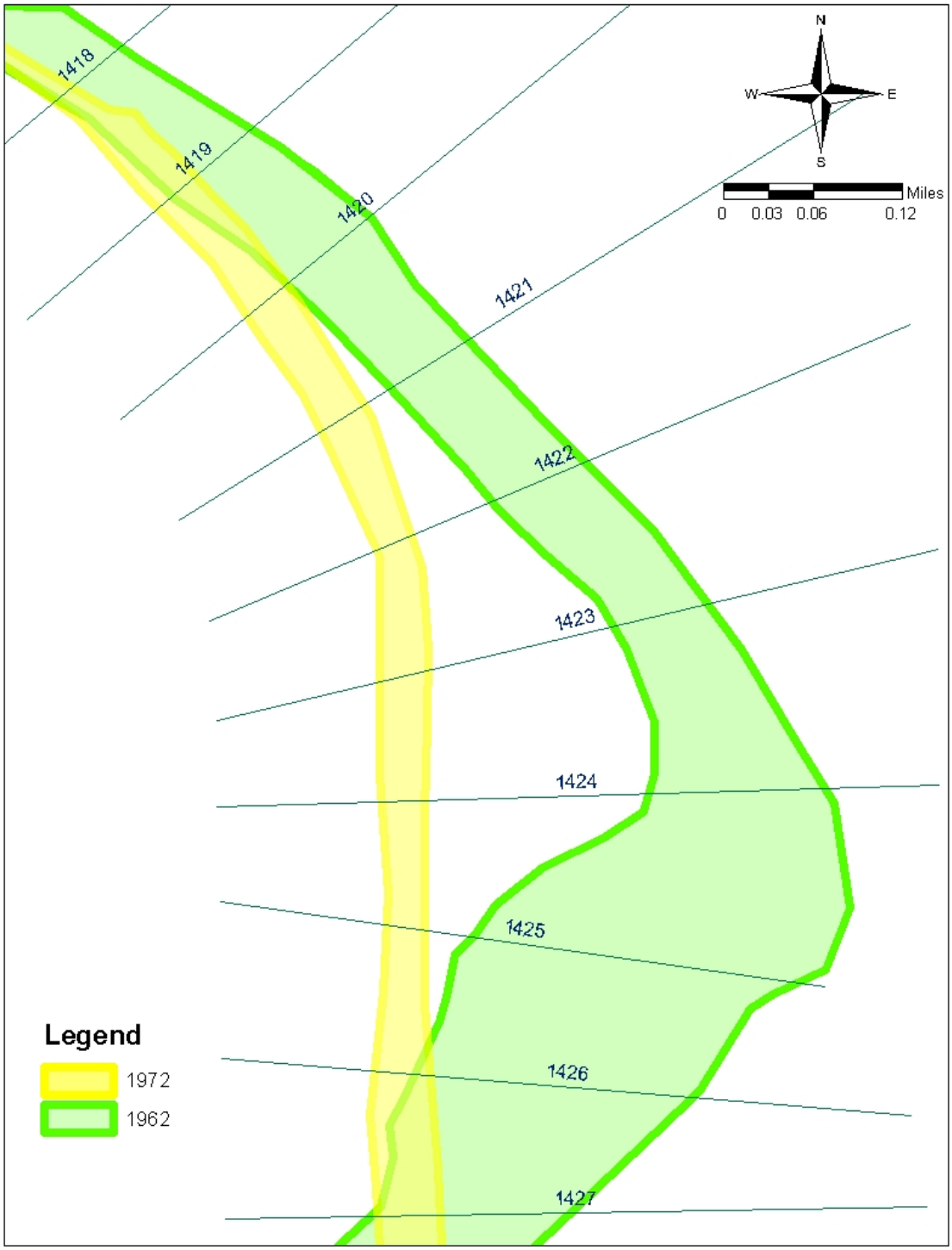

Figure 3.14 Bend migration at Agg/Deg 1419-1426

The migration of the bends show why the channel sinuosity has slightly decreased and a once wide channel with a tendency to braid at low flows is now more straight and narrow.

3.7. Material Analysis

3.7.1. Methods

The bed material surveys taken at SO-lines were used to determine the median bed grain size for each subreach. When appropriate data was not available at the SO-lines, bed material from the San Acacia and San Marcial gauges was used. In both 1962 and 1972, bed material data was not available, so the grain sizes from the closest available years were used. When SO-line data was used, the median grain size for the subreach was calculated using a weighted average based on the distance between SO-lines. The gauge data that was most similar to the available SO-line data was used in the absence of SO-line data. Grain size classification was determined using Figure 3.15 from Julien (1998).

	Size range	
Class name	mm	in.
Boulder		
Very large	4,096–2,048	160–80
Large	2,048–1,024	80–40
Medium	1,024–512	40–20
Small	512–256	20–10
Cobble		
Large	256–128	10–5
Small	128–64	5–2.5
Gravel		
Very coarse	64–32	2.5–1.3
Coarse	32–16	1.3–0.6
Medium	16–8	0.6–0.3
Fine	8–4	0.3–0.16
Very fine	4–2	0.16–0.08
Sand		
Very coarse	2.000–1.000	
Coarse	1.000–0.500	
Medium	0.500–0.250	
Fine	0.250–0.125	
Very fine	0.125–0.062	
Silt		
Coarse	0.062–0.031	
Medium	0.031–0.016	
Fine	0.016–0.008	
Very fine	0.008–0.004	
Clay		
Coarse	0.004–0.0020	
Medium	0.0020–0.0010	
Fine	0.0010–0.0005	
Very fine	0.0005–0.00024	

Figure 3.15 Grain size classification (Julien 1998)

3.7.2. Results

Figure 3.16 shows the change in grain size in each subreach. While the entire reach remains in the range of grain sizes for sand, there has been an overall increase in grain size in recent years.

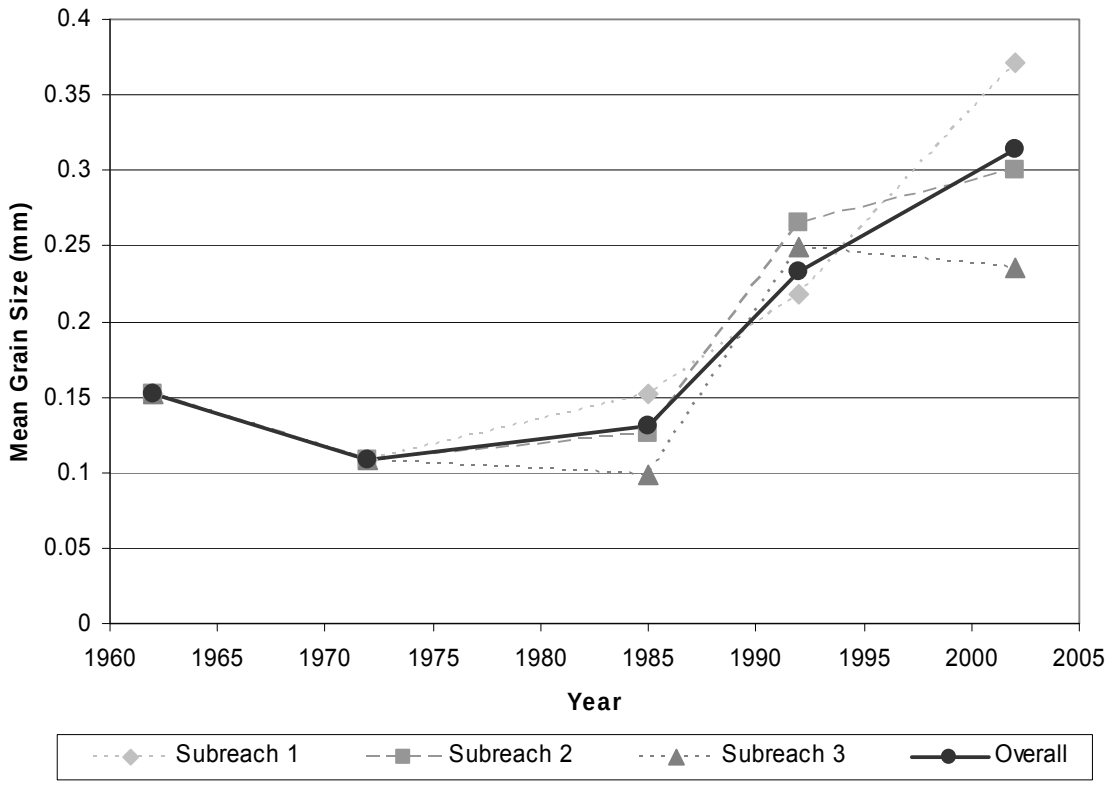

Figure 3.16 Bed material mean grain size

The bed material types are summarized in Table 3.7. The bed material size was obtained from SO-line surveys where available. When SO-line surveys were not available, San Acacia gauge data were used for subreach 1, San Marcial gauge data were used for subreach 3, and an average of San Acacia and San Marcial gauge data were used for subreach 2.

Table 3.7 Bed material type

Subreach	1962	1972	1985	1992	2002
1	Fine Sand	Very Fine Sand	Fine Sand	Fine Sand	Medium Sand
2	Fine Sand	Very Fine Sand	Fine Sand	Medium Sand	Medium Sand
3	Fine Sand	Very Fine Sand	Very Fine Sand	Fine Sand	Fine Sand
Total	Fine Sand	Very Fine Sand	Very Fine Sand	Fine Sand	Medium Sand

The bed material classification has been, increased from very fine sand in 1972 to medium sand in 2002. Average particle size distributions for each year are shown in Figure 3.17. This data were obtained from the San Marcial gage. The particle size distribution also indicates a recent trend toward increasing grain size. Particle-size distributions for each year and subreach are shown in Appendix D.

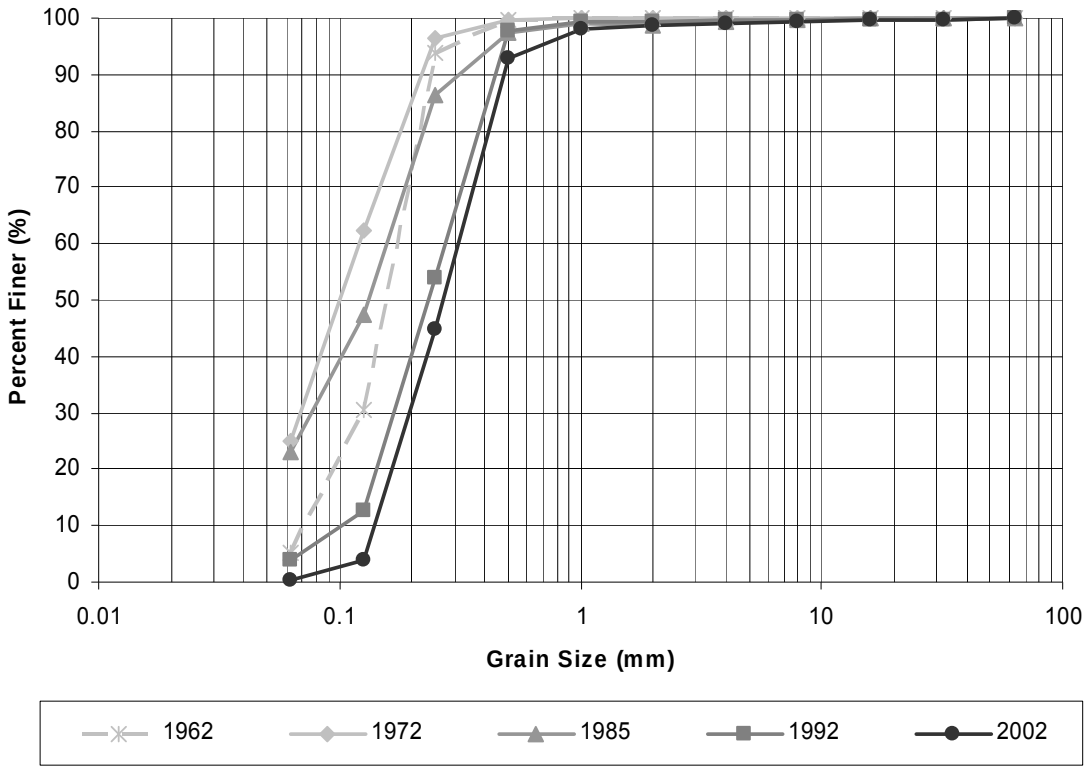

Figure 3.17 Bed material particle size distributions

4. Suspended Sediment and Water

Single and double mass curves were used to show trends in water discharge, suspended sediment discharge, and suspended sediment concentration. A difference mass curve was developed to show trends in suspended sediment continuity. Suspended sediment continuity compares the amount of sediment entering the reach versus the amount of sediment leaving the reach. Discharge and suspended sediment data were compiled from the USGS gauging stations at San Acacia and San Marcial. There were some large gaps in available data. When data were not available for one or both of the elements under consideration, the date was excluded from the cumulative analysis.

4.1. Methods

Trends in water and suspended sediment discharge were displayed in single mass curves for each gauge. These graphs show cumulative discharge versus time and cumulative suspended sediment discharge versus time. Suspended sediment discharge versus water discharge was graphed in a double mass curve to show the trends in suspended sediment concentration for both the San Acacia and San Marcial gauges.

To develop the difference mass curve for the suspended sediment continuity analysis, the cumulative difference between the San Acacia gauge, located upstream of the study reach, and the San Marcial gauge, located downstream of the study reach, was plotted versus time. A negative slope shows that more suspended sediment is leaving the reach than entering the reach. A positive slope shows that more suspended sediment is entering the reach than leaving the reach. The contributions of arroyos along the reach were not accounted for, so more sediment may have entered the reach than was recorded by the San Acacia gauge. In addition, because both gauges are located a considerable distance from the study reach, the suspended sediment readings taken at the gauges should be an indication but are liely not completely representatibe of the true amount of suspended sediment entering and leaving the reach.

4.2. Results

4.2.1. Single Mass Curves

The single mass curve for water discharge is shown in Figure 4.1. Both the San Acacia (SA) and San Marcial (SM) gauges have similar flow trends. Both curves show breaks around 1979 and 2000. In about 1979, the discharge increased from approximately 600 cfs to over 2000 cfs. A similar increase in discharge was observed in the San Felipe, Cochiti, and Rio Puerco reaches (Bauer 2000, Novak 2006, Vensel et al. 2005). However, the increase in discharge was not as great as in the Escondida reach. At the break around the year 2000, the gauge at San Acacia decreased from 2900 cfs to 1000 cfs, and the gauge at San Marcial

decreased from 2200 cfs to 750 cfs. Table 4.1 shows the average discharge for each period displayed on the graph.

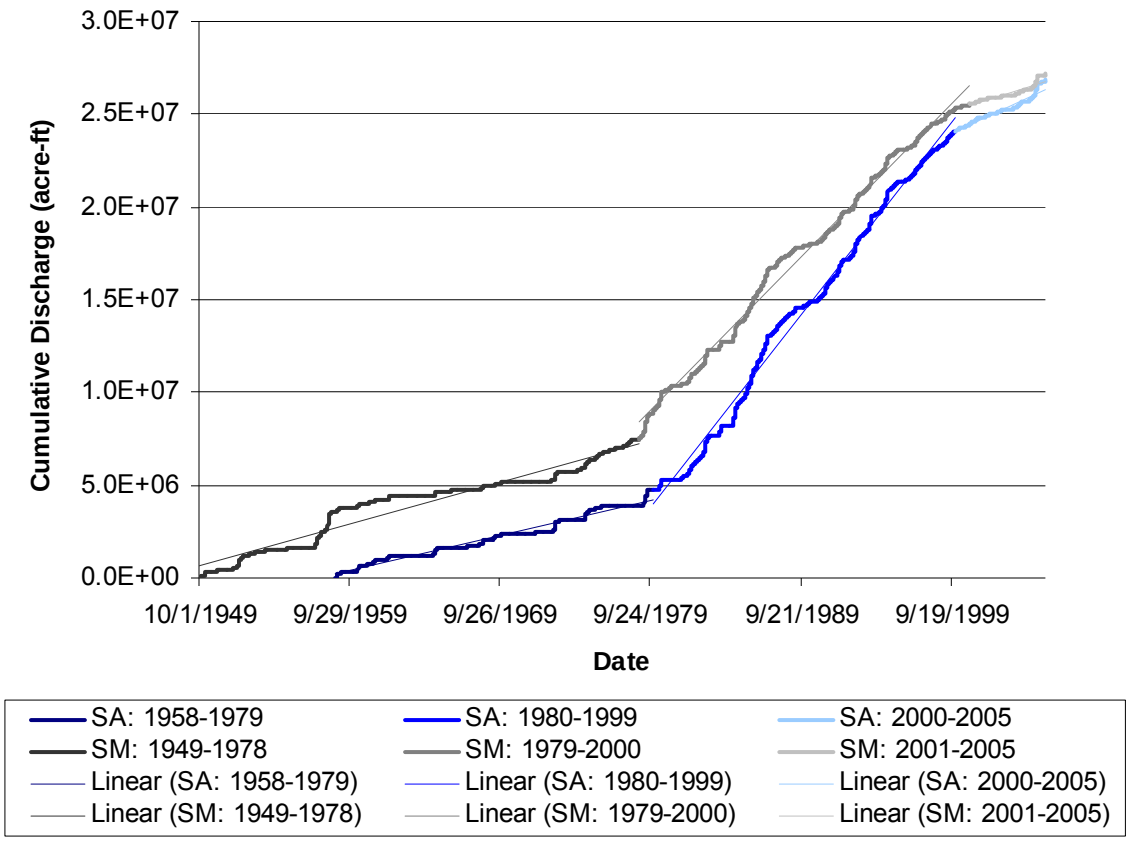

Figure 4.1 Water Discharge Single Mass Curve

Table 4.1 Water Discharge

Gauge	Years	acre-ft/day	acre-ft/year	R^2 value
San Acacia				
	1958-1979	522	190,530	0.98
	1980-1999	2856	1,042,440	0.99
	2000-2005	1055	385,075	0.93
San Marcial				
	1949-1978	621	226,665	0.94
	1979-2000	2263	825,995	0.99
	2001-2005	740	270,100	0.84

Figure 4.2 shows the single mass curve for suspended sediment discharge at the San Acacia and San Marcial gauges. The suspended sediment discharge at the two gauges does not correlate as well as the water discharge. The San Marcial gauge has a much higher suspended sediment discharge than the San Acacia gauge from 1956 until about 1968. From 1968 to 1991, the two gauges both have a suspended sediment discharge of about 10000 tons/day. From 1991 to 1996, the San Marcial gauge again shows a much higher suspended sediment discharge.

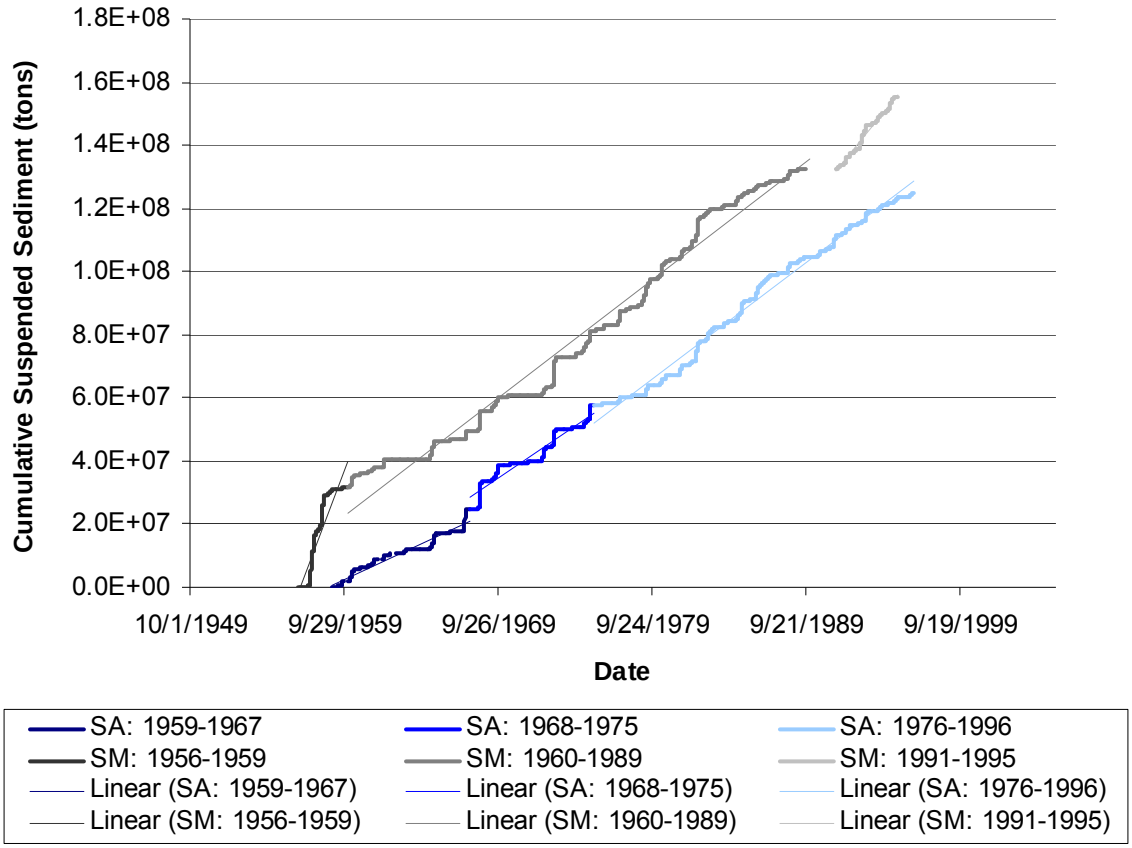

Figure 4.2 Suspended Sediment Discharge Single Mass Curve

Table 4.2 shows the average suspended sediment discharge for the periods shown on the graph. The R^2 value for each trend line is also shown.

Table 4.2 Suspended Sediment Discharge

Gauge	Years	tons/day	ton/year	R^2 value
San Acacia				
	1959-1967	6,062	2,212,630	0.94
	1968-1975	9,172	3,347,780	0.92
	1976-1996	10,066	3,674,090	0.99
San Marcial				
	1956-1959	35,276	12,875,740	0.88
	1960-1989	10,232	3,734,680	0.98
	1992-1995	16,707	6,098,055	0.98

4.2.2. Double Mass Curves

A double mass curve was developed at each gauge to show the changes in suspended sediment concentration over time. Figure 4.3 shows the two double mass curves.

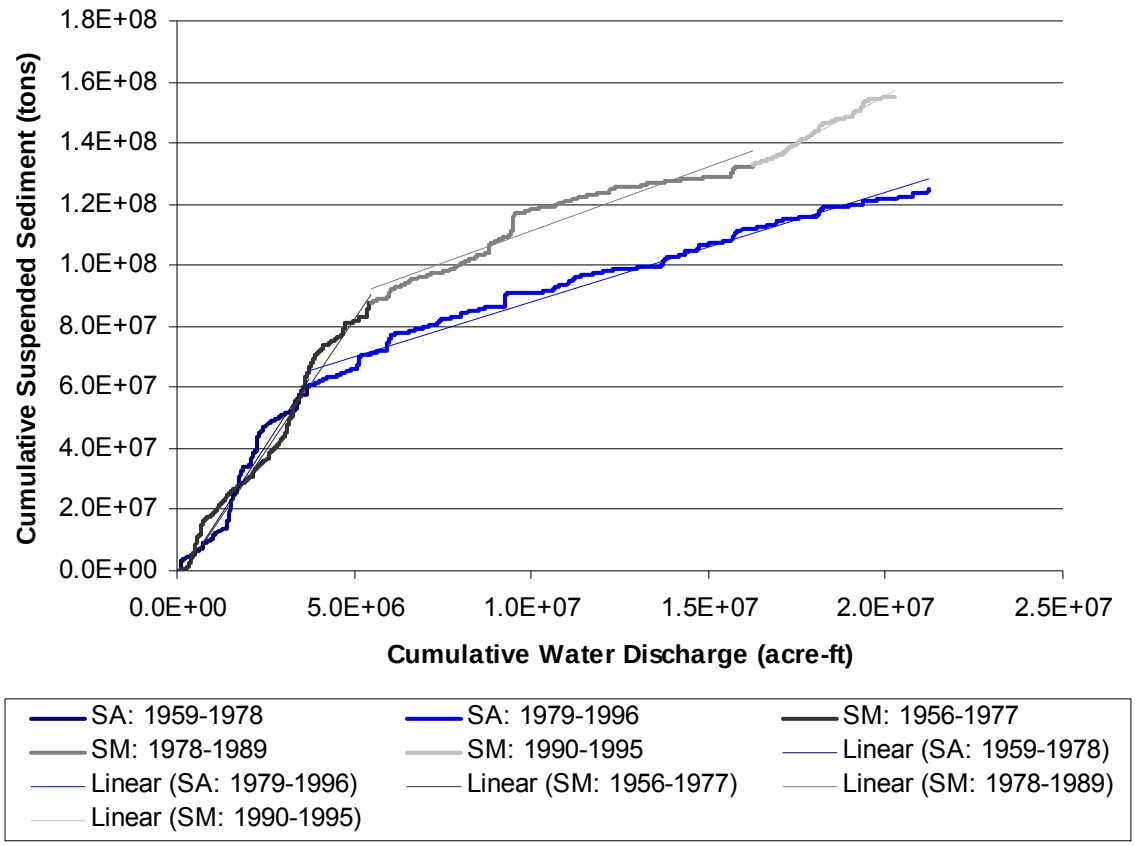

Figure 4.3 Suspended Sediment Concentration Double Mass Curve

From 1959 to 1978, the two curves are very similar, with an average suspended sediment concentration around 13,000 mg/L. Around 1978, both curves break, and the suspended sediment concentration drops to about 3000 mg/L. The concentration at the San Acacia gauge remains at about 3000 mg/L through the end of the available data. The San Marcial gauge, however, shows an increase in suspended sediment concentration from 3000 mg/L to 4500 mg/L around 1990. Table 4.3 shows the average concentration as well as the R^2 values for each segment of the graph.

Table 4.3 Suspended Sediment Concentration

Gauge	Years	tons/acre-ft	mg/L	R^2 value
San Acacia				
	1959-1978	17.9	13165	0.97
	1979-1996	3.58	2633	0.98
San Marcial				
	1956-1977	17.21	12657	0.97
	1978-1989	4.16	3060	0.92
	1990-1995	6.2	4560	0.98

4.2.3. Difference Mass Curve

The daily difference mass curves are shown in Figure 4.4. It is temporal and spatial representation of the increases and decreases in the suspended sediment volume present in the reach over time

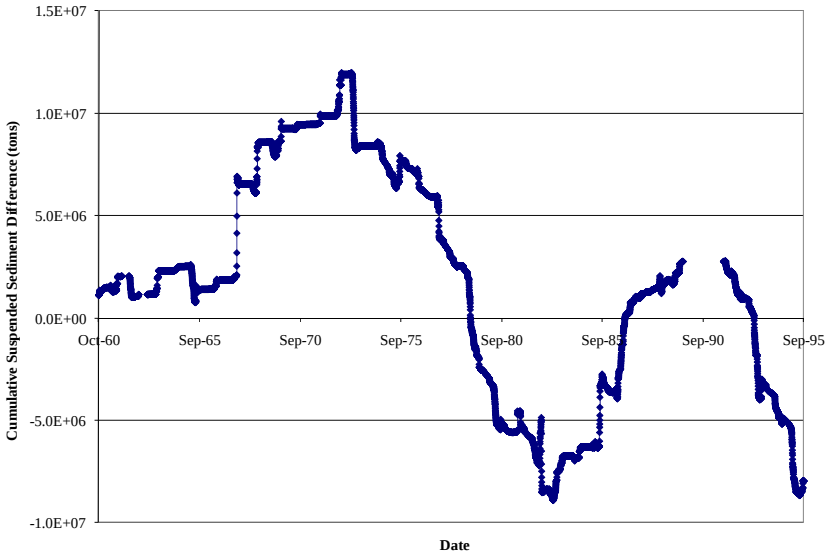

Figure 4.4 Suspended Sediment Difference Mass Curve

When more sediment is entering the reach than leaving the reach, aggradation is expected to occur because the sediment inflow that does not exit the reach must remain in the reach. Conversely, when more sediment is leaving the reach than entering, degradation of the channel is expected because the extra sediment leaving the reach is probably being eroded from the channel bed and banks. While arroyos and bank erosion could contribute some of the extra sediment, much of it is probably being mined from the bed.

The graph shows that from 1960 to 1973, more sediment was entering the reach than was leaving the reach indicating a trend toward aggradation. This trend reversed from 1973 to 1983, with more suspended sediment leaving the reach than entering the reach, indicating a trend toward degradation. The trend reversed towards aggradation from 1983 to1989, and returned to degradation from 1989 to 1995.

Based on the maximum sediment accumulation in the reach, the river should have aggraded by about 10 feet between 1960 and 1973, degraded by 6 feet between 1973 and 1983, aggraded by about less than a foot between 1983 and 1989, and finally degraded by about 7 feet between 1989 and 1995. These amounts of aggradation and degradation are much higher than the amounts of aggradation and degradation actually observed in the cross-section surveys.

The average observed values of aggradation and degradation were between 2 feet and 4 feet.

5. Floodplain Analysis

Observations by Reclamation indicate that an extended floodplain becomes active in the lower portion of the Escondida reach. The extent of the floodplain and the discharge at which the floodplain becomes inundated were investigated.

5.1. Methods

HEC-RAS was used to determine the top width at each cross-section at a series of discharges ranging from 1000 cfs to 6000 cfs. Initial observations from the HEC-RAS data showed two distinct regions of significant floodplain inundation. The average top width in each area was plotted versus discharge for each year of cross-section data to determine the discharge at which the floodplain becomes active. The floodplain becomes active when the top width becomes much greater with a small increase in discharge.

5.2. Results

The first area of interest stretches from about Agg/Deg 1406 to Agg/Deg 1418. The second area of interest stretches from about Agg/Deg 1456 to Agg/Deg 1476. Figures 5.1 and 5.2 show the top width vs. discharge for the two areas of interest and are both based on distance weighted averages.

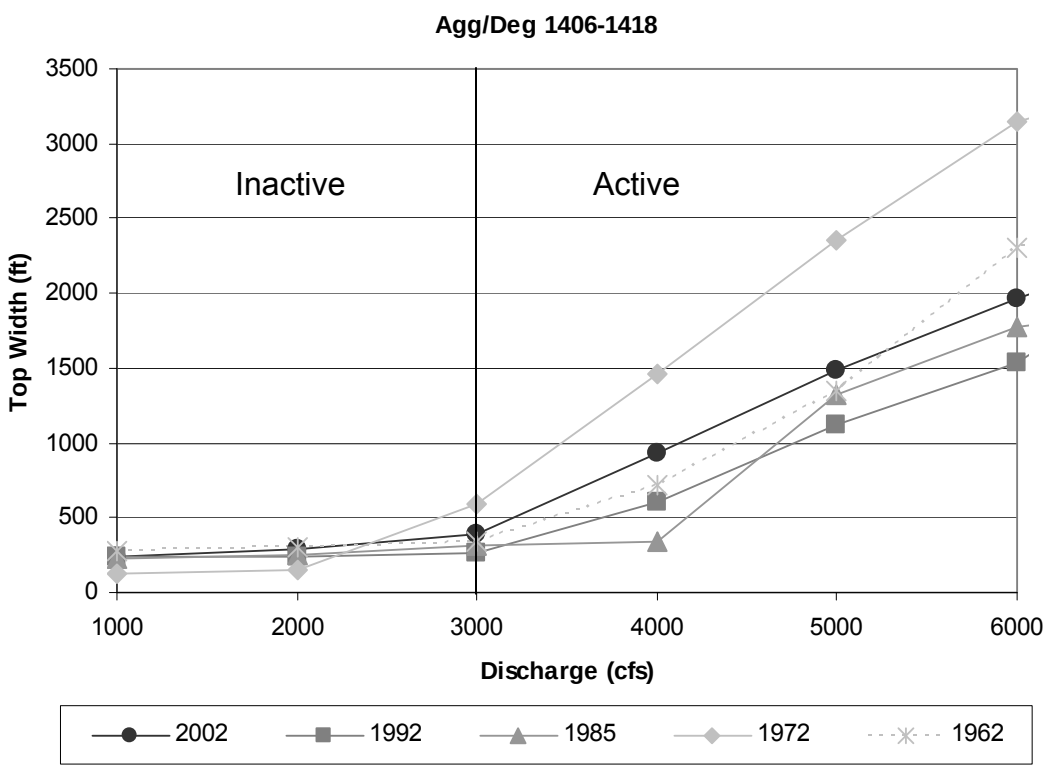

Figure 5.1 Top width vs. discharge for Agg/Deg 1406-1418

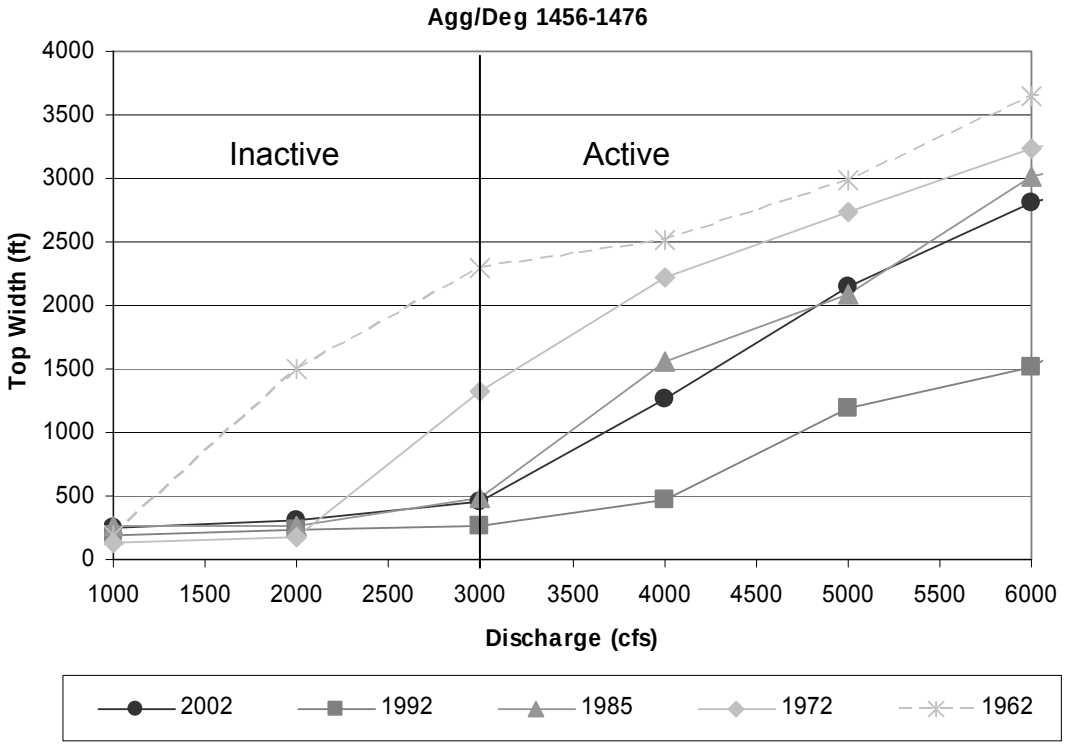

Figure 5.2 Top width vs. discharge for Agg/Deg 1456-1476

Both graphs show that the top width increases sharply around 3000 cfs, indicating that the floodplain becomes active in both areas of interest at about 3000 cfs. A discharge of 3000 cfs has a recurrence interval of less than 2 years. Based on this information, the floodplain will be inundated when the flows exceed a 2-year return period. The width increases by approximately 2 to 13 times between 3,000 cfs to 6,000 cfs.

6. Bedform Analysis

6.1. Methods

Two methods for predicting bedforms were selected for use in this analysis. The methods were developed by Simons and Richardson (from Julien 1998) and van Rijn (1984).

Simons and Richardson (from Julien 1998) performed laboratory experiments to develop a bedform prediction method based on stream power and median grain size diameter.

Stream power:

Where τ_o (lb/ft^2) is shear stress, V (ft/s) is velocity, γ (lb/ft^2) is the specific weight of water, q (ft^2/s) is unit discharge and S is channel slope. Figure 6.1 shows the region where each bedform is expected based on the observations from Simons and Richardson's experiments.

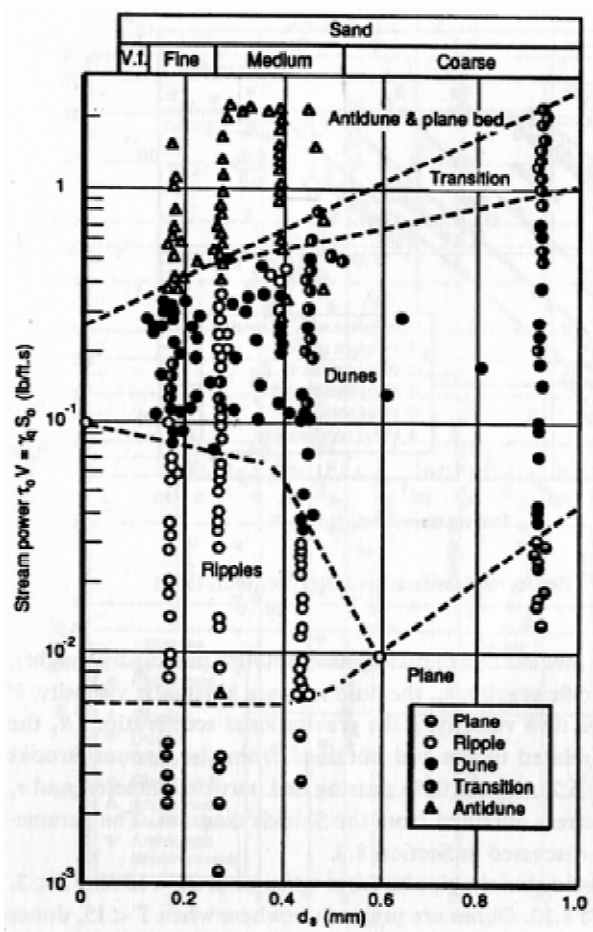

Figure 6.1 Bedform classification by Simons and Richardson (from Julien 1998)

van Rijn (1984) developed a bedform prediction method based on the dimensionless grain diameter and transport-stage parameter.

Dimensionless grain diameter: $$d_* = d_{50}\left[\frac{(G-1)g}{\nu^2}\right]^{1/3}$$

Where d_* is the dimensionless grain diameter, d_{50} (ft) is the median grain diameter, G is the specific gravity of the sediment and (lb*s/ft^2) is the kinematic viscosity of water.

Transport-stage parameter: $$T = \frac{\tau_*' - \tau_{*c}}{\tau_{*c}}$$

Where T is the transport-stage parameter, τ'_* is the grain Shield's parameter, and τ_{*c} is the critical Shield's parameter. Figure 6.2 shows the bedforms expected based on van Rijn's method.

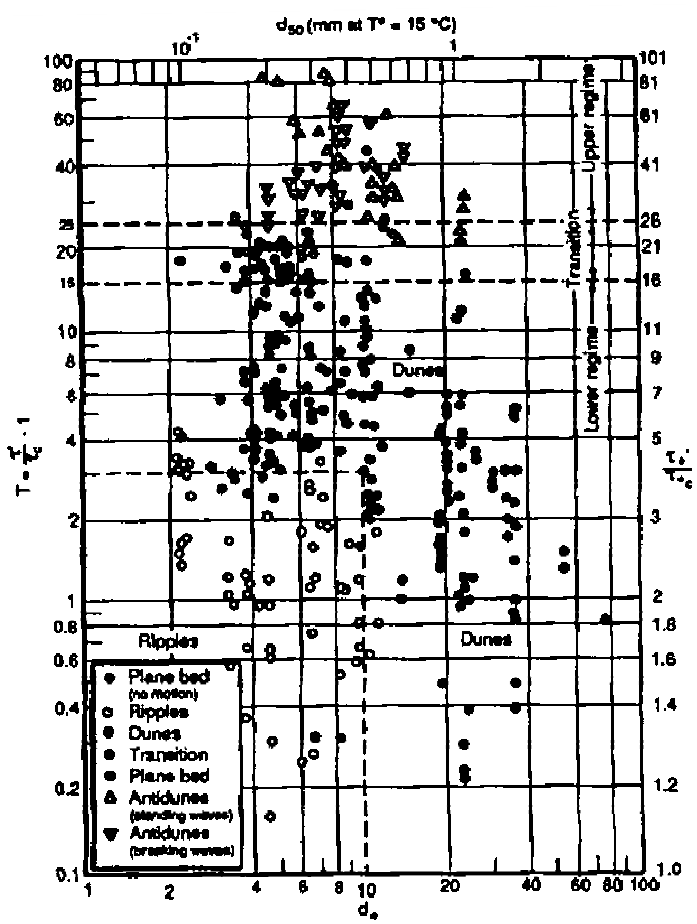

Figure 6.2 Bedform classification by van Rijn (1984, from Julien 1998)

Bedform data were collected by Reclamation at a number of SO-lines between 1990 and 1995. The dominant bedform was selected from the actual field notes as the bedform that covered the largest portion of the main flow area in a cross-section. The expected bedforms at each location were calculated using HEC-RAS, the discharge recorded at the San Acacia and San Marcial gauges on the dates the bedform data were collected, and bed material data. When possible, bed material samples taken at the same time as the bedform observations were used in the calculations. When this information was not available, bed material samples from the nearest SO-line were used. The predicted bedforms were then compared with the dominant bedform at each cross-section to determine the ability of the methods to correctly predict bedforms on the Middle Rio Grande.

6.2. Results

The bedform type observed at each location was plotted on the charts developed by Simons and Richardson and van Rijn based on the calculations performed for each method. Figures 6.3 – 6.6 show each of the four bedform types plotted on both graphs.

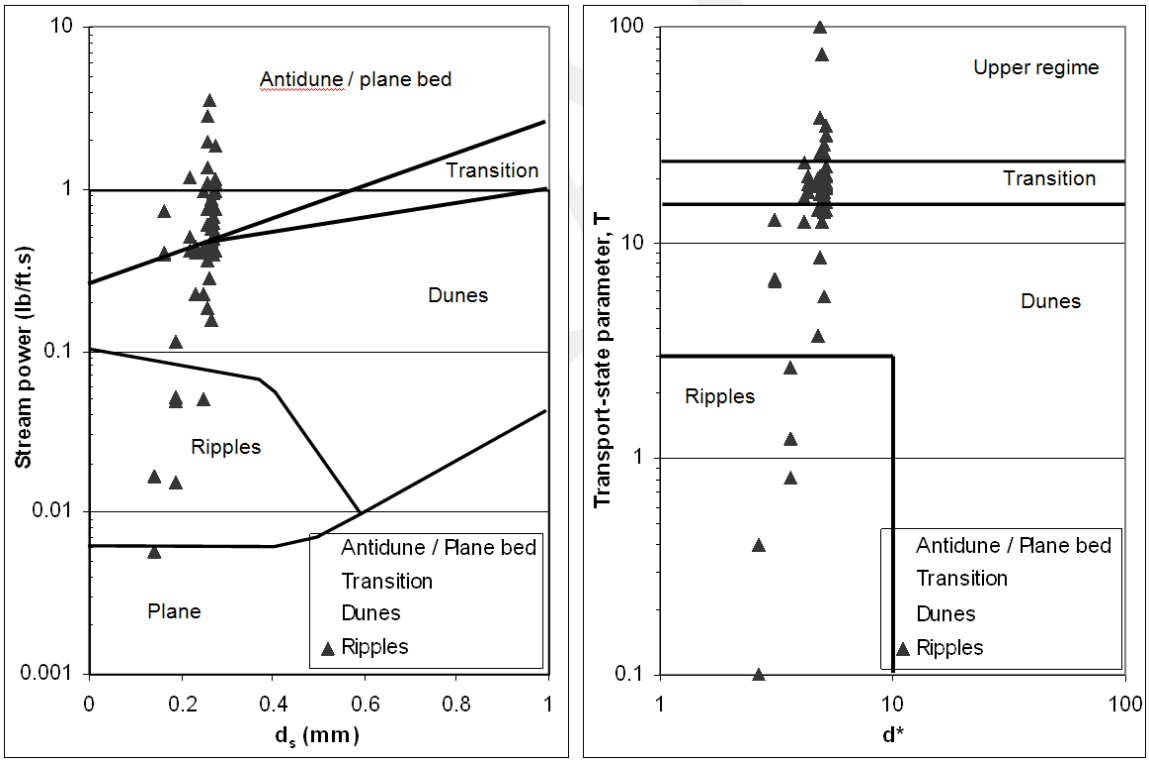

Figure 6.3 Observed ripples plotted on graphs from Simons and Richardson (L) and van Rijn (R) (after Julien 1998)

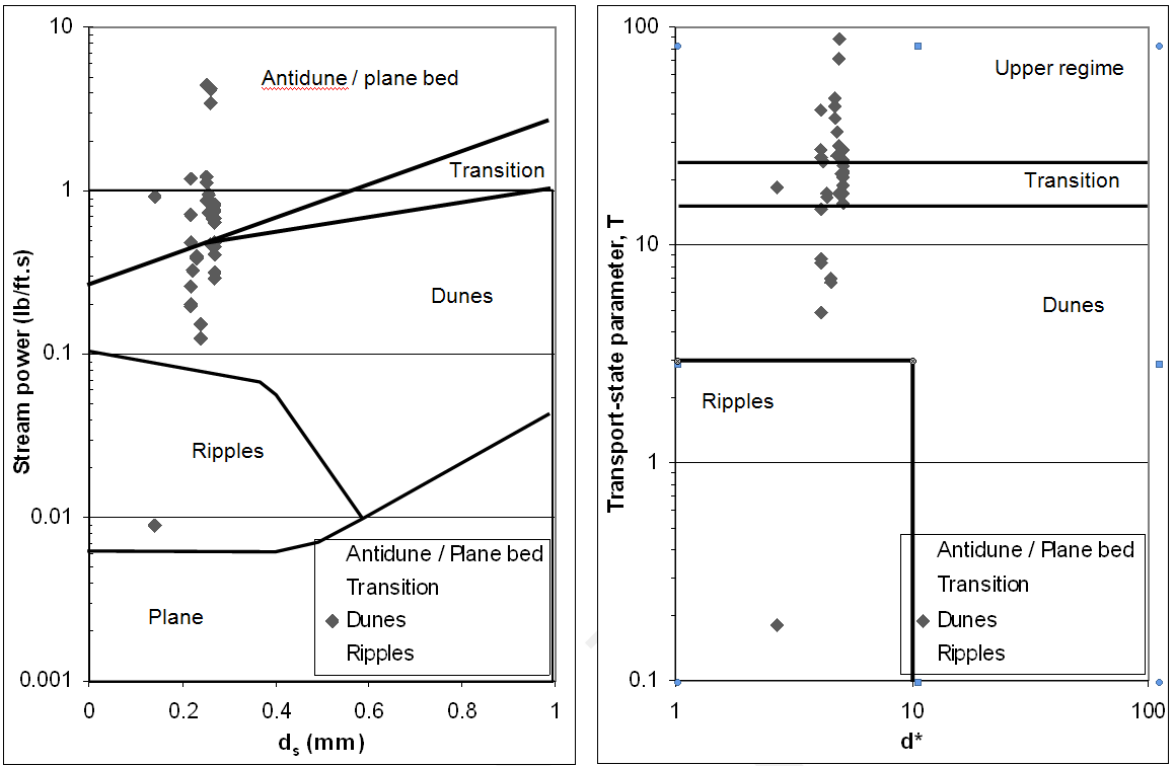

Figure 6.4 Observed dunes plotted on graph from Simons and Richardson (L) and van Rijn (R) (after Julein 1998)

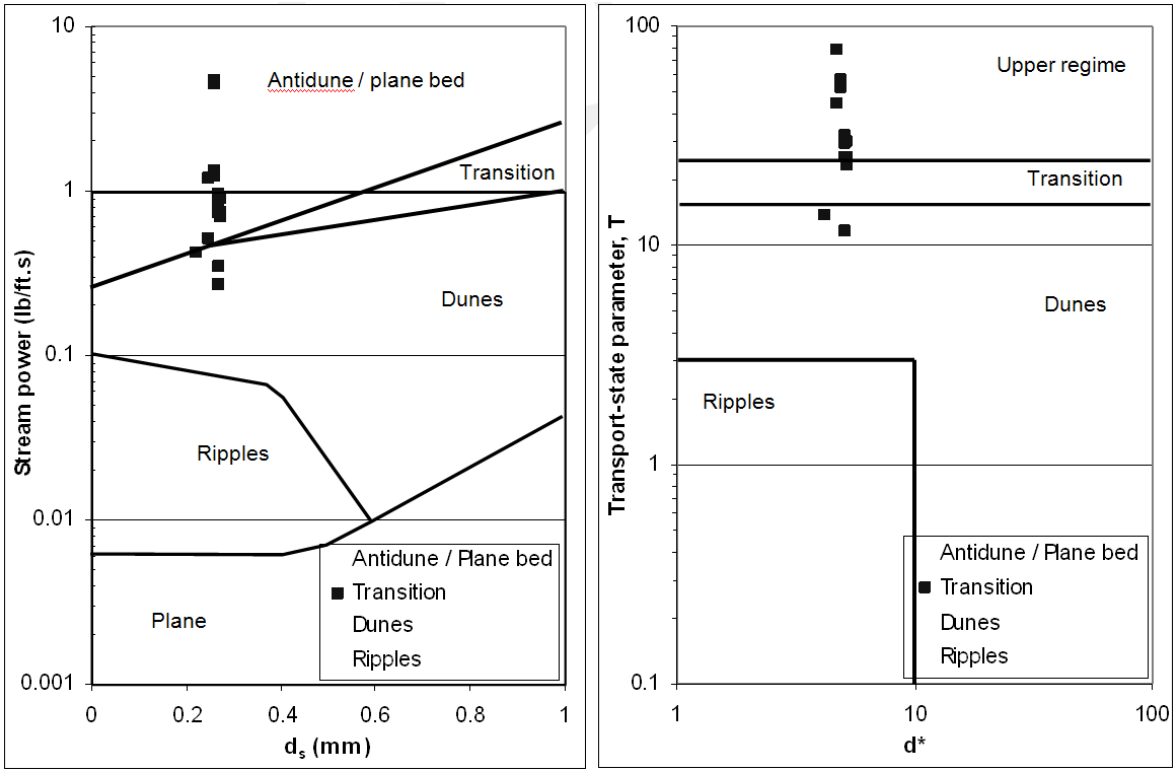

Figure 6.5 Observed transition bedforms plotted on graph from Simons and Richardson (L) and van Rijn (R) (after Julein 1998)

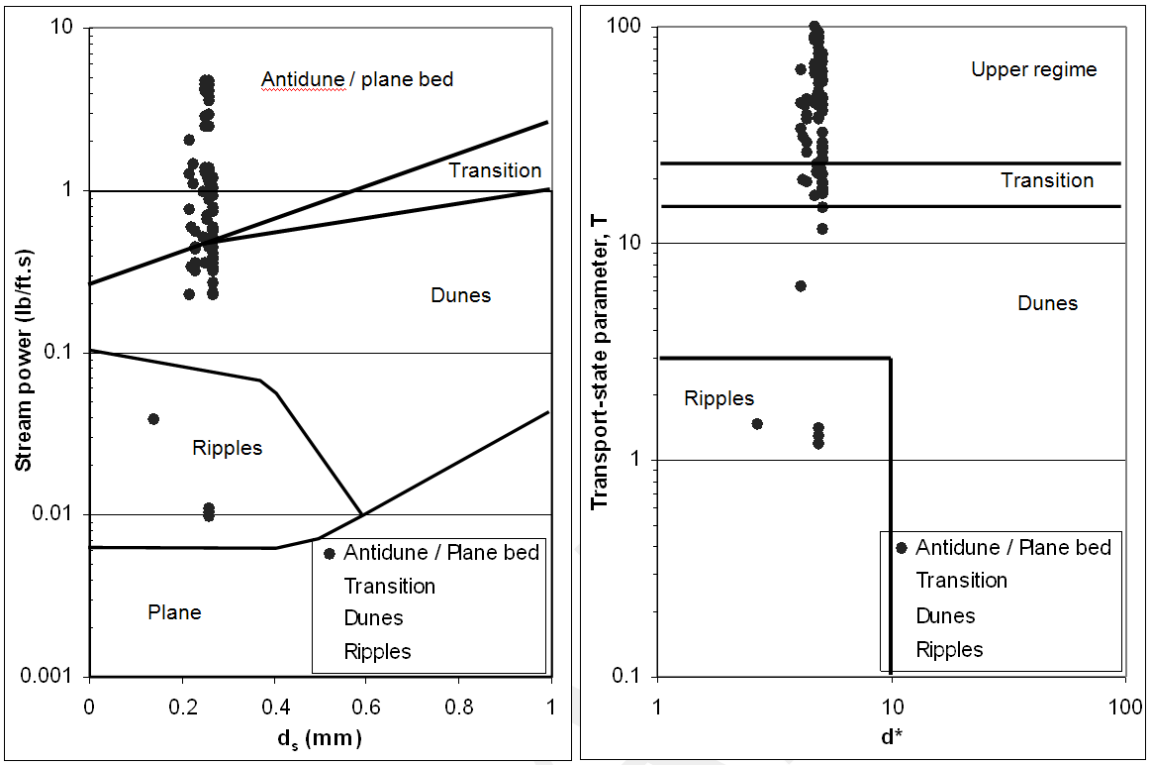

Figure 6.6 Observed antidunes/plane bed plotted on graph from Simons and Richardson (L) and van Rijn (R) (after Julien 1998)

Figures 6.3 – 6.6 show that the predicted bedforms match reasonably well with the predicted bedforms, but the plots show wide scatter. Antidunes were the most reliably predicted bedforms, while lower regime bedforms such as ripples and dunes were difficult to predict correctly. This can be attributed to the fact that observations are subjective, and the difficulty in predicting bedforms can be associated with not having reliable methods for field observations of bedforms.

A likely explanation for the discrepancy between the predicted and observed bedforms is the high variability in important parameters such as flow depth, slope and velocity across a cross-section. There was spatial variability can cause several different bedforms to exist in a single cross-section, which is observed in the field. The prediction methods are unable to account for the variability within the cross-section because they are based on cross-section average properties.

Figure 6.7 shows a typical cross-section with the bedform observations indicated on the cross-section. See Appendix E for the field notes for this cross-section. The width/depth ratio for this cross-section is about 400. This is typical of the Escondida reach and further explains the high variability in the cross-sections. The discharge at this cross-section was about 4400 cfs on the day of the survey. Simons and Richardson predicted antidunes and van Rijn predicted upper regime bedforms for this location. While upper regime bedforms were observed at the cross-section, lower regime bedforms were also observed. Both the upper

and lower regime bedforms were present in the main flow area of the channel and both occupied similar portions of the cross-section. Additional example cross-sections can be found in Appendix E.

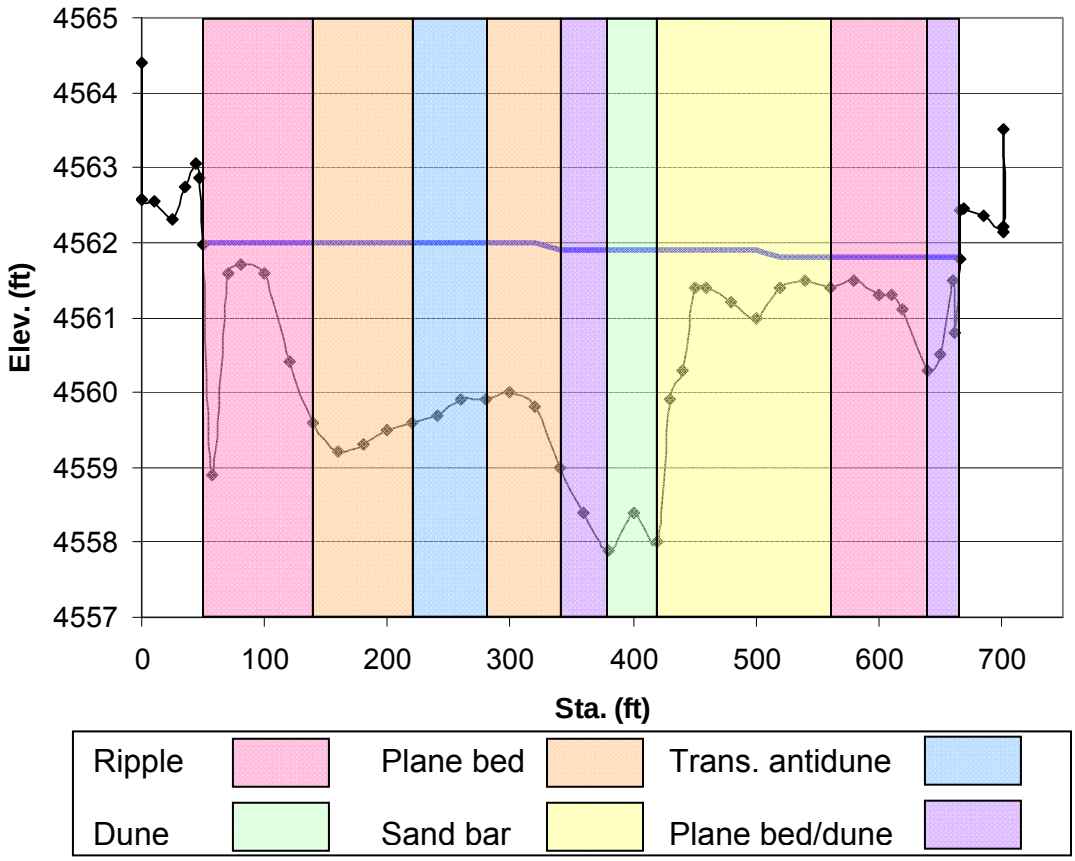

Figure 6.7 Typical cross-section with bedforms

7. Equilibrium State Predictors

7.1. Hydraulic Geometry

7.1.1. Methods

Several hydraulic geometry equations were used to determine the equilibrium channel width. These methods use channel characteristics such as channel width and slope, sediment concentration, and discharge. All of the equilibrium width equations were developed in simplified conditions such as man-made channels.

Julien and Wargadalam (1995) used the concepts of resistance, sediment transport, continuity, and secondary flow to develop semi-theoretical hydraulic geometry equations.

$$h = 0.2Q^{2/(5+6m)} d_s^{6m/(5+6m)} S^{-1/(5+6m)}$$
$$W = 1.33Q^{(2+4m)/(5+6m)} d_s^{-4m/(5+6m)} S^{-(1+2m)/(5+6m)}$$
$$V = 3.76Q^{(1+2m)/(5+6m)} d_s^{-2m(5+6m)} S^{(2+2m)/(5+6m)}$$
$$\tau^* = 0.121Q^{2/(5+6m)} d_s^{-5/(5+6m)} S^{(4+6m)/(5+6m)}$$
$$m = \frac{1}{\ln(\frac{12.2h}{d_{50}})}$$

Were h is the average depth, W (m) is the average width, V (m/s) is the average one-dimensional velocity, and τ^* is the Shield's parameter, and d_{50} (m) is the median grain size diameter.

Simons and Alberston (1963) used five sets of data from canals in India and America to develop equations to determine equilibrium channel width. Simons and Bender collected data from irrigation canals in Wyoming, Colorado and Nebraska. These canals had both cohesive and non cohesive bank material. Data were collected on the Punjab and Sind canals in India. The average bed material diameter found in the Indian canals varied from 0.43 mm in the Punjab canals to between 0.0346 mm and 0.1642 mm in the Sind canals. The USBR data was collected in the San Luis Valley in Colorado and consisted of coarse non-cohesive material. The final data set was collected in the Imperial Valley canal system, which have conditions similar to those seen in the Indian canals and the Simons and Bender canals (Simons and Albertson 1963).

Two figures were developed by Simons and Albertson to obtain the equilibrium width. Figures 7.1 and 7.2 show the relationships between wetted perimeter and discharge and average width and wetted perimeter, respectively.

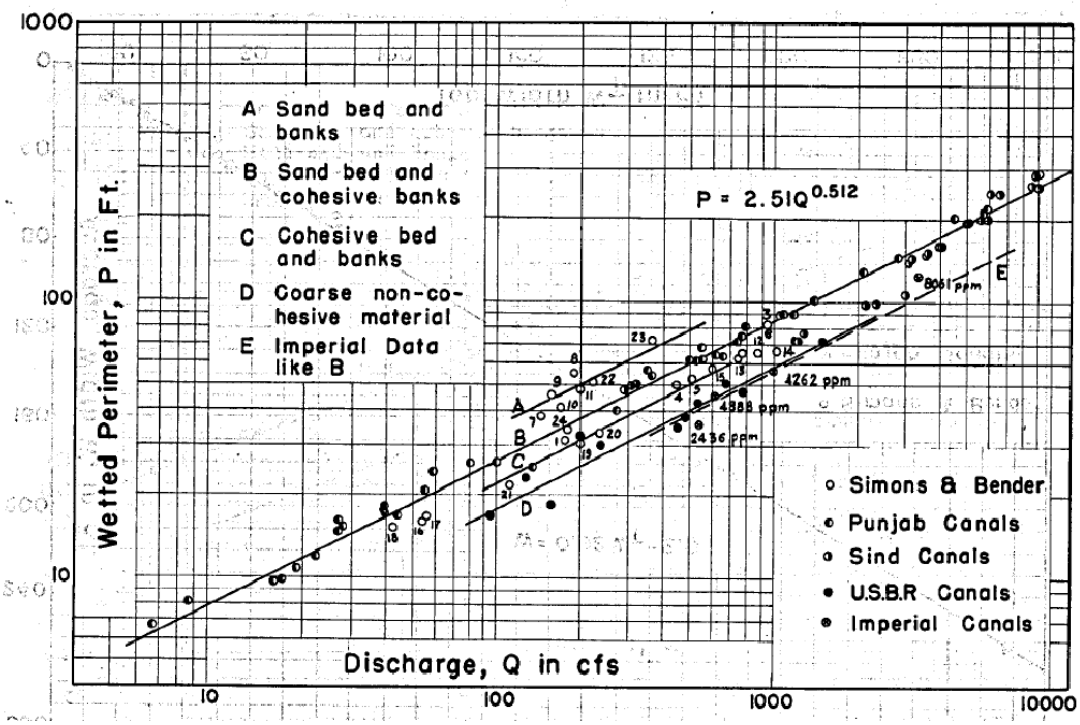

Figure 7.1 Variation of wetted perimeter P with discharge Q and type of channel (after Simons and Albertson 1963)

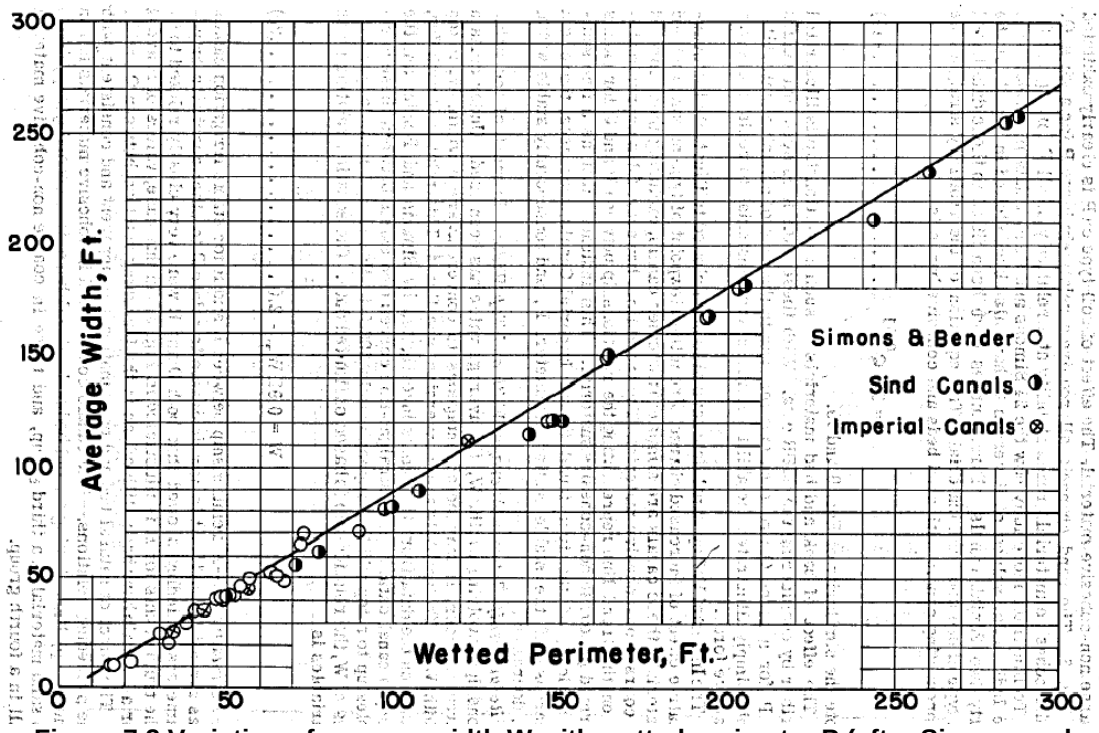

Figure 7.2 Variation of average width W with wetted perimeter P (after Simons and Albertson 1963)

Blench (1957) used flume data to develop regime equations. A bed and a side factor (F_s) were developed to account for differences in bed and bank material.

$$W = \left(\frac{9.6(1+0.012c)}{F_s} \right)^{1/2} d^{1/4} Q^{1/2}$$

Where W (ft) is channel width, c (ppm) is the sediment load concentration, d (mm) is the median grain diameter, and Q (cfs) is the discharge. The side factor, F_s = 0.1 for slight bank cohesiveness.

Lacey (from Wargadalam 1993) developed a power relationship for determining wetted perimeter based on discharge.

$$P = 2.667Q^{0.5}$$

Where P (ft) is wetted perimeter and Q (cfs) is discharge. For wide, shallow channels, the wetted perimeter is approximately equal to the width.

Klaassen-Vermeer (1988) used data from the Jamuna River in Bangladesh to develop a width relationship for braided rivers.

$$W = 16.1Q^{0.53}$$

Where W (m) is width, and Q (m^3/s) is discharge.

Nouh (1988) developed regime equations based on data collected in extremely arid regions of south and southwest Saudi Arabia.

$$W = 2.83\left(\frac{Q_{50}}{Q} \right)^{0.83} + 0.018(1+d)^{0.93} c^{1.25}$$

Where W (m) is channel width, Q_{50} (m^3/s) is the peak discharge for a 50 year return period, Q (m^3/s) is annual mean discharge, d (mm) is mean grain diameter, and c (kg/m^3) is mean suspended sediment concentration.

Table 7.1 shows the input values used to estimate channel width from the hydraulic geometry equations. The peak discharges for a 50-year return period were taken from Bullard and Lane (1993). The average sediment concentrations were obtained from the double mass curves (see Figure 4.3) developed for the San Acacia and San Marcial gauges. Suspended sediment data was only available until 1995, so all suspended sediment concentrations after 1995 were extrapolated from the double mass curves.

Table 7.1 Hydraulic geometry calculation inputs

	Q (cfs)	Q_{50} (cfs)	d_{50} (mm)	Channel Slope (ft/ft)	Sediment Concentration Avg C (ppm)
1962					
1	5000	28050	0.15	0.0009	13058
2	5000	28050	0.15	0.0008	12808
3	5000	28050	0.15	0.0005	12558
Total	5000	28050	0.15	0.0008	12808
1972					
1	5000	19800	0.11	0.0009	13058
2	5000	19800	0.11	0.0008	12808
3	5000	19800	0.11	0.0007	12558
Total	5000	19800	0.11	0.0008	12808
1985					
1	5000	19800	0.15	0.0008	2629
2	5000	19800	0.13	0.0009	2841
3	5000	19800	0.10	0.0005	3054
Total	5000	19800	0.13	0.0008	2841
1992					
1	5000	19800	0.22	0.0008	2629
2	5000	19800	0.27	0.0008	3588
3	5000	19800	0.25	0.0007	4547
Total	5000	19800	0.23	0.0008	3588
2002					
1	5000	19800	0.37	0.0008	2629
2	5000	19800	0.30	0.0008	3588
3	5000	19800	0.24	0.0008	4547
Total	5000	19800	0.31	0.0008	3588

An empirical width relationship was developed for the Escondida reach based on active channel widths determined from GIS channel planforms and peak flows for the 5 years prior to the survey date (Knighton 1998). Knighton (1998) suggests that it is the high magnitude, low frequency floods that may control the channel form in arid-zone rivers where the flow regime is very variable. For the hydraulic geometry equations, the peak discharge from the 5 years prior to the survey was used. Peak flows for the relationship were obtained from the gages located the San Acacia and San Marcial gauges. The resulting power relationship takes the form:

$$W = aQ^b$$

Where W (ft) is channel width and Q (cfs) is peak discharge. Table 6.2 shows the input values used to develop the empirical width relationship for the Escondida reach.

Table 7.2 Escondida empirical width-discharge inputs

Year	Average 5-year peak discharge (cfs)	GIS widths (ft)			
		Subreach 1	Subreach 2	Subreach 3	Overall
1962	3676	919	415	209	548
1972	2644	619	274	178	376
1985	6321	671	645	302	609
1992	4638	353	529	298	442
2001	2937	362	569	299	468
2002	2344	334	436	265	381
2005	3312	366	498	305	431

7.1.2. Results

The equilibrium channel widths predicted by the hydraulic geometry equations are shown in Table 7.3. All methods except Blench tend to under predict the channel width determined from HEC-RAS runs at 5000 cfs. Blench tends to over predict the channel widths determined from HEC-RAS, but shows the best overall agreement of the methods used to estimate the equilibrium channel width. This does not necessarily mean that Blench is the best predictor of equilibrium width because the channel was likely not in equilibrium between 1962 and 2002. Four methods, Simons and Albertson, Nouh, Lacey, and Julien-Wargadalam, predict similar equilibrium channel widths ranging from about 200 feet to about 300 feet. These methods may be a better indication of the expected equilibrium channel width because of their similar results. The channel is tending toward the narrower width predicted by the four methods discussed, but it is still much wider than the predicted equilibrium.

Table 7.3 Predicted equilibrium widths from hydraulic geometry equations

	Reach-Averaged HEC-RAS Main Channel Width (feet)	Predicted Width (ft)					
		Simons and Albertson	Klassen & Vermeer	Nouh	Blench	Lacey	Julien - Wargadalam
1962							
1	1417	274	729	390	2425	189	268
2	774	274	729	390	2402	189	277
3	3234	274	729	390	2378	189	298
Total	1291	274	729	390	2402	189	276
1972							
1	1416	274	729	293	2228	189	271
2	1296	274	729	293	2207	189	277
3	3158	274	729	293	2185	189	284
Total	1572	274	729	293	2207	189	275
1985							
1	1417	274	729	291	1102	189	273
2	774	274	729	291	1091	189	272
3	3239	274	729	291	1064	189	303
Total	1295	274	729	291	1102	189	275
1992							
1	468	274	729	291	1205	189	279
2	881	274	729	291	1474	189	275
3	1287	274	729	291	1629	189	281
Total	796	274	729	291	1427	189	277
2002							
1	505	274	729	291	1377	189	277
2	1024	274	729	291	1519	189	278
3	2000	274	729	291	1607	189	278
Total	982	274	729	291	1537	189	277

Julien-Wargadalam was also used to predict the equilibrium slope of the channel. Table 7.4 shows the predicted equilibrium slope and the observed channel slope for each subreach and the total reach between 1962 and 2002.

Table 7.4 Equilibrium slope predictions with Q = 5000 cfs

		1962	1972	1985	1992	2002
Observed Slope	1	0.00094	0.00089	0.00084	0.00076	0.00078
	2	0.00078	0.00080	0.00087	0.00081	0.00077
	3	0.00055	0.00070	0.00051	0.00072	0.00076
	Total	0.00080	0.00082	0.00081	0.00078	0.00077
Equilibrium Slope	1	0.00055	0.00036	0.00052	0.00075	0.00139
	2	0.00051	0.00035	0.00042	0.00098	0.00113
	3	0.00048	0.00033	0.00031	0.00089	0.00083
	Total	0.00051	0.00034	0.00044	0.00083	0.00117

The results of the equilibrium slope calculations indicate that the channel had a steeper slope than the predicted slope in 1962, 1972 and 1985. In 1992, however, the observed channel slope closely matches the predicted equilibrium slope. In 2002, the early trend is reversed with the predicted channel slope being steeper than the observed channel slope.

Figure 7.3 shows the plot and regressions used to find the empirical equations for the reach. The non-vegetated active channel width were measured using the GIS planforms (Section 3) and plotted against the 5-year average peak flow. Regressions were then developed for each subreach and the total reach. 1962 was the first year used in the regression because including data prior to 1962 would have resulted in regressions that predicted decreasing width with increasing discharge.

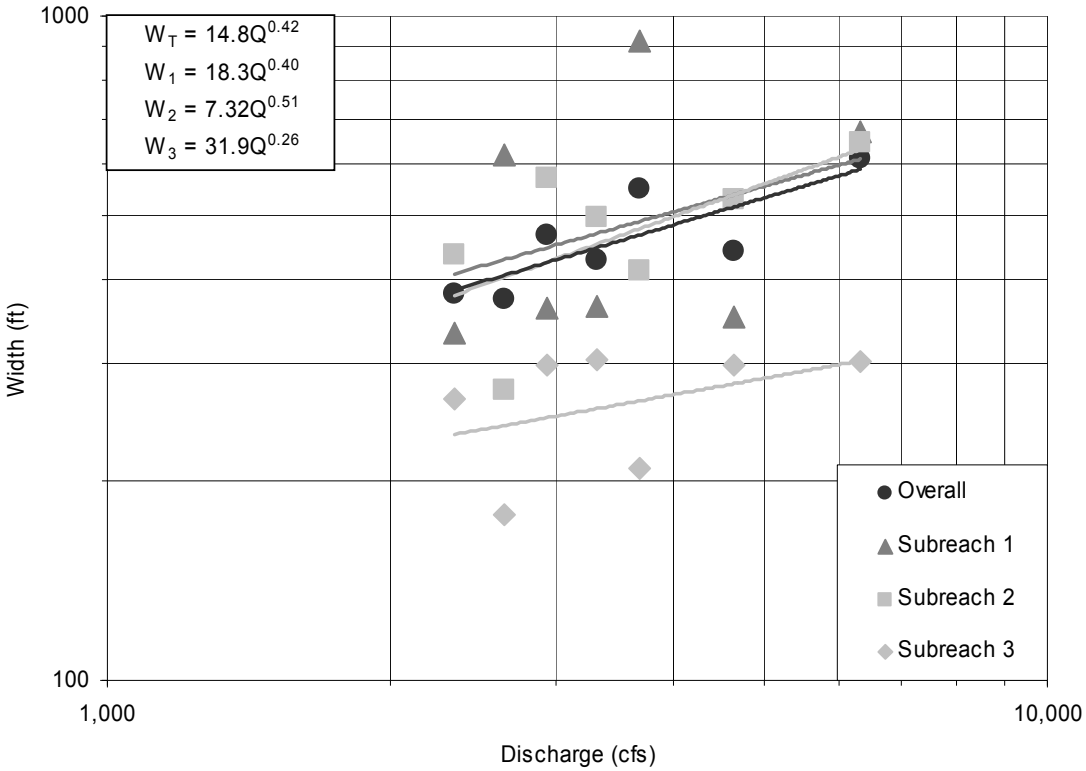

Figure 7.3 Escondida empirical width-discharge relationships

The results of the equilibrium width calculations performed using the empirical equation developed for the Escondida reach are shown in Table 7.5 along with the non-vegetated active channel widths.

Table 7.5 Escondida empirical width-discharge results

		1962	1972	1985	1992	2001	2002	2005
	Average 5-year peak discharge (cfs)	3676	2644	6321	4638	2937	2344	3312
GIS Width (ft)	1	919	619	671	353	362	334	366
	2	415	274	645	529	569	436	498
	3	209	178	302	298	299	265	305
	Total	548	376	609	442	468	381	431
Predicted Width (ft)	1	490	430	609	538	448	409	470
	2	478	404	630	538	426	380	453
	3	263	242	303	279	248	234	256
	Total	468	407	587	516	426	387	448

The predicted widths closely match the measured widths in all subreaches and in all years. The empirical equations may be good indicators of the actual expected width at a given discharge because they are based on the historical conditions rather than an ideal, equilibrium state. These equations, however, may not be reliable in predicting the equilibrium width of the channel.

7.2. Width Regression Model

7.2.1. Methods

<u>Hyperbolic Model</u>

The downstream effects of dams on alluvial rivers were studied by Williams and Wolman (1984). They found a hyperbolic equation to describe the changes in channel width with time.

$$\frac{1}{Y} = C_1 + C_2 \frac{1}{t}$$

Where C_1 and C_2 are empirical coefficients, t is the time in years after the initial change in the channel, and Y is the relative change in channel width and is equal to the ratio of the initial width (W_i) to the wide at time t (W_t). The coefficients may be a function of channel characteristics such as discharge and boundary material.

A hyperbolic equation was fit to the data from the each subreach. The initial time (t =0) was assumed to be the first year a narrowing trend was observed in the channel. The initial year was different in each subreach and in the total reach. To adjust the equations to an origin of 0, 1.0 was subtracted from the relative width ratio (W_t/W_i) before the regression was fit to the data. The constants C_1

and C_2 were determined by setting the R^2 of the regression as close to one as possible.

Exponential Model

Richard et al. (2005) developed prediction equations for active channel width, total channel width, migration rate and lateral mobility based on data collected in the Cochiti reach of the Middle Rio Grande and verified by data from four rivers including the Jemez river, the Arkansas river, Wolf creek and the North Canadian river. An exponential regression equation was developed to describe channel width as a function of time.

$$W(t) = W_e + (W_i - W_e)e^{-kt}$$

Where W_e is the equilibrium width, W_i is the channel width at the initial time, k is the rate of decay, and t is time after the initial time.

The exponential equation was fit to the GIS active channel width beginning in the first year showing a trend toward decreasing width. The decay constant k, and the equilibrium width, W_e, were determined by setting the R^2 of the exponential regression equation as close to one as possible. Table 7.6 shows the input information for the hyperbolic and exponential regression equations.

Table 7.6 Hyperbolic and exponential regression input

Subreach 1		
Year	t (year)	W(t) (ft)
1949	0	1591
1962	13	919
1972	23	619
1985	36	671
1992	43	353
2001	52	362
2002	53	334
2005	56	366

Subreach 2		
Year	t (year)	W(t) (ft)
1985	0	645
1992	7	529
2001	16	569
2002	17	436
2005	20	498

Subreach 3		
Year	t (year)	W(t) (ft)
1985	0	302
1992	7	298
2001	16	299
2002	17	265
2005	20	305

Total		
Year	t (year)	W(t) (ft)
1949	0	1081
1962	13	548
1972	23	376
1985	36	609
1992	43	442
2001	52	468
2002	53	381
2005	56	431

7.2.2. Results

Four hyperbolic and four exponential equations were developed for the Escondida reach. Figures 7.4 – 7.7 show the regression curves for each subreach and the total reach. All of the graphs start in the initial year and continue through 2020.

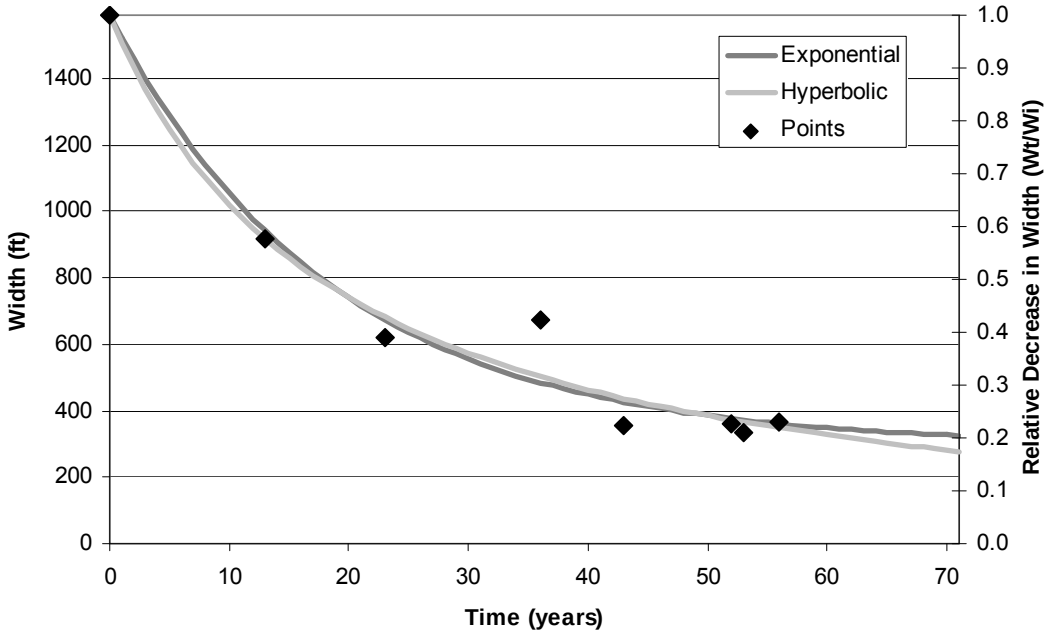

Figure 7.4 Hyperbolic and exponential regressions – subreach 1

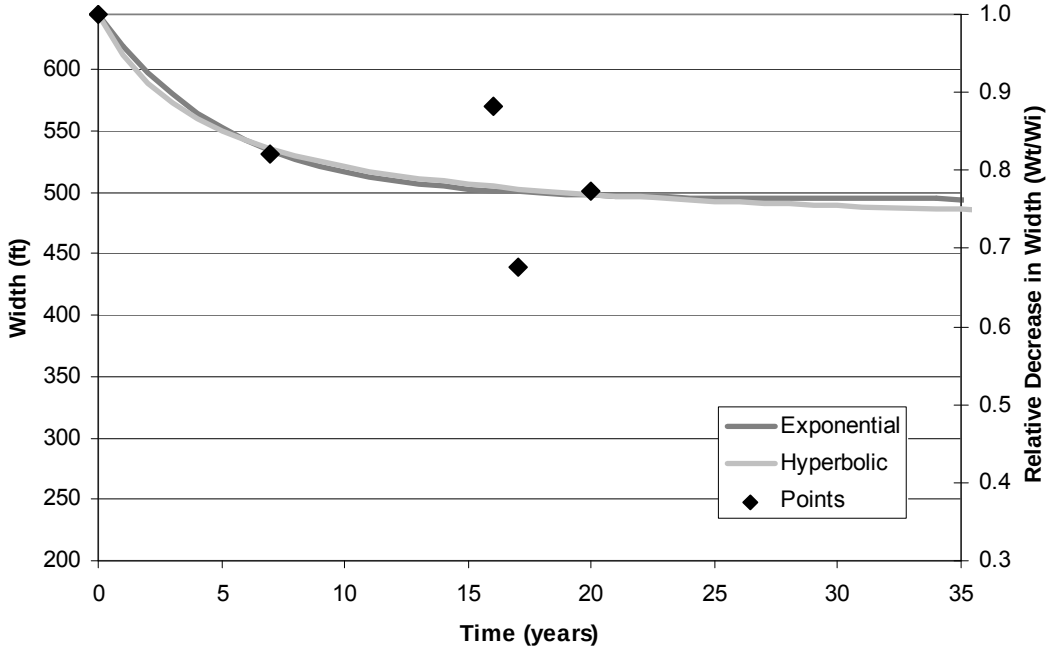

Figure 7.5 Hyperbolic and exponential regressions – subreach 2

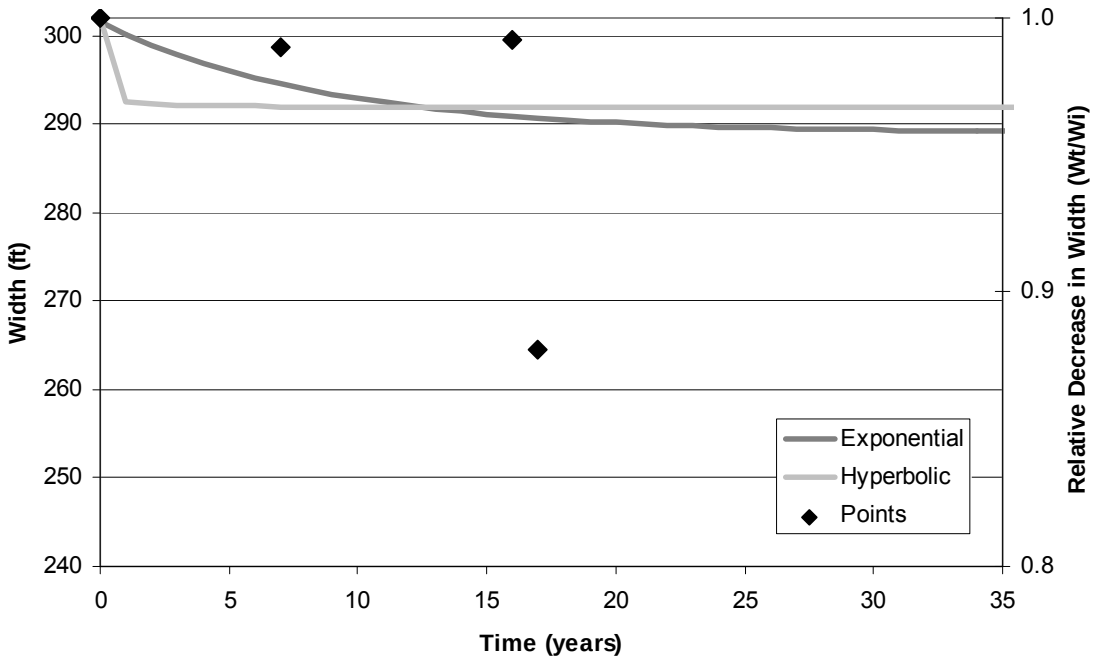

Figure 7.6 Hyperbolic and exponential regressions – subreach 3

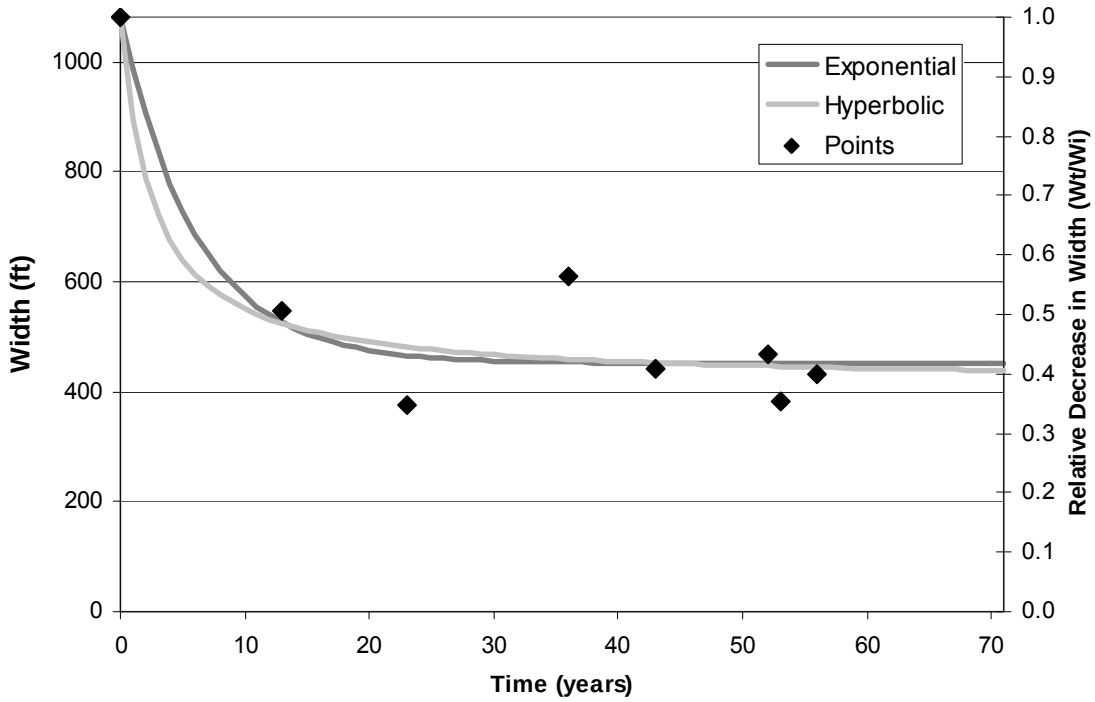

Figure 7.7 Hyperbolic and exponential regressions – total reach

As shown in Figures 7.4 – 7.7, the hyperbolic and exponential regression equations produce very similar results. Overall, the exponential regression seems to produce a smoother regression curves.

Table 7.7 shows the hyperbolic regressions for each subreach, along with the predicted width in 2020 and the predicted equilibrium width. The widths predicted in 2020 are reasonable for all reaches and, in most cases, are near the predicted equilibrium width. In subreach 1, the equilibrium width is negative. This indicates that this equation is not a reliable predictor of the ultimate equilibrium width of the channel, but it seems to be a reasonable predictor of the 2020 width. Additional data should be added to the regression equation for subreach 1 as they become available to better refine the equation for long-term predictions.

Table 7.7 Hyperbolic regression equations and predicted widths

Subreach	R^2	Regression Equation	W_{2020} (ft)	W_e (ft)
1	1.00	$\frac{W_t}{W_i} = \frac{t}{-0.95t - 18.34} + 1$	277	-79
2	1.00	$\frac{W_t}{W_i} = \frac{t}{-3.55t - 15.81} + 1$	484	463
3	1.00	$\frac{W_t}{W_i} = \frac{t}{-30.64t - 2.33} + 1$	292	292
Total	1.00	$\frac{W_t}{W_i} = \frac{t}{-1.62t - 4.13} + 1$	439	416

Table 7.8 shows the exponential regression equations and predicted equilibrium widths. All of the equations are able to produce reasonable equilibrium widths. The equilibrium widths predicted by the exponential regression are nearly identical to the equilibrium widths predicted by the hyperbolic regression, indicating that these methods may produce good predictions of the equilibrium channel width.

Table 7.8 Exponential regression equations and predicted widths

Subreach	R^2	Regression Equations	W_e (ft)
1	0.97	$W(t) = 296 + 1295e^{-0.045t}$	296
2	0.64	$W(t) = 494 + 151e^{-0.189t}$	494
3	0.10	$W(t) = 289 + 13e^{-0.117t}$	289
Total	0.90	$W(t) = 452 + 629e^{-0.164t}$	452

7.3. Sediment Transport

7.3.1. Methods

The equilibrium slope of the channel was estimated using sediment transport equations. Equilibrium is achieved when the incoming suspended sediment matches the sediment capacity of the reach. When supply and capacity are equal, the channel should not aggrade or degrade and a relatively constant slope should be maintained during lateral migration processes. The incoming sediment supply for each subreach was estimated using the Bureau of Reclamation Automated Modified Einstein Procedure (BORAMEP) and Psands programs. The channel slope was then varied in HEC-RAS until the calculated sediment transport capacity was within 20% of the incoming sediment supply.

The incoming sediment supply for subreach 1 was estimated using the BORAMEP). Suspended sediment and bed material gradations we obtained from the San Acacia gauge between 1990 and 2004. In addition, channel geometry, flow conditions, and suspended sediment concentration were also obtained at the San Acacia gauge for the dates of the suspended sediment and bed material samples. The input and output from BORAMEP can be found in the Appendix E. The total sand-sized sediment load calculated by BORAMEP was plotted vs. discharge. A power-law formula was fit to the data to obtain a regression used for estimating the incoming sediment load in subreach 1.

Psands was used to estimate the incoming sand-size sediment load for subreaches 2 and 3. The sediment load was calculated by Reclamation using Pasands for data collected at SO-lines between 1987 and 1996. A power-law formula was fit to a plot of sediment load vs. discharge to obtain an estimate of the incoming sand-sized sediment load.

HEC-RAS calculates sediment transport capacity using several different methods including those developed by, Ackers & White, Engelund & Hansen, Laursen, Meyer-Peter & Muller, Toffaleti, and Yang (sand). All methods except Meyer-Peter & Muller provide estimates of total load. Meyer-Peter & Muller estimates bed load only. For a complete listing of the limits of application for these methods as provided by HEC-RAS, see Appendix G.

The total load estimates from BORAMEP and Psands were compared directly with the HEC-RAS total load calculations for the five applicable methods. In 1992 geometry data was used for the HEC-RAS runs because the sediment data used in both BORAMEP and Psands was obtained around 1992. Estimating the incoming bed load for each reach was necessary before making comparisons with the Meyer-Peter & Muller bed load. The suspended load was estimated as the portion of the total load that was smaller than the d_{10} of the bed material samples collected at the San Acacia gauge for subreach 1 and at SO-lines for subreaches 2 and 3.

The total load for a discharge of 5000 cfs was determined from the rating curves developed from the BORAMEP and Psands results. The bed load was then determined by multiplying the total load by the percent of material considered to be wash load. The slope of the channel was varied until a slope was reached that matched incoming sediment supply and transport capacity. The equilibrium slope was determined for each method in each subreach.

7.3.2. Results

The total load rating curve for the incoming sand-sized sediment is shown in Figure 7.8. Table 7.9 shows the total load obtained from the regression curves at a discharge of 500 cfs, the average d_{10} of the bed material for each subreach, the percent of the suspended sediment that is smaller than the d_{10} of the bed material, and the bed load for each subreach.

Table 7.9 Total load and bed load calculations

	Total Load (tons/day)	Bed material d_{10} (mm)	% smaller than d_{10} of bed	Bed Load (tons/day)
Subreach 1	33298	0.0625	71.9	9344
Subreach 2	35460	0.125	82.3	6263
Subreach 3	38790	0.125	81.8	7068

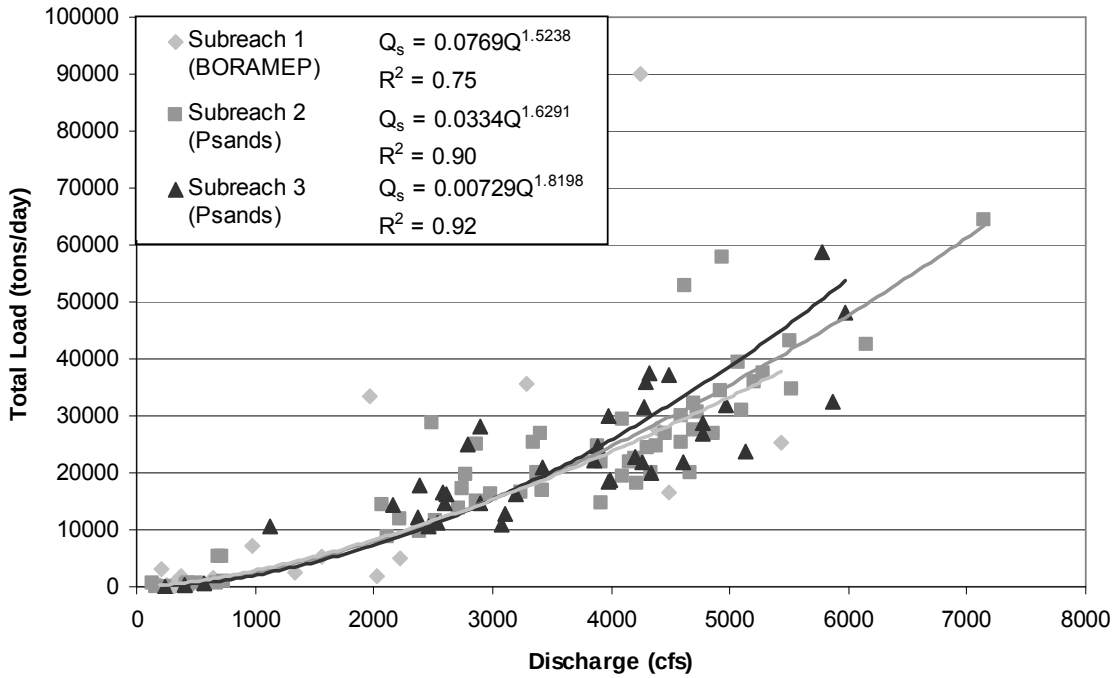

Figure 7.8 Total load rating curves from BORAMEP and Psands

The equilibrium sediment transport capacity and slope are shown for each reach and each method in Table 7.10. Some of the methods did not approach the target transport capacity within a reasonable range of slopes. A reasonable range of slope is a condition where a slope is predicted. These reaches do not show a specific equilibrium slope or transport capacity.

Table 7.10 Equilibrium slope determined from transport capacity equations

	Subreach 1		Subreach 2		Subreach 3	
Estimated Total Load (tons/day)	33298		35460		38790	
Estimated Bed Material Load (tons/day)	9344		6263		7068	
Existing Channel Slope (from 1992)	0.000759		0.000809		0.000723	
Sediment Transport Equations	**Transport Capacity (tons/day)**	**Slope**	**Transport Capacity (tons/day)**	**Slope**	**Transport Capacity (tons/day)**	**Slope**
Ackers & White	-	<0.00009	31255	0.00015	-	<0.00009
Engelund & Hansen	33234	0.00052	35020	0.00062	38141	0.00009
Laursen	-	<0.00009	40306	0.00041	-	<0.00009
Meyer-Peter & Muller	-	>0.01	6913	0.01	5668	0.01
Toffaleti	32519	0.00047	29191	0.00052	39097	0.00021
Yang - Sand	31348	0.00041	36112	0.00072	-	<0.00009
Average Slope		0.00193		0.00207		0.0018
Median Slope		0.00044		0.00057		0.00009

Methods by Engelund & Hansen and Toffaleti were the only methods able to determine an equilibrium slope for all subreaches, while Laursen and Ackers & White were only able to determine an equilibrium slope for subreach 2. The methods that predicted equilibrium slopes closest o the current slope were Engelund & Hansend in subreach 1, Yang in subreach 2, and Toffaleti in subreach 3. Meyer-Peter & Muller estimated very high slopes for all reaches. This may be due to the large amount of bed material load typically transported as suspended load in this section of the river, leaving very little material to be transported as bed load. Based on their ability to predict reasonable slopes in all subreaches, Engelun & Hansend and Toffaleti seem to be the best methods for determining transport capacity in the Escondida reach.

The average equilibrium slopes predicted by the sediment transport methods are much higher than expected for all reaches due to the influence of the Meyer-Peter & Muller method. This occurred because the Meyer-Peter & Muller method is more applicable for coarser bed rivers. The median slopes, however, present a reasonable estimate of the equilibrium slopes for subreaches 1 and 2. The median slope estimated for subreach 3 is very low when compared to the other subreaches and the other methods used to predict the equilibrium slope. Based on the median slope estimates, the channel slope will decrease by 42% in subreach 1, 30% in subreach 2 and 88% in subreach 3. The decrease in slope correlates well with the aggradational trend seen recently in subreach 3, but does not correlate well with the degradational trend seen in subreaches 1 and 2.

7.4. SAM

7.4.1. Methods

HEC-RAS stable channel design program, know as SAM, was used to determine the equilibrium slope and width for a series of suspended sediment inputs. SAM was developed for use as a preliminary design tool for flood control channels. The program assumes a trapezoidal channel and steady uniform flow in calculations. Given suspended sediment and water discharges, as well as a bed material gradation, SAM computes combinations of stable depth, width, and slope for the channel using Copeland's flow resistance and sediment transport equations. The series of slope and width combinations can then be plotted. The minimum point on the resulting slope vs. width graph is the point of minimum stream power for the input conditions.

The 2002 channel properties were used for the SAM analysis. The inputs included a bank slope of 2H:1V, a bank roughness of n=0.4, a discharge of 5000 cfs, and bed material gradation of d84 = 0.45 mm, d50=0.3 mm, d16=0.18 mm. A series of suspended sediment concentrations between 800 mg/L and 4500 mg/L were input into SAM as well.

7.4.2. Results

Figure 7.9 shows the slope vs. width curves for each suspended sediment concentration. The width and slope of the channel for 2002 conditions are plotted for comparison. The width was determined from GIS planform measurements and the channel slope was determined from HEC-RAS. The point of minimum stream power on the graph predicts a width of about 150 ft regardless of the bed material concentration (HEC-RAS Manual). The predicted width is much less than the equilibrium width predicted by any other method.

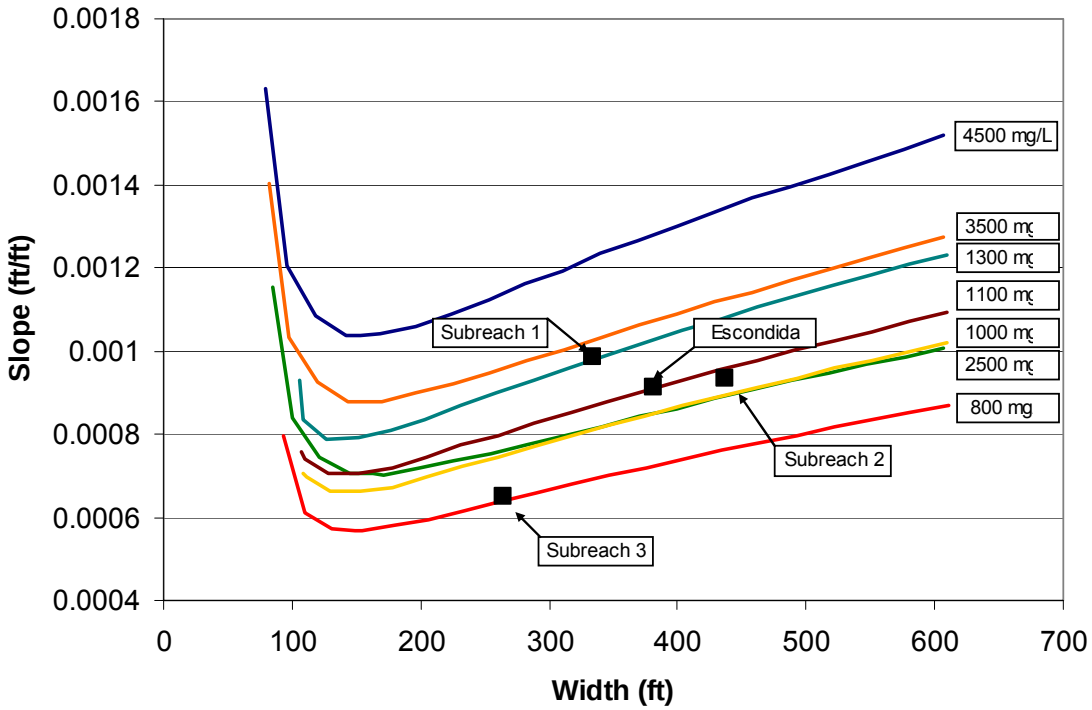

Figure 7.9 Results from SAM for 2002 conditions at Q = 5000 cfs

Table 7.11 shows the width and slope for each subreach and the entire reach for the 2002 conditions. This width and slope are also plotted in Figure 7.9. Table 7.11 also shows the suspended sediment concentration at each location and the width and slope calculated by SAM for those suspended sediment concentrations. While the equilibrium width is much lower than other methods predict, the equilibrium slope is reasonable when compared with other methods.

Table 7.11 Current conditions and equilibrium slope and width from SAM

		Subreach 1	Subreach 2	Subreach 3	Total
	SS C (mg/L)	2629	3588	4547	3588
2002	Slope	0.00099	0.00093	0.00065	0.00091
	Width (ft)	334	436	265	381
SAM	Slope	0.000704	0.000878	0.001037	0.000878
	Width (ft)	163.5	155.9	153.3	155.9

8. Discussion

8.1. Historic trends and current conditions in the Escondida reach

Observed Channel Planform Change Over Time

Based on visual observations of the GIS non-vegetated active channel planforms, the channel planform has become straighter since 1918. This observation is confirmed by a steady decrease in sinuosity (see Figure 3.6). The decrease in sinuosity is larger in subreach 3 between 1918 and 1935 than the other reaches. The straightening was likely caused by flood control and irrigation efforts implemented during the 1920's and 1930's. At the same time, the upper portion of the channel transitioned from a braided, multi-thread channel to a much narrower, single thread channel.

The total channel has narrowed slightly between 1962 and 2002, with the greatest decrease in width occurring between 1985 and 1992 (see Figure 3.12). The decrease in top width is likely related to a corresponding increase in depth in the channel at the same time. It has been observed that during low flows this reach has low flow braids and at higher flows acts an essentially straight single treaded channel.

Channel classification

The results of the channel classification methods indicated that the channel was primarily a straight or braided channel. The methods that most closely estimated the actual channel planform were those that indicated a straight planform, as braiding is only seen in localized areas of the channel during low flows. Leopold and Wolman, Schumm and Kahn, and Nanson and Croke all indicated a straight channel planform. Rosgen's method also provides a good description of the channel planform. Rosgen describes the channel as slightly to moderately entrenched with well-developed floodplains.

Vertical movement

Both aggradation and degradation were observed through changes in the mean bed elevation over time (see Figure 3.8 and Figure 3.9). Between 1962 and 1985, subreach 1 and subreach 2 showed 2 to 4 feet of aggradation, while subreach 3 showed about 4 feet of degradation. This trend was reversed between 1985 and 2002. The cyclical nature of the aggradation and degradation may be caused by complex response. Complex response results in several periods of aggradation and degradation in a reach due to a change in the system (Schumm 1979). The Escondida reach has been subjected to many changes, such as levee and dam construction and channelization. Any combination of these changes could have led to the complex response seen in the mean bed elevation.

The difference mass curve developed from suspended sediment gauge data also shows a cycle of aggradation and degradation. Aggradation was seen between

1960 and 1978. This was followed by about 5 years of degradation, then 6 years of aggradation. Finally, another cycle of degradation occurred from about 1992 until the end of the data in 1995. Continuing to analyze the difference mass curve as more data becomes available may give an indication as to when the channel is approaching equilibrium. As the channel approaches equilibrium, the oscillations between aggradation and degradation should become smaller.

Channel geometry

Table 8.1 shows the changes in each channel geometry parameter. A plus (+) indicates an increase, a minus (-) a decrease, and an equals (=) no change in the parameter value.

Table 8.1 Channel geometry changes

Subreach	Area	Top Width	Wetted Perimeter	Hydraulic Depth	Max Depth	W/D	Velocity	Froude Number
1962-1972								
1	+	=	=	+	+	-	+	=
2	+	+	+	+	+	+	+	+
3	-	-	-	+	+	=	+	+
Total	+	+	+	+	+	+	+	+
1972-1985								
1	=	=	-	+	-	-	+	+
2	-	-	=	-	-	-	-	-
3	-	+	-	-	=	+	-	-
Total	-	-	-	-	-	-	-	-
1985-1992								
1	-	-	-	+	-	-	+	+
2	-	+	-	+	+	+	+	+
3	-	-	-	+	-	-	+	+
Total	-	-	-	+	+	-	+	+
1992-2002								
1	=	=	=	-	-	+	+	+
2	+	+	+	-	-	+	-	-
3	+	+	+	-	-	+	-	+
Total	+	+	+	-	-	+	-	-
1962-2002								
1	+	+	+	-	=	+	-	-
2	-	-	-	+	+	-	+	-
3	+	+	+	+	-	+	-	-
Total	+	+	+	-	+	+	-	-

Lateral movement

Significant channel migration occurred at numerous locations throughout the reach (see Table 3.5). Shifts in channel banks of more than 100 feet were not uncommon. The largest channel movements were seen between 1962 and 1972. The channel migration may be due to the placement of improvements such as

levees that both straighten the channel and restrict the locations were migration is possible between 1949 and 1962 primarily. The migration may also be a response to earlier channelization efforts.

Bed material

Sand-sized particles are the primary bed material throughout the reach. Historically, the bed material has ranged from very find sand to medium sand. A slight coarsening of the bed material has been seen between 1972 and 2002 (See Figure 3.17). This may be due to the effects of dam installation and reduced sediment supply from upstream ephemeral tributaries. The coarsening may also be due to new inputs of coarse material from tributaries and arroyos, a decreased supply of fine sediments, or increased transport capacity due to higher discharges.

Discharge

The daily discharge at both the San Acacia and San Marcail gauges increased to about 4 times the previous daily discharge around 1979. The daily discharge decreased by about 3 times around 2000 (see Figure 4.1). These changes may have occurred to the installation and operation of the Cochiti Dam as well as the operation of the San Acacia Diversion Dam.

Suspended sediment

The daily suspended sediment discharge recorded at both gauges has changed little since early 1960's (see Figure 4.2). As a result, the suspended sediment concentration has varied inversely with discharge over time. The concentration decreased by about 5 times following the increase in discharge in 1979. The effects of the recent decrease in discharge are not known because suspended sediment data is unavailable after 1996. Based on Table 4.2 the sediment load in tons/day is greater at San Marcial than at San Acacia. In the late 1950's the sediment load at San Marcial is 5 times greater than San Acacia. In the late 1960's the sediment load is still greater at San Marcial, however the magnitude is not as high.

Floodplain Inundation

Two locations in the lower portion of the reach have large, active floodplains. These floodplains typically become active at about 3000 cfs. The recurrence interval of a 3000 cfs flow indicates that the floodplain is inundated on about an annual basis. The floodplain became active between 1000 cfs and 2000 cfs before 1985 in the lowest section of the reach, indicating that the channel has entrenched since 1972.

Bedforms

Neither of the bedform predictors was able to adequately predict the bedforms observed in the Escondida reach. Upper regime anti-dues and plane bedforms

were predicted correctly most often. The difficulty in calculating the expected bedforms stems from the high variability of the cross-sections in the reach. Two or more different types of bedforms were typically observed at a typical cross-section. Upper regime bedforms were easier to predict because the cross-section variability had less of an effect at the high flows necessary to produce upper regime bedforms.

8.2. Channel response models

8.2.1. Schumm's (1969) river metamorphosis model

Schumm (1969) developed a model to describe a channel's response to changes in water and sediment discharge. Schumm hypothesized that changes in water and sediment discharge would effect channel width, depth, width/depth ratio, channel slope, sinuosity and meander wavelength. The response of these parameters can be described by the following equations where a plus (+) exponent indicates an increase and a minus (-) exponent indicates a decrease.

Decreased bed material load:

$$Q_s^- \sim W^- D^+ P^+ L^- S^-$$

Increase bed material load:

$$Q_s^+ \sim W^+ D^- P^- L^+ S^+$$

Decreased water discharge:

$$Q^- \sim W^- D^- L^- S^+$$

Increased water discharge:

$$Q^+ \sim W^+ D^+ L^+ S^-$$

Decreased water discharge and bed material load:

$$Q^- Q_t^- \sim W^- D^\pm F^- L^- S^\pm P^+$$

Increased water discharge and bed material load:

$$Q^+ Q_t^+ \sim W^+ D^\pm F^+ L^+ S^\pm P^-$$

Where Q is water discharge, Qs is bed material load, Qt is the percent of the total load that is sand or bed material load, W is channel width, D is flow depth, F is width/depth ratio, L is meander wavelength, P is sinuosity, and S is channel slope.

Table 8.2 shows Schumm's equations in tabular form. In addition, Table 8.3 shows the observed changes in the Escondida reach for each year and subreach.

Table 8.2 Schumm's (1969) channel metamorphosis model

	W	D	S	F = W/D	P	L
Qs^-	-	+	-		+	-
Qs^+	+	-	+		-	+
Q^-	-	-	+			-
Q^+	+	+	-			+
Q^-Qt^-	-	+ -	+ -	-	+	-
Q^+Qt^+	+	+ -	+ -	+	-	+

Table 8.3 Observed channel changes at Q = 5000 cfs

Subreach	W	D	S	F = W/D	P
1962-1972					
1	=	+	-	-	+
2	+	+	+	+	-
3	-	+	+	=	=
Total	+	+	+	+	+
1972-1985					-
1	=	+	-	-	-
2	-	-	+	-	-
3	+	-	-	+	+
Total	-	-	=	-	-
1985-1992					
1	-	+	-	-	-
2	+	+	-	+	+
3	-	+	+	-	-
Total	-	+	-	-	+
1992-2002					
1	=	-	+	+	-
2	+	-	-	+	-
3	+	-	+	+	+
Total	+	-	-	+	-
1962-2002					
1	+	-	-	+	-
2	-	+	=	-	-
3	+	+	+	+	+
Total	+	-	=	+	-

Comparing the observed changes in channel properties to Schumm's equations gives an indication of what the channel may be responding to. Schumm's model seems to work best in the Escondida reach between 1985 and 2002. Few of the changes in the earlier years match the model. The model indicates that between 1985 and 1992, the channel was likely responding to a decrease in discharge and sediment load. This observation is opposite to the changes in discharge and

sediment load observed at the San Acacia and San Marcial gauges at the same time. In addition, the model indicates that between 1992 and 2002, the channel was responding to an increase in both discharge and sediment load. An increase in sediment load was observed during this time, but an increase in discharge was not. This may indicate that the channel is responding more to the changes in sediment supply than to changes in discharge.

8.2.2. Lane's (1955) balance

Lane's (1955) balance model is illustrated in Figure 8.1. The channel parameters examined by Lane were channel slope, discharge, median grain size, and sediment discharge. The model states that a change in any of the four driving variables will result in a change of the other three variables such that the channel will tend toward a new equilibrium state.

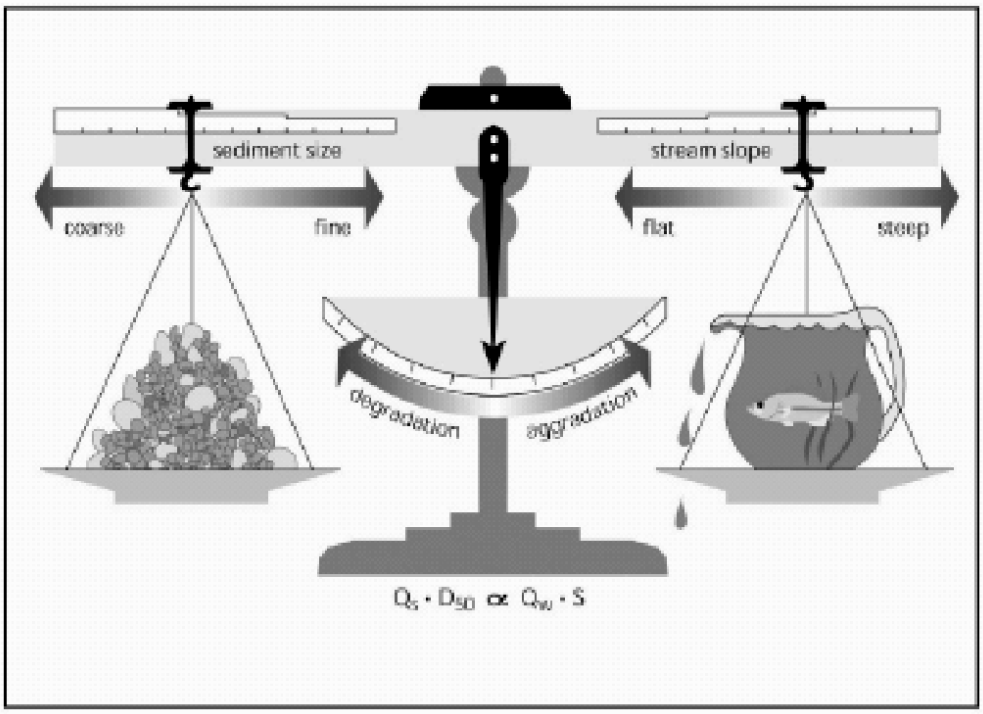

Figure 8.1 Lane's balance(1955)

Table 8.4 shows the observed channel changes from 1962 to 2002 as well as the variable to which the channel may be reacting. The variable initiating change was determined by selecting a variable as the initial point of change, and evaluating the changes in the other variables to determine if they followed the pattern outlined by Lane. If the changes balanced according to Lane, the variable could have been the trigger of channel change. Discharge and suspended sediment discharge were always considered first because the channel cannot change the amount or water or sediment entering the reach from upstream. Suspended sediment data was not available after 1996, so the

change from 1992 to 2002 is unknown. The suspended sediment discharge for the unknown time was assumed to be constant for the purpose of this analysis.

Table 8.4 Observed Changes in Lane Balance Parameters and the Corresponding Trigger Variable

Subreach	Q	S	Q_s	d_{50}	Trigger variable
1962-1972					
1	=	-	+	-	d_{50}
2	=	+	+	-	Q_s
3	=	+	+	-	Q_s
Total	=	+	+	-	Q_s
1972-1985					
1	+	-	+	+	Q
2	+	+	+	+	None
3	+	-	+	-	None
Total	+	=	+	+	None
1985-1992					
1	=	-	=	+	None
2	=	-	=	+	None
3	=	+	+	+	S or d_{50}
Total	=	-	=	+	None
1992-2002					
1	-	+		+	None
2	-	-		+	d_{50}
3	-	+		-	Q
Total	-	-		+	d_{50}

According to Lane's balance, between 1962 and 1972, the channel was primarily reacting to a change in the incoming suspended sediment discharge because d_{50} did not change much. Between 1985 and 1992, the channel did not change in a way that was predicted by Lane. Assuming a relatively constant suspended sediment discharge, the channel seemed to be reacting to an increase in median grain diameter. It is likely that the channel is actually under the influence of multiple channel changes at any given time. However, this simplified approach gives some idea of what changes may be having the greatest influence on the channel morphology.

8.3. Potential future equilibrium conditions

8.3.1. Equilibrium Width

<u>Hydraulic Geometry</u>

The hydraulic geometry equation developed by Blench (1957) gave equilibrium widths that most closely matched the current channel conditions. However, Blench may not be the best method for predicting equilibrium width because the channel was likely not in equilibrium between 1962 and 2002. Simons and Albertson (1963), Nouh (1988), Lacey (from Wargadalam 1993), and Julien-Waradalam (1995) all predicted similar equilibrium widths between 200 ft and

300 ft. The consistent prediction by these four methods indicates that they may be the most effective in predicting equilibrium width.

Hyperbolic and Exponential Models

The hyperbolic model developed by Williams and Wolman (1984) fit well with historic width data from the Escondida reach. The widths predicted by the hyperbolic model ranged from about 300 ft to about 450 ft. The method predicted a negative equilibrium width for subreach 1, but predicted a reasonable width for 2020. More data should be added to the model to improve the equilibrium prediction for subreach 1.

The exponential model developed by Richard et al. (2005) produced results very similar to those calculated by the hyperbolic model. However, this model was able to predict reasonable equilibrium widths for all subreaches and the total reach.

SAM

The final equilibrium width prediction method used was the HEC-RAS stable channel design program (SAM). Based on the incoming suspended sediment concentration estimated for each subreach and the total reach, the equilibrium widths for the channel were all about 160 ft. This width is less than the widths predicted by the other methods, but it still provides a reasonable estimate of equilibrium channel width.

8.3.2. Equilibrium Slope

Hydraulic Geometry

Julien and Wargadalam (1995) predicted equilibrium slopes for the 2002 channel geometry between 0.00083 and 0.00139. These slopes are much steeper than the slopes observed in the channel during that time, indicating that the channel may not be in equilibrium. The predicted slopes are, however, reasonable when compared to historic channel slopes.

SAM

The equilibrium slope was also estimated from the HEC-RAS stable channel design program. The program estimated the equilibrium slope to between 0.00065 and 0.00099 depending upon the incoming suspended sediment concentration. These results are very similar to the predictions made by Julien-Wargadalam.

Sediment Transport

The HEC-RAS sediment transport analysis was used to determine an equilibrium slope for the channel based on sediment transport. The equilibrium slope was estimated as the slope at which sediment supply equals sediment transport capacity. Engelund & Hansen and Toffaleti were the only methods able to provide reasonable slope predictions for all subreaches. These methods estimated the equilibrium slope to be between 0.00009 and 0.00062. This slope

range is much less steep than the slopes estimated by Julien-Wargadalam and SAM. The slopes are also much less steep than the historic slopes in the reach. This method may not be the best for predicting equilibrium slope for this reach. A better accounting of incoming sediment from all sources, such as arroyos and other ungauged tributaries may improve the predictions provided by the sediment transport analysis.

9. Summary

The Escondida reach was analyzed for this study. The reach covers 17.7 miles of the Middle Rio Grande in central New Mexico. Important changes occurring in the Escondida reach between 1918 and 2005 were analyzed using a number of techniques. Changes in channel geometry and morphology, and water and sediment discharge were observed. In addition, historic bedform data were analyzed. Finally, the equilibrium conditions of the reach were estimated.

Spatial and temporal trends in channel geometry and morphology were identified using visual observations of aerial photographs and GIS active channel planforms, cross-section surveys, hydraulic modeling using HEC-RAS, and channel classification methods. Observations of the GIS active channel planforms and aerial photographs show that the channel has narrowed between 1918 and 2005. The most significant narrowing has occurred in the upper portion of the reach. Analysis of channel geometry trends using HEC-RAS hydraulic modeling output shows a series of increases and decreases in most channel properties. The fluctuations in channel geometry may be the result of a complex response to past channel changes. Bed material samples obtained from cross-section surveys and at the San Acacia and San Marcial gauges between 1962 and 2002 show a slight coarsening of the bed from a mean diameter of 0.15 mm to 0.31 mm.

Historic bedform observations were compiled and compared to predicted bedforms at the survey locations. Simons and Richardson and van Rijn were used to calculate the expected bedforms at each survey locations. These predictions were compared with field observations of bedforms. The bedform predictor methods produced adequate results. Large scatter was observed in the data, especially in the prediction of lower regime bedforms. This scatter is likely due to the wide variability across individual cross-sections in the reach.

Trends in water and sediment discharge were analyzed using mass curves developed from USGS gauge data. The mass curves show a wet period between 1979 and 2000. This increase in discharge was also observed in upstream reaches. The increase in discharge caused the Escondida reach to carry a similar magnitude of discharge as the upstream reaches, where, historically, the reach carried much lower discharges. The daily mean suspended sediment discharge remained nearly constant for the entire period of record. The difference mass curve shows periods of aggradation and degradation that approximately correlate with changes in mean bed elevation.

Estimates of potential equilibrium slope and width conditions were made using hydraulic geometry equations, hyperbolic and exponential regressions, stable channel geometry, and sediment transport relationships. An equilibrium width of around 300 ft was estimated by several methods, indicating that this is a reasonable estimate of the future channel width. Julien-Wargadalam and SAM

predicted equilibrium slopes between 0.00065 and 0.00139, depending on the subreach and the method used. These slopes are within a reasonable range of the current slope and provide a good estimate of the direction of potential slope change in each subreach since the reach currently has a slope of 0.0008.

The main conclusions of this study are:

- The active channel has narrowed and the sinuosity decreased from 1.19 to 1.09 between 1918 and 2005. In addition, the mean bed material diameter increased from 0.15 mm to 0.31 mm between 1962 and 2002.

- Bedform prediction methods by van Rijn and Simons and Richardson produced a reasonable fit to the observed bedform data. The data showed wide scatter, likely caused by the high degree of variability across a cross-section.

- The water discharge indicated a period of increased water discharge between 1979 and 2000. The increase in discharge that occurred in 1979 was observed in upstream reaches, but was more dramatic in the Escondida reach.

- Equilibrium width and slope predictors forecast a channel width of about 300 ft and a slope between 0.00065 and 0.00139. These estimates were confirmed by multiple methods and seem to be reasonable estimates.

The collective observations of the reach indicate that this is a very dynamic reach that has not yet reached an equilibrium state. The channel will likely continue to narrow. Lateral movement and sinuosity changes are also likely as the channel attempts to reach an equilibrium slope.

10. References

Ackers, P. (1982). Meandering Channels and the Influence of Bed Material. *Gravel Bed Rivers. Fluvial Processes, Engineering and Management.* Edited by R.D. Hey, J.C. Bathurst and C.R. Thorne. John Wiley & Sons Ltd. pp. 389-414.

Ackers, P. and F. G. Charlton (1970). The slope and resistance of small meandering channels. Proc. Insitit. Civil Engrs., Paper 7362S, Supplement XV, pp 329-370.

Bauer, T.R. (2000). Morphology of the Middle Rio Grande from Bernalillo Bridge to the San Acacia Diversion Dam, New Mexico. M.S. Thesis. Colorado State University, Fort Collins, CO. 308 p.

Blench, T. (1957). *Regime Behavior of Canals and Rivers.* London: Butterworths Scientific Publications. 138p.

Bogan, M., Alllen, C., Muldavin, E., Platania, S., Stuart, J., Farley, G., Mehlhop, P., Belnap, J. (2006). "Southwest." *United States Geological Survey.* < http://biology.usgs.gov/s+t/SNT/noframe/sw152.htm> (June 27, 2006).

Brown, M. (2006). Personal Communication. Graduate Student. Colorado State University. Fort Collins, CO.

Bullard, K.L. and Lane, W.L. (1993). Middle Rio Grande Peak Flow Frequency Study. U.S. Department of the Interior, Bureau of Reclamation, Albuquerque, NM.
36 p.

Chang, H.H. (1979). Minimum Stream Power and River Channel Patterns. *Journal of Hydrology*. 41, pp. 303-327.

Clark, I. G. (1987). *Water in New Mexico: A History of its Management and Use.* Albuquerque, NM: University of New Mexico Press. 839 p.

Earick, D. (1999). The History and Development of the Rio Grande River in the Albuquerque Region. Available at http://www.unm.edu/~abqteach/EnvirCUs/99-03-04.htm. Accessed June 27, 2006).

Hawley, J.W. (1987). Guidebook to Rio Grande Rift in New Mexico and Colorado. *New Mexico Bureau Mines & Mineral Resources*. Circular 163. 241+ p.

Henderson, F.M. (1966). *Open Channel Flow.* New York, NY: Macmillan Publishing Co., Inc. 544 p.

Julien, P.Y. (1998). *Erosion and Sedimentation.* New York, NY: Cambridge University Press. 280 p.

Julien, P.Y. and Wargadalam, J. (1995). Alluvial Channel Geometry: Theory and Applications. *Journal of Hydraulic Engineering,* 121(4), pp. 312-325.

Klaassen, G.J. and Vermeer, K. (1988). Channel Characteristics of the Braiding Jamuna River, Bangladesh. *International Conference on River Regime,* 18-20 May 1988. W.R. White (ed.), Hydraulics Research Ltd., Wallingford, UK. pp. 173-189.

Lane, E.W. (1955). The importance of fluvial morphology in hydraulic engineering. *Proc. ASCE,* 81(745):1-17.

Larsen, S. and Reilinger, R. (1983). "Recent measurements of crustal deformation related to the Socorro Magma Body, New Mexico." *New Mexico Geological Society Guidebook, 34th Field Conference.* pp. 119-121.

Leopold, L.B. and Wolman, M.G. (1957). River Channel Patterns: Braided, Meandering, and Straight. *USGS Professional Paper 282-B.* 85 p.

Middle Rio Grande Conservancy District. (2006). About the District. Available at http://www.mrgcd.com/?cmd=pages&what=About%20the%20District. Accessed on June 27, 2006.

Middle Rio Grande Conservancy District v. Norton, 2002 10CIR 685, 294 F.3d 1220, (2002).

Middle Rio Grande Endangered Species Act Collaborative Program. (2006a). The Rio Grande Silvery Minnow. Available at http://www.fws.gov/mrgesacp/MRGSM.cfm. Accessed on June 6, 2006.

Middle Rio Grande Endangered Species Act Collaborative Program. (2006b). The Southwestern Willow Flycatcher. Available at http://www.fws.gov/mrgesacp/SWWFC.cfm. Accessed on June 6 ,2006.

Nanson, G.C. and Croke, J.C. (1992). A genetic classification of floodplains. *Geomorphology*. 4, pp. 459-486.

Nouh, M. (1988). Regime Channels of an Extremely Arid Zone. *International Conference of River Regime*, 18-20 May 1988. W.R. White (ed.). Hydraulics Research Ltd., Wallingford, UK. pp 55-66.

Novak, S.J. (2006). Hydraulic modeling anlysis of the Middle Rio Grande River from Cochiti Dam to Galisteo Creek, New Mexico. M.S thesis, Civil Engineering Department, Colorado State University, Fort Collins, CO. 168 p.

Ouchi, S. (1983). Response of alluvial rivers to active tectonics. PhD. dissertation, Earth Resources Department, Colorado State University, Fort Collins, CO. 205 p.

Parker, G. (1976). On the Cause and Characteristic Scales of Meandering and Braiding in Rivers." *Journal of Fluid Mechanics*. vl. 76, part 3, pp. 457-480.

Porter, M. and Massong, T. (2004). *Habitat fragmentation and modifications affecting distribution of the Rio Grande silvery minnow.* United States Department of the Interior, Bureau of Reclamation, Fishery and Aquatic GIS Research Group, Albuquerque, NM. pp. 421-432.

Raff, D., Bledsoe, B. P. and Flores, A. N. (2004). *Geo Tool Version 3.* Engineering Research Center Colorado State University.

Reclamation. (2003). *Geomorphologic assessment of the Rio Grande, San Acacia reach.* United States Department of the Interior, Bureau of Reclamation, Albuquerque Area Office, Albuquerque, NM. 75 p.

Richard, G., Julien, P.Y., Baird, D.C., (2005). Case Study: Modeling the Lateral Mbility of the Rio Grande below Cochiti Dam, New Mexico. *Journal of Hydraulic Engineering.* 131(11), pp. 931-941.

Richardson, E.V., Simons, D.B., Lagasee, P.F. (2001). *River Engineering for Highway Encroachments, Highways in the River Environment.* United States Department of the Transportation, Federal Highway Administration. 644 p.

Rosgen, D. (1996). *Applied River Morphology.* Pagosa Springs, CO: Wildland Hydrology. 360 p.

Schumm, S.A. (1969). River Metamorphosis. *Journal of Hydraulics Division, ASCE.* Vol. 95, No.1. pp. 255-273.

Schumm, S.A. (1979). Geomorphic Thresholds: The Concept and Its Applications. *Transactions of the Institute of British Geographers.* New Series, Vol. 4, No. 4. pp. 485-515.

Schumm, S.A and Khan, H.R. (1972). Experimental Study of Channel Patterns. *Geological Society of America Bulletin.* 83, pp. 1755-1770.

Scurlock, D. (1998). *From the Rio to the Sierra: An Environmental History of the Middle Rio Grande Basin.* General Technical Report RMRS-GTR5. United States Department of Agriculture, Forest Service, Rocky Mountain Research Station, Fort Collins, CO. 440 p.

Simons, D.B. and Albertson, M.L. (1963). Uniform Water Conveyance Channels in Alluvial Material. *Transactions of the American Society of Civil Engineers.* Paper No. 3399. Vol. 128, Part I. pp. 65-107.

Tetra Tech, Inc. (2002). *Development of the Middle Rio Grande FLO-2D Flood Routing Model Cochiti Dam to Elephant Butte Reservoir.* Tetra Tech, Inc. 48 p.

U.S. Army Corps of Engineers, USACE (2005). HEC-RAS River Analysis System. v.3.1.3. U.S Army Corps of Engineers Institute for Water Resources. Hydrologic Engineering Center, Davis, CA.

van den Berg, J.H. (1995). Prediction of Alluvial Channel Pattern of Perennial Rivers. *Geomorphology*. 12, pp. 259-279.

van Rijn, L.C. (1984). Sediment Transport, part III: Bedforms and Alluvial Roughness. *Journal of the Hydraulic Division, ASCE*. 110 (12), pp. 1733-1754.

Vensel, C., Richard, G., Leon, C.L., and Julien, P.Y. (2005). Hydraulic Modeling on the Middle Rio Grande, New Mexico. Rio Puerco Reach. Prepared for U.S. Bureau of Reclamation. Albuquerque, New Mexico. Colorado State University, Fort Collins, CO. 100 p.

Wargadalam, J. (1993). Hydraulic Geometry of Alluvial Channels. Ph.D. Dissertation. Colorado State University, Fort Collins, CO. 203 p.

Williams, G. and Wolman, G. (1984). Downstream Effects of Dams on Alluvial Rivers. U.S. Geological Survey Professional Paper 1286, 83 p.

Appendix A – Socorro Line Survey Plots

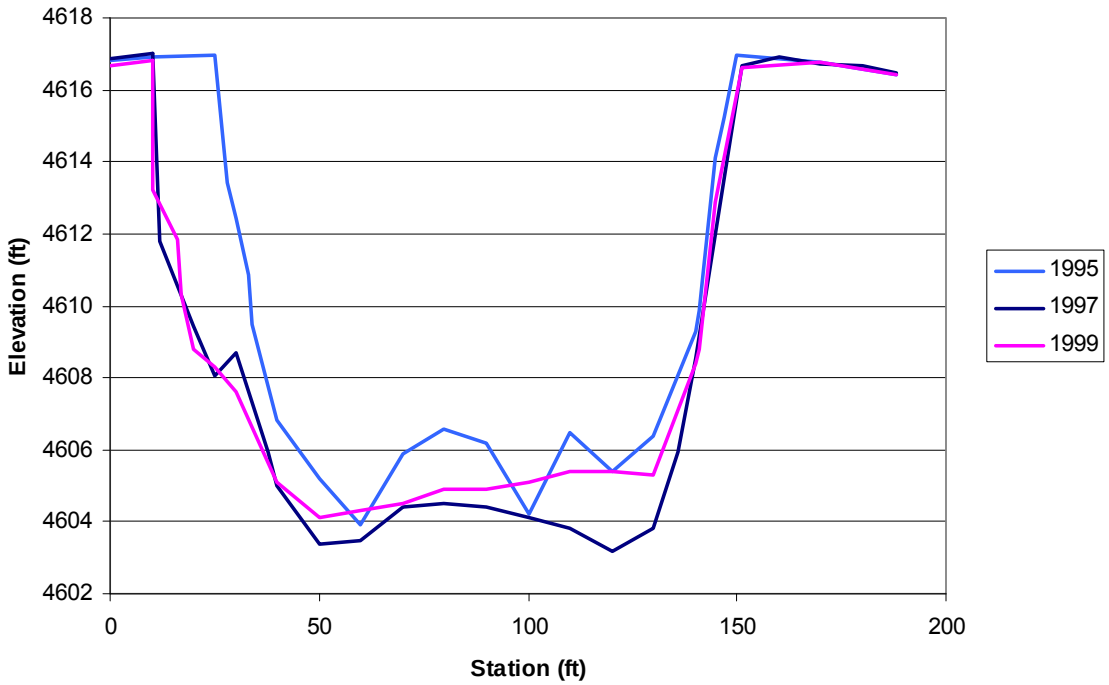

Figure A.1 Cross-section survey at SO-line 1313

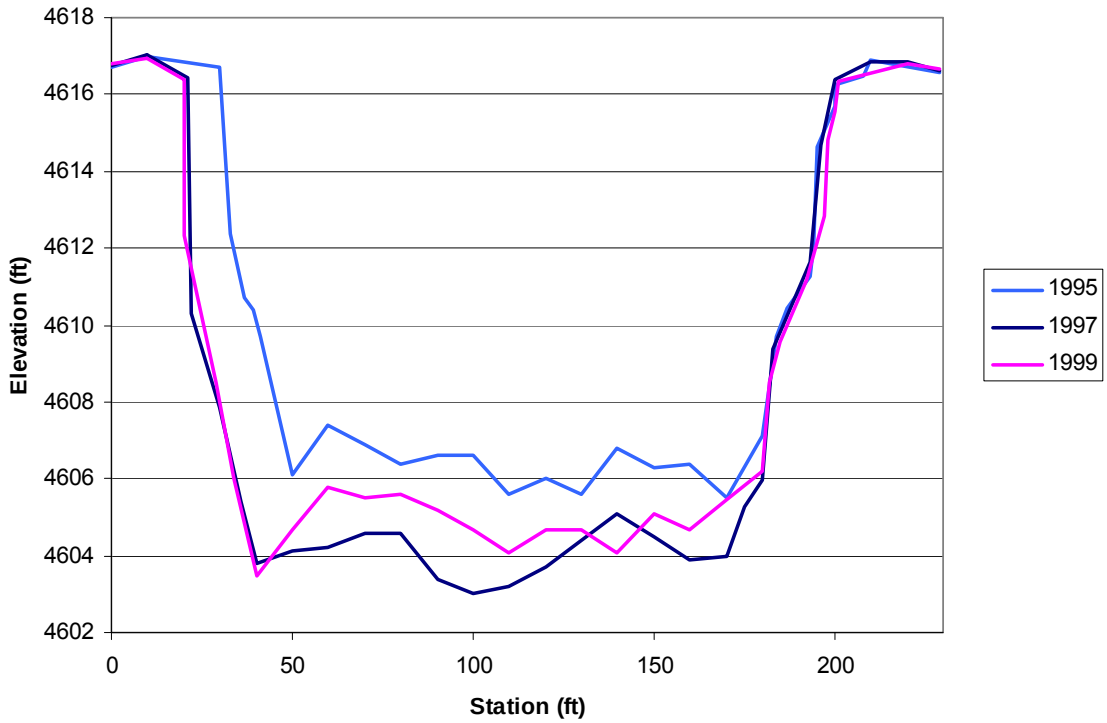

Figure A.2 Cross-section survey at SO-line 1314

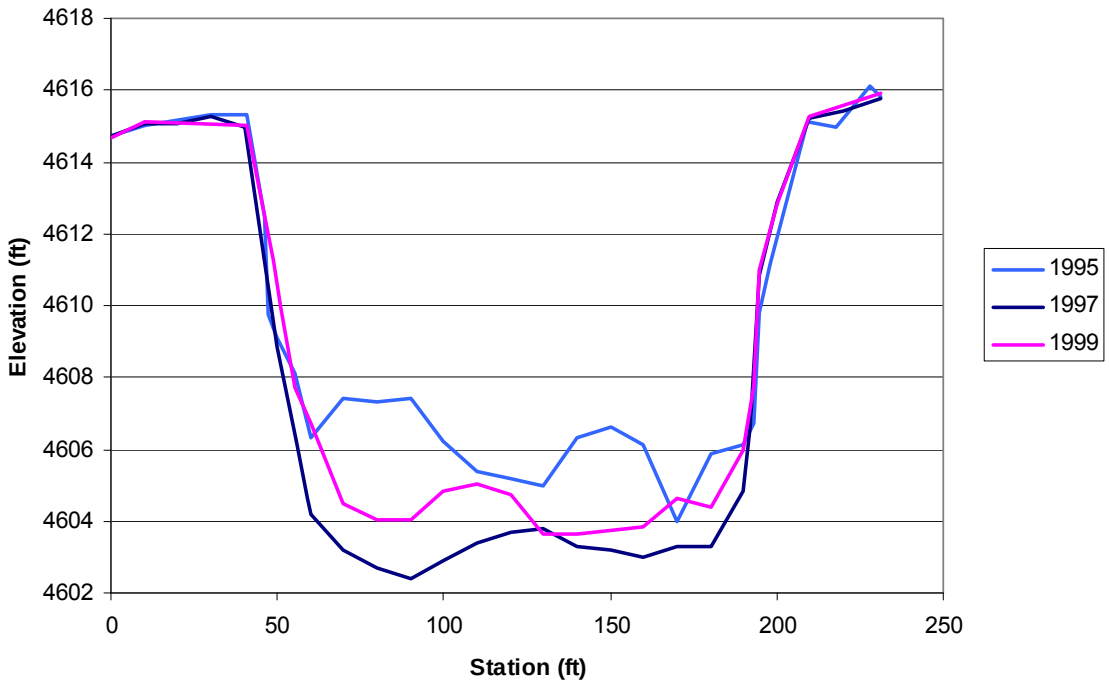

Figure A.3 Cross-section survey at SO-line 1316

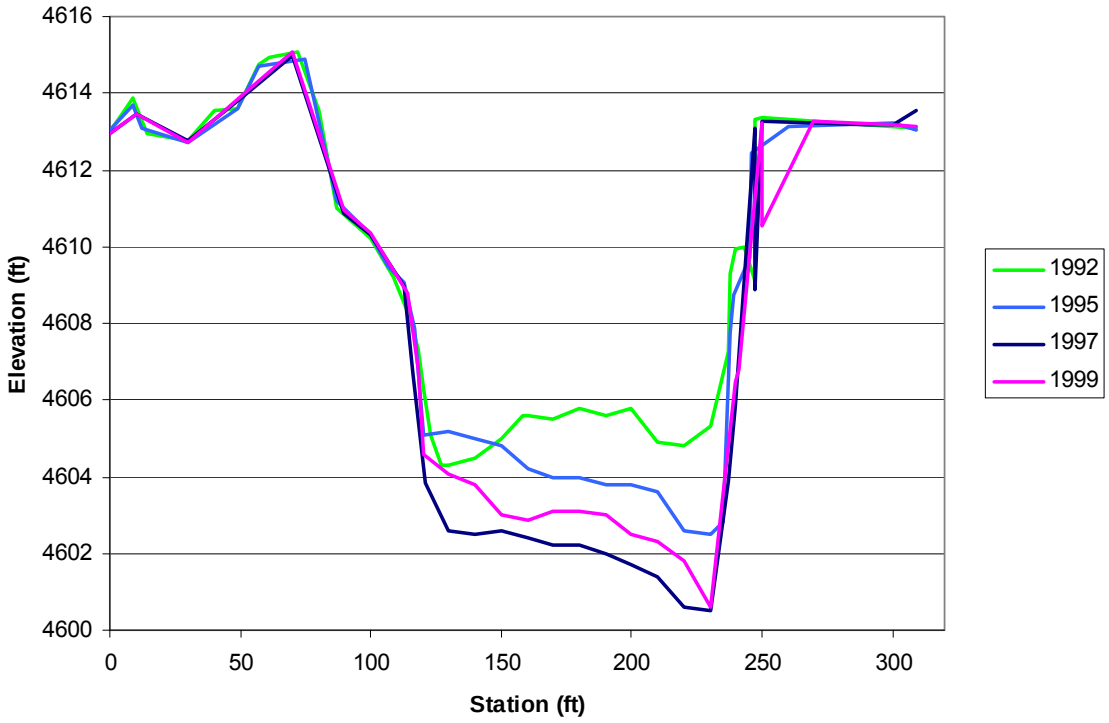

Figure A.4 Cross-section survey at SO-line 1320

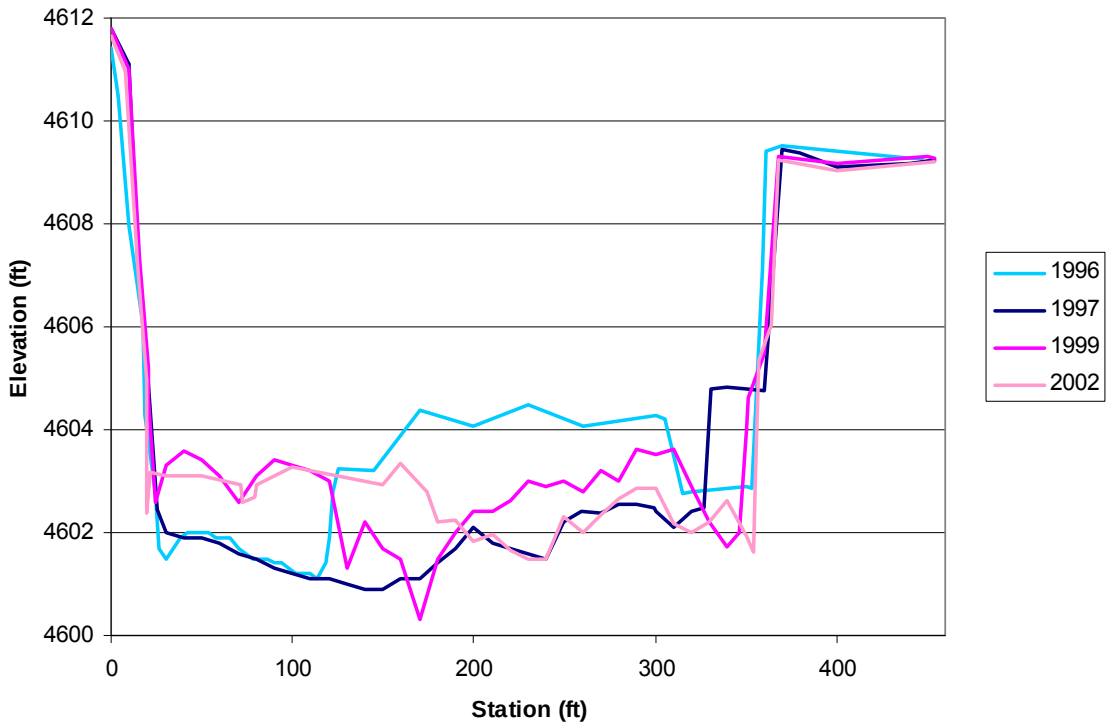

Figure A.5 Cross-section survey at SO-line 1327

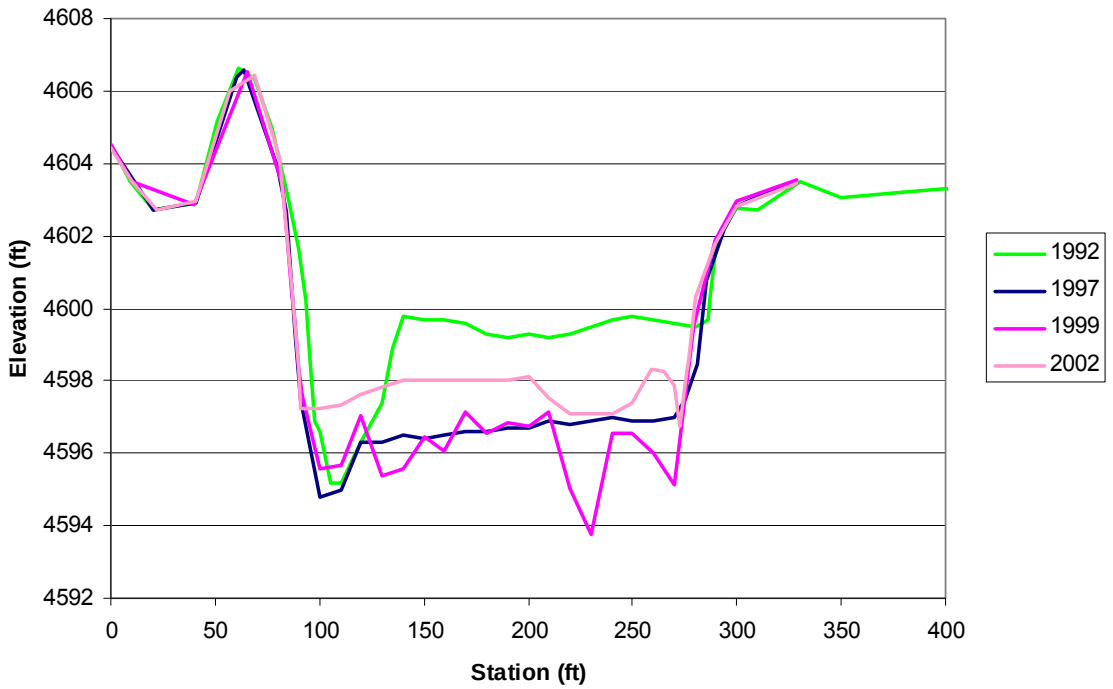

Figure A.6 Cross-section survey at SO-line 1339

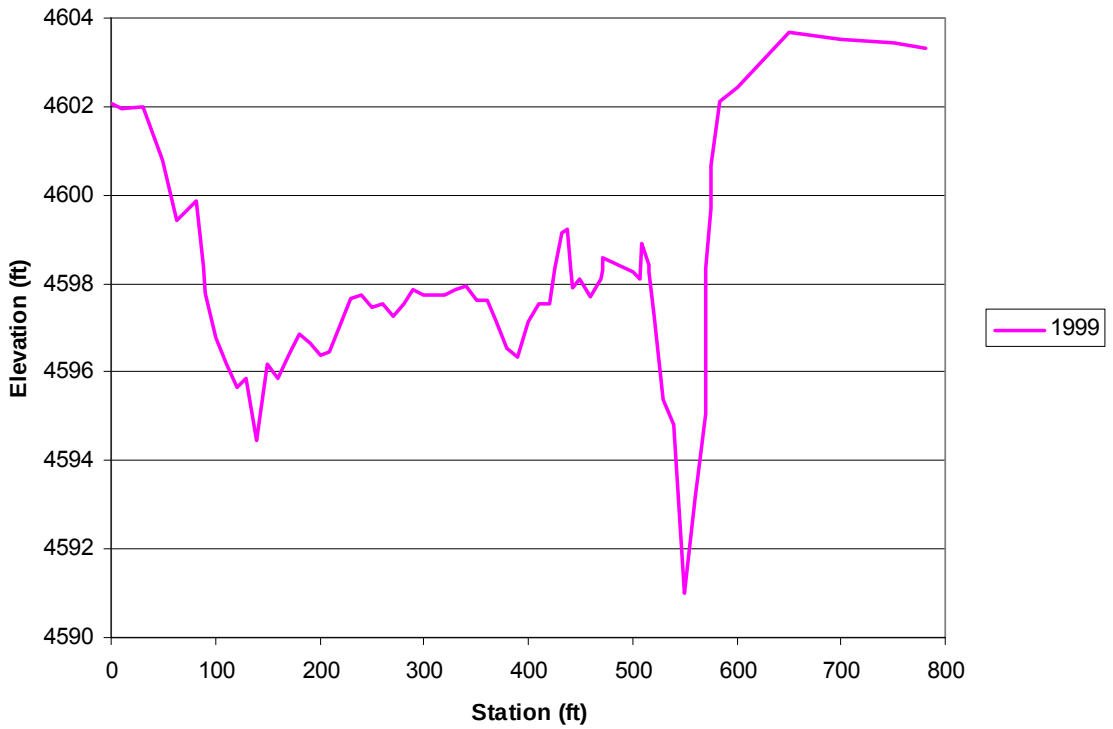

Figure A.7 Cross-section survey at SO-line 1342.5

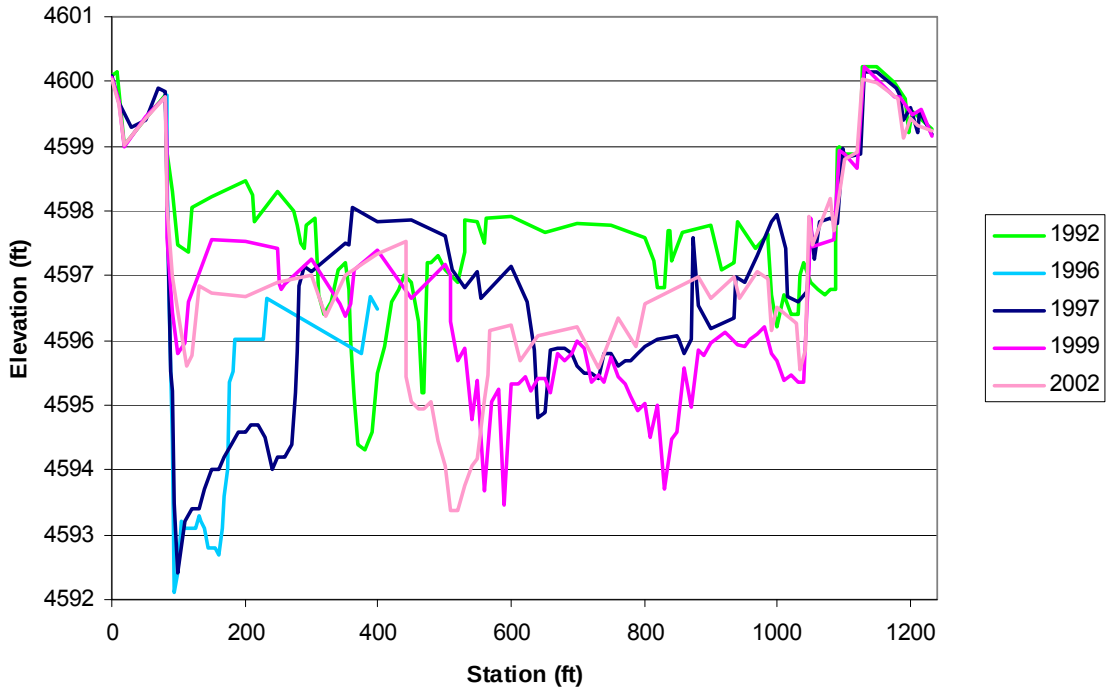

Figure A.8 Cross-section survey at SO-line 1346

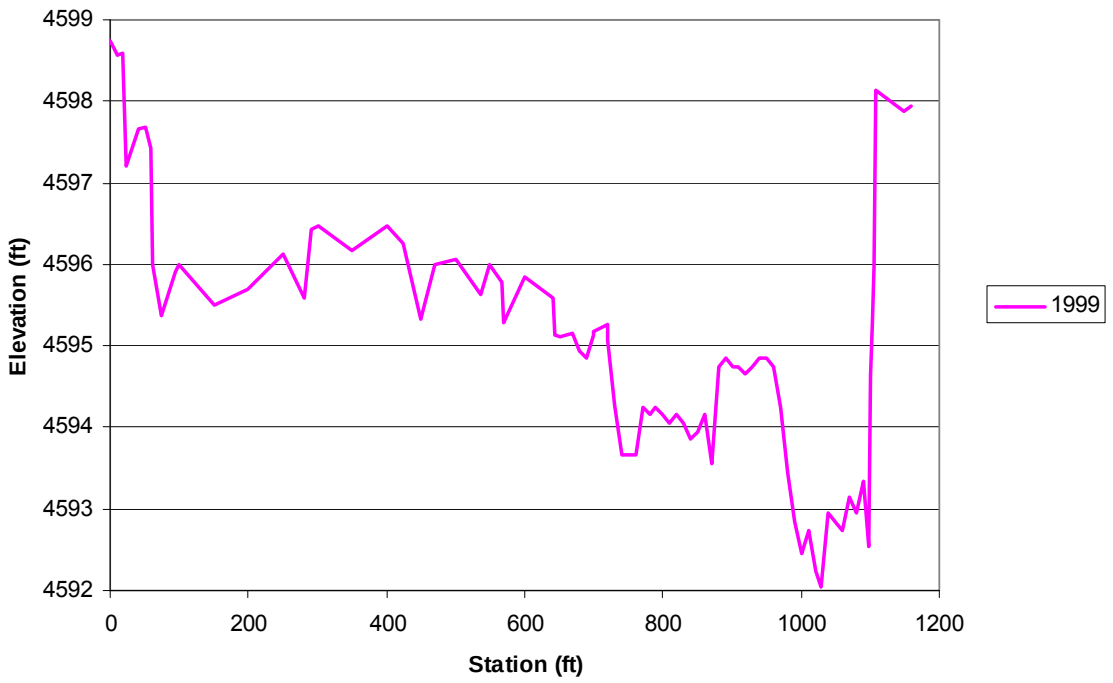

Figure A.9 Cross-section survey at SO-line 1349

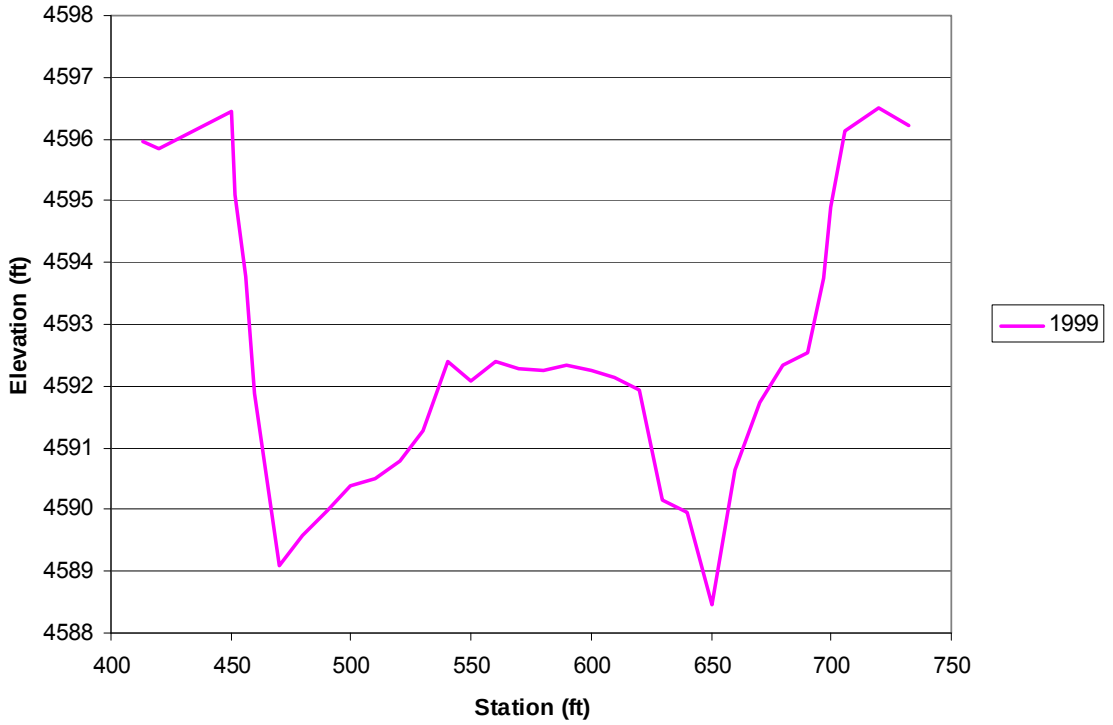

Figure A.10 Cross-section survey at SO-line 1352

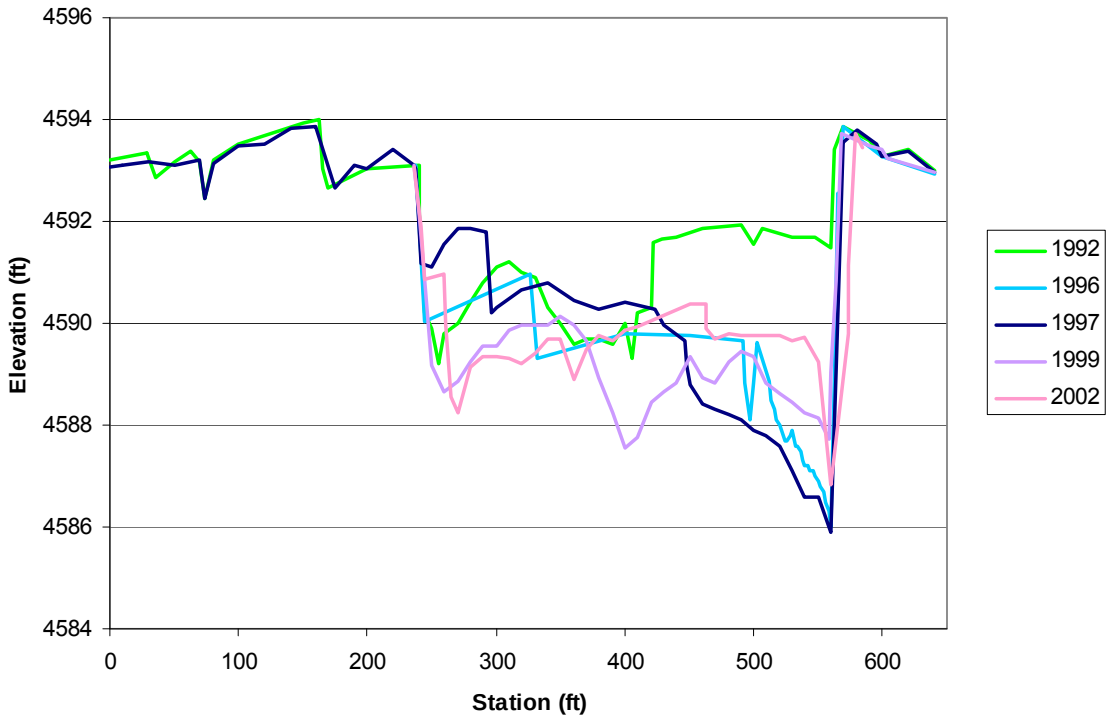

Figure A.11 Cross-section survey at SO-line 1360

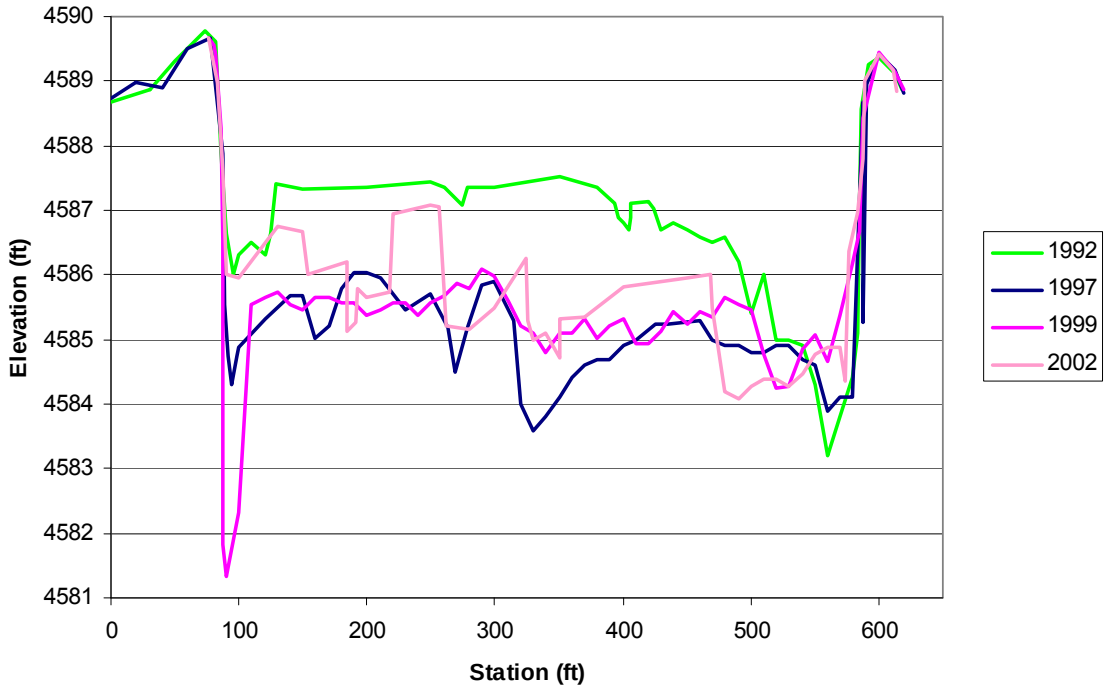

Figure A.12 Cross-section survey at SO-line 1371

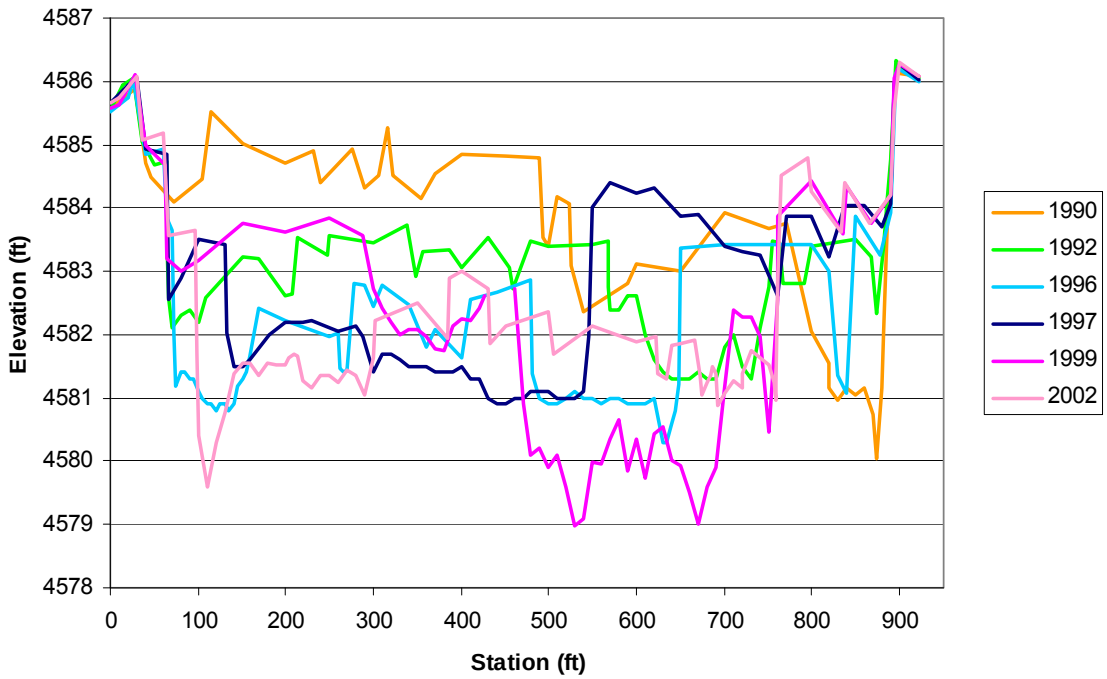

Figure A.13 Cross-section survey at SO-line 1380

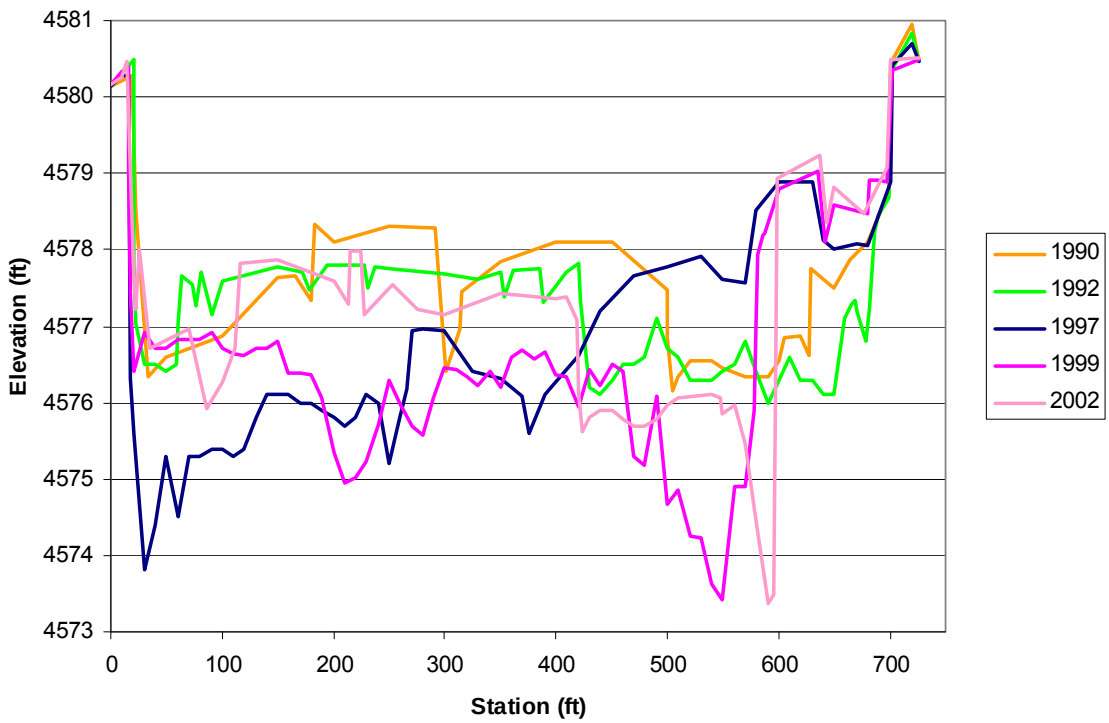

Figure A.14 Cross-section survey at SO-line 1394

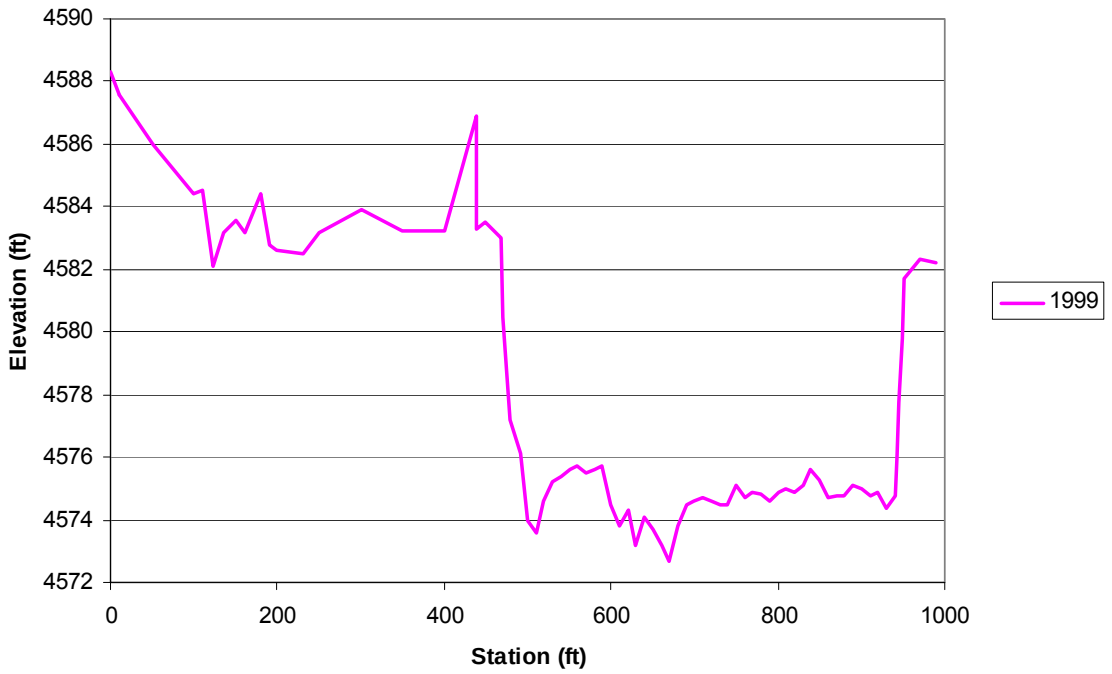

Figure A.15 Cross-section survey at SO-line 1396.5

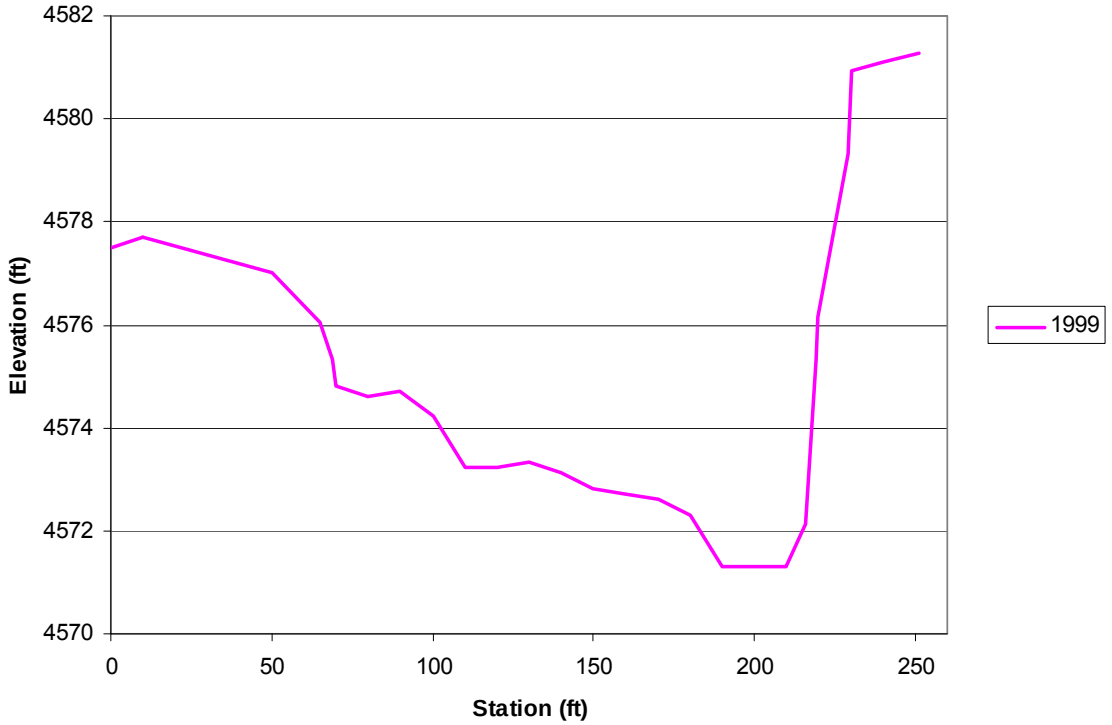

Figure A.16 Cross-section survey at SO-line 1398

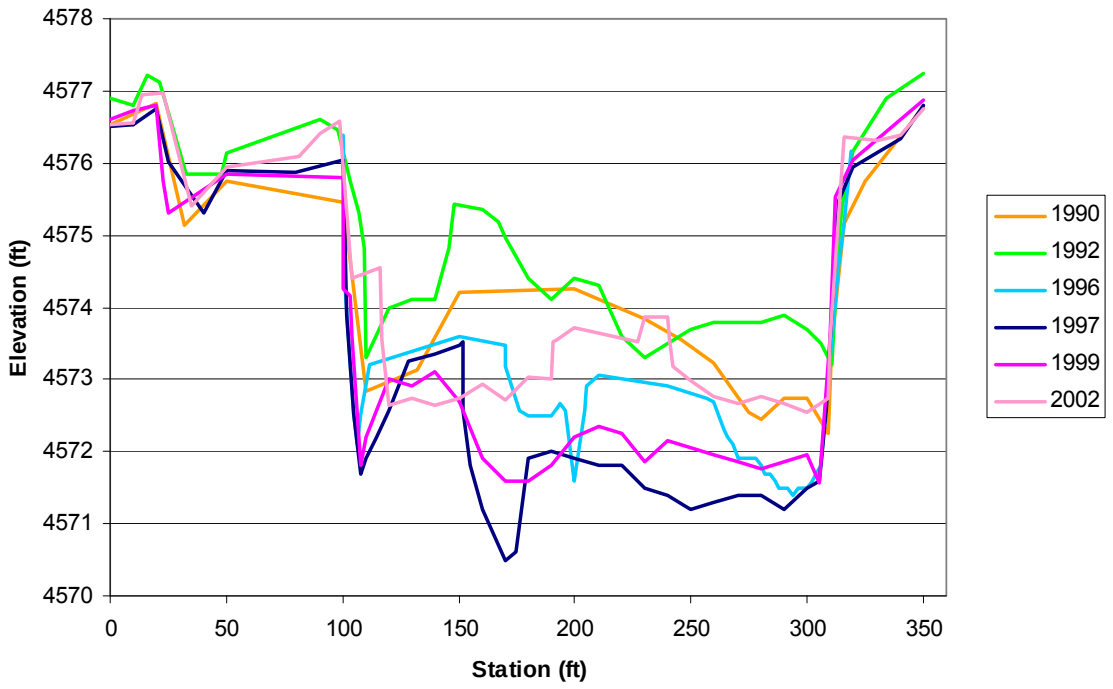

Figure A.17 Cross-section survey at SO-line 1401

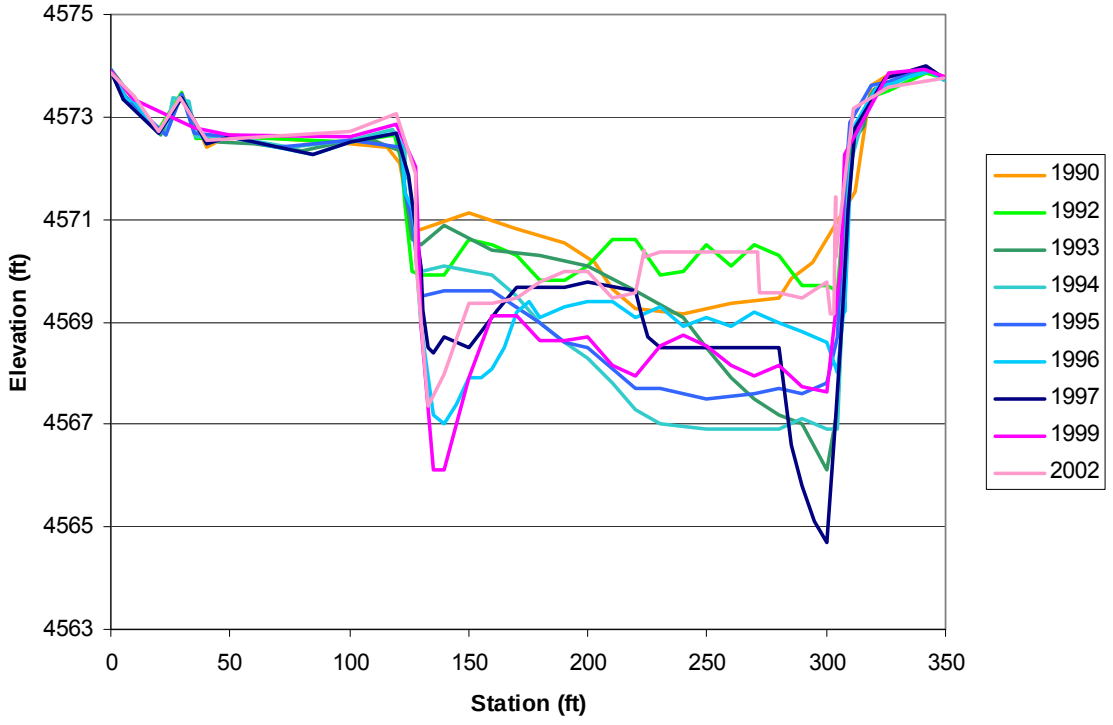

Figure A.18 Cross-section survey at SO-line 1410

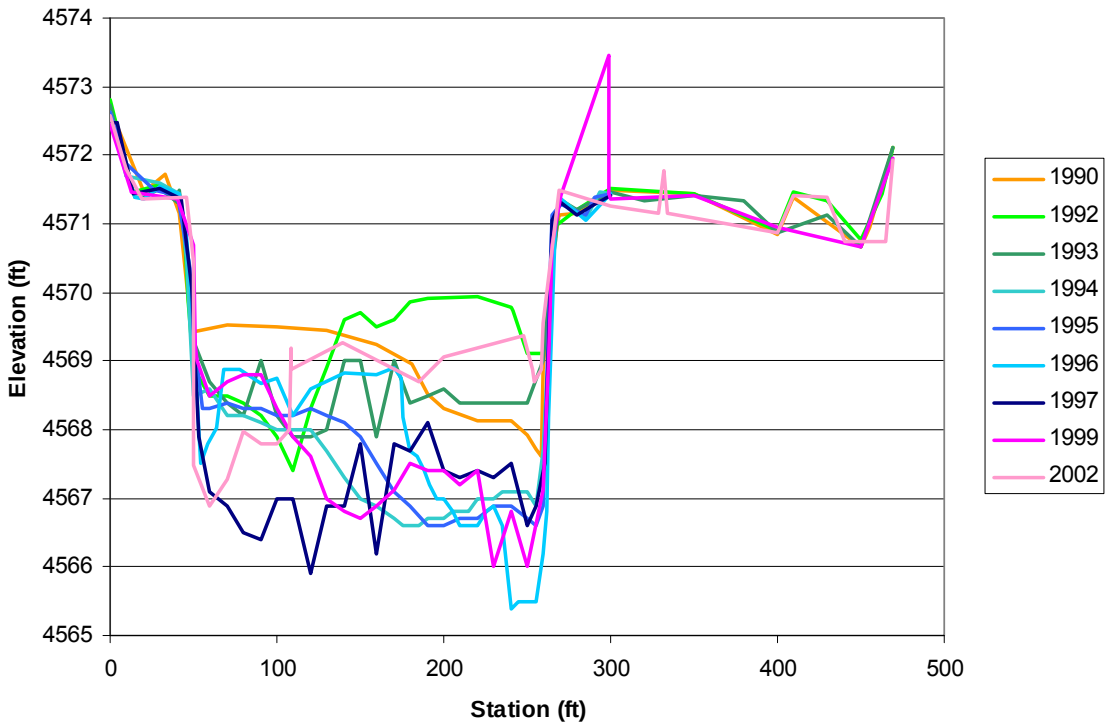

Figure A.19 Cross-section survey at SO-line 1414

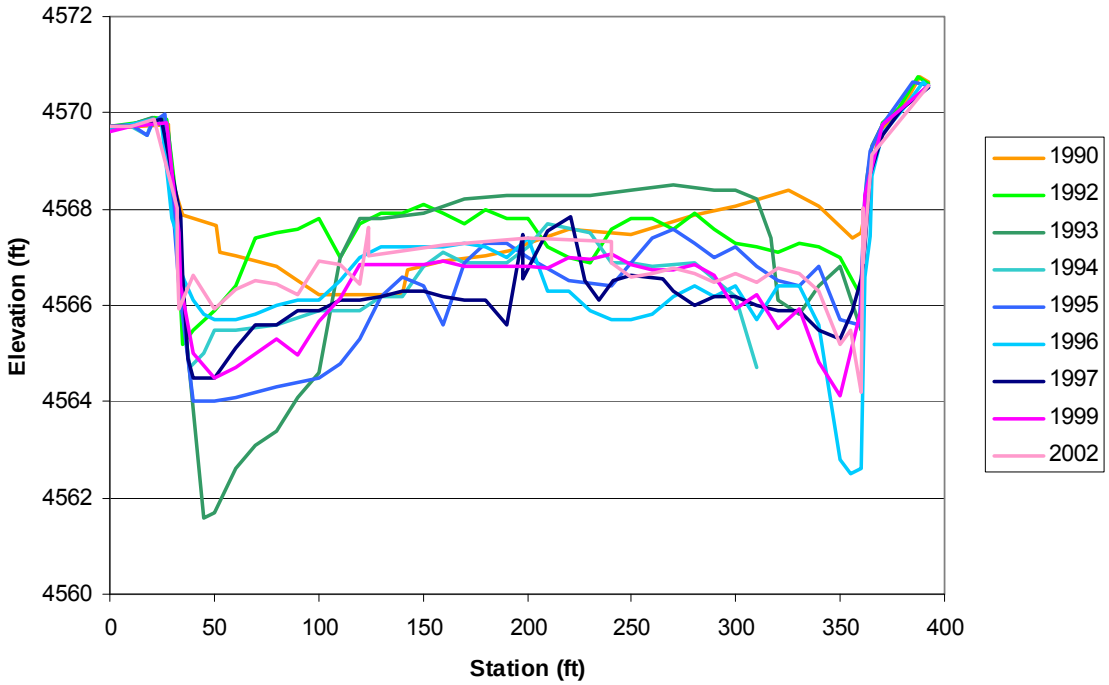

Figure A.20 Cross-section survey at SO-line 1420

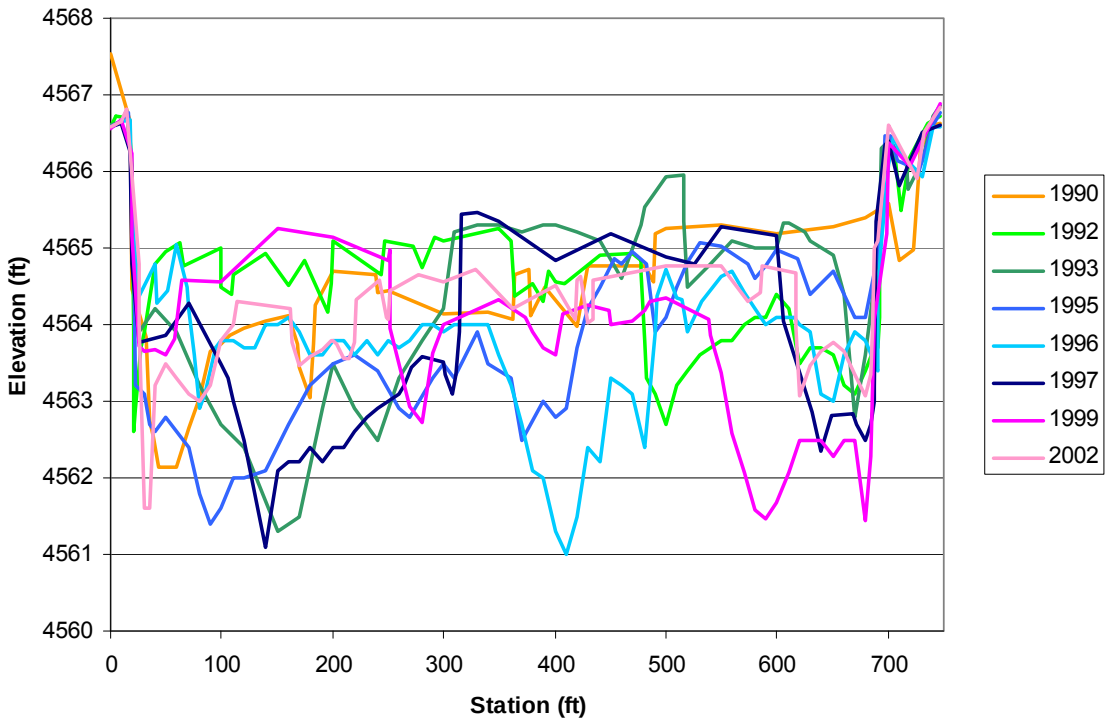

Figure A.21 Cross-section survey at SO-line 1428

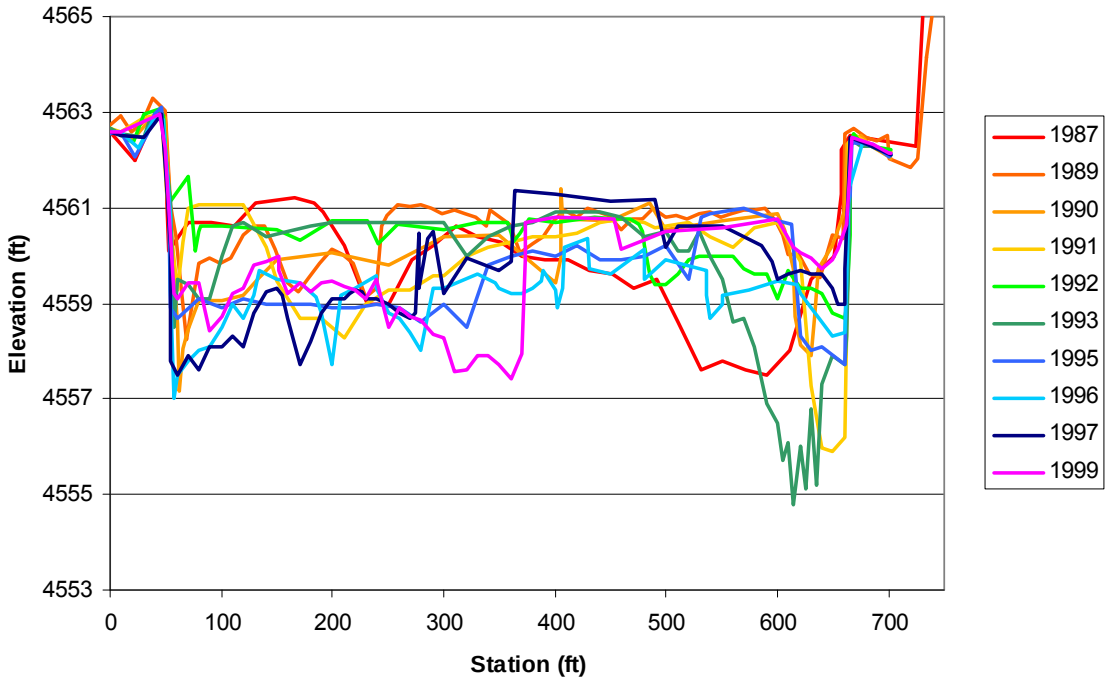

Figure A.22 Cross-section survey at SO-line 1437.9

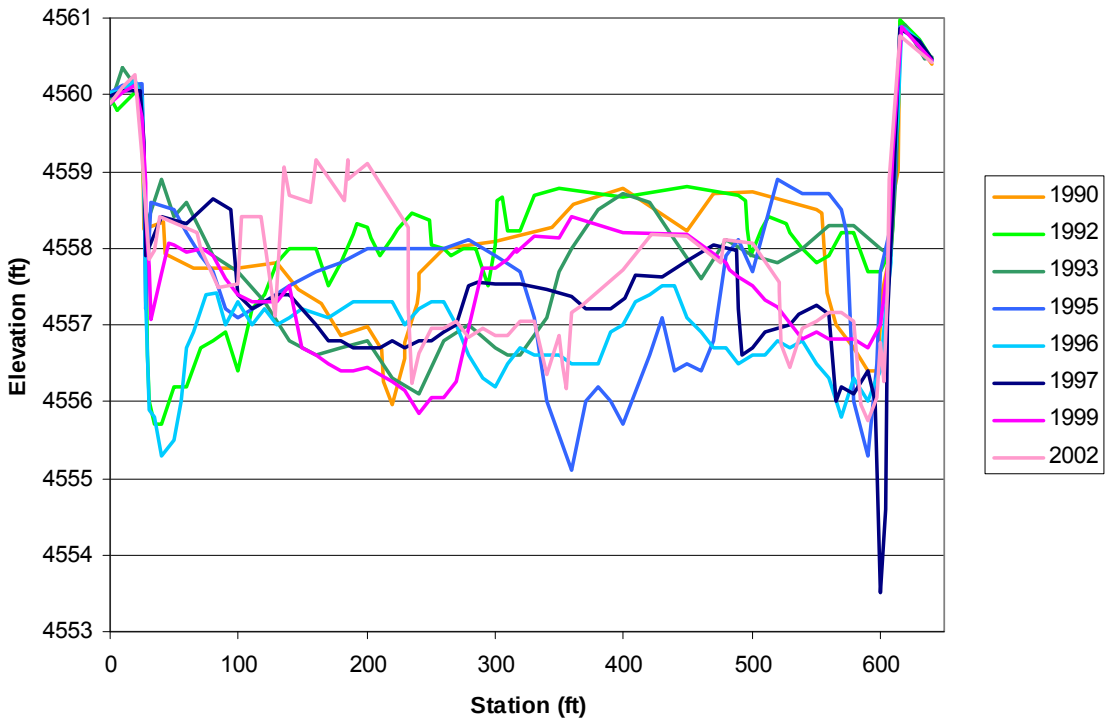

Figure A.23 Cross-section survey at SO-line 1443

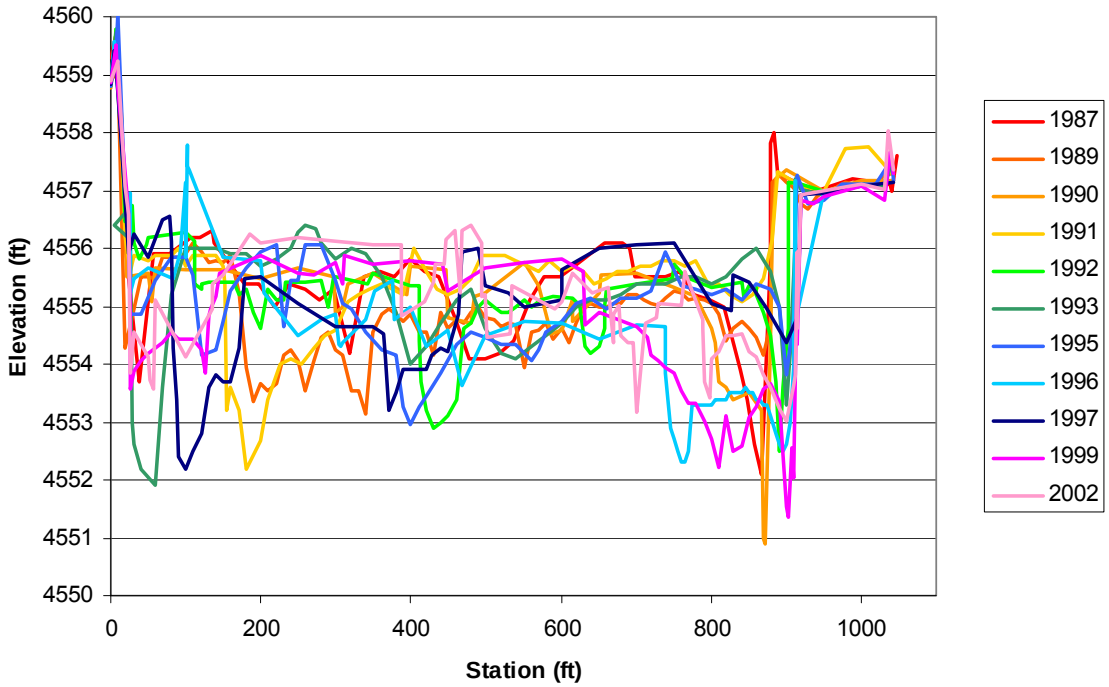

Figure A.24 Cross-section survey at SO-line 1450

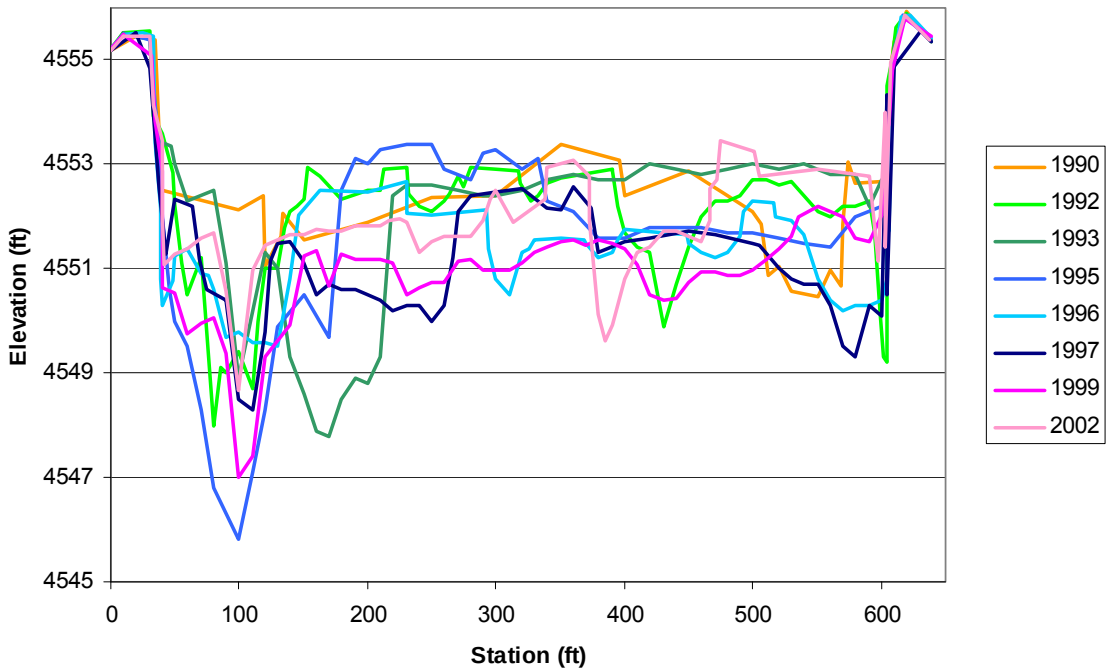

Figure A.25 Cross-section survey at SO-line 1456

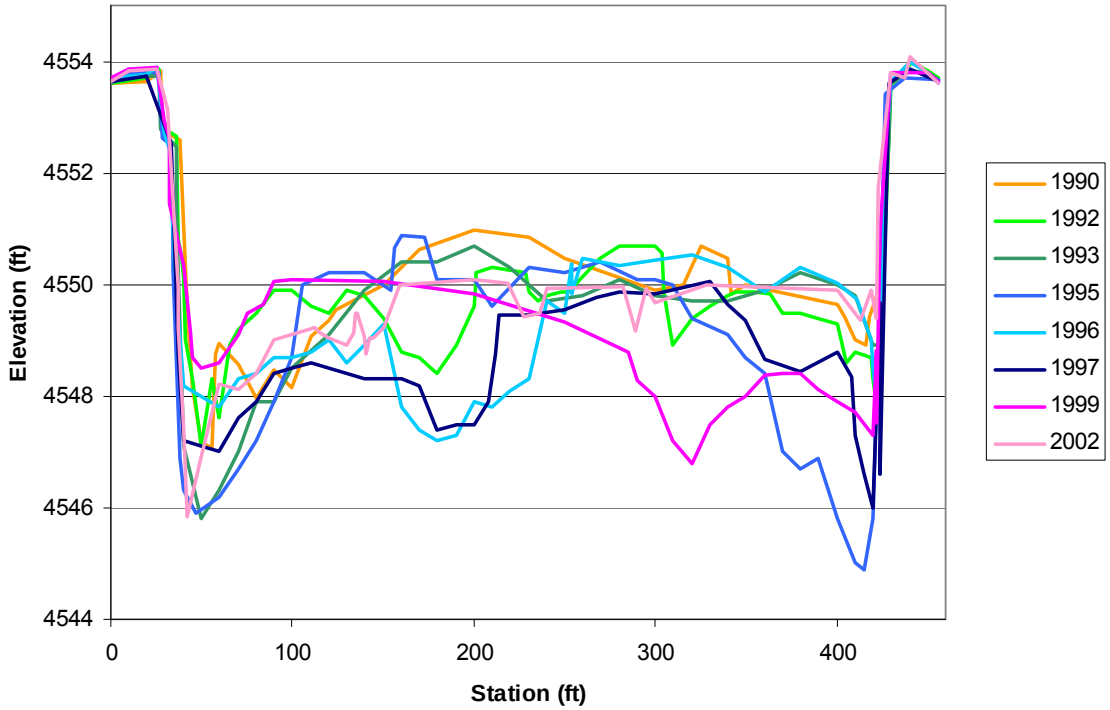

Figure A.26 Cross-section survey at SO-line 1462

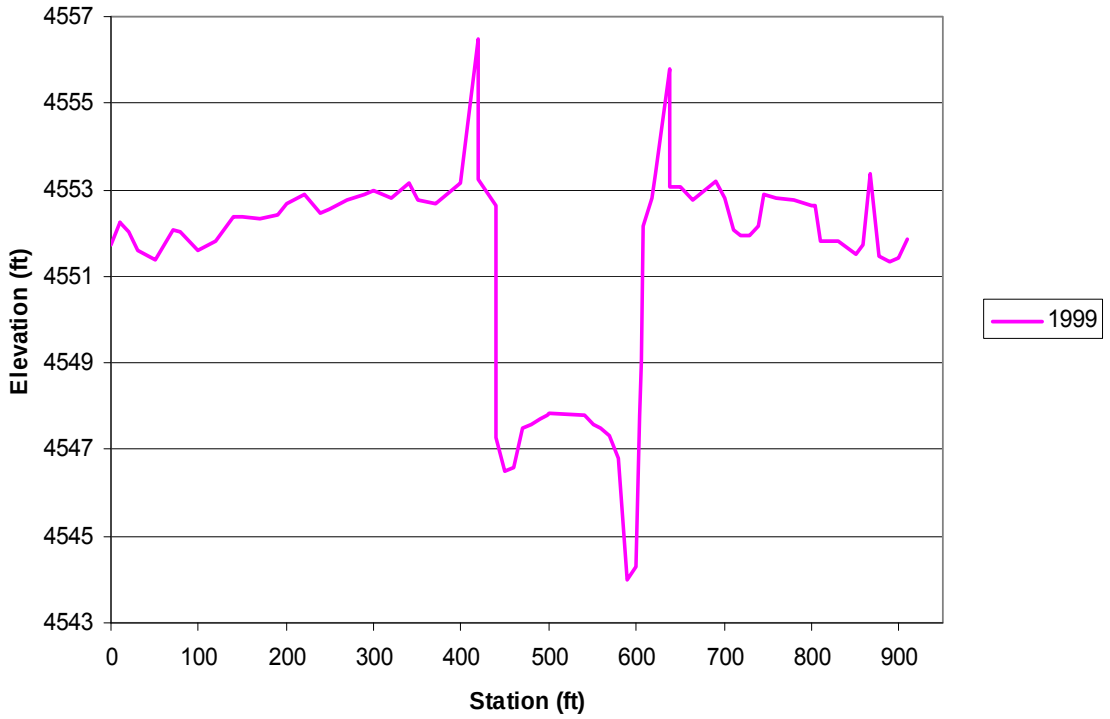

Figure A.27 Cross-section survey at SO-line 1464.5

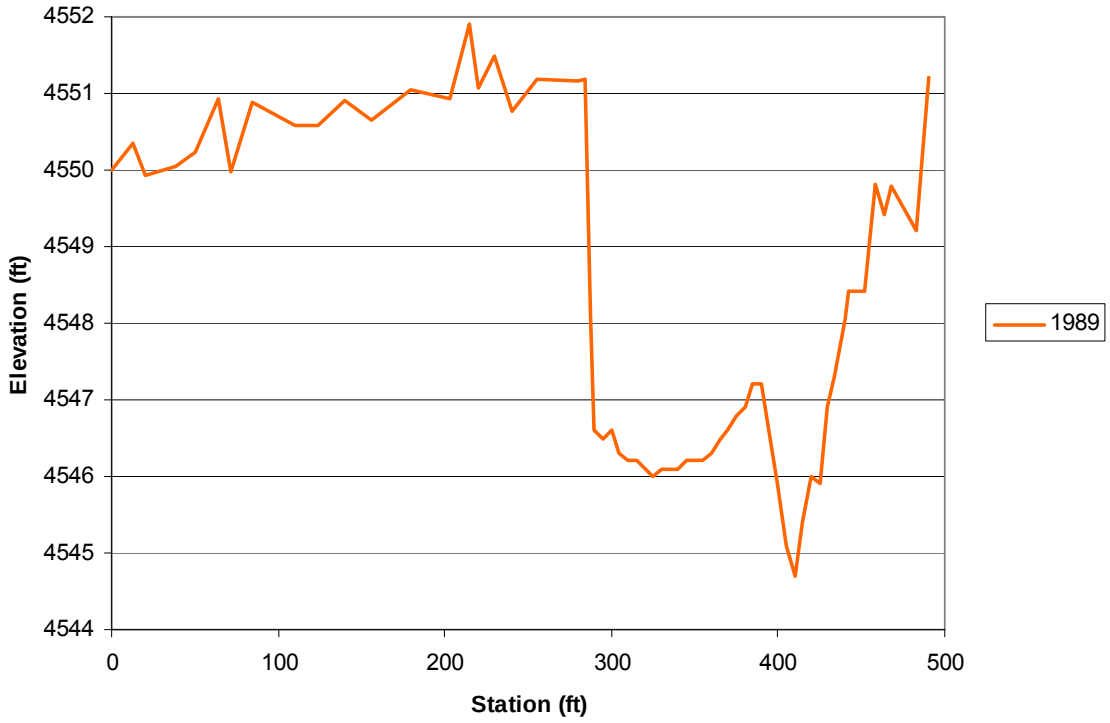

Figure A.28 Cross-section survey at SO-line 1469.5

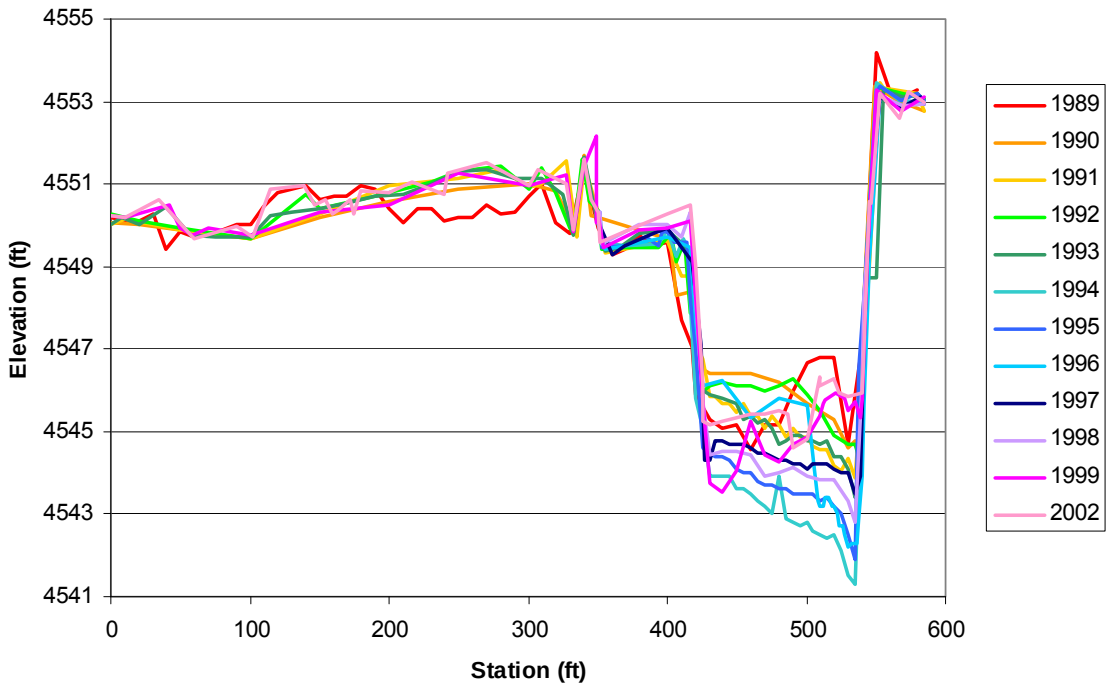

Figure A.29 Cross-section survey at SO-line 1470.5

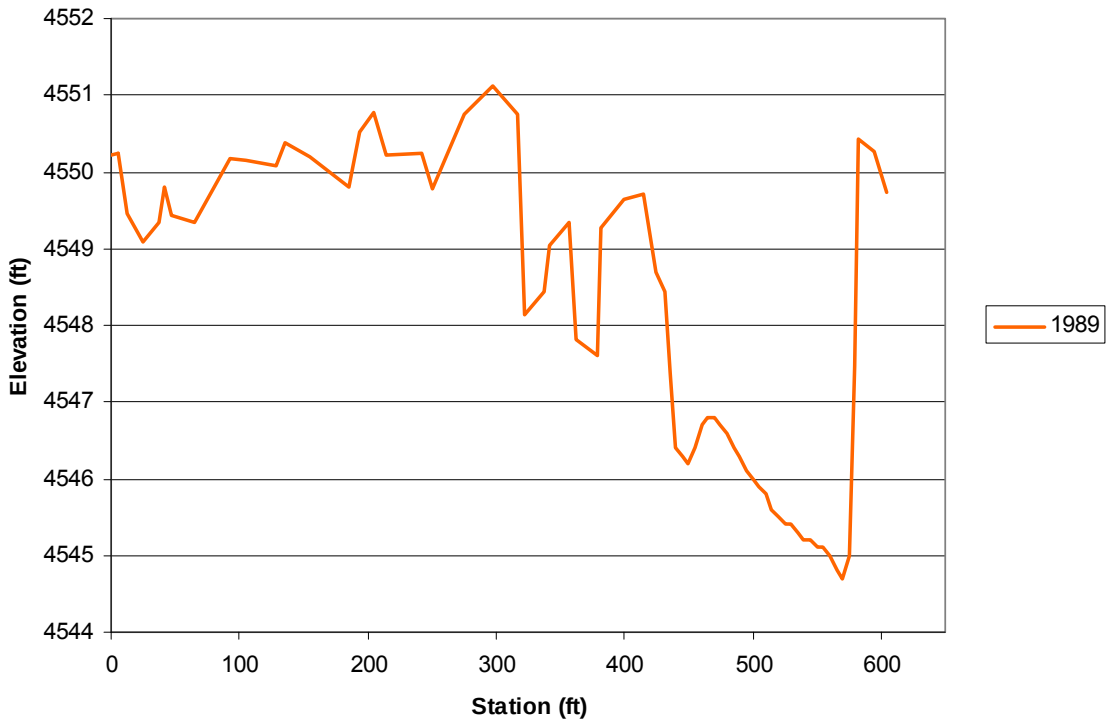

Figure A.30 Cross-section survey at SO-line 1471.2

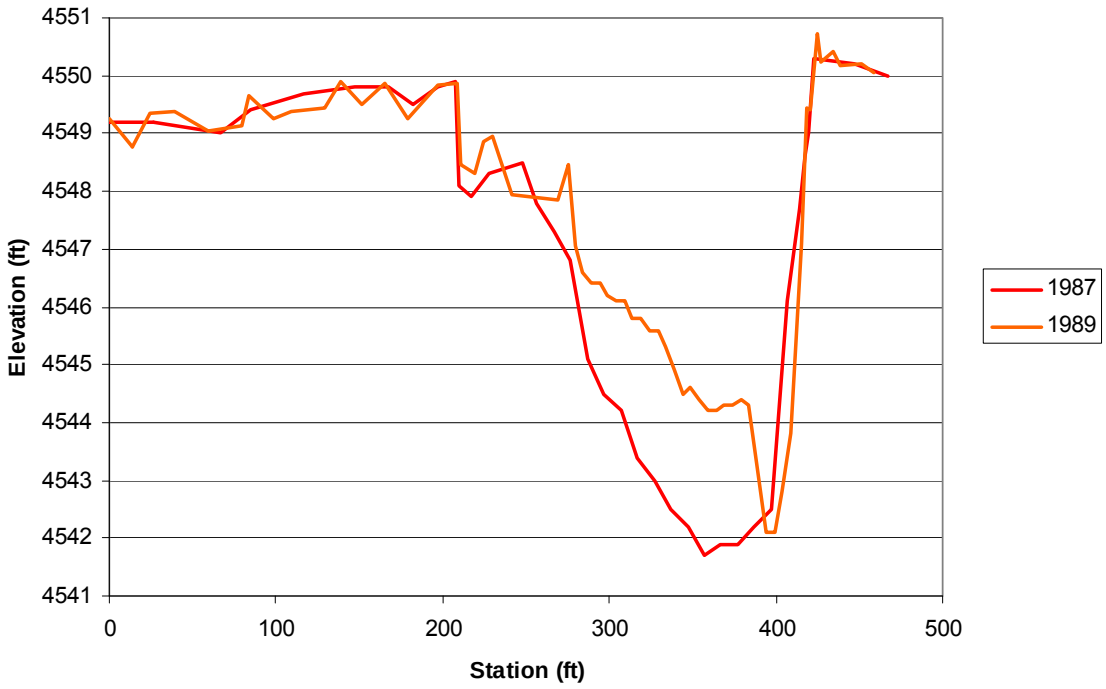

Figure A.31 Cross-section survey at SO-line 1472

Appendix B – Aerial Photography Information

Table B.1 Aerial photography survey dates and information

	Mean Daily Discharge			
Date	**San Acacia**	**San Marcial**	**Scale**	**Notes (1918-2002:from Novak 2006 2005: from ArcGIS metadata)**
1918	No Data	No Data	1:12,000	Hand-drafted linens (39 sheets). USBR Albuquerque Area Office. Surveyed in 1918. Published in 1922.
1935	No Data	No Data	1:8,00	Black and white photography. USBR Albuquerque Area Office. Flown in 1935. Published in 1936.
1949	No Data	No Data	1:5,000	Photo-mosaic. J-Ammann Photogrammetric Engineers, San Antonio, TX. USBR Albuquerque Area Office.
March 1962	25 cfs	0 cfs	1:4,800	Photo-mosaic. Abram Aerial Survey Corp, Lansing, MI. USBR Albuquerque Area Office.
April 1972	4 cfs	0 cfs	1:4,800	Photo-mosaic. Limbaugh Engineers, Inc., Albuquerque, NM. USBR Albuquerque Area Office.
March 1985	1900 cfs	1320 cfs	1:4,800	Orthophoto. M&I Consulting Engineers, Fort Collins, CO. Aero-Metric Engineering, Sheboygan, MN. USBR Albuquerque Area Office.
February 1992	1020 cfs	630 cfs	1:4,800	Ratio-rectified photo-mosaic. Koogle and Poules Engineering, Albuquerque, NM. USBR Albuquerque Area Office.
February 2001	770 cfs	560 cfs	1:4,800	Ratio-rectified photo-mosaic. Pacific Western Technologies, Ltd., Albuquerque, NM. USBR Albuquerque Area Office.
March 2002	310 cfs	150 cfs	1:4,800	Digital ortho-imagery. Pacific Western Technologies, Ltd., Albuquerque, NM. USBR Albuquerque Area Office.
April 2005	2270 cfs	1680 cfs	1:4,800	Digital ortho-rectified imagery. Aero-Metric, Inc., Fort Collins, Co. USBR Albuquerque Area Office.

Appendix C – HEC-RAS Model Output

1962
1972
1985
1992
2002

Table C.1 HEC-RAS output for 1962 geometry

HEC-RAS Plan: 1962(8-7-06) River: Middle Rio Grande Reach: Socorro Profile: PF 1

Agg/Deg #	Discharge	Min. Channel Elev.	W.S. Elev.	E.G. Elev.	E.G. Slope	Velocity	Flow Area	Top Width	Froude #	Frctn Slope	Hydr Radius	Wetted Perimeter	Hydr Depth
	(cfs)	(ft)	(ft)	(ft)	(ft/ft)	(ft/s)	(sq ft)	(ft)		(ft/ft)	(ft)	(ft)	(ft)
1313	5000	4610.8	4615.57	4616.04	0.001525	5.55	948.55	301.71	0.52	0.000873	3.13	303.47	3.14
1314	5000	4610.7	4615.29	4615.43	0.000565	3.26	2115.41	871.06	0.32	0.000462	2.43	872.05	2.43
1315	5000	4610.9	4615.12	4615.18	0.000385	2.74	3593.21	1396.01	0.26	0.000436	2.57	1399.44	2.57
1316	5000	4610.7	4614.92	4614.99	0.000498	2.81	3074.4	1169.95	0.29	0.000785	2.62	1172.92	2.63
1317	5000	4609.9	4614.31	4614.6	0.001418	4.7	1401.96	563.79	0.49	0.001703	2.48	565.21	2.49
1318	5000	4609.6	4613.37	4613.69	0.002085	4.69	1185.99	611.7	0.56	0.001869	1.93	613.84	1.94
1319	5000	4608.7	4612.52	4612.65	0.001686	3.35	2131.56	1489.74	0.48	0.001054	1.43	1492.73	1.43
1320	5000	4608.6	4612.01	4612.09	0.000721	2.65	2586.3	1474.03	0.33	0.000733	1.75	1475.92	1.75
1321	5000	4608.4	4611.64	4611.72	0.000744	2.49	2612.82	1471.74	0.33	0.001083	1.77	1474.01	1.78
1322	5000	4607.6	4611.01	4611.16	0.001717	3.42	1855.28	1449.29	0.49	0.001115	1.28	1450.18	1.28
1323	5000	4606.9	4610.49	4610.59	0.000782	2.63	2105.17	1293.4	0.34	0.000875	1.63	1294.4	1.63
1324	5000	4606.9	4610	4610.12	0.000986	3.03	2033.83	1211.97	0.38	0.001242	1.68	1213.53	1.68
1325	5000	4605.6	4609.29	4609.48	0.001611	3.51	1514.84	991.65	0.48	0.001081	1.53	992.55	1.53
1326	5000	4605.1	4608.79	4608.88	0.000776	2.46	2208.75	1413.86	0.33	0.001091	1.56	1414.56	1.56
1327	5000	4605.1	4608.16	4608.28	0.001646	2.81	1808.38	1607.33	0.46	0.001226	1.12	1607.98	1.13
1328	5000	4604.2	4607.58	4607.65	0.000948	2.24	2248.78	1779.35	0.35	0.001007	1.26	1780.2	1.26
1329	5000	4603.4	4607.06	4607.14	0.001072	2.26	2226.33	1915.85	0.37	0.000963	1.16	1917.28	1.16
1330	5000	4602.7	4606.55	4606.63	0.000869	2.23	2255.24	1680.59	0.34	0.001262	1.34	1682.74	1.34
1331	5000	4603.3	4605.84	4605.98	0.001997	3.02	1653.72	1447.28	0.5	0.001677	1.14	1447.76	1.14
1332	5000	4601.2	4605.06	4605.2	0.001428	2.99	1674.51	1161.07	0.44	0.001501	1.44	1162.48	1.44
1333	5000	4599.6	4604.37	4604.5	0.001581	2.9	1722.89	1345.04	0.45	0.001053	1.28	1345.87	1.28
1334	5000	4600.4	4603.89	4603.96	0.000752	2.06	2430.36	1820.33	0.31	0.000863	1.33	1821.22	1.34

1335	5000	4600.8	4603.47	4603.55	0.001001	2.14	2335.1	2041.55	0.35	0.000833	1.14	2042.45	1.14
1336	5000	4600	4603.08	4603.14	0.000704	1.89	2651.15	2153.26	0.3	0.000952	1.23	2154.78	1.23
1337	5000	4599.4	4602.6	4602.68	0.00136	2.37	2107.58	1988.85	0.41	0.00073	1.06	1989.5	1.06
1338	5000	4598.9	4602.28	4602.32	0.000454	1.68	2970.12	2060.53	0.25	0.000616	1.44	2061.53	1.44
1339	5000	4598.5	4601.95	4602.03	0.000883	2.24	2231.37	1658.15	0.34	0.000743	1.34	1659.35	1.35
1340	5000	4596.9	4601.61	4601.67	0.000634	2.12	2786.61	2018.11	0.3	0.000906	1.38	2020.23	1.38
1341	5000	4596.3	4601.07	4601.22	0.0014	3.15	1595.04	1023.58	0.44	0.001375	1.55	1026.96	1.56
1342	5000	4596.1	4600.45	4600.56	0.00135	2.68	1864.92	1461.06	0.42	0.001297	1.28	1462.59	1.28
1343	5000	4593.5	4599.79	4599.89	0.001247	2.58	1992.03	1794.2	0.4	0.001078	1.11	1800.45	1.11
1344	5000	4595.6	4599.23	4599.32	0.000941	2.32	2327.23	2176.72	0.35	0.000961	1.07	2178.71	1.07
1345	5000	4593.9	4598.74	4598.83	0.000982	2.4	2083.18	1511.62	0.36	0.000772	1.38	1513.9	1.38
1346	5000	4593.3	4598.37	4598.42	0.000623	1.89	2988.73	2746.23	0.29	0.000521	1.09	2749.54	1.09
1347	5000	4592.7	4598.09	4598.14	0.000443	1.75	2921.33	2023.98	0.25	0.00062	1.44	2026.83	1.44
1348	5000	4593.1	4597.64	4597.77	0.00093	2.92	1715.11	892.72	0.37	0.001136	1.92	893.91	1.92
1349	5000	4592.4	4596.99	4597.12	0.001418	3	1870.07	1642.06	0.44	0.001226	1.14	1643.96	1.14
1350	5000	4591.9	4596.35	4596.49	0.001071	2.99	1724.06	1313.12	0.45	0.001092	1.31	1315.43	1.31
1351	5000	4592.6	4595.89	4596.03	0.001113	3.07	1679.11	1387.34	0.46	0.00131	1.21	1388.08	1.21
1352	5000	4590.8	4595.27	4595.42	0.001564	3.12	1604.39	1464.84	0.52	0.001251	1.09	1468.71	1.1
1353	5000	4591.7	4594.68	4594.85	0.001023	3.27	1529.78	947.33	0.45	0.001604	1.61	948.2	1.61
1354	5000	4589.6	4593.71	4593.99	0.002868	4.26	1175	1061.24	0.71	0.001014	1.11	1062.24	1.11
1355	5000	4589.3	4593.32	4593.4	0.000514	2.24	2230.78	1465.45	0.32	0.000466	1.52	1466.16	1.52
1356	5000	4589.5	4593.1	4593.16	0.000425	2.04	2470.63	1636.76	0.29	0.00047	1.51	1637.96	1.51
1357	5000	4588.6	4592.83	4592.92	0.000523	2.36	2116.76	1291.54	0.33	0.000642	1.64	1292.18	1.64
1358	5000	4588.7	4592.43	4592.54	0.000807	2.75	1821.83	1234.65	0.4	0.000664	1.47	1235.42	1.48
1359	5000	4588.6	4592.14	4592.23	0.000556	2.48	2038.51	1238.18	0.34	0.000623	1.64	1239.53	1.65
1360	5000	4587.4	4591.79	4591.91	0.000704	2.78	1798.81	1078.3	0.38	0.001222	1.66	1080.65	1.67

1361	5000	4588.6	4590.99	4591.29	0.002628	4.39	1138.03	917.88	0.7	0.001193	1.24	918.55	1.24
1362	5000	4586.8	4590.48	4590.63	0.000678	3.08	1623.75	807.83	0.38	0.000525	2.01	808.72	2.01
1363	5000	4585.2	4590.22	4590.34	0.000418	2.73	1834.07	761.64	0.31	0.000547	2.4	762.93	2.41
1364	5000	4586.4	4589.89	4590.04	0.000746	3.15	1586.47	818.36	0.4	0.000356	1.94	819.53	1.94
1365	5000	4583.4	4589.76	4589.84	0.000208	2.27	2241.55	800.83	0.23	0.000289	2.79	803.12	2.8
1366	5000	4585.4	4589.54	4589.69	0.000429	3.08	1621.38	570.54	0.32	0.000441	2.84	571.66	2.84
1367	5000	4584.4	4589.29	4589.48	0.000453	3.43	1513.91	586.77	0.34	0.000322	2.57	588.3	2.58
1368	5000	4583.5	4589.18	4589.3	0.00024	2.82	1847.3	581.54	0.25	0.000347	3.17	582.9	3.18
1369	5000	4583.5	4588.89	4589.12	0.000545	3.9	1282.6	377.63	0.37	0.000486	3.37	380.86	3.4
1370	5000	4582.4	4588.69	4588.89	0.000435	3.56	1403.21	398.01	0.33	0.000561	3.49	402.4	3.53
1371	5000	4583.3	4588.28	4588.61	0.000751	4.63	1126.79	423.06	0.44	0.001053	2.65	425.02	2.66
1372	5000	4582.2	4587.59	4588.12	0.001585	5.8	861.7	310.81	0.61	0.001226	2.75	313.55	2.77
1373	5000	4582.2	4587.07	4587.44	0.000977	4.9	1037.09	405.84	0.49	0.000482	2.55	407.41	2.56
1374	5000	4581.6	4587.03	4587.15	0.000287	3.06	2880.83	1737.9	0.28	0.000562	1.66	1740.57	1.66
1375	5000	4580.5	4586.26	4586.85	0.001564	6.21	913.49	481.47	0.62	0.00095	1.88	486.31	1.9
1376	5000	4580.4	4586.01	4586.28	0.000638	4.34	1514.48	788.25	0.41	0.00071	1.92	789.8	1.92
1377	5000	4578.2	4585.62	4585.91	0.000796	4.54	1453.97	705.16	0.44	0.000855	2.05	710.88	2.06
1378	5000	4579.4	4585.15	4585.46	0.000921	4.56	1291.51	749.33	0.47	0.000632	1.72	751.69	1.72
1379	5000	4579.4	4584.99	4585.17	0.000461	3.5	1745.43	786.26	0.34	0.00064	2.21	788.64	2.22
1380	5000	4579.4	4584.57	4584.9	0.000947	4.63	1133.81	469.78	0.48	0.001075	2.41	470.79	2.41
1381	5000	4578.7	4584.08	4584.47	0.001229	5.01	1043.42	479	0.54	0.001292	2.17	481.05	2.18
1382	5000	4578.2	4583.48	4583.85	0.00136	4.85	1074.27	560.72	0.56	0.001012	1.91	562.16	1.92
1383	5000	4578.2	4583.18	4583.35	0.000782	3.26	1534.25	779.87	0.41	0.000658	1.96	780.86	1.97
1384	5000	4577.9	4582.91	4583.04	0.000562	2.88	1738.53	853.31	0.35	0.000772	2.03	855.77	2.04
1385	5000	4578.3	4582.41	4582.67	0.001128	4.1	1242.83	613.2	0.5	0.000679	2.02	614.53	2.03
1386	5000	4578	4582.19	4582.3	0.000454	2.72	1965.55	1025.71	0.32	0.000538	1.91	1026.68	1.92

1387	5000	4576.4	4581.9	4582.05	0.00065	3.15	1680.3	838.56	0.38	0.000556	2	840.86	2
1388	5000	4576.4	4581.64	4581.77	0.000482	2.87	1740.21	743.82	0.33	0.00057	2.34	744.75	2.34
1389	5000	4576.1	4581.25	4581.46	0.000684	3.68	1370.77	529.63	0.4	0.000557	2.58	531.72	2.59
1390	5000	4575.9	4580.98	4581.18	0.000462	3.73	1798.74	865.89	0.35	0.000796	2.07	868.37	2.08
1391	5000	4575.7	4580.22	4580.76	0.001686	6.16	1170.04	862.19	0.64	0.001	1.36	863.07	1.36
1392	5000	4574.9	4579.91	4580.16	0.000661	4.45	2028.4	1212.63	0.41	0.000612	1.67	1214.31	1.67
1393	5000	4574.3	4579.62	4579.85	0.000569	4.14	2018.38	1197.46	0.38	0.000586	1.68	1200.45	1.69
1394	5000	4573.8	4579.31	4579.55	0.000605	4.07	1562.24	857.86	0.39	0.00079	1.82	860.65	1.82
1395	5000	4573.9	4578.85	4579.17	0.001075	4.48	1116.62	443.47	0.5	0.000546	2.49	448.18	2.52
1396	5000	4572.9	4578.74	4578.86	0.00033	2.72	1946.29	880.17	0.28	0.0004	2.2	883.16	2.21
1397	5000	4572.2	4578.46	4578.65	0.000494	3.61	1698.13	746.24	0.35	0.00048	2.27	748.65	2.28
1398	5000	4572.6	4578.19	4578.4	0.000466	3.68	1461.94	590.55	0.35	0.000717	2.47	592.05	2.48
1399	5000	4572.2	4577.49	4578.01	0.00124	5.93	1021.75	470.23	0.56	0.001292	2.16	472.08	2.17
1400	5000	4572.5	4576.85	4577.32	0.001347	5.51	948.71	498.28	0.57	0.000997	1.9	499.76	1.9
1401	5000	4571.6	4576.48	4576.77	0.000767	4.36	1146.09	369.72	0.44	0.00035	3.09	371.31	3.1
1402	5000	4570.9	4576.45	4576.54	0.000199	2.51	2653.24	1133.78	0.23	0.000248	2.33	1137.98	2.34
1403	5000	4570.1	4576.32	4576.4	0.000316	2.71	3018.29	1168.63	0.28	0.000458	2.57	1172.42	2.58
1404	5000	4571.1	4575.84	4576.15	0.000724	4.47	1120.66	339.83	0.43	0.000933	3.28	341.25	3.3
1405	5000	4570.7	4575.25	4575.65	0.001248	5.13	980.68	388.03	0.55	0.001302	2.52	389.85	2.53
1406	5000	4570.2	4574.54	4574.98	0.001359	5.33	938.55	343.66	0.57	0.000229	2.71	345.93	2.73
1407	5000	4569.3	4574.73	4574.74	0.000091	1.64	7968.58	3562.84	0.15	0.000073	2.23	3566.02	2.24
1408	5000	4569.4	4574.7	4574.71	0.00006	1.28	9561.79	3562.69	0.12	0.000149	2.68	3565.62	2.68
1409	5000	4569.1	4574.22	4574.6	0.000826	4.99	1117.71	451.21	0.46	0.001586	2.47	453.11	2.48
1410	5000	4568.7	4572.56	4573.75	0.004205	8.74	573.57	254.59	0.98	0.000184	2.25	255.37	2.25
1411	5000	4567.7	4573.22	4573.23	0.000057	1.25	10146.49	4009.95	0.12	0.000135	2.53	4012.2	2.53
1412	5000	4567.7	4572.89	4573.14	0.000624	4.1	1352.77	501.17	0.4	0.000552	2.69	502.86	2.7

1413	5000	4567.2	4572.61	4572.85	0.000492	4.02	1392.79	477.54	0.36	0.000455	2.9	479.71	2.92
1414	5000	4566.9	4572.44	4572.59	0.000421	3.19	1719.82	669.8	0.32	0.000479	2.56	672.13	2.57
1416	5000	4566.8	4572.08	4572.34	0.000549	4.11	1274.67	406.78	0.38	0.000475	3.12	408.26	3.13
1417	5000	4565.5	4571.89	4572.09	0.000415	3.61	1427.21	454.67	0.33	0.000614	3.12	457.52	3.14
1418	5000	4566.3	4571.43	4571.77	0.000999	4.83	1297.01	776.41	0.49	0.001133	1.67	778.3	1.67
1419	5000	4566.6	4570.78	4571.16	0.001295	5.03	1122.98	558.39	0.55	0.001104	2.01	559.25	2.01
1420	5000	4565.6	4570.31	4570.57	0.000952	4.29	1437.41	715.58	0.47	0.001064	2.01	716.74	2.01
1421	5000	4565.3	4569.69	4570	0.001196	4.5	1116.85	489.54	0.52	0.001403	2.28	490.77	2.28
1422	5000	4564.7	4568.83	4569.21	0.001668	5.06	1199.36	741.13	0.61	0.001667	1.62	742.32	1.62
1423	5000	4562.2	4567.86	4568.22	0.001666	4.89	1090.23	586.59	0.6	0.001106	1.85	589.94	1.86
1424	5000	4563	4567.33	4567.47	0.000787	3.02	1718.76	1073.46	0.4	0.000693	1.6	1074.67	1.6
1425	5000	4563.1	4566.93	4567.03	0.000615	2.49	2008.71	1278.33	0.35	0.000681	1.57	1279.45	1.57
1426	5000	4562.8	4566.56	4566.69	0.000758	2.94	1805.98	1174.87	0.39	0.000375	1.53	1177.06	1.54
1427	5000	4562.2	4566.39	4566.46	0.000223	2.05	2433.81	966.15	0.23	0.0003	2.52	967.09	2.52
1428	5000	4561.2	4566.16	4566.3	0.000425	2.96	1747.67	684.65	0.32	0.000437	2.54	687.52	2.55
1429	5000	4560.3	4565.92	4566.07	0.000449	3.16	1644.9	618.57	0.33	0.000666	2.65	620.98	2.66
1430	5000	4559.8	4565.41	4565.71	0.001088	4.41	1171.7	513.2	0.5	0.00063	2.28	514.47	2.28
1431	5000	4559.6	4565.18	4565.34	0.000411	3.14	1591.88	527.26	0.32	0.000492	3.01	528.21	3.02
1432	5000	4559.2	4564.8	4565.06	0.000601	4.08	1225.88	364.95	0.39	0.000699	3.35	365.67	3.36
1433	5000	4558.7	4564.34	4564.68	0.000825	4.68	1069.32	329.42	0.46	0.000939	3.23	331.48	3.25
1434	5000	4558.5	4563.81	4564.2	0.001078	5.05	1004.24	435.86	0.51	0.000808	2.29	437.88	2.3
1435	5000	4558	4563.48	4563.73	0.000629	3.97	1263.68	439.66	0.4	0.000765	2.86	441.29	2.87
1436	5000	4557.7	4563.02	4563.31	0.000951	4.32	1159.88	447.56	0.47	0.000812	2.57	451.06	2.59
1437	5000	4557.4	4562.61	4562.86	0.000701	3.99	1254.49	436.5	0.41	0.000635	2.86	438.33	2.87
1438	5000	4556.4	4562.31	4562.51	0.000578	3.64	1391.58	538.63	0.38	0.000449	2.57	541.33	2.58
1439	5000	4556.3	4562.11	4562.26	0.000359	3.08	1675.54	549.25	0.3	0.000646	3.04	550.36	3.05

1440	5000	4556.2	4561.23	4561.87	0.001495	6.46	813.6	270.64	0.62	0.0006	2.98	272.64	3.01
1441	5000	4555.6	4561.3	4561.41	0.000322	3.33	3522.16	1944.45	0.29	0.000583	1.81	1946.37	1.81
1442	5000	4555.7	4560.61	4561.09	0.001369	5.55	905.73	330.19	0.58	0.001416	2.73	331.29	2.74
1443	5000	4555.5	4559.91	4560.35	0.001465	5.34	955.07	438.55	0.59	0.001307	2.17	439.51	2.18
1444	5000	4554.9	4559.37	4559.68	0.001172	4.46	1120.56	481.53	0.52	0.001376	2.32	482.39	2.33
1445	5000	4554.5	4558.66	4558.95	0.001637	4.29	1165.65	682.05	0.58	0.001273	1.7	683.73	1.71
1446	5000	4553.6	4558.04	4558.29	0.001018	4.03	1239.53	556.7	0.48	0.000929	2.22	558.3	2.23
1447	5000	4553	4557.59	4557.81	0.000851	3.77	1408.45	689.74	0.44	0.000803	2.04	690.95	2.04
1448	5000	4552	4557.18	4557.41	0.000758	3.81	1313.08	515.16	0.42	0.000584	2.54	517.01	2.55
1449	5000	4551.9	4556.95	4557.12	0.000464	3.24	1542.32	531.8	0.34	0.000561	2.88	534.89	2.9
1450	5000	4552	4556.69	4556.85	0.000693	3.18	1571.88	755.33	0.39	0.000547	2.07	757.67	2.08
1451	5000	4550.7	4556.45	4556.58	0.000443	2.83	1814.85	763.88	0.32	0.000306	2.37	766.35	2.38
1452	5000	4551.4	4556.34	4556.4	0.000224	2.15	2936.52	1204.6	0.23	0.000315	2.43	1206.47	2.44
1453	5000	4551.3	4556.1	4556.24	0.000476	3.08	1740.07	708.91	0.33	0.00052	2.44	711.92	2.45
1454	5000	4550.5	4555.82	4555.98	0.000571	3.33	1937.65	1433.5	0.37	0.000549	1.35	1435.65	1.35
1455	5000	4550.6	4555.52	4555.72	0.000528	3.61	1482.13	558.73	0.36	0.000476	2.65	560.16	2.65
1456	5000	4550.9	4555.31	4555.48	0.000432	3.25	1611.94	601.55	0.33	0.000725	2.67	602.62	2.68
1457	5000	4550.3	4554.6	4555.1	0.001462	5.69	919.57	458.21	0.59	0.000041	2	460.08	2.01
1458	5000	4550.1	4554.93	4554.93	0.000012	0.6	18959.91	5313.99	0.06	0.000012	3.57	5316.43	3.57
1459	5000	4550.1	4554.93	4554.93	0.000012	0.56	19043.94	5323.2	0.06	0.000044	3.58	5325.66	3.58
1460	5000	4549.9	4553.96	4554.82	0.003073	7.78	914.06	687.07	0.85	0.000028	1.33	688.27	1.33
1461	5000	4549.9	4554.36	4554.36	0.000008	0.48	23078.19	5768.61	0.04	0.000028	4	5770.98	4
1462	5000	4549.7	4552.51	4554.18	0.006689	10.45	515.83	304.76	1.22	0.000065	1.69	305.9	1.69
1463	5000	4549.2	4552.39	4552.39	0.000018	0.63	17484.53	5588.97	0.07	0.000013	3.13	5590.44	3.13
1464	5000	4548.3	4552.38	4552.38	0.00001	0.47	20802.79	5588.35	0.05	0.000009	3.72	5590.27	3.72
1465	5000	4548.2	4552.38	4552.38	0.000008	0.45	22550.46	5594.13	0.04	0.000008	4.03	5596.49	4.03

1466	5000	4547.7	4552.38	4552.38	0.000009	0.53	21818.23	5716.61	0.05	0.00001	3.82	5718.48	3.82
1467	5000	4547.8	4552.37	4552.37	0.000012	0.57	19538.56	5440.42	0.05	0.000042	3.59	5442.72	3.59
1468	5000	4547.7	4550.93	4552.22	0.004183	9.11	548.84	209.54	0.99	0.000108	2.61	210.25	2.62
1469	5000	4547.5	4551.4	4551.41	0.000032	0.86	13642.11	4732.27	0.09	0.000029	2.88	4734.18	2.88
1470	5000	4547.4	4551.39	4551.39	0.000026	0.82	13821.17	4216.51	0.08	0.000031	3.28	4218.26	3.28
1471	5000	4546.8	4551.37	4551.38	0.000038	1.1	11079.49	3372.58	0.1	0.000125	3.28	3373.93	3.29
1472	5000	4546.3	4549.85	4551.18	0.003857	9.26	557.44	225.77	0.97	0.000614	2.46	226.5	2.47
1473	5000	4546.2	4549.36	4549.38	0.000239	1.82	5510.32	2668.38	0.23	0.00026	2.06	2669.25	2.07
1474	5000	4546.1	4549.23	4549.26	0.000284	2.11	5039.72	2473	0.25	0.000286	2.04	2473.68	2.04
1475	5000	4545.9	4549.07	4549.09	0.000287	2.12	5513.46	3061.9	0.25	0.000555	1.8	3063.27	1.8
1476	5000	4545	4548.24	4548.72	0.001501	5.71	1132.87	767.55	0.6		1.47	768.3	1.48

Table C.2 HEC-RAS output for 1972 geometry

HEC-RAS Plan: 1972(8-7-06) River: Middle Rio Grande Reach: Socorro Profile: PF 1

Agg/Deg #	Discharge	Min. Channel Elev.	W.S. Elev.	E.G. Elev.	E.G. Slope	Velocity	Flow Area	Top Width	Froude #	Frctn Slope	Hydr Radius	Wetted Perimeter	Hydr Depth
	(cfs)	(ft)	(ft)	(ft)	(ft/ft)	(ft/s)	(sq ft)	(ft)		(ft/ft)	(ft)	(ft)	(ft)
1313	5000	4611.3	4616.02	4617.37	0.004129	9.37	611.54	291.61	0.87	0.001404	2.09	292.78	2.1
1314	5000	4609.5	4616.02	4616.2	0.000699	4.14	3116.85	1302.48	0.36	0.000635	2.39	1305.61	2.39
1315	5000	4609.9	4615.74	4615.88	0.000579	3.87	3910.56	1404.76	0.33	0.000581	2.77	1409.75	2.78
1316	5000	4610.5	4615.49	4615.61	0.000583	3.79	4185.73	1455.91	0.33	0.00054	2.87	1460.58	2.87
1317	5000	4610	4615.26	4615.36	0.000501	3.55	4514.7	1498.46	0.31	0.000882	3.01	1502.07	3.01
1318	5000	4609.3	4614.33	4614.86	0.001951	6.16	1238.44	520.97	0.59	0.001028	2.36	523.98	2.38
1319	5000	4607.9	4614.09	4614.21	0.000633	3.49	3666.07	1491.06	0.33	0.000962	2.45	1496.89	2.46
1320	5000	4606.7	4613.24	4613.68	0.001632	5.5	1226.42	533.81	0.53	0.000909	2.29	536.47	2.3
1321	5000	4607.2	4613.01	4613.11	0.000578	2.99	3538.51	1491.69	0.31	0.000948	2.37	1495.42	2.37
1322	5000	4608.1	4612.17	4612.61	0.001835	5.32	945.19	344.63	0.56	0.001128	2.72	346.97	2.74
1323	5000	4607.7	4611.8	4611.96	0.000763	3.18	1572.69	622.9	0.35	0.000623	2.52	624.29	2.52
1324	5000	4607	4611.51	4611.61	0.000519	2.65	2232.15	937.98	0.29	0.00071	2.37	939.95	2.38
1325	5000	4606.7	4611.03	4611.24	0.00103	3.91	1807.3	757.29	0.41	0.001221	2.38	758.31	2.39
1326	5000	4606.3	4610.31	4610.59	0.001469	4.38	1566.38	783.08	0.49	0.001395	2	785.01	2
1327	5000	4605.4	4609.63	4609.78	0.001326	3.21	1636.46	1003.86	0.43	0.00124	1.63	1005.1	1.63
1328	5000	4605.1	4609.04	4609.15	0.001162	2.65	1932.91	1414.4	0.39	0.001119	1.36	1416.26	1.37
1329	Cross-section removed - incorrect geometry data												
1330	5000	4604	4607.92	4608.02	0.001078	2.46	2171.43	1703.87	0.38	0.001167	1.27	1707.88	1.27
1331	5000	4602.4	4607.3	4607.42	0.001269	2.81	1830.38	1323.62	0.41	0.001341	1.38	1325.09	1.38
1332	5000	4601.2	4606.63	4606.78	0.001419	3.15	1914.09	1373	0.44	0.001425	1.39	1375.03	1.39
1333	5000	4601.6	4605.96	4606.1	0.001431	2.99	1699.96	1215.68	0.44	0.00106	1.4	1218.48	1.4
1334	5000	4601.4	4605.41	4605.49	0.000816	2.23	2335.16	1651.03	0.33	0.000688	1.41	1653.29	1.41

1335	5000	4600.4	4605.09	4605.15	0.000588	2	2719.71	1949.25	0.28	0.000411	1.39	1952	1.4
1336	5000	4599.9	4604.89	4604.95	0.000304	1.84	2754.17	1253.82	0.22	0.000521	2.19	1256.38	2.2
1337	5000	4600.6	4604.56	4604.69	0.00109	2.92	1784.04	1090.12	0.39	0.001369	1.63	1091.85	1.64
1338	5000	4600.2	4603.8	4604.03	0.001769	3.83	1373.12	853.31	0.5	0.001649	1.6	856.37	1.61
1339	5000	4599.9	4603.05	4603.23	0.001541	3.7	2559.14	2103.33	0.48	0.001103	1.22	2106.17	1.22
1340	5000	4598.6	4602.55	4602.7	0.000828	3.36	2531.66	1594.25	0.37	0.000924	1.59	1596.52	1.59
1341	5000	4598	4601.9	4602.05	0.001038	3.11	1682.3	906.64	0.39	0.000881	1.85	907.23	1.86
1342	5000	4596.9	4601.41	4601.5	0.000757	2.49	2170.42	1302.09	0.33	0.000964	1.66	1303.69	1.67
1343	5000	4595.9	4600.86	4600.95	0.001269	2.66	3235.96	2733.42	0.41	0.000854	1.18	2735.33	1.18
1344	5000	4595	4600.42	4600.47	0.000614	2.17	4666.91	3396.84	0.29	0.001252	1.37	3399.7	1.37
1345	5000	4595	4599.33	4599.75	0.003834	5.26	951.41	591.99	0.73	0.001605	1.61	592.73	1.61
1346	5000	4594.5	4598.68	4598.78	0.000877	2.69	2638.62	1767.12	0.36	0.000791	1.49	1768.19	1.49
1347	5000	4593.1	4598.28	4598.36	0.000717	2.35	2683.65	1864.1	0.32	0.00088	1.44	1865.77	1.44
1348	5000	4593.2	4597.74	4597.87	0.001104	2.85	1755.15	1075.94	0.39	0.000885	1.63	1077	1.63
1349	5000	4592.9	4597.29	4597.39	0.000725	2.5	2002.34	1091.03	0.32	0.000379	1.83	1092.76	1.84
1350	5000	4592.4	4597.13	4597.18	0.000232	1.84	2712.99	1305.5	0.23	0.000238	2.08	1306.81	2.08
1351	5000	4591.8	4597.03	4597.08	0.000243	1.87	3538.29	2203.09	0.23	0.000204	1.6	2205.1	1.61
1352	5000	4590.8	4596.94	4596.98	0.000174	1.72	4119.34	2310.09	0.2	0.000118	1.78	2311.56	1.78
1353	5000	4590.4	4596.88	4596.92	0.000085	1.74	5316.21	2448.03	0.15	0.000108	2.17	2449.73	2.17
1354	5000	4591.1	4596.8	4596.85	0.000141	2.01	5405.14	2450.42	0.19	0.000194	2.2	2452.86	2.21
1355	5000	4591.4	4596.6	4596.72	0.000286	2.85	1921.66	663.67	0.27	0.000264	2.89	664.91	2.9
1356	5000	4590.4	4596.51	4596.6	0.000244	2.79	4397.85	2153.96	0.25	0.000392	2.04	2156.75	2.04
1357	5000	4591.2	4596.16	4596.44	0.000729	4.53	2241.12	1260.36	0.43	0.001198	1.78	1262.32	1.78
1358	5000	4590.2	4594.65	4595.64	0.002327	8.32	1169.25	982.78	0.78	0.001924	1.19	984.65	1.19
1359	5000	4588.3	4593.97	4594.62	0.001618	6.85	1668.16	1355.25	0.65	0.001247	1.23	1357.62	1.23
1360	5000	4588.6	4593.44	4593.82	0.000991	5.6	2597.26	1478.05	0.51	0.000831	1.75	1481.18	1.76
1361	5000	4587.1	4593.1	4593.35	0.000707	4.64	3260.76	1770.83	0.43	0.000663	1.84	1775.29	1.84

1362	5000	4586.7	4592.8	4592.97	0.000624	4.32	4460.67	2279.76	0.4	0.000457	1.95	2286.2	1.96
1363	5000	4587	4592.63	4592.71	0.000349	3.21	5819.4	2479.88	0.3	0.000844	2.34	2484.61	2.35
1364	5000	4586.8	4590.98	4592.17	0.004266	8.75	571.25	234.44	0.99	0.001235	2.42	235.82	2.44
1365	5000	4583	4590.36	4590.54	0.000578	3.77	3316.84	2277.36	0.38	0.000489	1.45	2285.59	1.46
1366	5000	4584.3	4590.18	4590.3	0.000419	2.98	3393.56	1886.24	0.32	0.000314	1.8	1889.14	1.8
1367	5000	4585.3	4590.07	4590.14	0.000244	2.27	3936.17	1991.32	0.24	0.000261	1.98	1992.32	1.98
1368	5000	4585.2	4589.93	4590.01	0.000279	2.47	3530.14	1770.29	0.26	0.000263	1.99	1771.98	1.99
1369	5000	4584.6	4589.79	4589.89	0.000249	2.68	3098.48	1424.73	0.25	0.000253	2.17	1426.72	2.17
1370	5000	4583.5	4589.65	4589.77	0.000258	2.88	3159.28	1405.76	0.26	0.000399	2.24	1408.2	2.25
1371	5000	4583.9	4589.25	4589.56	0.000696	4.5	1219.93	479.54	0.42	0.000685	2.53	481.57	2.54
1372	5000	4583.8	4588.95	4589.25	0.000675	4.67	2307.1	1262.51	0.42	0.000542	1.82	1266.47	1.83
1373	5000	4582.3	4588.73	4588.94	0.000445	4.01	3204.4	1721.78	0.35	0.000426	1.86	1723.76	1.86
1374	5000	4582.5	4588.56	4588.74	0.000409	3.7	3205.69	1857.39	0.33	0.000459	1.72	1860.49	1.73
1375	5000	4582.4	4588.26	4588.52	0.000519	4.41	2961.01	2224.88	0.38	0.000789	1.33	2227.55	1.33
1376	5000	4581.7	4587.53	4588.07	0.001344	6.78	2161.41	1190.12	0.6	0.001317	1.81	1192.76	1.82
1377	5000	4581.2	4586.87	4587.39	0.001291	6.53	2034.48	1116.97	0.59	0.00112	1.82	1118.91	1.82
1378	5000	4580.4	4586.35	4586.78	0.00098	5.78	2156.55	1410.44	0.51	0.000977	1.53	1413.39	1.53
1379	5000	4580.4	4586	4586.38	0.000974	5.52	2080.8	878.81	0.51	0.000876	2.36	882.41	2.37
1380	5000	4580.3	4585.68	4586.02	0.000792	5.01	1893.21	813.73	0.46	0.000483	2.32	816.4	2.33
1381	5000	4579.6	4585.63	4585.76	0.000325	3.31	3735.14	1868.77	0.3	0.000452	1.99	1873.3	2
1382	5000	4579	4585.25	4585.54	0.000671	4.38	1576.17	670.55	0.42	0.000595	2.34	673.01	2.35
1383	5000	4579	4585	4585.24	0.000532	4	1456.28	543.31	0.37	0.000873	2.67	545.42	2.68
1384	5000	4578.4	4584.32	4584.82	0.001689	5.74	1060.34	495.81	0.63	0.001376	2.12	499.19	2.14
1385	5000	4578.1	4583.7	4584.13	0.001143	5.27	1005.83	454.76	0.53	0.00072	2.21	455.8	2.21
1386	5000	4577.3	4583.5	4583.68	0.000495	3.66	2762.7	1793.26	0.35	0.000545	1.54	1798.32	1.54
1387	5000	4577.5	4583.18	4583.42	0.000603	4.16	2557.48	1791.19	0.39	0.000916	1.42	1797.51	1.43
1388	5000	4577.3	4582.44	4582.93	0.001554	5.6	904.95	368.26	0.61	0.001373	2.45	369.58	2.46

1389	5000	4576.4	4581.81	4582.14	0.001221	4.64	1077.47	450.37	0.53	0.000541	2.39	450.96	2.39
1390	5000	4575.5	4581.69	4581.8	0.000304	2.69	1857.98	618.45	0.27	0.000527	2.99	620.63	3
1391	5000	4575.3	4581.17	4581.51	0.001125	4.66	1141.84	597.01	0.51	0.000821	1.9	599.54	1.91
1392	5000	4574.8	4580.86	4581.04	0.000625	3.44	1490.26	645.69	0.38	0.000797	2.3	648.7	2.31
1393	5000	4574.6	4580.09	4580.61	0.001051	5.83	858.11	227.34	0.53	0.000892	3.76	228.11	3.77
1394	5000	4573.8	4579.67	4580.15	0.000767	5.56	898.59	200.44	0.46	0.00049	4.45	201.97	4.48
1395	5000	4574.6	4579.67	4579.81	0.00034	2.95	1692.8	532.1	0.29	0.000161	3.17	534.14	3.18
1396	5000	4573.4	4579.65	4579.7	0.000094	1.8	2891.68	756.07	0.16	0.000167	3.78	764.17	3.82
1397	5000	4573	4579.36	4579.59	0.000374	3.85	1322.79	344.76	0.32	0.000463	3.83	345.35	3.84
1398	5000	4572.4	4579.03	4579.35	0.000587	4.58	1444.19	783.9	0.4	0.000465	1.84	786.26	1.84
1399	5000	4571.2	4578.82	4579.1	0.000378	4.58	2397.17	834.33	0.34	0.000449	2.86	837.31	2.87
1400	5000	4572	4578.53	4578.86	0.000544	4.75	1910.71	901.8	0.39	0.000556	2.11	905.02	2.12
1401	5000	4571.8	4578.22	4578.56	0.000569	4.93	1911.71	835.61	0.4	0.001065	2.28	838.16	2.29
1402	5000	4571.6	4576.59	4577.94	0.002668	9.31	537.89	144.74	0.84	0.001557	3.68	146.27	3.72
1403	5000	4570	4576.4	4576.92	0.001019	6.62	2392.88	1282.47	0.54	0.00064	1.86	1285.81	1.87
1404	5000	4570.7	4576.36	4576.46	0.000439	3.53	4880.45	1833.09	0.34	0.000307	2.66	1835.52	2.66
1405	5000	4569.9	4576.26	4576.31	0.000227	2.65	6956.9	2298.81	0.24	0.000425	3.02	2300.71	3.03
1406	5000	4569.5	4575.44	4576.05	0.001069	6.3	808.62	236.36	0.54	0.000377	3.39	238.19	3.42
1407	5000	4569.1	4575.65	4575.7	0.000191	2.58	8564	3532.81	0.23	0.000466	2.42	3535.9	2.42
1408	5000	4568.6	4574.18	4575.35	0.002425	8.72	683.95	423.08	0.8	0.000125	1.61	424.44	1.62
1409	5000	4568.1	4574.93	4574.94	0.00004	1.4	18110.83	5118.67	0.11	0.000031	3.54	5122.4	3.54
1410	5000	4567.6	4574.92	4574.93	0.000025	1.16	20866.35	5089.76	0.09	0.000031	4.1	5093.59	4.1
1411	5000	4567.7	4574.91	4574.91	0.000039	1.4	17738.37	4877.65	0.11	0.000112	3.63	4881.75	3.64
1412	5000	4567.5	4573.93	4574.78	0.001254	7.72	1172.25	465	0.6	0.00188	2.5	469	2.52
1413	5000	4567.3	4572.17	4573.73	0.003128	10.13	640.78	403.24	0.91	0.000298	1.58	405.22	1.59
1414	5000	4566.5	4573.01	4573.03	0.000104	2.18	12860	4925.82	0.17	0.000272	2.61	4929.33	2.61
1416	5000	4565.9	4571.84	4572.81	0.001827	7.92	700.31	273.1	0.7	0.000302	2.55	274.2	2.56

1417	5000	4565.5	4572.34	4572.37	0.000119	2.48	11799.05	4601.34	0.19	0.000295	2.56	4605.38	2.56
1418	5000	4564.6	4571.07	4572.13	0.001637	8.26	669.75	219.93	0.68	0.001408	3.03	221.4	3.05
1419	5000	4565.6	4570.58	4571.25	0.001224	6.59	759	186.88	0.58	0.001188	4.03	188.14	4.06
1420	5000	4564.1	4570.02	4570.64	0.001153	6.31	792.55	198.86	0.56	0.001268	3.95	200.47	3.99
1421	5000	4564.1	4569.24	4569.99	0.001401	6.95	734.49	232.22	0.61	0.000951	3.15	233.35	3.16
1422	5000	4562.8	4569.08	4569.4	0.000688	4.59	1089.78	308.56	0.42	0.00057	3.51	310.08	3.53
1423	5000	4563.2	4568.85	4569.12	0.00048	4.19	1436.94	524.75	0.36	0.000525	2.7	532.99	2.74
1424	5000	4562.7	4568.63	4568.88	0.000576	4.02	1242.85	365.9	0.38	0.000516	3.39	366.75	3.4
1425	5000	4562.5	4568.31	4568.64	0.000465	4.71	1569.8	522.88	0.37	0.000399	2.99	524.51	3
1426	5000	4562	4568.17	4568.41	0.000346	4.17	2064.45	543.52	0.32	0.00056	3.75	549.88	3.8
1427	5000	4562.4	4567.49	4568.09	0.001059	6.23	802.81	193.35	0.54	0.000972	4.14	194.13	4.15
1428	5000	4561.6	4567.13	4567.53	0.000895	5.97	2604.39	1584.15	0.5	0.000714	1.64	1590.73	1.64
1429	5000	4561	4566.86	4567.11	0.000582	4.02	1323.85	436.72	0.39	0.000536	3.01	439.22	3.03
1430	5000	4560.2	4566.63	4566.81	0.000494	3.48	1519.56	534.36	0.35	0.000369	2.83	536.09	2.84
1431	5000	4560.5	4566.48	4566.6	0.000286	2.79	1870.25	599.13	0.27	0.00061	3.11	600.65	3.12
1432	5000	4559.4	4565.33	4566.2	0.002105	7.56	819.66	397.36	0.73	0.001664	2.05	399.25	2.06
1433	5000	4559.8	4564.65	4565.23	0.001349	6.21	991.52	492.27	0.59	0.001258	2.01	493.62	2.01
1434	5000	4558.4	4564.06	4564.56	0.001176	5.69	985.8	470.54	0.55	0.000435	2.08	473.21	2.1
1435	5000	4558.4	4564.13	4564.23	0.000224	3.16	6046.04	2530.55	0.25	0.00018	2.39	2533.22	2.39
1436	5000	4556.8	4564.07	4564.14	0.000148	2.71	7052.48	2645.39	0.21	0.000302	2.66	2648.64	2.67
1437	5000	4558	4563.46	4563.94	0.000924	5.72	1340.1	560.32	0.5	0.000989	2.38	562.14	2.39
1438	5000	4558	4562.92	4563.43	0.001062	5.98	1481.74	662.81	0.53	0.000815	2.23	664.15	2.24
1439	5000	4557.4	4562.66	4562.91	0.000645	4.77	3430.79	1642.28	0.42	0.000747	2.08	1645.68	2.09
1440	5000	4557	4562.27	4562.55	0.000876	5.2	3277.04	1697.19	0.48	0.001162	1.93	1700.32	1.93
1441	5000	4557.5	4561.56	4561.96	0.001614	6.1	2759.54	1855.2	0.63	0.001506	1.49	1856.94	1.49
1442	5000	4556.7	4560.86	4561.21	0.001408	6	3441.16	2493.19	0.59	0.000831	1.38	2496.36	1.38
1443	5000	4554.9	4560.58	4560.77	0.000548	4.39	4455.8	2578.94	0.38	0.00052	1.73	2582.64	1.73

1444	5000	4554.2	4560.36	4560.52	0.000494	3.95	4555.66	2414.57	0.36	0.000494	1.88	2417.9	1.89
1445	5000	4555.2	4560.11	4560.26	0.000494	3.89	4407.57	2394.59	0.36	0.000497	1.84	2398.48	1.84
1446	5000	4555.1	4559.9	4560.02	0.0005	3.57	4499.06	2203.75	0.35	0.00039	2.04	2208.41	2.04
1447	5000	4554.2	4559.74	4559.82	0.000313	2.89	5224.67	2366.07	0.28	0.000706	2.21	2369.34	2.21
1448	5000	4553.8	4558.41	4559.39	0.002855	7.93	630.83	226.97	0.83	0.002642	2.75	229.28	2.78
1449	5000	4552.9	4557.29	4558.21	0.002452	7.67	663.04	240.67	0.78	0.00136	2.73	242.6	2.75
1450	5000	4552.1	4557.09	4557.38	0.000863	4.33	1154.51	410.41	0.46	0.000464	2.8	413.04	2.81
1451	5000	4551.7	4557.02	4557.11	0.000289	2.5	1996.59	713.35	0.26	0.000505	2.79	714.82	2.8
1452	5000	4550.9	4556.53	4556.84	0.001098	4.44	1125.18	462.51	0.5	0.000466	2.43	463.97	2.43
1453	5000	4550.9	4556.46	4556.55	0.000256	2.35	2130.08	772.46	0.25	0.000136	2.74	776.4	2.76
1454	5000	4550.4	4556.43	4556.46	0.000084	1.62	8142.39	4207.88	0.15	0.000136	1.93	4212.24	1.94
1455	5000	4550.8	4556.26	4556.39	0.000255	2.92	2786.65	1783.55	0.26	0.000464	1.56	1786.24	1.56
1456	5000	4550.1	4555.67	4556.13	0.001097	5.43	942.06	356.75	0.53	0.001266	2.63	358.37	2.64
1457	5000	4549.9	4554.98	4555.5	0.001476	5.77	907.33	447.09	0.6	0.00011	2.03	447.8	2.03
1458	5000	4549.6	4555.3	4555.3	0.000037	1.11	18941.09	5310.22	0.1	0.000034	3.56	5318.02	3.57
1459	5000	4549.3	4555.29	4555.29	0.000031	1.08	20506.08	5373.71	0.09	0.000104	3.81	5376.38	3.82
1460	5000	4548.2	4553.5	4555.08	0.004281	10.12	523.61	244.76	1.03	0.000181	2.13	246.2	2.14
1461	5000	4548.6	4553.58	4553.58	0.000056	1.27	18063.49	5465.18	0.12	0.000059	3.3	5467.38	3.31
1462	5000	4549.2	4553.55	4553.55	0.000062	1.06	17869.78	5745.51	0.12	0.000049	3.11	5748.26	3.11
1463	5000	4547	4553.52	4553.53	0.000039	1.1	20046.26	5703.18	0.1	0.000037	3.51	5706.48	3.51
1464	5000	4547.8	4553.51	4553.51	0.000035	0.95	20799.56	5612.03	0.09	0.000102	3.7	5616.55	3.71
1465	5000	4546.4	4552.76	4553.4	0.00124	6.55	1128.58	487.04	0.58	0.001603	2.3	490.8	2.32
1466	5000	4546.7	4551.79	4552.58	0.002152	7.11	703.54	236.54	0.73	0.0002	2.96	237.61	2.97
1467	5000	4545.8	4552.23	4552.24	0.00007	1.46	15837.7	5423.06	0.14	0.000071	2.92	5426.89	2.92
1468	5000	4546.1	4552.2	4552.21	0.000072	1.57	15320.33	5288.22	0.14	0.00007	2.9	5291.13	2.9
1469	5000	4545.6	4552.16	4552.17	0.000069	1.71	15278.64	5088.98	0.14	0.000069	3	5093.35	3
1470	5000	4546	4552.12	4552.14	0.000069	1.66	14102.42	4254.76	0.14	0.000079	3.31	4256.76	3.31

1471	5000	4545.2	4552.07	4552.09	0.000092	1.93	11338.88	3427.11	0.16	0.000275	3.31	3429.13	3.31
1472	5000	4545.7	4550.13	4551.79	0.003814	10.35	483.04	141.5	0.99	0.001074	3.39	142.56	3.41
1473	5000	4544.3	4550.41	4550.57	0.000497	4.25	4880.54	2294.02	0.37	0.000475	2.12	2297.5	2.13
1474	5000	4544.2	4550.2	4550.35	0.000454	4.03	4780.13	2267.22	0.35	0.00046	2.11	2268.99	2.11
1475	5000	4543.5	4549.93	4550.08	0.000467	3.98	4841.74	2463.12	0.35	0.001047	1.96	2466.65	1.97
1476	5000	4543.6	4548.01	4549.33	0.004146	9.23	541.99	201.67	0.99		2.68	202.41	2.69

Table C.3 HEC-RAS output for 1985 geometry

HEC-RAS Plan: 1985(8-7-06) River: Middle Rio Grande Reach: Socorro Profile: PF 1

Agg/Deg #	Discharge	Min. Channel Elev.	W.S. Elev.	E.G. Elev.	E.G. Slope	Velocity	Flow Area	Top Width	Froude #	Frctn Slope	Hydr Radius	Wetted Perimeter	Hydr Depth
	(cfs)	(ft)	(ft)	(ft)	(ft/ft)	(ft/s)	(sq ft)	(ft)		(ft/ft)	(ft)	(ft)	(ft)
1313	5000	4610.3	4616.31	4617.3	0.001846	7.96	627.93	117.7	0.61	0.000871	5.18	121.25	5.34
1314	5000	4608.6	4616.29	4616.57	0.000505	4.28	1167.49	213.64	0.32	0.000556	5.4	216.2	5.46
1315	5000	4609.7	4616.05	4616.28	0.000614	4.14	2688.47	1393.78	0.35	0.000699	1.93	1396.37	1.93
1316	5000	4609.7	4615.76	4615.95	0.000802	3.89	2880.79	1458.2	0.38	0.000309	1.97	1461.5	1.98
1317	5000	4606.2	4615.66	4615.78	0.000163	2.96	4036.11	1493.67	0.19	0.000271	2.69	1499.22	2.7
1318	5000	4609.6	4615.48	4615.63	0.000539	3.64	3331.48	1489.41	0.32	0.000429	2.23	1492.33	2.24
1319	5000	4606.9	4615.28	4615.39	0.00035	3.13	3783.05	1493.73	0.26	0.000526	2.52	1501.01	2.53
1320	5000	4608.6	4614.79	4615.1	0.000877	4.5	1232.36	404.47	0.4	0.001813	3.03	406.05	3.05
1321	5000	4609.4	4612.58	4614.07	0.00574	9.8	510.2	167.56	0.99	0.001721	3.02	168.95	3.04
1322	5000	4607.5	4612.28	4612.6	0.000816	4.71	1809.44	1373.97	0.4	0.000433	1.32	1375.41	1.32
1323	5000	4605.6	4612.19	4612.32	0.000268	3.06	2745.58	1288.7	0.23	0.00038	2.13	1291.78	2.13
1324	5000	4605.4	4611.96	4612.12	0.000579	3.29	1789.62	669.43	0.32	0.00053	2.66	672.74	2.67
1325	5000	4607	4611.68	4611.83	0.000487	3.17	1578.37	440.57	0.29	0.00068	3.53	447.32	3.58
1326	5000	4607	4611.21	4611.45	0.001015	3.86	1293.95	469.88	0.41	0.000554	2.74	471.93	2.75
1327	5000	4605.8	4611.01	4611.11	0.000348	2.55	2695.05	1171.61	0.25	0.000209	2.29	1177.29	2.3
1328	5000	4605	4610.93	4610.99	0.00014	1.91	3354.93	1116.2	0.16	0.00012	2.99	1123.87	3.01
1329	5000	4605.4	4610.88	4610.92	0.000104	1.66	3882	1136.52	0.14	0.000225	3.41	1139.34	3.42
1330	5000	4605.6	4610.41	4610.77	0.000799	4.83	1035.04	222.58	0.39	0.001155	4.59	225.68	4.65
1331	5000	4605.1	4609.47	4610.18	0.001816	6.77	738.02	177.15	0.58	0.000535	4.11	179.39	4.17
1332	5000	4604.8	4609.65	4609.75	0.000252	2.72	3694.82	1451.79	0.22	0.000122	2.54	1456.15	2.55
1333	5000	4603.5	4609.64	4609.67	0.000072	1.44	5387.37	1423.84	0.12	0.000077	3.77	1427.89	3.78
1334	5000	4602.8	4609.6	4609.63	0.000083	1.66	5766.42	1509.33	0.13	0.000142	3.81	1514.99	3.82

1335	5000	4603.4	4609.42	4609.56	0.000299	3.4	3493.79	1017.22	0.25	0.000194	3.42	1022.06	3.43
1336	5000	4602.8	4609.4	4609.43	0.000136	2.1	8529.88	2461.54	0.16	0.00031	3.46	2467.2	3.47
1337	5000	4603.1	4608.61	4609.21	0.001282	6.19	807.53	169.1	0.5	0.00235	4.67	172.95	4.78
1338	5000	4602.8	4606.3	4607.98	0.005634	10.4	480.92	140.9	0.99	0.004052	3.35	143.72	3.41
1339	5000	4602.2	4605	4605.4	0.003053	5.48	1575.32	1151.21	0.68	0.001089	1.37	1152.3	1.37
1340	5000	4601.2	4604.74	4604.85	0.000554	2.67	2249.59	1088.58	0.3	0.000638	2.06	1090.14	2.07
1341	5000	4600.9	4604.41	4604.52	0.000744	3.4	4418.1	2439.03	0.35	0.000961	1.81	2440.87	1.81
1342	5000	4601.1	4603.96	4604.06	0.001288	3.23	3172.49	1542.88	0.43	0.002655	2.06	1543.53	2.06
1343	5000	4600.3	4602.02	4602.47	0.008339	5.41	1020.24	1168.47	0.98	0.000585	0.87	1169.8	0.87
1344	5000	4597.6	4601.52	4601.55	0.000194	1.66	6577.56	3341.77	0.18	0.000274	1.97	3344.37	1.97
1345	5000	4597.8	4601.33	4601.39	0.000414	2.42	5407.58	3186.9	0.26	0.000451	1.7	3189.31	1.7
1346	5000	4597.5	4601.05	4601.13	0.000492	3.03	5332.23	2832.13	0.29	0.000801	1.88	2833.52	1.88
1347	5000	4598.3	4600.6	4600.71	0.001529	3.68	3753.32	2223.09	0.47	0.000907	1.69	2224.93	1.69
1348	5000	4597	4600.14	4600.2	0.000599	2.33	4051.28	2006.74	0.3	0.000242	2.02	2008.73	2.02
1349	5000	4594.9	4600.03	4600.05	0.00013	1.32	5786.96	2569.21	0.15	0.000262	2.25	2572.02	2.25
1350	5000	4595.5	4599.75	4599.91	0.000776	3.14	1593.56	852.11	0.4	0.000639	1.87	854.11	1.87
1351	5000	4596	4599.52	4599.63	0.000535	2.6	1921.61	1029.55	0.34	0.000644	1.86	1031.82	1.87
1352	5000	4596.3	4599.24	4599.37	0.00079	3.04	2302.66	1409.55	0.4	0.001165	1.63	1411.06	1.63
1353	5000	4595.8	4598.35	4598.58	0.001884	3.88	1509.86	1360.19	0.6	0.00164	1.11	1360.71	1.11
1354	5000	4594.7	4597.18	4597.42	0.00144	3.98	1257.25	749.94	0.54	0.000698	1.68	750.27	1.68
1355	5000	4592.9	4596.9	4597.02	0.00041	2.79	1789.64	706.38	0.31	0.000856	2.53	707.71	2.53
1356	5000	4592.4	4595.97	4596.59	0.00277	6.33	789.69	382.77	0.78	0.001545	2.06	383.24	2.06
1357	5000	4591.5	4595.56	4595.94	0.000984	4.95	1010.16	325.41	0.5	0.000935	3.09	326.39	3.1
1358	5000	4591.2	4595.06	4595.36	0.00089	4.36	1147.79	415.13	0.46	0.001153	2.75	416.71	2.76
1359	5000	4590.7	4594.45	4594.8	0.00155	4.73	1165.6	859.9	0.58	0.001454	1.35	861.01	1.36
1360	5000	4590.5	4593.62	4593.91	0.001366	4.36	1496.11	1358.49	0.54	0.000824	1.1	1359.56	1.1

1361	5000	4590	4593.31	4593.43	0.00055	3.17	3502.65	1814	0.36	0.0007	1.93	1815.2	1.93
1362	5000	4589.2	4592.81	4593.05	0.000921	3.95	1265.15	543.71	0.46	0.001185	2.32	544.98	2.33
1363	5000	4588.6	4592.14	4592.54	0.001581	5.02	995.87	448.24	0.59	0.00042	2.22	449.44	2.22
1364	5000	4588.3	4592.16	4592.19	0.00019	1.58	6108.45	2559.76	0.2	0.000333	2.38	2562.95	2.39
1365	5000	4588.7	4591.93	4592.01	0.000726	2.84	4408.66	2366.85	0.38	0.000697	1.86	2368.62	1.86
1366	5000	4588.1	4591.57	4591.67	0.000669	3.05	4061.79	2259.89	0.38	0.000613	1.8	2261.65	1.8
1367	5000	4587.5	4591.25	4591.37	0.000563	3.25	3851.43	1973.61	0.36	0.000561	1.95	1974.77	1.95
1368	5000	4587.2	4590.98	4591.09	0.000559	3.16	3740.22	1777.9	0.36	0.000517	2.1	1779.67	2.1
1369	5000	4587.2	4590.73	4590.84	0.00048	2.87	3153.49	1449.27	0.33	0.000684	2.17	1451.33	2.18
1370	5000	4587	4590.26	4590.49	0.001053	3.87	1291.38	633.34	0.48	0.000926	2.03	634.66	2.04
1371	5000	4587	4589.86	4590.01	0.00082	3.29	2527.8	1506.38	0.42	0.001245	1.68	1507.88	1.68
1372	5000	4585.9	4589.03	4589.42	0.00211	5.01	998.44	559.4	0.66	0.000874	1.78	561.69	1.78
1373	5000	4585.5	4588.76	4588.88	0.000475	2.81	2403.2	1653.44	0.33	0.000657	1.45	1655.68	1.45
1374	5000	4585.9	4588.44	4588.59	0.000966	3.16	1580.28	984.31	0.44	0.000621	1.6	985.39	1.61
1375	5000	4585.3	4588.16	4588.24	0.000433	2.29	2207.92	1365.83	0.3	0.001059	1.62	1366.88	1.62
1376	5000	4585	4587.1	4587.59	0.005586	5.75	1048.61	1064.43	0.99	0.001294	0.98	1065.25	0.99
1377	5000	4583.7	4586.24	4586.35	0.000561	2.6	1922.18	1068.54	0.34	0.000572	1.8	1069.61	1.8
1378	5000	4582.9	4585.92	4586.04	0.000584	2.87	2290.82	1249.68	0.36	0.000528	1.83	1250.83	1.83
1379	5000	4582	4585.72	4585.83	0.00048	2.73	2528.45	1424.31	0.33	0.000405	1.77	1426.38	1.78
1380	5000	4582.2	4585.57	4585.65	0.000347	2.39	2379.7	1251.79	0.28	0.000519	1.9	1253.62	1.9
1381	5000	4582.9	4585.31	4585.44	0.000859	2.97	2013.6	1339.07	0.41	0.000741	1.5	1341.73	1.5
1382	5000	4581.7	4584.99	4585.09	0.000646	2.58	2161.92	1381.44	0.36	0.001214	1.56	1384.08	1.56
1383	5000	4581.2	4584.21	4584.49	0.003069	4.26	1173.56	1111.32	0.73	0.000823	1.05	1114.38	1.06
1384	5000	4580.5	4583.91	4583.98	0.000375	2.16	2393.59	1665.55	0.28	0.000364	1.43	1668.72	1.44
1385	5000	4580.6	4583.72	4583.79	0.000353	2.19	2593.93	1674.36	0.28	0.00045	1.55	1676.11	1.55
1386	5000	4580.5	4583.44	4583.56	0.000593	2.75	1961.34	1315.26	0.35	0.0008	1.49	1316.6	1.49

1387	5000	4580	4583.02	4583.19	0.001139	3.27	1530.43	1027.95	0.47	0.001126	1.49	1028.99	1.49
1388	5000	4579.8	4582.43	4582.62	0.001113	3.45	1450.26	882.95	0.47	0.000679	1.64	884.13	1.64
1389	5000	4578.7	4582.14	4582.25	0.000457	2.64	1890.83	878.27	0.32	0.000385	2.15	880.72	2.15
1390	5000	4579.1	4581.96	4582.04	0.000329	2.35	2130.21	924.53	0.27	0.000463	2.3	926.83	2.3
1391	5000	4577.5	4581.63	4581.8	0.0007	3.32	1508.43	700.24	0.39	0.000864	2.14	703.28	2.15
1392	5000	4577.4	4581.13	4581.35	0.001094	3.77	1328.68	729.6	0.48	0.002091	1.82	731.36	1.82
1393	5000	4577.9	4579.68	4580.29	0.005488	6.27	797.69	655.32	1	0.000576	1.22	656.32	1.22
1394	5000	4575.3	4579.48	4579.56	0.000205	2.31	2247.59	833.05	0.23	0.00024	2.69	834.45	2.7
1395	5000	4575.6	4579.36	4579.45	0.000284	2.32	2154.17	852.33	0.26	0.000171	2.52	853.72	2.53
1396	5000	4574.2	4579.3	4579.35	0.000114	1.88	3414.89	1097.18	0.17	0.000227	3.11	1098.99	3.11
1397	5000	4575	4578.98	4579.22	0.00066	3.9	1281.78	436.68	0.4	0.000985	2.92	438.58	2.94
1398	5000	4574.4	4578.28	4578.68	0.001626	5.07	985.43	446.1	0.6	0.000879	2.2	447.19	2.21
1399	5000	4573.6	4577.96	4578.2	0.00055	3.99	1476.54	569.97	0.38	0.000584	2.58	573.21	2.59
1400	5000	4573.6	4577.67	4577.92	0.000622	4.01	1283.04	498.38	0.39	0.000394	2.56	501.51	2.57
1401	5000	4571.4	4577.54	4577.69	0.000272	3.23	2005.73	763.55	0.27	0.000361	2.62	765.26	2.63
1402	5000	4572.7	4577.25	4577.49	0.000503	3.99	1621.09	681.88	0.36	0.000537	2.37	683.23	2.38
1403	5000	4573	4577	4577.2	0.000575	3.97	2837.25	1404.06	0.38	0.000732	2.02	1405	2.02
1404	5000	4572.7	4576.58	4576.82	0.000964	3.95	1343.43	696.41	0.46	0.000436	1.93	697.82	1.93
1405	5000	4572	4576.48	4576.58	0.000247	2.49	2056.65	752.67	0.25	0.000278	2.73	753.94	2.73
1406	5000	4572	4576.31	4576.44	0.000314	2.86	1747.13	544.06	0.28	0.000124	3.2	545.17	3.21
1407	5000	4572.2	4576.33	4576.34	0.000066	1.32	12716.66	4095.31	0.13	0.000087	3.1	4097.12	3.11
1408	5000	4570.9	4576.26	4576.3	0.000121	2.19	8808.12	3885.51	0.18	0.000289	2.27	3888.15	2.27
1409	5000	4571.6	4575.7	4576.11	0.0014	5.17	967.04	379.81	0.57	0.002293	2.54	381.14	2.55
1410	5000	4570.9	4573.84	4574.9	0.004422	8.25	605.81	279.02	0.99	0.000178	2.16	280.58	2.17
1411	5000	4570.1	4574.3	4574.31	0.000055	1.14	15669.67	4916.94	0.12	0.000135	3.19	4918.91	3.19
1412	5000	4569.5	4574.01	4574.23	0.000713	3.72	1405.77	615.97	0.41	0.000879	2.27	619.26	2.28

1413	5000	4569.8	4573.51	4573.76	0.001112	4.03	1276.45	662.34	0.49	0.0013	1.92	663.54	1.93
1414	5000	4569.5	4572.77	4573.1	0.001539	4.64	1078.21	536.55	0.58	0.00162	2.01	537.31	2.01
1416	5000	4568.7	4571.93	4572.31	0.001706	4.94	1030.74	538.57	0.61	0.001533	1.91	539.67	1.91
1417	5000	4568.2	4571.24	4571.51	0.001384	4.2	1189.18	632.42	0.54	0.000814	1.88	633.85	1.88
1418	5000	4567.1	4570.94	4571.07	0.000535	2.99	1692.37	857.59	0.35	0.000504	1.97	858.61	1.97
1419	5000	4566.1	4570.68	4570.81	0.000476	2.83	1808.78	851.13	0.33	0.000664	2.12	853.01	2.13
1420	5000	4566.8	4570.27	4570.51	0.00103	3.87	1290.55	621.83	0.47	0.001159	2.07	622.92	2.08
1421	5000	4566.6	4569.7	4569.92	0.001314	3.71	1398.72	897.53	0.51	0.001526	1.56	899.48	1.56
1422	5000	4566	4568.78	4569.19	0.001794	5.11	1040.18	620.99	0.63	0.000707	1.67	622.01	1.68
1423	5000	4565.5	4568.68	4568.77	0.000375	2.44	2140.41	1011.87	0.29	0.000346	2.11	1013.57	2.12
1424	5000	4564.7	4568.51	4568.6	0.000319	2.47	2513.74	1269.61	0.27	0.000413	1.98	1272.03	1.98
1425	5000	4565	4568.23	4568.4	0.000554	3.66	3095.37	1903.76	0.37	0.000514	1.62	1905.07	1.63
1426	5000	4563.9	4567.99	4568.13	0.000478	2.96	2354.17	1469.03	0.33	0.00095	1.6	1470.62	1.6
1427	5000	4564.5	4567.27	4567.6	0.002728	4.71	1203.17	881.48	0.72	0.00205	1.36	882.59	1.36
1428	5000	4564.1	4566.28	4566.53	0.001596	4.06	1232.21	769.96	0.57	0.000481	1.6	770.98	1.6
1429	5000	4561.4	4566.15	4566.23	0.000228	2.35	3201.01	1673.99	0.24	0.000268	1.91	1675.65	1.91
1430	5000	4562.4	4565.99	4566.09	0.00032	2.65	2865.56	1804.51	0.28	0.000398	1.59	1806.25	1.59
1431	5000	4562.4	4565.76	4565.88	0.000509	2.95	2911	1968.88	0.34	0.000816	1.48	1970.57	1.48
1432	5000	4562.7	4565.12	4565.43	0.001516	4.42	1194.36	752.88	0.57	0.000705	1.58	753.92	1.59
1433	5000	4562.2	4564.9	4564.98	0.000406	2.69	4433.72	1996.53	0.3	0.000254	2.22	1998.2	2.22
1434	5000	4561.2	4564.81	4564.83	0.000174	1.76	7300.98	2282.8	0.2	0.000382	3.2	2283.79	3.2
1435	5000	4560.7	4564.33	4564.64	0.001422	4.44	1160.11	639.06	0.55	0.001	1.81	640.2	1.82
1436	5000	4560.7	4563.87	4564.08	0.000742	3.72	1345.37	539.44	0.41	0.001057	2.49	540.69	2.49
1437	5000	4560.1	4563.16	4563.51	0.001625	4.75	1052.56	525.74	0.59	0.001449	2	526.88	2
1438	5000	4559.3	4562.43	4562.71	0.001301	4.24	1180.14	591.29	0.53	0.001255	1.99	593.56	2
1439	5000	4558.4	4561.82	4561.99	0.001212	3.62	2262.3	1485.44	0.5	0.000593	1.52	1487.19	1.52

1440	5000	4557.5	4561.58	4561.67	0.00035	2.6	3161.94	1610.18	0.29	0.000359	1.96	1611.34	1.96
1441	5000	4557.5	4561.41	4561.5	0.000367	2.56	3415.48	1821.37	0.29	0.000297	1.87	1822.24	1.88
1442	5000	4557.2	4561.27	4561.35	0.000245	2.43	4080.6	2381.18	0.25	0.00038	1.71	2383.21	1.71
1443	5000	4557.5	4561.01	4561.16	0.00067	3.34	2942.36	2374.23	0.39	0.00112	1.24	2376.59	1.24
1444	5000	4557.8	4560.25	4560.6	0.002237	4.74	1054.69	672.22	0.67	0.000937	1.57	673.02	1.57
1445	5000	4557.4	4559.92	4560.05	0.000512	2.81	1781.06	823.92	0.34	0.001097	2.16	824.92	2.16
1446	5000	4556.6	4559.12	4559.49	0.003816	4.9	1021.1	925.46	0.82	0.00217	1.1	926.59	1.1
1447	5000	4554.9	4558.15	4558.36	0.001398	3.61	1384.44	930.75	0.52	0.001168	1.48	934.04	1.49
1448	5000	4554.4	4557.59	4557.78	0.000991	3.5	1428.45	779.05	0.46	0.001027	1.83	780.22	1.83
1449	5000	4554.5	4557.08	4557.29	0.001065	3.71	1346.26	709.34	0.48	0.000804	1.9	710.19	1.9
1450	5000	4553.9	4556.74	4556.88	0.000628	2.94	1698.72	853.39	0.37	0.00079	1.99	855.06	1.99
1451	5000	4553.9	4556.36	4556.52	0.001024	3.26	1532.96	953.1	0.45	0.000934	1.61	954.09	1.61
1452	5000	4553.4	4555.92	4556.08	0.000855	3.23	1547.85	853.02	0.42	0.001313	1.81	853.68	1.81
1453	5000	4553.1	4555.11	4555.42	0.002268	4.81	1828.18	1474.2	0.67	0.000753	1.24	1475.25	1.24
1454	5000	4551.4	4554.86	4554.96	0.000371	2.67	3397.59	1884.54	0.29	0.000338	1.8	1886.95	1.8
1455	5000	4550	4554.7	4554.8	0.000308	2.49	2008.72	759.97	0.27	0.000342	2.64	762.08	2.64
1456	5000	4549.8	4554.49	4554.63	0.000382	3.04	1643.64	540.46	0.31	0.000449	3.03	541.79	3.04
1457	5000	4550.5	4554.26	4554.42	0.000536	3.23	1703.08	998.79	0.35	0.000415	1.7	999.58	1.71
1458	5000	4549.7	4554.08	4554.21	0.00033	2.92	1711.12	536	0.29	0.000425	3.18	537.39	3.19
1459	5000	4549.8	4553.85	4554.02	0.000566	3.36	1486.7	565.03	0.37	0.000336	2.62	566.53	2.63
1460	5000	4549.2	4553.73	4553.83	0.000222	2.55	1961.41	560.17	0.24	0.000088	3.49	561.45	3.5
1461	5000	4548	4553.74	4553.76	0.000047	1.32	14595.67	5685.52	0.11	0.00005	2.57	5688.32	2.57
1462	5000	4548	4553.72	4553.73	0.000053	1.4	15118.16	5631	0.12	0.0001	2.68	5632.42	2.68
1463	5000	4548.5	4553.52	4553.67	0.000253	3.11	1610.04	376.22	0.26	0.000527	4.26	377.53	4.28
1464	5000	4548.6	4552.53	4553.34	0.001712	7.21	693.13	191.59	0.67	0.001608	3.59	192.84	3.62
1465	5000	4547.5	4551.78	4552.52	0.001512	6.91	723.76	195.04	0.63	0.001219	3.7	195.76	3.71

1466	5000	4546.1	4551.22	4551.88	0.001004	6.6	1049.49	507.67	0.53	0.000239	2.06	509.66	2.07
1467	5000	4545.2	4551.53	4551.57	0.000105	2.39	11377.17	4754.64	0.18	0.00009	2.39	4758.53	2.39
1468	5000	4544.4	4551.5	4551.52	0.000078	1.57	13397.1	5109.48	0.14	0.000072	2.62	5115.46	2.62
1469	5000	4543.3	4551.46	4551.48	0.000067	1.67	12523.34	4691.2	0.14	0.000087	2.67	4696.23	2.67
1470	5000	4545	4551.41	4551.44	0.000119	2.22	11006.55	4190.94	0.18	0.000089	2.63	4192.49	2.63
1471	5000	4543.1	4551.35	4551.39	0.000069	2.07	10811.87	3406.36	0.15	0.000084	3.17	3409.76	3.17
1472	5000	4543.2	4551.27	4551.34	0.000106	2.49	6885.17	2552.45	0.18	0.000125	2.69	2555.87	2.7
1473	5000	4543.4	4551.17	4551.28	0.00015	3	5575.7	2425.83	0.21	0.000183	2.29	2429.53	2.3
1474	5000	4543.4	4551	4551.19	0.000229	3.94	4310.79	2220.94	0.27	0.000328	1.94	2225.55	1.94
1475	5000	4544.7	4550.71	4550.98	0.000508	4.68	3352.09	2001.92	0.38	0.000192	1.67	2004.37	1.67
1476	5000	4544.7	4550.75	4550.79	0.0001	2.29	9130.32	2865.36	0.17		3.18	2867.26	3.19

Table C.4 HEC-RAS output for 1992 geometry

HEC-RAS Plan: 1992(8-7-06) River: Middle Rio Grande Reach: Socorro Profile: PF 1													
Agg/Deg #	Discharge	Min. Channel Elev.	W.S. Elev.	E.G. Elev.	E.G. Slope	Velocity	Flow Area	Top Width	Froude #	Frctn Slope	Hydr Radius	Wetted Perimeter	Hydr Depth
	(cfs)	(ft)	(ft)	(ft)	(ft/ft)	(ft/s)	(sq ft)	(ft)		(ft/ft)	(ft)	(ft)	(ft)
1313	5000	4608.1	4614.9	4615.55	0.000996	6.44	776.11	124.1	0.45	0.000989	5.99	129.61	6.25
1314	5000	4608.2	4614.46	4614.92	0.000983	5.44	919.47	192	0.44	0.000999	4.69	196.06	4.79
1315	5000	4607.8	4613.85	4614.42	0.001017	6.09	854.08	175.96	0.46	0.000969	4.75	179.83	4.85
1316	5000	4607.5	4613.45	4613.96	0.000924	5.75	869.97	158.84	0.43	0.001012	5.34	163.07	5.48
1317	5000	4607.4	4612.95	4613.48	0.001112	5.87	851.71	173.77	0.47	0.000879	4.79	177.66	4.9
1318	5000	4606.1	4612.56	4612.99	0.000712	5.31	942.25	158.79	0.38	0.000683	5.76	163.6	5.93
1319	5000	4605.5	4612.23	4612.63	0.000657	5.04	991.14	169.98	0.37	0.000976	5.67	174.85	5.83
1320	5000	4604.65	4611.39	4612.1	0.001601	6.74	741.77	161.56	0.55	0.001452	4.49	165.23	4.59
1321	5000	4605.7	4610.75	4611.34	0.001324	6.17	810.15	174.71	0.51	0.001151	4.53	178.67	4.64
1322	5000	4605.5	4610.29	4610.72	0.001009	5.29	945.78	211.1	0.44	0.00091	4.41	214.64	4.48
1323	5000	4605	4609.88	4610.24	0.000824	4.8	1041.4	231.4	0.4	0.000827	4.44	234.64	4.5
1324	5000	4605	4609.46	4609.8	0.00083	4.7	1064.59	244.66	0.4	0.000853	4.27	249.09	4.35
1325	5000	4604.8	4609.05	4609.35	0.000878	4.45	1122.92	291.87	0.4	0.001042	3.78	297.07	3.85
1326	5000	4604.6	4608.45	4608.8	0.001255	4.72	1059.33	330.34	0.46	0.001102	3.16	335.58	3.21
1327	5000	4603.7	4607.9	4608.18	0.000975	4.29	1166.79	346.49	0.41	0.001308	3.3	353.51	3.37
1328	5000	4604	4607.27	4607.56	0.001848	4.31	1196.88	611.76	0.53	0.001137	1.94	615.5	1.96
1329	5000	4603.4	4606.8	4606.95	0.000769	3.11	1644.11	790.14	0.35	0.000558	2.07	793.19	2.08
1330	5000	4602.5	4606.53	4606.65	0.000423	2.76	1813.47	560.32	0.27	0.000523	3.18	569.58	3.24
1331	5000	4602.2	4606.2	4606.38	0.000661	3.39	1476.95	471.82	0.34	0.000443	3.1	476.36	3.13
1332	5000	4601.5	4606.05	4606.15	0.000318	2.51	1989.9	569.51	0.24	0.000321	3.44	579.26	3.49
1333	5000	4601.6	4605.89	4606	0.000324	2.69	1861.7	489.26	0.24	0.000229	3.74	497.55	3.81
1334	5000	4600.7	4605.81	4605.88	0.00017	2.07	2416.96	581.75	0.18	0.000242	4.1	590.06	4.15

1335	5000	4600.5	4605.59	4605.75	0.00037	3.16	1581.12	355.78	0.26	0.000608	4.33	365.51	4.44
1336	5000	4600.4	4604.94	4605.42	0.001176	5.55	900.92	209.84	0.47	0.000861	4.23	213.15	4.29
1337	5000	4599.7	4604.66	4604.96	0.000658	4.42	1131.75	240.76	0.36	0.000624	4.64	243.95	4.7
1338	5000	4599	4604.36	4604.66	0.000593	4.38	1140.8	225.76	0.34	0.000915	4.96	230.11	5.05
1339	5000	4595.73	4603.69	4604.21	0.001595	5.81	861.22	236.69	0.54	0.000791	3.6	239.37	3.64
1340	5000	4598.3	4603.57	4603.79	0.000471	3.78	1420.45	556.94	0.3	0.001007	2.53	560.58	2.55
1341	5000	4598.2	4602.12	4603.23	0.003485	8.46	590.79	165.21	0.79	0.002026	3.52	167.65	3.58
1342	5000	4597.9	4601.54	4601.93	0.001323	4.96	1007.95	313.72	0.48	0.001046	3.17	317.73	3.21
1343	5000	4597.6	4601.13	4601.28	0.000847	3.04	1645.83	746.34	0.36	0.001319	2.19	751.83	2.21
1344	5000	4597.5	4600.26	4600.56	0.002333	4.4	1136.83	632.35	0.58	0.001291	1.78	637.42	1.8
1345	5000	4596.9	4599.7	4599.84	0.000818	3.07	1627.46	708.56	0.36	0.000867	2.29	712.07	2.3
1346	5000	4594.39	4599.26	4599.38	0.000921	2.73	1830.94	1042.3	0.36	0.000626	1.75	1044.82	1.76
1347	5000	4596	4598.97	4599.04	0.000453	2.11	2365.36	1159.56	0.26	0.000443	2.03	1163.38	2.04
1348	5000	4595.4	4598.73	4598.8	0.000433	2.08	2403.38	1169.36	0.26	0.000366	2.05	1171.9	2.06
1349	5000	4594.5	4598.53	4598.59	0.000313	2.1	2681.93	1380.87	0.23	0.000405	1.94	1383.67	1.94
1350	5000	4593.5	4598.08	4598.37	0.000543	4.28	1167.69	294.02	0.38	0.000658	3.89	300.04	3.97
1351	5000	4593.8	4597.71	4598.09	0.000814	4.94	1156.05	682.29	0.46	0.000896	1.69	684.58	1.69
1352	5000	4593.6	4597.24	4597.66	0.000991	5.2	1009.48	498.3	0.5	0.000743	2.02	500.27	2.03
1353	5000	4593.2	4597	4597.26	0.000578	4.17	1596.87	669.23	0.39	0.000399	2.38	671.48	2.39
1354	5000	4592.6	4596.84	4596.96	0.000292	2.8	1782.57	536.19	0.27	0.000349	3.29	542.21	3.32
1355	5000	4592.2	4596.59	4596.73	0.000425	3.06	1635.12	575.62	0.32	0.000487	2.82	579.71	2.84
1356	5000	4592.1	4596.35	4596.53	0.000563	3.43	1457.02	533.68	0.37	0.000975	2.72	536.6	2.73
1357	5000	4591.3	4595.22	4596.12	0.002079	7.61	656.8	191.99	0.73	0.001022	3.37	195	3.42
1358	5000	4591.2	4595.05	4595.34	0.000606	4.38	1188.33	433.84	0.4	0.000866	2.72	437.07	2.74
1359	5000	4590.9	4594.49	4594.92	0.001339	5.32	1235.51	840.54	0.56	0.001244	1.46	845.45	1.47
1360	5000	4589.2	4593.88	4594.3	0.001158	5.19	1025.5	399.49	0.53	0.000878	2.55	402.15	2.57

1361	5000	4589.5	4593.54	4593.81	0.000688	4.21	1187.72	370.78	0.41	0.000461	3.18	374.05	3.2
1362	5000	4589	4593.36	4593.54	0.00033	3.37	1483.33	372.62	0.3	0.000544	3.95	375.65	3.98
1363	5000	4588.9	4592.88	4593.23	0.001062	4.76	1051.05	386.84	0.5	0.000723	2.68	392.24	2.72
1364	5000	4588.4	4592.6	4592.82	0.000524	3.85	1401.34	512.15	0.37	0.000448	2.71	516.71	2.74
1365	5000	4588.4	4592.41	4592.58	0.000387	3.3	1513.84	443.61	0.31	0.000478	3.37	449.61	3.41
1366	5000	4588	4592.1	4592.35	0.000605	4.03	1239.44	371.43	0.39	0.000837	3.28	377.98	3.34
1367	5000	4587.6	4591.42	4591.93	0.001234	5.74	871.62	263.93	0.56	0.001213	3.26	267.4	3.3
1368	5000	4587.1	4590.86	4591.34	0.001193	5.57	898.14	276	0.54	0.000817	3.2	281.01	3.25
1369	5000	4587.1	4590.65	4590.89	0.000595	3.89	1284.49	402.8	0.38	0.000581	3.15	407.83	3.19
1370	5000	4586.5	4590.41	4590.61	0.000567	3.54	1410.59	491.92	0.37	0.00087	2.83	497.63	2.87
1371	5000	4584.22	4589.83	4590.17	0.001501	4.72	1060.04	502.64	0.57	0.001069	2.1	505.4	2.11
1372	5000	4585.6	4589.43	4589.67	0.0008	3.91	1290.26	560.02	0.43	0.00086	2.28	565.19	2.3
1373	5000	4585.5	4589.01	4589.23	0.000928	3.77	1325.45	608.94	0.45	0.000647	2.15	616.08	2.18
1374	5000	4585.2	4588.78	4588.91	0.000476	2.88	1743.11	759.66	0.33	0.000425	2.27	767.38	2.29
1375	5000	4585.1	4588.61	4588.71	0.000381	2.59	1969.95	882.63	0.29	0.000727	2.22	888	2.23
1376	5000	4584.9	4587.97	4588.26	0.001902	4.32	1158.12	751.11	0.61	0.001035	1.54	752.94	1.54
1377	5000	4583.4	4587.57	4587.71	0.00065	3.09	1649.8	823.75	0.38	0.001429	1.99	828.1	2
1378	5000	4582.8	4586.18	4586.82	0.005345	6.43	777.15	599.15	1	0.001036	1.29	602.86	1.3
1379	5000	4581.9	4585.99	4586.11	0.000426	2.8	1815.04	765.01	0.31	0.000465	2.35	771.3	2.37
1380	5000	4582.03	4585.81	4585.93	0.000511	2.78	1815.12	884.72	0.34	0.000361	2.05	886.66	2.05
1381	5000	4581.3	4585.7	4585.77	0.000268	2.2	2275.21	930.66	0.25	0.00015	2.43	937.93	2.44
1382	5000	4580.6	4585.65	4585.69	0.000096	1.64	3869.05	1596.59	0.16	0.000161	2.41	1605.23	2.42
1383	5000	4580.3	4585.46	4585.61	0.000321	3.19	2613.39	1539.4	0.29	0.000441	1.69	1544.27	1.7
1384	5000	4580.2	4585.19	4585.41	0.000644	3.91	2271.88	1637.41	0.4	0.000783	1.38	1642.9	1.39
1385	5000	4580.2	4584.75	4585.06	0.000974	4.95	2526.58	1673.97	0.49	0.001203	1.51	1677.93	1.51
1386	5000	4580.1	4584.09	4584.48	0.001524	5.57	2177.77	1603.17	0.6	0.001783	1.36	1606.5	1.36

1387	5000	4579.3	4582.86	4583.58	0.002114	7.04	1258.11	1171.03	0.72	0.001575	1.07	1174.1	1.07
1388	5000	4578.9	4582.47	4582.67	0.001219	3.67	1503.33	985.06	0.5	0.00174	1.52	988.54	1.53
1389	5000	4578.7	4581.36	4581.71	0.002684	4.72	1060.09	777.37	0.71	0.000845	1.36	781.42	1.36
1390	5000	4577.3	4581.1	4581.2	0.000408	2.5	2044.87	988.99	0.3	0.000531	2.06	994.66	2.07
1391	5000	4577.2	4580.8	4580.93	0.00072	2.91	1719.48	972.28	0.39	0.000766	1.76	975.78	1.77
1392	5000	4576.8	4580.36	4580.53	0.000817	3.26	1532.24	800.9	0.42	0.000567	1.9	804.49	1.91
1393	5000	4576.1	4580.11	4580.24	0.000417	2.89	1731.62	651.6	0.31	0.000372	2.63	659.43	2.66
1394	5000	4576	4579.94	4580.05	0.000334	2.67	1985.88	930.92	0.28	0.000285	2.12	937.36	2.13
1395	5000	4575.7	4579.82	4579.9	0.000246	2.23	2246.28	843.19	0.24	0.000186	2.64	849.58	2.66
1396	5000	4575	4579.75	4579.81	0.000146	1.97	2892.93	1084.36	0.19	0.000148	2.65	1090.18	2.67
1397	5000	4574.2	4579.63	4579.73	0.00015	2.56	2004.76	436.26	0.21	0.000283	4.53	442.66	4.6
1398	5000	4573.7	4579.15	4579.56	0.000719	5.21	1122.82	305.21	0.44	0.000938	3.64	308.75	3.68
1399	5000	4573.9	4578.49	4579.07	0.001276	6.24	1149.15	593.78	0.58	0.000733	1.93	596.87	1.94
1400	5000	4573.2	4578.33	4578.61	0.000475	4.33	1556.31	527.76	0.36	0.000738	2.92	533.42	2.95
1401	5000	4573.2	4577.7	4578.22	0.001301	5.97	1284.91	734.82	0.57	0.000816	1.74	737.91	1.75
1402	5000	4572.5	4577.42	4577.76	0.000559	4.76	1420.54	640.21	0.39	0.000529	2.21	643.53	2.22
1403	5000	4572	4577.17	4577.48	0.000501	4.53	1495.67	637.34	0.37	0.000498	2.33	641.4	2.35
1404	5000	4571.7	4576.95	4577.22	0.000495	4.2	1579.04	672.01	0.36	0.000688	2.31	682.61	2.35
1405	5000	4571.8	4576.53	4576.87	0.001021	4.72	1209.98	606.91	0.49	0.00064	1.98	611.23	1.99
1406	5000	4571.7	4576.32	4576.5	0.000438	3.38	1631.77	623.69	0.33	0.000117	2.61	626.3	2.62
1407	5000	4570.9	4576.38	4576.4	0.000053	1.49	11859.53	3908.71	0.12	0.000121	3.03	3915.6	3.03
1408	5000	4570.9	4576.05	4576.31	0.000508	4.1	1218.96	311.15	0.37	0.001117	3.84	317.82	3.92
1409	5000	4571.1	4574.38	4575.68	0.00418	9.18	544.84	203.29	0.99	0.000128	2.64	206.31	2.68
1410	5000	4570.36	4574.98	4574.99	0.000038	1.08	19125.62	4973.22	0.1	0.000112	3.84	4976.54	3.85
1411	5000	4570.6	4574.3	4574.88	0.00133	6.18	915.9	344.22	0.58	0.000806	2.64	346.59	2.66
1412	5000	4569.6	4574.11	4574.37	0.00054	4.1	1313.15	516.68	0.38	0.000733	2.52	520.2	2.54

1413	5000	4568.9	4573.53	4573.98	0.001053	5.43	1143.54	622.27	0.51	0.001718	1.82	628.92	1.84
1414	5000	4567.59	4572.09	4573.07	0.003287	8.01	777.02	524.86	0.88	0.001465	1.47	527.32	1.48
1416	5000	4567.7	4571.8	4572.17	0.000825	4.89	1119.4	519.13	0.46	0.000499	2.14	522.7	2.16
1417	5000	4567.4	4571.69	4571.85	0.000334	3.27	1711.73	677.57	0.3	0.000447	2.5	684	2.53
1418	5000	4566.8	4571.44	4571.64	0.000628	3.54	1413.58	532.72	0.38	0.000475	2.62	539.89	2.65
1419	5000	4566.8	4571.22	4571.38	0.000372	3.3	2054.51	822.88	0.31	0.000724	2.48	827.5	2.5
1420	5000	4565.85	4570.46	4570.98	0.001974	5.87	1095.3	607.63	0.67	0.001303	1.79	610.48	1.8
1421	5000	4566.3	4569.92	4570.28	0.000924	4.79	1043.16	331.91	0.48	0.00164	3.09	337.39	3.14
1422	5000	4566	4568.81	4569.43	0.00368	6.32	790.84	471.35	0.86	0.001868	1.66	476.03	1.68
1423	5000	4565.1	4568.12	4568.31	0.001127	3.53	1416.7	832.43	0.48	0.000351	1.68	841.74	1.7
1424	5000	4563	4568.02	4568.08	0.000169	1.96	2800.99	1416.18	0.2	0.000165	1.96	1427.46	1.98
1425	5000	4563.4	4567.93	4568	0.000162	2.03	3062.87	1725.15	0.2	0.000298	1.76	1736.28	1.78
1426	5000	4563.4	4567.71	4567.84	0.000722	2.95	1692.23	933.36	0.39	0.00067	1.8	940.19	1.81
1427	5000	4563.4	4567.36	4567.49	0.000623	2.93	1904.58	1366.67	0.37	0.000732	1.39	1370.8	1.39
1428	5000	4563	4566.91	4567.1	0.000873	3.56	1406.01	676.92	0.43	0.000888	2.06	681.75	2.08
1429	5000	4562.5	4566.42	4566.65	0.000903	3.88	1287.79	556.85	0.45	0.000785	2.29	561.41	2.31
1430	5000	4562.3	4566.05	4566.23	0.000689	3.44	2252.76	1688.84	0.39	0.00099	1.33	1696.71	1.33
1431	5000	4562.3	4565.39	4565.7	0.001541	4.46	1121.24	586.76	0.57	0.000774	1.89	593.05	1.91
1432	5000	4561.2	4565.11	4565.24	0.000464	2.98	2870.88	1808.5	0.33	0.000876	1.58	1815.72	1.59
1433	5000	4560.6	4564.33	4564.74	0.002231	5.15	970.23	537.11	0.68	0.000459	1.78	545.22	1.81
1434	5000	4560	4564.32	4564.41	0.000192	2.51	1991.13	518.53	0.23	0.000427	3.81	522.55	3.84
1435	5000	4560.4	4563.79	4564.16	0.001654	4.91	1019	487.18	0.6	0.001176	2.07	492.46	2.09
1436	5000	4560.5	4563.26	4563.51	0.000879	4.02	1245.11	502.23	0.45	0.000861	2.46	505.95	2.48
1437	5000	4559.6	4562.81	4563.04	0.000844	3.86	1296.51	539.19	0.44	0.001175	2.39	542.77	2.4
1438	5000	4558.7	4562.12	4562.44	0.001748	4.53	1103.75	623.49	0.6	0.000974	1.76	626.69	1.77
1439	5000	4558.2	4561.72	4561.87	0.00062	3.15	2136.28	1350.06	0.37	0.000977	1.58	1353.21	1.58

1440	5000	4558.1	4561.06	4561.37	0.001762	4.5	1112.13	637.73	0.6	0.001382	1.73	642.41	1.74
1441	5000	4557.3	4560.43	4560.66	0.001113	3.91	1304.52	708	0.49	0.000401	1.82	715.01	1.84
1442	5000	4556.7	4560.33	4560.42	0.000205	2.42	2089.86	668.52	0.23	0.000459	3.11	672.51	3.13
1443	5000	4555.7	4559.83	4560.17	0.001809	4.69	1067.05	587.92	0.61	0.001094	1.81	591.03	1.81
1444	5000	4556.4	4559.43	4559.6	0.000732	3.35	1494.42	692.05	0.4	0.000716	2.15	695.62	2.16
1445	5000	4555.7	4559.09	4559.23	0.0007	3.02	1653.82	863.34	0.38	0.001016	1.91	867.07	1.92
1446	5000	4555.2	4558.54	4558.75	0.001606	3.64	1374.85	1013.86	0.55	0.000738	1.35	1018.54	1.36
1447	5000	4554.5	4558.25	4558.35	0.000422	2.49	2004.8	955.42	0.3	0.000328	2.09	960.43	2.1
1448	5000	4554.5	4558.11	4558.19	0.000262	2.31	2160.28	801.46	0.25	0.00033	2.67	808.27	2.7
1449	5000	4554.6	4557.9	4558.03	0.000428	2.86	1750.91	686.09	0.32	0.000719	2.53	691.34	2.55
1450	5000	4553.26	4557.45	4557.67	0.001453	3.74	1337.05	876.97	0.53	0.001332	1.52	881.29	1.52
1451	5000	4554	4556.83	4557.03	0.001226	3.58	1396.27	860.14	0.5	0.002324	1.62	864.56	1.62
1452	5000	4553.5	4555.58	4556.04	0.005984	5.47	914.61	981.99	1	0.000596	0.93	985.92	0.93
1453	5000	4552.1	4555.46	4555.51	0.00021	1.7	3029.65	1572.47	0.21	0.0002	1.92	1581.35	1.93
1454	5000	4551.8	4555.37	4555.41	0.000191	1.64	3164.33	1678.91	0.2	0.000219	1.88	1685.53	1.88
1455	5000	4551.5	4555.25	4555.3	0.000255	1.92	2793.27	1598.14	0.24	0.000425	1.74	1604.35	1.75
1456	5000	4548.54	4554.86	4555.08	0.000844	3.72	1344.78	588.85	0.43	0.000392	2.26	595.07	2.28
1457	5000	4550.4	4554.75	4554.85	0.000225	2.56	2217.03	1020.45	0.24	0.000304	2.16	1028.31	2.17
1458	5000	4550.2	4554.54	4554.7	0.000431	3.18	1570.04	523.48	0.32	0.00062	2.97	529.49	3
1459	5000	4550.4	4554.2	4554.43	0.000965	3.87	1290.76	588.09	0.46	0.00063	2.17	593.53	2.19
1460	5000	4549.7	4553.93	4554.08	0.000443	3.13	1597.34	555.96	0.33	0.000099	2.83	564.04	2.87
1461	5000	4549	4553.98	4553.99	0.000043	1.09	16622.59	5561.51	0.1	0.000105	2.99	5566.94	2.99
1462	5000	4547.92	4553.7	4553.92	0.000552	3.75	1413.16	628.37	0.37	0.000408	2.23	632.95	2.25
1463	5000	4548.3	4553.52	4553.7	0.000313	3.34	1496.58	363.59	0.29	0.000389	4.05	369.6	4.12
1464	5000	4547.5	4553.11	4553.49	0.000496	4.92	1015.74	192.55	0.38	0.000103	5.13	198.02	5.28
1465	5000	4546.6	4553.32	4553.33	0.000043	1.35	17991.64	5702.45	0.11	0.000112	3.15	5707.83	3.16

1466	5000	4546.7	4552.65	4553.21	0.000744	6.04	828.07	156.91	0.46	0.000769	5.14	161	5.28
1467	5000	4546.5	4552.25	4552.82	0.000796	6.08	821.81	162.3	0.48	0.001024	4.94	166.2	5.06
1468	5000	4546.1	4551.41	4552.3	0.001367	7.56	661.19	140.46	0.61	0.000344	4.57	144.78	4.71
1469	5000	4545	4551.8	4551.88	0.000153	2.87	8825.27	4577.03	0.21	0.000294	1.93	4584.52	1.93
1470	5000	4544.6	4551.12	4551.68	0.000777	6.02	830.55	161.58	0.47	0.000765	4.95	167.63	5.14
1471	5000	4544.5	4550.69	4551.28	0.000752	6.22	889.63	239.68	0.47	0.000776	3.63	245.22	3.71
1472	5000	4544.4	4550.4	4550.86	0.000801	5.94	2478.62	1837.33	0.47	0.000438	1.35	1842.75	1.35
1473	5000	4544.3	4550.38	4550.59	0.000275	3.86	2642.01	1595	0.29	0.0003	1.65	1599.42	1.66
1474	5000	4544.3	4550.25	4550.43	0.000329	3.53	2624.16	1601.93	0.3	0.000616	1.63	1609.87	1.64
1475	5000	4544	4549.32	4550.01	0.001548	6.64	753.1	216.16	0.63	0.002357	3.42	220.02	3.48
1476	5000	4544	4547.07	4548.51	0.004016	9.61	520.15	175.88	0.99		2.92	178.3	2.96

Table C.5 HEC-RAS output for 2002 geometry

HEC-RAS Plan: 2002(8-7-06) River: Middle Rio Grande Reach: Socorro Profile: PF 1													
Agg/Deg #	Discharge	Min. Channel Elev.	W.S. Elev.	E.G. Elev.	E.G. Slope	Velocity	Flow Area	Top Width	Froude #	Frctn Slope	Hydr Radius	Wetted Perimeter	Hydr Depth
	(cfs)	(ft)	(ft)	(ft)	(ft/ft)	(ft/s)	(sq ft)	(ft)		(ft/ft)	(ft)	(ft)	(ft)
1313	5000	4607.93	4614.14	4614.69	0.000631	5.95	840.13	140.97	0.43	0.000842	5.7	147.44	5.96
1314	5000	4608.96	4613.51	4614.19	0.001181	6.65	752.18	177.05	0.57	0.000818	4.2	179.02	4.25
1315	5000	4607.18	4613.24	4613.74	0.0006	5.7	877.49	153.7	0.42	0.000771	5.54	158.34	5.71
1316	5000	4607.64	4612.69	4613.37	0.001028	6.6	757.63	162.09	0.54	0.000719	4.61	164.3	4.67
1317	5000	4606.5	4612.51	4612.96	0.00053	5.38	929.62	161.67	0.4	0.000826	5.57	166.83	5.75
1318	5000	4607.08	4611.65	4612.49	0.001458	7.38	677.47	158.66	0.63	0.0009	4.2	161.45	4.27
1319	5000	4605.94	4611.47	4611.9	0.000611	5.28	947.47	191.46	0.42	0.000715	4.87	194.44	4.95
1320	5000	4602.69	4610.87	4611.52	0.000848	6.47	773.37	142.82	0.49	0.000873	5.17	149.68	5.41
1321	5000	4605.53	4610.49	4611.06	0.000899	6.06	824.77	180.61	0.5	0.001097	4.49	183.73	4.57
1322	5000	4605.98	4609.84	4610.5	0.001368	6.55	763.22	205.52	0.6	0.000944	3.68	207.34	3.71
1323	5000	4604.5	4609.56	4609.95	0.00069	5.01	998.68	240.23	0.43	0.00141	4.11	243.11	4.16
1324	5000	4605.38	4607.93	4609.12	0.004334	8.75	571.47	237.62	0.99	0.002006	2.39	238.85	2.4
1325	5000	4603.91	4607.27	4607.72	0.001152	5.35	934.42	300.48	0.53	0.001358	3.09	302.35	3.11
1326	5000	4603.37	4606.5	4606.99	0.001625	5.65	885.46	337.28	0.61	0.000932	2.59	342.06	2.63
1327	5000	4601.48	4606.15	4606.42	0.000603	4.15	1205.84	346.85	0.39	0.000794	3.43	351.98	3.48
1328	5000	4602.42	4605.76	4606.04	0.001093	4.22	1200.38	575.36	0.49	0.001075	2.07	579.24	2.09
1329	5000	4602.08	4605.26	4605.49	0.001057	3.83	1306.8	669.18	0.48	0.001054	1.94	672.49	1.95
1330	5000	4601.19	4604.72	4604.95	0.00105	3.86	1296.26	632.07	0.47	0.000709	2.03	639.37	2.05
1331	5000	4601.69	4604.42	4604.56	0.00051	2.93	1705.5	735.83	0.34	0.000231	2.31	738.82	2.32
1332	5000	4600.85	4604.37	4604.42	0.000131	1.86	2699.99	851.01	0.18	0.000227	3.15	857.87	3.17
1333	5000	4600.83	4604.15	4604.31	0.000489	3.21	1558.14	567.74	0.34	0.000486	2.73	570.51	2.74
1334	5000	4601.11	4603.92	4604.07	0.000484	3.12	1603.96	607.37	0.34	0.000355	2.64	608.64	2.64

1335	5000	4599.75	4603.78	4603.89	0.000271	2.72	1843.93	563.9	0.26	0.000358	3.23	570.36	3.27
1336	5000	4600.29	4603.51	4603.71	0.000494	3.55	1407.69	444.44	0.35	0.000314	3.16	446.15	3.17
1337	5000	4598.3	4603.4	4603.55	0.000217	3.11	1605.68	329.38	0.25	0.000329	4.81	334.11	4.87
1338	5000	4598.3	4603.01	4603.37	0.000559	4.79	1043.95	238.4	0.39	0.000602	4.31	242.19	4.38
1339	5000	4596.76	4602.67	4603.08	0.000651	5.14	973.3	215.1	0.43	0.000673	4.46	218.23	4.52
1340	5000	4598.05	4602.46	4602.78	0.000695	4.53	1103.42	310.62	0.42	0.001273	3.52	313.62	3.55
1341	5000	4598.08	4601.08	4602.11	0.003046	8.17	612.02	216.34	0.86	0.001542	2.81	217.63	2.83
1342	5000	4596.9	4600.79	4601.18	0.000928	5.02	996.6	297.53	0.48	0.00111	3.3	302.07	3.35
1343	5000	4597.6	4600.3	4600.54	0.001352	3.95	1266.27	741.2	0.53	0.001297	1.7	743.53	1.71
1344	5000	4596.76	4599.63	4599.85	0.001246	3.8	1317.27	753.94	0.51	0.001455	1.74	756.33	1.75
1345	5000	4596.76	4598.84	4599.09	0.001722	4.01	1247.23	840.29	0.58	0.000583	1.48	841.17	1.48
1346	5000	4593.37	4598.66	4598.73	0.00029	2.18	2298.32	1016.17	0.25	0.000255	2.26	1018.22	2.26
1347	5000	4594.91	4598.53	4598.59	0.000226	2.01	2674.05	1189.86	0.23	0.000348	2.24	1195.97	2.25
1348	5000	4594.78	4598.26	4598.4	0.000603	3.06	2076.08	1223.56	0.36	0.000524	1.69	1231.26	1.7
1349	5000	4594.8	4597.97	4598.11	0.00046	3.11	2545.01	1353.19	0.33	0.000587	1.88	1354.78	1.88
1350	5000	4594.65	4597.59	4597.8	0.000775	3.72	1346.34	578.97	0.42	0.000782	2.32	579.97	2.33
1351	5000	4594.02	4597.23	4597.48	0.00079	4.02	1252.42	563.02	0.43	0.000725	2.22	564.03	2.22
1352	5000	4593.38	4596.88	4597.14	0.000668	4.09	1409.12	655.69	0.41	0.0011	2.14	657.12	2.15
1353	5000	4593.33	4596.18	4596.61	0.002142	5.29	962.08	599.24	0.67	0.001214	1.6	600.07	1.61
1354	5000	4592.65	4595.73	4595.94	0.000781	3.69	1374.2	611.7	0.42	0.000569	2.24	613.99	2.25
1355	5000	4592.25	4595.49	4595.63	0.000433	3.06	1679.41	738.27	0.32	0.000385	2.27	739.6	2.27
1356	5000	4591.79	4595.33	4595.47	0.000344	2.96	1688.95	533.26	0.29	0.000705	3.15	536.46	3.17
1357	5000	4591.28	4594.55	4595.14	0.00218	6.41	1068.05	479	0.71	0.001339	2.22	480.92	2.23
1358	5000	4590.46	4593.98	4594.28	0.000905	4.34	1151.26	422.97	0.46	0.000772	2.71	424.95	2.72
1359	5000	4590.08	4593.74	4593.91	0.000666	3.34	1494.77	647.34	0.39	0.000707	2.3	648.59	2.31
1360	5000	4587.09	4593.23	4593.54	0.000753	4.47	1118.45	340.98	0.43	0.000971	3.25	344.32	3.28

1361	5000	4589.69	4592.66	4593.05	0.001302	5	1000.9	392.15	0.55	0.001269	2.54	393.38	2.55
1362	5000	4589.04	4592.03	4592.4	0.001238	4.89	1022.53	398.18	0.54	0.001243	2.56	399.65	2.57
1363	5000	4588.62	4591.38	4591.73	0.001248	4.73	1127.57	594.6	0.54	0.001119	1.89	595.64	1.9
1364	5000	4587.69	4590.85	4591.15	0.001009	4.44	1566.1	987.94	0.49	0.000954	1.58	989.19	1.59
1365	5000	4587.04	4590.39	4590.65	0.000903	4.09	1221.07	490.56	0.46	0.00065	2.48	491.52	2.49
1366	5000	4586.17	4590.12	4590.34	0.00049	3.72	1351.31	484.2	0.35	0.000597	2.77	487.68	2.79
1367	5000	4585.94	4589.69	4590.04	0.000742	4.75	1051.72	290.06	0.44	0.000508	3.6	292.05	3.63
1368	5000	4584.96	4589.54	4589.76	0.00037	3.83	1305.42	293.24	0.32	0.000562	4.39	297.3	4.45
1369	5000	4586.34	4589.18	4589.49	0.000954	4.49	1114.44	406.43	0.48	0.001057	2.73	407.79	2.74
1370	5000	4585.93	4588.7	4589	0.001176	4.4	1137.17	499.15	0.51	0.000872	2.27	501.59	2.28
1371	5000	4584.09	4588.35	4588.56	0.000672	3.7	1350.23	503.04	0.4	0.000922	2.67	506.55	2.68
1372	5000	4585.3	4587.83	4588.14	0.001342	4.49	1132.56	639.26	0.54	0.001267	1.76	642.46	1.77
1373	5000	4585.1	4587.23	4587.48	0.001198	4.05	1237.42	659.99	0.51	0.001317	1.87	661.32	1.87
1374	5000	4584.67	4586.67	4586.93	0.001455	4.06	1231.36	715.58	0.55	0.001275	1.72	717.79	1.72
1375	5000	4583.45	4586.14	4586.34	0.001127	3.61	1383.8	791.66	0.48	0.001094	1.74	793.72	1.75
1376	5000	4582.87	4585.57	4585.77	0.001063	3.59	1391.35	768.87	0.47	0.000605	1.81	769.99	1.81
1377	5000	4582.01	4585.35	4585.46	0.00039	2.67	1874.77	781.91	0.3	0.000599	2.39	785.93	2.4
1378	5000	4582.76	4584.94	4585.15	0.001038	3.64	1372.27	730.2	0.47	0.000851	1.88	730.87	1.88
1379	5000	4581.82	4584.62	4584.81	0.00071	3.5	1427.75	604.56	0.4	0.000543	2.35	606.88	2.36
1380	5000	4579.59	4584.46	4584.57	0.000429	2.69	1860.54	802.13	0.31	0.000346	2.31	806.09	2.32
1381	5000	4581.22	4584.35	4584.43	0.000285	2.36	3129.01	1509.71	0.26	0.00022	2.07	1513.64	2.07
1382	5000	4580.83	4584.27	4584.31	0.000175	1.86	3815.22	1636.27	0.2	0.000159	2.32	1643.68	2.33
1383	5000	4579.96	4584.19	4584.24	0.000145	1.89	3524.73	1548.7	0.19	0.000214	2.27	1555.13	2.28
1384	5000	4579.42	4584.03	4584.14	0.000346	2.73	1910.63	725.11	0.29	0.000488	2.62	729.34	2.63
1385	5000	4578.83	4583.76	4583.92	0.000739	3.43	2429.97	1681.41	0.4	0.001033	1.44	1686.57	1.45
1386	5000	4579.17	4583.14	4583.41	0.001547	4.62	2269.33	1626.36	0.58	0.001423	1.39	1628.87	1.4

1387	5000	4578.46	4582.5	4582.81	0.001314	4.62	1593.34	1005.32	0.54	0.001288	1.58	1007.64	1.58
1388	5000	4578.18	4581.9	4582.19	0.001263	4.34	1415.21	807.51	0.53	0.001396	1.75	809.29	1.75
1389	5000	4578.14	4581.15	4581.49	0.001551	4.72	1411.19	1014.55	0.58	0.001922	1.39	1016.71	1.39
1390	5000	4577.83	4580.1	4580.54	0.002445	5.31	957.89	584.04	0.71	0.001136	1.64	585.81	1.64
1391	5000	4576.86	4579.74	4579.89	0.000654	3.15	1653.2	811.78	0.38	0.000663	2.03	813.62	2.04
1392	5000	4576.1	4579.45	4579.54	0.000673	2.83	2862.25	1141.48	0.37	0.000506	2.5	1144.78	2.51
1393	5000	4575.35	4579.19	4579.29	0.000395	2.65	2861.83	1135.81	0.3	0.000361	2.5	1144.05	2.52
1394	5000	4572.55	4578.99	4579.11	0.000331	2.79	2005.8	770.12	0.28	0.000188	2.59	774.56	2.6
1395	5000	4574.71	4578.94	4579	0.000121	1.98	3297.59	1004.58	0.18	0.0001	3.27	1009.12	3.28
1396	5000	4574.24	4578.91	4578.95	0.000084	1.8	4454.27	1087.77	0.15	0.000124	4.08	1092.78	4.09
1397	5000	4573.64	4578.76	4578.88	0.0002	2.79	1863.77	462.46	0.24	0.0003	4.02	464.2	4.03
1398	5000	4572.41	4578.43	4578.71	0.000498	4.23	1185.13	304.55	0.37	0.000744	3.85	307.88	3.89
1399	5000	4573.19	4577.76	4578.31	0.001232	6.18	1320.44	620.34	0.57	0.000689	2.11	624.36	2.13
1400	5000	4572.78	4577.61	4577.88	0.000439	4.25	1543.07	532.8	0.35	0.000681	2.87	537.15	2.9
1401	5000	4572.55	4577.06	4577.52	0.001196	5.6	1252.78	755.23	0.55	0.00099	1.65	757.96	1.66
1402	5000	4572.18	4576.59	4577.02	0.000833	5.49	1702.77	1151.21	0.48	0.000698	1.48	1154.37	1.48
1403	5000	4572.04	4576.38	4576.6	0.000594	4.35	3090.34	1331.12	0.4	0.00029	2.32	1334.23	2.32
1404	5000	4570.5	4576.36	4576.41	0.000171	2.37	5932.6	1857.68	0.21	0.000261	3.18	1865.59	3.19
1405	5000	4571.7	4576.02	4576.27	0.000444	4.07	1497.35	657.22	0.35	0.000574	2.27	660.63	2.28
1406	5000	4572.01	4575.73	4575.98	0.000771	4.07	1403.18	635.89	0.43	0.000489	2.19	640.58	2.21
1407	5000	4571.24	4575.56	4575.71	0.000337	3.14	1591.14	453.03	0.3	0.000639	3.49	455.45	3.51
1408	5000	4571.96	4574.82	4575.35	0.001645	5.87	853.62	323.23	0.63	0.001958	2.63	324.83	2.64
1409	5000	4570.12	4573.81	4574.43	0.002369	6.3	793.77	342.46	0.73	0.00025	2.3	345.3	2.32
1410	5000	4567.37	4574.11	4574.12	0.000089	1.47	13846.12	4985.72	0.15	0.000274	2.77	4994.17	2.78
1411	5000	4570.04	4572.95	4573.91	0.004589	7.86	635.85	323.72	0.99	0.000293	1.95	325.58	1.96
1412	5000	4569.6	4573.1	4573.1	0.000096	1.34	13539.34	5076.82	0.15	0.000184	2.67	5080.1	2.67

1413	5000	4567.52	4572.79	4573.01	0.000488	3.7	1364.52	433.51	0.35	0.000725	3.12	437.4	3.15
1414	5000	4566.88	4572.39	4572.64	0.001186	4.03	1240.68	630.77	0.5	0.001803	1.95	635.73	1.97
1416	5000	4568.17	4571.2	4571.73	0.003066	5.87	935.73	639.96	0.79	0.000554	1.46	641.34	1.46
1417	5000	4566.05	4571.23	4571.31	0.000223	2.39	2092.63	656.03	0.24	0.000334	3.16	662.79	3.19
1418	5000	4567.86	4570.98	4571.15	0.000552	3.24	1585.9	724.17	0.36	0.000402	2.19	725.75	2.19
1419	5000	4566.42	4570.82	4570.92	0.000306	2.48	2013.19	759.23	0.27	0.000434	2.64	761.7	2.65
1420	5000	4564.18	4570.53	4570.69	0.000662	3.23	1547.72	719.36	0.38	0.000544	2.13	727.35	2.15
1421	5000	4566.49	4570.29	4570.41	0.000455	2.72	1928.82	912.62	0.32	0.001089	2.11	915.75	2.11
1422	5000	4566.88	4569.17	4569.81	0.005325	6.42	779.26	603.38	0.99	0.002038	1.29	605.25	1.29
1423	5000	4565.86	4568	4568.18	0.001068	3.4	1537.96	986.56	0.47	0.000498	1.56	987.64	1.56
1424	5000	4564.22	4567.79	4567.88	0.000287	2.45	2480.79	1141.19	0.26	0.000452	2.17	1145.25	2.17
1425	5000	4564.74	4567.46	4567.63	0.000812	3.28	1531.04	800.77	0.42	0.000659	1.91	803.45	1.91
1426	5000	4564.46	4567.16	4567.29	0.000545	2.9	1793.71	996.44	0.35	0.000486	1.8	998.11	1.8
1427	5000	4564.17	4566.95	4567.05	0.000435	2.59	1933.71	896.05	0.31	0.000453	2.15	897.56	2.16
1428	5000	4561.6	4566.68	4566.82	0.000472	2.94	1778.57	801.8	0.33	0.000748	2.21	806.32	2.22
1429	5000	4563.71	4566.16	4566.42	0.001362	4.22	1808.11	1478.67	0.54	0.000859	1.22	1480.98	1.22
1430	5000	4563.28	4565.81	4565.94	0.00059	3.19	2775.66	1719.41	0.37	0.000799	1.61	1720.18	1.61
1431	5000	4562.94	4565.29	4565.52	0.001143	3.85	1593.01	1700.26	0.49	0.000986	0.94	1702.27	0.94
1432	5000	4562.68	4564.83	4564.98	0.00086	3.48	3050.47	1982.71	0.43	0.000807	1.54	1985.39	1.54
1433	5000	4561.88	4564.37	4564.55	0.000759	3.45	2305.25	2147.16	0.41	0.000519	1.07	2148.06	1.07
1434	5000	4561.19	4564.15	4564.26	0.000378	2.91	3721.7	1988.14	0.3	0.000495	1.87	1989.54	1.87
1435	5000	4560.91	4563.79	4564	0.000678	3.69	1400.49	639.27	0.4	0.001192	2.19	640.41	2.19
1436	5000	4560.62	4562.88	4563.35	0.002627	5.54	903.31	514.58	0.74	0.001529	1.75	515.5	1.76
1437	5000	4558.97	4562.2	4562.46	0.000999	4.07	1227.28	535.2	0.47	0.001221	2.28	537.11	2.29
1438	5000	4559.53	4561.6	4561.83	0.001527	4	1827.67	1362.43	0.55	0.000867	1.34	1363.2	1.34
1439	5000	4558.63	4561.21	4561.34	0.000558	3	2403.07	1433.1	0.35	0.000915	1.67	1434.83	1.68

1440	5000	4558.1	4560.56	4560.87	0.00177	4.44	1126.87	663.85	0.6	0.001681	1.69	666.28	1.7
1441	5000	4557.05	4559.74	4560.04	0.001598	4.4	1140.25	696.04	0.58	0.000456	1.63	697.62	1.64
1442	5000	4554.83	4559.66	4559.75	0.000212	2.38	2109.06	691.54	0.23	0.000466	3	702.13	3.05
1443	5000	4555.4	4559.17	4559.5	0.001724	4.62	1082.27	586.58	0.6	0.00079	1.83	590.57	1.85
1444	5000	4555.95	4558.96	4559.06	0.000451	2.69	3586.72	2249.19	0.32	0.00056	1.59	2256.3	1.59
1445	5000	4556.29	4558.63	4558.77	0.000714	3.02	1658.36	883.66	0.39	0.00073	1.87	885.81	1.88
1446	5000	4555.96	4558.3	4558.42	0.000747	2.82	1770.27	1076.84	0.39	0.000697	1.64	1079.54	1.64
1447	5000	4555.61	4557.95	4558.08	0.000651	2.84	1763	961.77	0.37	0.00064	1.83	963.88	1.83
1448	5000	4554.85	4557.63	4557.77	0.00063	2.96	1711.05	977.44	0.37	0.00075	1.75	979.12	1.75
1449	5000	4554.9	4557.22	4557.41	0.000909	3.55	1497.13	994.83	0.44	0.001225	1.5	997.67	1.5
1450	5000	4553.02	4556.57	4556.81	0.001741	3.91	1301.31	997.18	0.58	0.001466	1.3	1004.71	1.3
1451	5000	4553.64	4555.92	4556.1	0.001251	3.41	1467.79	992.25	0.49	0.000767	1.48	994.21	1.48
1452	5000	4552.91	4555.52	4555.6	0.000518	2.32	2158.87	1344.46	0.32	0.000404	1.6	1347.16	1.61
1453	5000	4552.47	4555.39	4555.45	0.000323	1.9	2636.37	1553.51	0.26	0.000376	1.69	1558.55	1.7
1454	5000	4552.04	4555.2	4555.26	0.000444	2.08	2424.15	1651.59	0.3	0.000394	1.46	1661.55	1.47
1455	5000	4552.65	4555	4555.08	0.000353	2.13	2363.5	1332.44	0.27	0.000402	1.77	1333.98	1.77
1456	5000	4548.67	4554.72	4554.87	0.000463	3.13	1598.83	575.06	0.33	0.000768	2.74	583.98	2.78
1457	5000	4551.97	4554.13	4554.48	0.001518	4.72	1059.66	512.63	0.58	0.000549	2.07	513.12	2.07
1458	5000	4550.38	4554.04	4554.16	0.000281	2.78	1817.04	605.48	0.27	0.000342	2.99	608.72	3
1459	5000	4550.64	4553.86	4554.01	0.000427	3.09	1667.36	657.73	0.32	0.000406	2.52	660.8	2.54
1460	5000	4550.03	4553.67	4553.8	0.000387	2.92	1746.2	669.19	0.31	0.000072	2.6	672.04	2.61
1461	5000	4548.8	4553.72	4553.73	0.000029	1.11	17201	5689.29	0.09	0.000032	3.02	5693.03	3.02
1462	5000	4545.56	4553.71	4553.71	0.000036	1.12	17719.79	5785.57	0.1	0.000032	3.06	5791.14	3.06
1463	5000	4548.44	4553.69	4553.7	0.000028	1.07	18575.22	5025.32	0.09	0.000075	3.69	5029.68	3.7
1464	5000	4547.91	4553.47	4553.64	0.000521	3.33	1502.27	543.21	0.35	0.000719	2.75	546.42	2.77
1465	5000	4547.95	4552.86	4553.25	0.001056	5.13	1273.98	512.08	0.51	0.001173	2.48	514.43	2.49

1466	5000	4546.82	4552.14	4552.67	0.001312	6	1146.06	510.95	0.58	0.000176	2.23	513.8	2.24
1467	5000	4545.99	4552.41	4552.43	0.000066	1.7	15322.64	5309.26	0.14	0.00018	2.88	5313.92	2.89
1468	5000	4546.31	4551.52	4552.27	0.001484	7.05	955.74	487.23	0.63	0.00174	1.95	489.99	1.96
1469	5000	4546.43	4550.65	4551.38	0.002068	6.93	835.01	425.1	0.71	0.000492	1.96	426.72	1.96
1470	5000	4545.53	4550.87	4550.93	0.000215	3.04	8648.08	4086.25	0.25	0.00023	2.11	4089.7	2.12
1471	5000	4545.15	4550.75	4550.8	0.000247	2.65	7087.71	3110.51	0.25	0.000298	2.28	3114.27	2.28
1472	5000	4544.23	4550.53	4550.64	0.000368	3.42	5047.54	2382.58	0.31	0.000336	2.11	2387.91	2.12
1473	5000	4544.82	4550.32	4550.48	0.000308	3.49	3282.61	2043.24	0.29	0.000336	1.6	2047.7	1.61
1474	5000	4544.69	4550.14	4550.33	0.000367	3.59	2656.29	1761.86	0.31	0.000562	1.5	1765.24	1.51
1475	5000	4544.73	4549.55	4549.97	0.000964	5.27	1235.28	764.11	0.5	0.001371	1.61	767.02	1.62
1476	5000	4544.6	4548.33	4549.1	0.002104	7.16	962.1	645.72	0.72		1.49	647.08	1.49

Appendix D – Bed Material Grain Size Distributions

Table D.1 Grain size distribution (subreach 1)

Bed Material Percent Finer					
(mm)	1962	1972	1985	1992	2002
0.0625	5	25	15	14	0
0.125	30	62	38	27	3
0.25	94	96	81	66	21
0.5	100	100	96	90	73
1	100	100	98	95	86
2	100	100	98	96	91
4	100	100	99	97	94
8	100	100	100	97	95
16	100	100	100	98	96
32	100	100	100	98	96
64	100	100	100	100	100

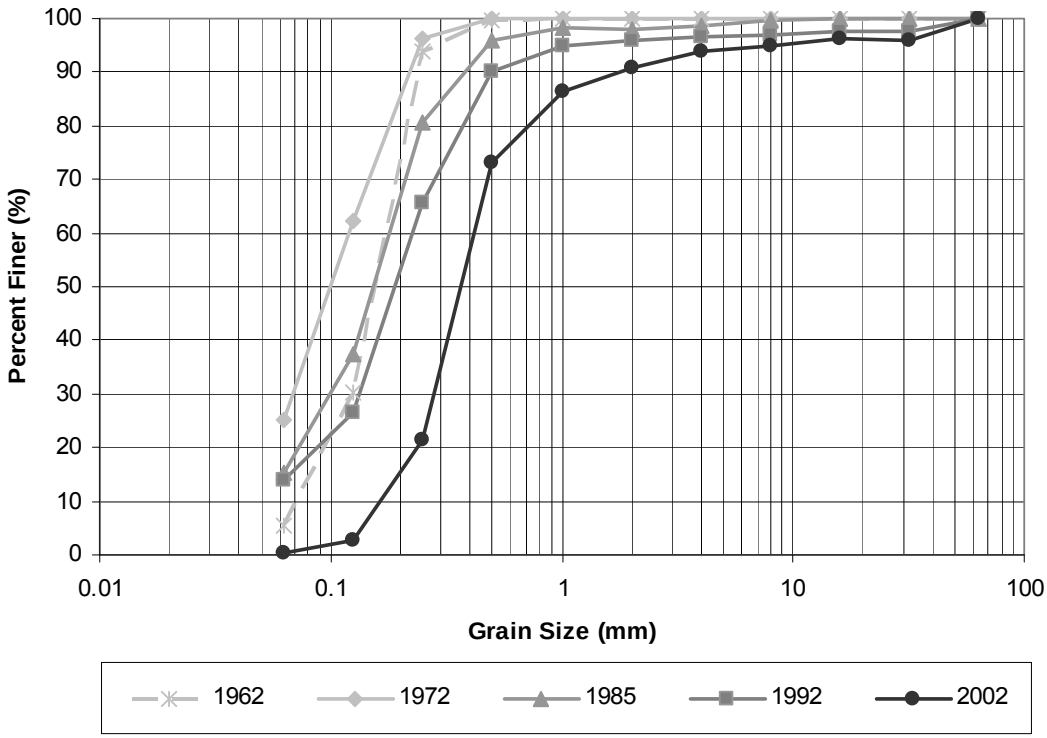

Figure D.1 Bed material grain size distribution (subreach 1)

Table D.2 Grain size distribution (subreach 2)

Bed Material Percent Finer					
(mm)	1962	1972	1985	1992	2002
0.0625	5	25	25	5	0
0.125	30	62	50	12	1
0.25	94	96	88	49	33
0.5	100	100	98	99	90
1	100	100	99	100	99
2	100	100	99	100	100
4	100	100	99	100	100
8	100	100	100	100	100
16	100	100	100	100	100
32	100	100	100	100	100
64	100	100	100	100	100

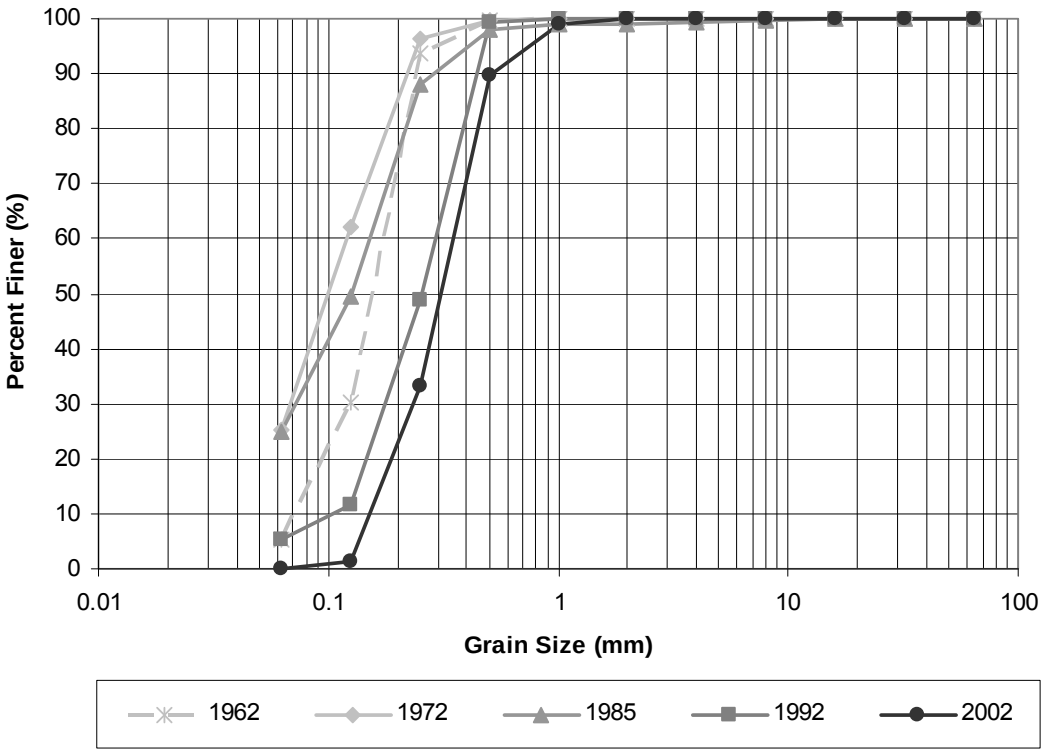

Figure D.2 Bed material grain size distribution (subreach 2)

Table D.3 Grain size distribution (subreach 3)

Bed Material Percent Finer					
(mm)	1962	1972	1985	1992	2002
0.0625	5	25	35	1	0
0.125	30	62	62	10	5
0.25	94	96	95	54	54
0.5	100	100	100	99	98
1	100	100	100	100	100
2	100	100	100	100	100
4	100	100	100	100	100
8	100	100	100	100	100
16	100	100	100	100	100
32	100	100	100	100	100
64	100	100	100	100	100

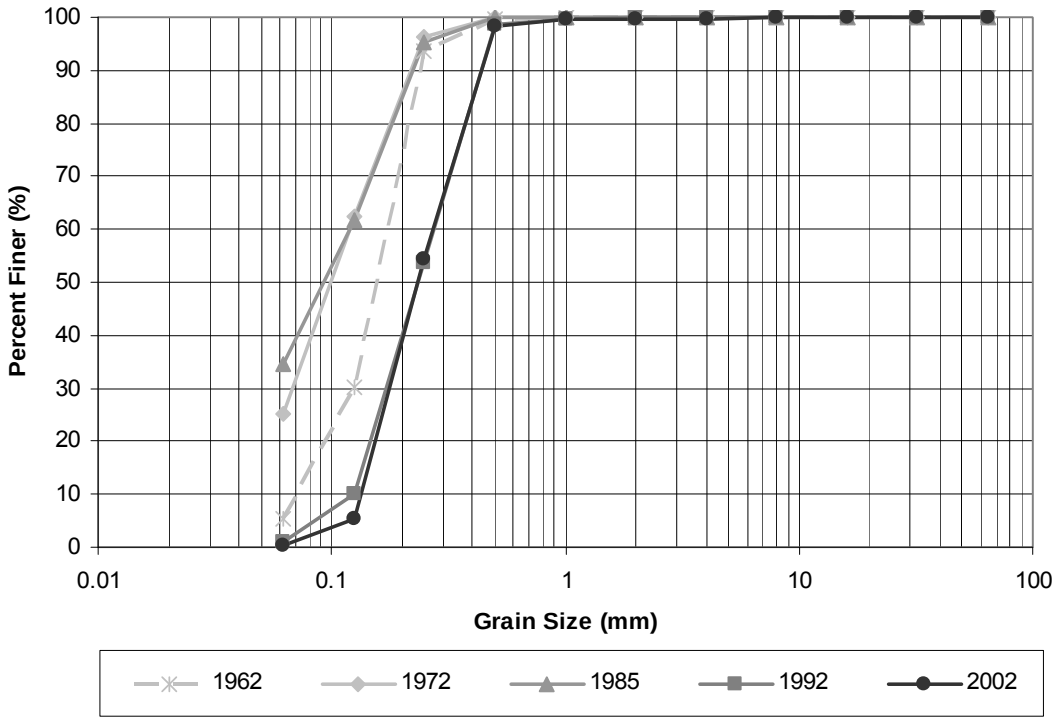

Figure D.3 Bed material grain size distribution (subreach 3)

Table D.4 Grain size distribution (Escondida reach)

Bed Material Percent Finer					
(mm)	1962	1972	1985	1992	2002
0.0625	5	25	23	4	0
0.125	30	62	47	13	4
0.25	94	96	86	54	45
0.5	100	100	97	98	93
1	100	100	99	99	98
2	100	100	99	99	99
4	100	100	99	100	99
8	100	100	100	100	99
16	100	100	100	100	100
32	100	100	100	100	100
64	100	100	100	100	100

Appendix E – Bedforms

Example Bedform Field Notes
Example Cross-sections with Bedform Information
Summary of Bedform Observations

U.S.B.R. ALBUQUERQUE PROJECT OFFICE CROSS SECTION FIELD NOTES

Cross Section SO-1437.9 Party WTT, GRS, BAP, RET Page 1 of 3

Date 6-5-94 Weather Sunny, 80°F Length 702

LEP B&C 4562.57 TLP 4564.94 REP B&C 4562.14 FLO 4-30-94 TLP 4563.51

TOTAL LOST & PHOTOS FLO 4-30-94 HI#1 4568.00 HI#2 HI#3

Station	Rod	Depth	Elevation	Notes
0	5.43		4562.57	LEP B&C
0	3.59		4564.41	LEP +LP
0	5.43		4562.57	GRND TRANS
10	5.45		4562.55	
25	5.69		4562.31	
35	5.26		4562.74	
44	4.95		4563.05	
47	5.13		4562.87	TOP of BANK
50	6.02	0	4561.98	LEW
57		3.1	4558.9	Trans Ripples / Dunes (USE W.S. 4562.
70		0.4	4561.6	Ripples
80		0.3	4561.7	
100		0.4	4561.6	
120		1.6	4560.4	PLANE BED
140		2.4	4559.6	
160		2.8	4559.2	
180		2.7	4559.3	
200		2.5	4559.5	TRANS PLANE Bd / ANTI DUNES
220		2.4	4559.6	
240		~~2.9~~ 2.3	4559.7	
260		2.1	4559.9	PLANE Bd
280		2.1	4559.9	
300		2.0	4560.0	
320		2.2	4559.8	

RECD	CHKD	ENTER	FN=

Figure E.1 Field notes for example cross-section (pg.1)

U.S.B.R. ALBUQUERQUE PROJECT OFFICE CROSS SECTION FIELD NOTES

Cross Section SO-1437.9 Party W+F GRS BAP RET Page 2 of 3

Date 6-5-94 Weather Length 702

LEP B&C 4562.57 TLP 4564.94 REP B&C 4562.14 TLP 4563.51

AVG. WS. F/B 4-30-94 HI#1 4568.00 HI#2 HI#3 F/B 4-30-94 E/C +/- =

Station	Rod	Depth	Elevation	Notes
340		2.9	4559.0	TRANS PLANE Bd / DUNES (USE W.S. 4561.9)
360		3.5	4558.4	↓ ↓
380		4.0	4557.9	DUNES
400		3.5	4558.4	"
420		3.9	4558.0	SAND DEP BELOW LARGE BAR
430		2.0	4559.9	↓ ↓ ↓
440		1.6	4560.3	
450		0.5	4561.4	DEP ON LARGE BAR
460		0.5	4561.4	↓ ↓ ↓
480		0.7	4561.2	LARGE TRANSIENT BAR
500		0.9	4561.0	" " "
520		0.4	4561.4	" " " (USE W.S. 4561.8)
540		0.3	4561.5	" " "
560		0.4	4561.4	RIPPS
580		0.3	4561.5	↓
600		0.5	4561.3	
610		0.5	4561.3	
620		0.7	4561.1	TRANS RIPP / DUNE
640		1.5	4560.3	TRANS DUNES / PLANE Bd
650		1.3	4560.5	↓ ↓
660		1.3	4560.5	
662		1.0	4560.8	
666	6.21	0	4561.79	REW
666	5.58		4562.42	TOB
				RECD CHKD ENTER FN=

Figure E.2 Field notes for example cross-section (pg.2)

U.S.D.H. ALBUQUERQUE PROJECT OFFICE CROSS SECTION FIELD NOTES

Cross Section SO 1437.9 Party WTF, GRJ, BAP, RET Page 3 of 3

Date 6-5-94 Weather _____ Length _____

LEP B&C 4562.57 TLP 4564.94 REP B&C 4562.14 TLP 4563.51

AVG. WS. PIO 4-30-94 HI#1 4568.00 HI#2 _____ HI#3 _____ E/C +/- = _____

Station	Rod	Depth	Elevation	Notes
670	5.55		4562.45	TAM'S
685	5.64		4562.36	℄ JACK
702	5.79		4562.21	REP GRND
707	4.49		4563.51	REP TLP
702	5.87		4562.13	REP B&C Δ = -0.01 ok

RECD	CHKD	ENTER	FN=

Figure E.3 Field notes for example cross-section (pg.3)

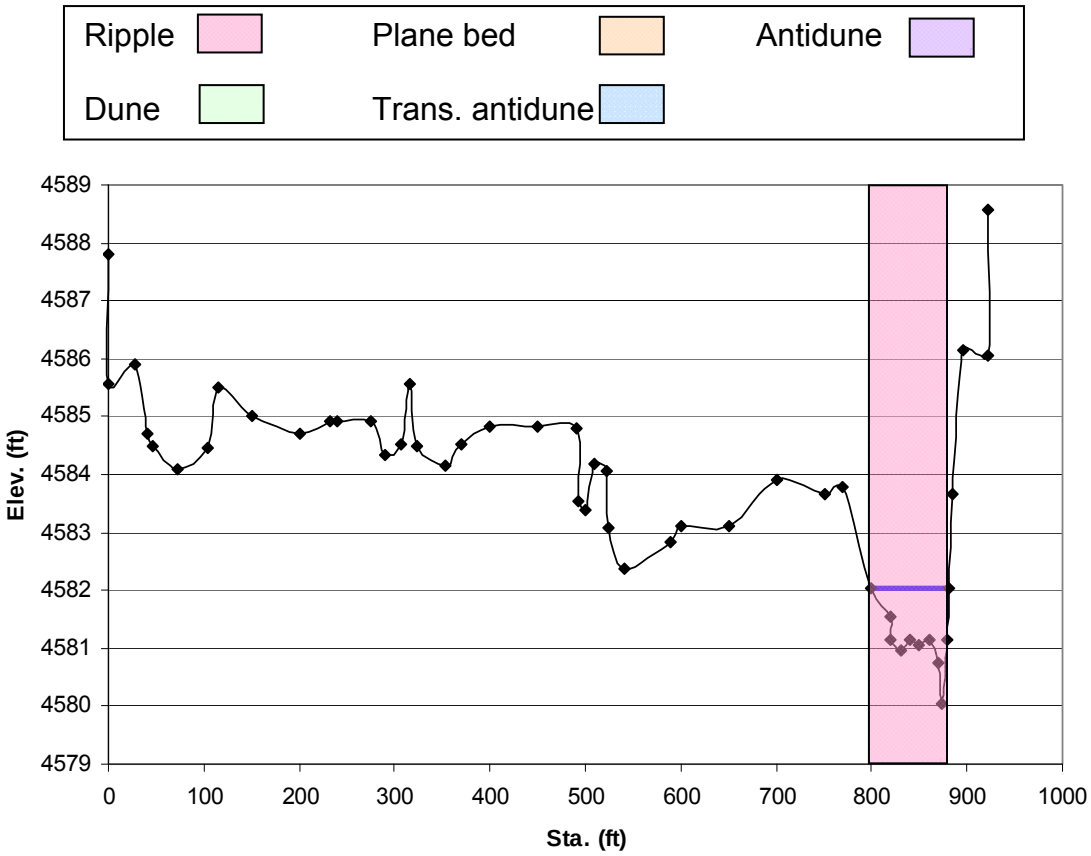

Figure E.4 Cross-section 1380 (surveyed 9/12/1990, Q =70 cfs)

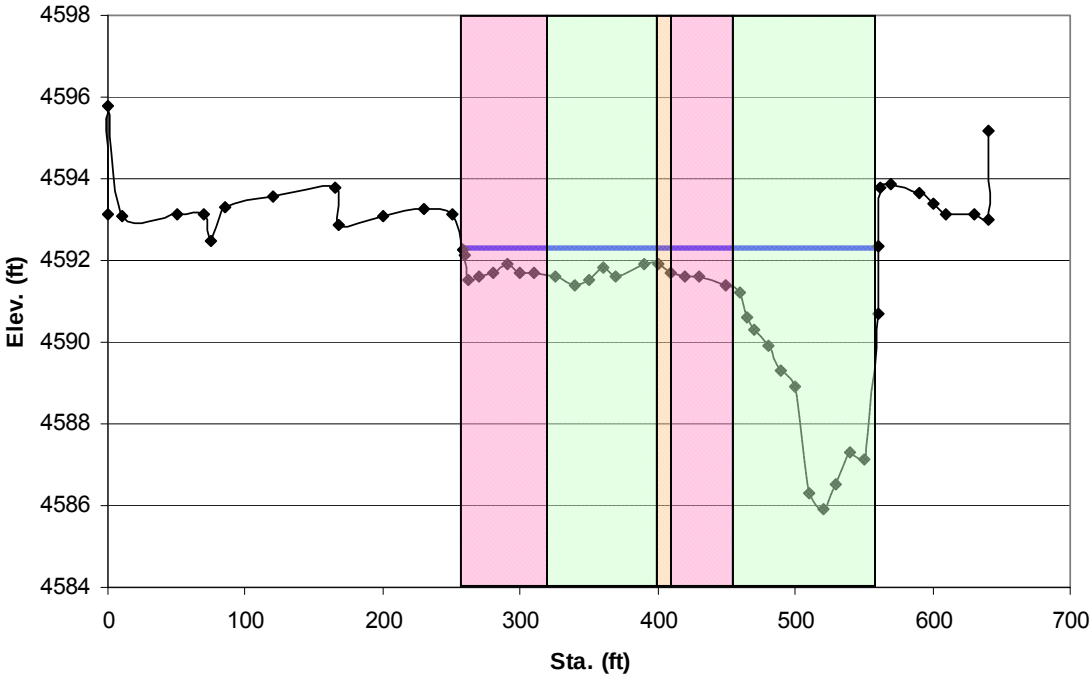

Figure E.5 Cross-section 1360 (surveyed 4/23/1991, Q = 2300 cfs)

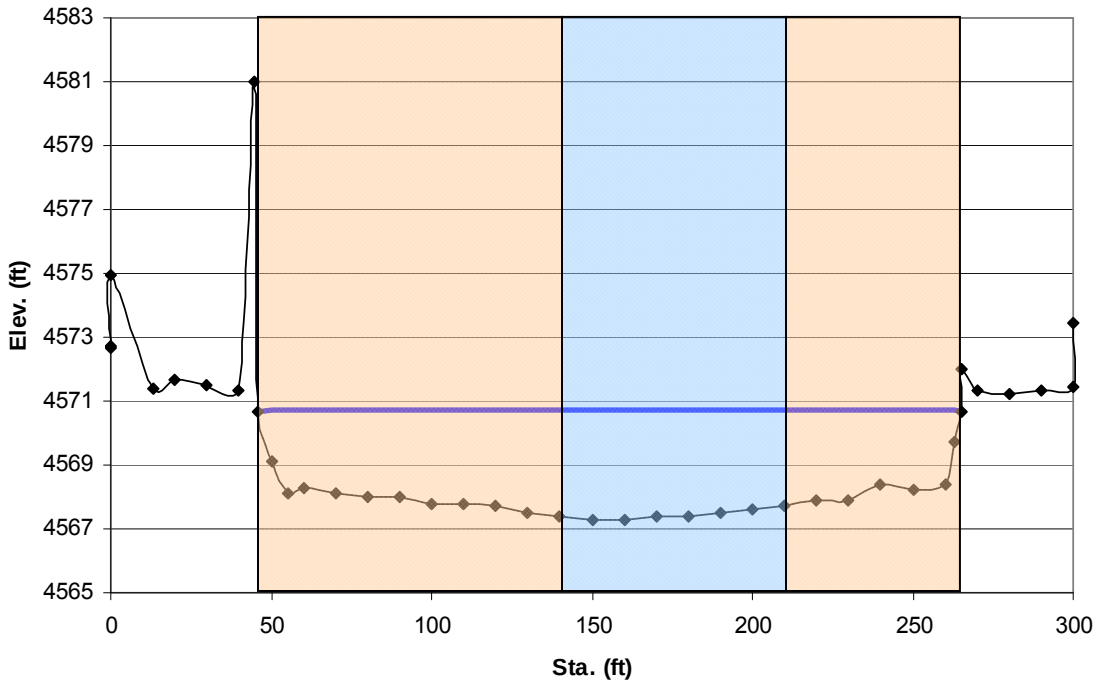

Figure E.6 Cross-section 1414 (surveyed 5/23/1992, Q = 3800 cfs)

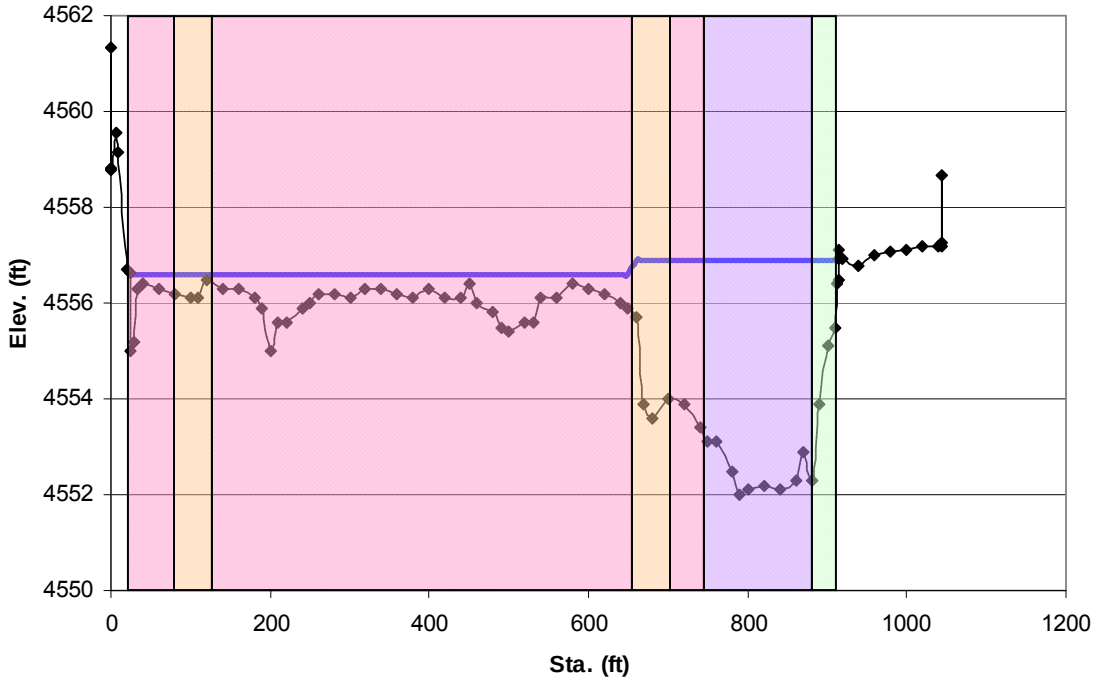

Figure E.7 Cross-section 1450 (surveyed 5/27/1993, Q = 5000 cfs)

Table E.1 Summary of bedform observations

Date	SO-line	Dominate Bedform	Description	Discharge (cfs)		
				Calculated at cross-section	San Acacia	San Marcial
9/12/1990	1380	R	ripples		92	58
9/12/1990	1394	R	ripples		92	58
9/12/1990	1401	R	ripples		92	58
9/12/1990	1410	R	ripples		92	58
9/13/1990	1414	R	ripples		186	31
9/13/1990	1428	R	ripples		186	31
9/13/1990	1437.9	R	ripples		186	31
9/13/1990	1443	PB-R	flat bed w/ no motion, ripples		186	31
9/13/1990	1450	PB	flat bed w/ motion		186	31
9/14/1990	1456	R-D	dunes, ripples		114	52
9/14/1990	1462	R-D	dunes, ripples, flat bed		114	52
9/14/1990	1470.5	R	ripples		114	52
4/23/1991	1320	D	dunes		2300	1660
4/23/1991	1346	UPB	upper regime plane bed, dunes, ripples		2300	1660
4/23/1991	1360	R-D	ripples, small dunes, flat bed		2300	1660
4/24/1991	1380	D-UPB	flat bed, dunes, ripples, anti-dunes		2430	1820
4/24/1991	1401	UPB	dunes, flat bed		2430	1820
4/25/1991	1437.9	PB-R	dunes, ripples, plane bed w/ motion		2760	1880
4/25/1991	1450	R	dunes, plane bed, ripples		2760	1880
4/26/1991	1470.5	D-UPB	plane bed w/ motion, dunes		2740	2020
6/4/1991	1437.9	PB	ripples, small dunes, flat bed		3460	3030
6/5/1991	1450	UPB-AD	ripples, flat bed, anti-dunes, dunes		3470	3130
6/5/1991	1470.5	PB	flat bed		3470	3130
6/11/1991	1306	PB	plane bed w/ motion, dunes		3560	3100
6/11/1991	1320	PB	plane bed		3560	3100
6/11/1991	1346	R-D	plane bed, ripples, dunes		3560	3100
6/11/1991	1360	PB	plane bed, dunes		3560	3100
6/12/1991	1380	D	plane bed, ripples, dunes		3280	2920
6/12/1991	1401	PB	plane bed w/ motion		3280	2920
2/20/1992	1306	R-D	ripples, dunes		615	375
2/21/1992	1320	R-D	ripples, small dunes		609	357
2/21/1992	1339	R	ripples		609	357
2/21/1992	1346	R-D	ripples, dunes		609	357

2/21/1992	1360	R-D	ripples, dunes		609	357
2/21/1992	1371	R-D	ripples, small dunes		609	357
2/21/1992	1380	PB	ripples, plane bed		609	357
2/21/1992	1394	PB-R	ripples, flat bed		609	357
2/21/1992	1401	PB-R	ripples, flat bed		609	357
2/22/1992	1410	PB-R	ripples, flat bed		668	380
2/22/1992	1414	PB-R	flat bed, ripples, dunes		668	380
2/22/1992	1420	R	ripples		668	380
2/22/1992	1428	R	ripples, flat bed		668	380
2/22/1992	1437.9	R	ripples, flat bed		668	380
2/22/1992	1443	R	small dunes, ripples		668	380
2/22/1992	1450	R	ripples, flat bed		668	380
2/22/1992	1456	PB-R	ripples, flat bed w/o motion, flat bed w/ motion		668	380
2/22/1992	1462	R	small dunes, ripples, flat bed		668	380
2/22/1992	1470.5	PB-R	ripples, flat bed		668	380
4/25/1992	1414	UPB	flat bed		4010	3950
4/26/1992	1437.9	UPB-AD	flat bed, small anti-dunes, ripples		4330	3890
4/27/1992	1414	UPB-AD	flat bed, slight anti-dunes		4340	3960
4/27/1992	1470.5	UPB	flat bed		4340	3960
5/8/1992	1410	UPB	flat bed w/ movement, ripples		5460	5230
5/8/1992	1414	R	ripples		5460	5230
5/8/1992	1420	UPB-AD	dunes, flat bed w/ movement, anti-dunes		5460	5230
5/9/1992	1428	PB-R	ripples, flat bed, dunes		5400	4930
5/9/1992	1437.9	UPB-AD	ripples, flat bed, trans. anti-dunes,dunes		5400	4930
5/10/1992	1443	PB-R	ripples, dunes, flat bed		5380	4760
5/10/1992	1450	R	ripples, flat bed, small anti-dunes, dunes		5380	4760
5/10/1992	1456	R	anti-dunes, flat bed, dunes, ripples		5380	4760
5/10/1992	1462	PB-R	flat bed, ripples		5380	4760
5/10/1992	1470.5	PB	flat bed		5380	4760
5/11/1992	1414	UPB	flat bed w/ movement		5500	4700
5/11/1992	1470.5	UPB	flat bed w/ movement, dunes		5500	4700
5/23/1992	1414	UPB-AD	flat bed, slight anti-dunes		3790	3920
5/23/1992	1470.5	UPB-AD	flat bed, slight anti-dunes		3790	3920
5/24/1992	1414	UPB-AD	flat bed, slight anti-dunes		4190	4620
5/24/1992	1437.9	UPB-AD	flat bed, slight anti-dunes, anti-dunes, ripples		4190	4620
5/25/1992	1470.5	UPB-AD	flat bed, slight anti-dunes		3690	5570

3/29/1993	1470.5	PB	plane bed		2750	2600
3/30/1993	1410	PB	plane bed		3200	2880
3/30/1993	1414	PB	plane bed		3200	2880
3/30/1993	1420	PB	plane bed, ripples		3200	2880
3/30/1993	1428	PB	plane bed, ripples, dunes		3200	2880
3/31/1993	1437.9	R	dunes, plane bed, ripples		3090	3880
3/31/1993	1443	PB-D	ripples, trans. dunes, plane bed		3090	3880
3/31/1993	1450	PB-R	ripples, dunes, plane bed		3090	3880
3/31/1993	1456	PB	ripples, plane bed		3090	3880
3/31/1993	1462	PB	plane bed, ripples		3090	3880
4/2/1993	1414	PB	plane bed		2400	2790
4/2/1993	1470.5	PB	plane bed		2400	2790
4/20/1993	1414	PB	ripples, plane bed		3250	3570
4/22/1993	1437.9	PB-R	plane bed, ripples		3030	2950
4/23/1993	1470.5	PB	plane bed		3060	2520
4/24/1993	1470.5	PB	plane bed, small anti-dunes		3060	2230
4/25/1993	1414	PB-R	ripples, plane bed		3290	2020
5/26/1993	1410	PB	plane bed		5200	4820
5/26/1993	1414	PB	plane bed		5200	4820
5/26/1993	1420	PB	plane bed		5200	4820
5/26/1993	1428	PB-R	ripples, plane bed		5200	4820
5/26/1993	1443	UPB-AD	plane bed, small anti-dunes		5200	4820
5/27/1993	1437.9	D-AD	small dunes, ripples, plane bed, anti-dunes		5340	4980
5/27/1993	1450	AD	ripples, plane bed, small anti-dunes, dunes		5340	4980
5/27/1993	1456	PB	ripples, dunes, plane bed		5340	4980
5/27/1993	1462	D	dunes, plane bed, ripples		5340	4980
5/28/1993	1414	PB	plane bed		5240	4900
5/28/1993	1470.5	PB	plane bed		5240	4900
6/11/1993	1414	PB	plane bed		5790	5290
6/11/1993	1470.5	PB	plane bed		5790	5290
6/12/1993	1437.9	PB-R	plane bed, ripples, small dunes		5510	5440
6/16/1993	1414	PB	ripples, plane bed		3590	2030
6/16/1993	1470.5	PB	plane bed		3590	2030
6/18/1993	1414	PB	plane bed		4030	2080
6/18/1993	1470.5	PB	plane bed		4030	2080
6/21/1993	1410	UPB-AD	ripples, plane bed, small anti-dunes		4350	4040
6/21/1993	1420	PB	plane bed, small anti-dunes		4350	4040
6/22/1993	1462	PB	plane bed		4590	4730

6/24/1993	1428	PB	ripples, plane bed, dunes		3350	4560
6/24/1993	1437.9	PB-R	ripples, plane bed, dunes		3350	4560
6/24/1993	1443	PB-D	ripples, plane bed, dunes		3350	4560
6/24/1993	1450	PB-D	ripples, plane bed, dunes		3350	4560
6/24/1993	1456	PB	ripples, plane bed, dunes		3350	4560
6/25/1993	1414	PB-D	plane bed, dunes		3110	3080
6/25/1993	1470.5	UPB-AD	plane bed, trans. anti-dunes		3110	3080
4/29/1994	1410	PB	plane bed		4240	3680
4/29/1994	1414	PB	plane bed		4240	3680
4/30/1994	1420	PB	plane bed, dunes		3080	3350
4/30/1994	1428	R	ripples, plane bed, small dunes		3080	3350
4/30/1994	1437.9	PB-R	ripples, plane bed, small dunes		3080	3350
4/30/1994	1443	PB	ripples, plane bed, small dunes		3080	3350
4/30/1994	1450	PB-R	ripples, plane bed, small dunes		3080	3350
4/30/1994	1456	D	ripples, dunes		3080	3350
4/30/1994	1462	PB-R	plane bed, ripples		3080	3350
5/1/1994	1470.5	PB	plane bed		2960	2920
5/4/1994	1414	D	ripples, plane bed, small dunes		2710	2250
5/4/1994	1470.5	PB	ripples, plane bed		2710	2250
5/19/1994	1414	PB	ripples, plane bed		5120	4150
5/19/1994	1437.9	PB-R	small dunes, plane bed, ripples		5120	4150
5/20/1994	1414	PB	plane bed, ripples		5150	4190
5/20/1994	1470.5	PB	plane bed		5150	4190
5/20/1994	1470.5	PB	plane bed		5150	4190
5/21/1994	1410	PB	plane bed, dunes		5010	4230
5/21/1994	1414	PB	plane bed		5010	4230
5/21/1994	1420	PB	plane bed		5010	4230
5/21/1994	1428	PB	plane bed, dunes, ripples		5010	4230
5/21/1994	1437.9	R-D	plane bed, dunes, ripples		5010	4230
5/21/1994	1462	R	plane bed, ripples, anti-dunes		5010	4230
5/22/1994	1414	PB	plane bed		4740	4120
5/22/1994	1443	R-D	ripples, plane bed, dunes		4740	4120
5/22/1994	1450	R-D	plane bed, dunes, ripples		4740	4120
5/22/1994	1456	R	plane bed, ripples, dunes		4740	4120
5/22/1994	1470.5	PB	plane bed		4740	4120
5/22/1994	1470.5	PB	plane bed		4740	4120
6/5/1994	1410	PB	plane bed		4810	3990

6/5/1994	1414	PB	plane bed		4810	3990
6/5/1994	1420	PB	plane bed, dunes, ripples		4810	3990
6/5/1994	1428	PB-R	ripples, plane bed		4810	3990
6/5/1994	1437.9	R-D	ripples, plane bed, trans. anti-dunes, dunes		4810	3990
6/6/1994	1443	PB	plane bed, ripples, dunes		3200	3760
6/6/1994	1450	R	ripples, dunes, plane bed		3200	3760
6/6/1994	1456	R-D	ripples, dunes, plane bed		3200	3760
6/6/1994	1462	PB	ripples, plane bed		3200	3760
6/6/1994	1470.5	PB	plane bed		3200	3760
6/10/1994	1414	PB	plane bed		4270	3590
6/10/1994	1470.5	PB	plane bed		4270	3590
4/14/1995	1312	D	ripples, dunes		1930	1370
4/14/1995	1314	D	ripples, plane bed, dunes		1930	1370
4/14/1995	1316	D	ripples, plane bed, dunes		1930	1370
4/19/1995	1306	PB	ripples, plane bed, dunes		2450	2040
4/19/1995	1308	PB-D	ripples, plane bed, dunes		2450	2040
4/19/1995	1310	PB-R	ripples, plane bed, trans. dunes		2450	2040
4/19/1995	1311	PB	ripples, plane bed, dunes		2450	2040
4/19/1995	1312	PB	plane bed		2450	2040
4/19/1995	1320	PB	plane bed		2450	2040
5/12/1995	1410	PB-D	plane bed, trans. dunes		3100	2940
5/12/1995	1414	PB	plane bed, trans. dunes		3100	2940
5/12/1995	1420	R-D	plane bed, dunes, ripples		3100	2940
5/12/1995	1428	D-AD	plane bed, trans. anti-dunes, ripples, trans. dunes		3100	2940
5/12/1995	1437.9	PB-R	plane bed, dunes, ripples		3100	2940
5/13/1995	1443	R-D	ripples, plane bed, dunes		3340	2830
5/13/1995	1450	PB-R	ripples, plane bed, dunes, trans. anti-dunes		3340	2830
5/13/1995	1456	PB-R	plane bed, ripples, trans. anti-dunes		3340	2830
5/13/1995	1462	PB-R	plane bed, ripples		3340	2830
5/13/1995	1470.5	PB	plane bed		3340	2830
5/13/1995	1470.5	R-D	ripples, small dunes		3340	2830
5/15/1995	1414	PB	plane bed		3580	3140
5/15/1995	1470.5	PB	plane bed	3240 cfs	3580	3140
5/22/1995	1414	PB	plane bed		4790	4050
5/22/1995	1437.9	UPB-AD	plane bed, trans. anti-dunes, ripples		4790	4050
5/23/1995	1470.5	PB	plane bed		5280	4220
5/27/1995	1414	PB	plane bed		5900	4590

5/27/1995	1470.5	PB	plane bed		5900	4590
5/30/1995	1410	PB	plane bed, dunes		4410	4580
5/30/1995	1414	PB	plane bed, dunes		4410	4580
5/30/1995	1437.9	PB-R	plane bed, dunes, ripples		4410	4580
5/30/1995	1443	R	dunes, ripples		4410	4580
5/30/1995	1450	R-D	ripples, dunes, plane bed		4410	4580
5/30/1995	1456	PB-D	ripples, dunes, plane bed		4410	4580
5/30/1995	1462	PB	plane bed, ripples		4410	4580
5/30/1995	1470.5	PB	plane bed		4410	4580
6/1/1995	1414	PB	plane bed, dunes		4920	4190
6/1/1995	1437.9	PB-R	plane bed, dunes, ripples	4588 cfs	4920	4190
6/1/1995	1443	R	plane bed, ripples		4920	4190
6/1/1995	1450	PB-R	ripples, dunes, plane bed		4920	4190
6/1/1995	1470.5	PB	plane bed	4279 cfs	4920	4190
6/15/1995	1414	PB	plane bed	4100 cfs	4530	3880
6/15/1995	1437.9	D	plane bed, dunes, ripples	3920 cfs	4530	3880
6/15/1995	1470.5	PB	plane bed	3861 cfs	4530	3880
6/20/1995	1414	PB-D	plane bed, trans. dunes	4342 cfs	4760	4030
6/20/1995	1470.5	PB	plane bed	4200 cfs	4760	4030
6/28/1995	1410	PB	plane bed		4590	4090
6/28/1995	1414	PB	plane bed		4590	4090
6/28/1995	1420	PB-D	plane bed, dunes, ripples		4590	4090
6/28/1995	1428	PB	ripples, plane bed		4590	4090
6/28/1995	1437.9	PB	plane bed, trans. anti-dunes, ripples		4590	4090
6/29/1995	1443	PB-D	ripples, plane bed, dune, trans. anti-dunes		4580	4010
6/29/1995	1450	PB-R	plane bed, ripples, dunes		4580	4010
6/29/1995	1456	PB	plane bed, dunes		4580	4010
6/29/1995	1462	R-D	dunes, ripples, plane bed, anti-dunes		4580	4010
6/29/1995	1470.5	PB	plane bed	3999.09 cfs	4580	4010
7/1/1995	1414	PB	plane bed, dunes, ripples	4490 cfs	5350	4290
7/1/1995	1470.5	PB	plane bed	4469.56 cfs	5350	4290
9/12/1990	1380	R	ripples		92	58

Appendix F – BORAMEP

Table F.1 BORAMEP Input – general information

Input Variables	Title	Date	Time	S_energy	g (ft/s2)	γw (lb/ft3)	γs (lb/ft3)	Q (cfs)	Vavg (ft/s)	h (ft)	W (ft)	T (F)	dn (ft)	Cs (ppm)	d65 (mm)	d35 (mm)	ds (ft)
###	5/2/1990	5/2/1990	1430	0.00011	32.17	62.4	165	648	2.08	1.8	197	49.1	0.3	636	0.21	0.15	4.8
###	6/9/1990	6/9/1990	1430	0.00011	32.17	62.4	165	18	1.1	0.46	60	78.8	0.3	1678	0.48	0.33	4.8
###	5/22/1991	5/22/1991	1430	0.00011	32.17	62.4	165	4530	4.97	5.4	160	62.6	0.3	2107	0.21	0.09	4.8
###	6/17/1991	6/17/1991	1430	0.00011	32.17	62.4	165	4070	5.1	5.1	160	73.4	0.3	3701	0.16	0.08	4.8
###	5/7/1992	5/7/1992	1430	0.00011	32.17	62.4	165	5560	4.39	6.3	203	64.4	0.3	2486	2.83	0.13	4.8
###	5/21/1992	5/21/1992	1430	0.00011	32.17	62.4	165	3230	4.07	5.1	155	68	0.3	1209	0.06	0.01	4.8
###	6/4/1992	6/4/1992	1430	0.00011	32.17	62.4	165	3940	4.78	5.2	161	64.4	0.3	603	0.10	0.04	4.8
###	6/18/1992	6/18/1992	1430	0.00011	32.17	62.4	165	2030	2.69	4.9	155	71.6	0.3	219	0.34	0.21	4.8
###	5/17/1994	5/17/1994	1430	0.00011	32.17	62.4	165	5440	5.12	6.3	170	60.8	0.3	1298	0.37	0.24	4.8
###	6/22/1994	6/22/1994	1430	0.00011	32.17	62.4	165	4490	5.07	5.3	167	77	0.3	866	0.35	0.21	4.8
###	5/16/1995	5/16/1995	1430	0.00011	32.17	62.4	165	3370	3.86	5.3	165	65.84	0.3	950	0.23	0.17	4.8
###	6/8/1995	6/8/1995	1430	0.00011	32.17	62.4	165	4390	4.63	5.7	165	63.5	0.3	1848	0.47	0.24	4.8
###	6/19/1996	6/19/1996	1430	0.00011	32.17	62.4	165	5010	2.23	1.4	74	73.94	0.3	213	0.43	0.28	4.8
###	5/20/1997	5/20/1997	1430	0.00011	32.17	62.4	165	4250	4.59	5.7	162	62.6	0.3	7376	16.00	0.63	4.8
###	6/24/1997	6/24/1997	1430	0.00011	32.17	62.4	165	978	2.85	3	114	71.06	0.3	1788	0.35	0.22	4.8
###	5/18/1998	5/18/1998	1430	0.00011	32.17	62.4	165	2510	4.49	4.8	160	60.8	0.3	1259	2.00	0.17	4.8
###	4/7/1999	4/7/1999	1430	0.00011	32.17	62.4	165	418	2.1	2	106	51.8	0.3	100	0.64	0.39	4.8
###	5/21/1999	5/21/1999	1430	0.00011	32.17	62.4	165	2220	2.65	5.2	162	69.8	0.3	787	1.57	0.55	4.8
###	4/7/2000	4/7/2000	1430	0.00011	32.17	62.4	165	375	2.14	2	104	65	0.3	1638	0.84	0.49	4.8
###	5/3/2000	5/3/2000	1430	0.00011	32.17	62.4	165	321	1.92	1.7	109	77	0.3	83	0.85	0.41	4.8
###	4/21/2001	4/21/2001	1430	0.00011	32.17	62.4	165	664	2.27	1.9	162	59.9	0.3	217	0.71	0.40	4.8
###	5/22/2001	5/22/2001	1430	0.00011	32.17	62.4	165	1340	2.41	3.6	164	72.5	0.3	673	1.17	0.41	4.8
###	6/20/2001	6/20/2001	1430	0.00011	32.17	62.4	165	274	1.78	1.8	92	51.44	0.3	98	0.76	0.38	4.8
###	5/7/2002	5/7/2002	1430	0.00011	32.17	62.4	165	210	1.64	1.1	122	68	0.3	84.3	0.27	0.03	4.8
###	4/3/2003	4/3/2003	1430	0.00011	32.17	62.4	165	199	1.6	1	142	59.9	0.3	289	0.02	0.01	4.8
###	5/12/2003	5/12/2003	1430	0.00011	32.17	62.4	165	193	1.58	0.99	137	73.4	0.3	260	0.39	0.27	4.8
###	6/6/2003	6/6/2003	1430	0.00011	32.17	62.4	165	254	1.7	1.3	107	64.4	0.3	573	0.47	0.33	4.8
###	4/15/2004	4/15/2004	1430	0.00011	32.17	62.4	165	1960	4.72	2.5	162	62.6	0.3	4756	0.40	0.28	4.8
###	5/24/2004	5/24/2004	1430	0.00011	32.17	62.4	165	1560	2.56	4	158	68	0.3	1139	0.78	0.43	4.8

Table F.2 BORAMEP Input – suspended sediment percent in range

Title	0.001 0.002 mm	0.002 0.004 mm	0.004 0.016 mm	0.016 0.0625 mm	0.0625 0.125 mm	0.125 0.25 mm	0.25 0.5 mm	0.5 1 mm	1 2 mm	2 4 mm	4 8 mm	8 16 mm	16 32 mm	32 64 mm	64 128 mm	128 256 mm
5/2/1990	0	0	0	40	22	34	4	0	0	0	0	0	0	0	0	0
6/9/1990	0	0	0	36	3	30	31	0	0	0	0	0	0	0	0	0
5/22/1991	0	27	7	25	29	12	0	0	0	0	0	0	0	0	0	0
6/17/1991	0	76	12	11	1	0	0	0	0	0	0	0	0	0	0	0
5/7/1992	26	2	7	27	25	13	0	0	0	0	0	0	0	0	0	0
5/21/1992	40	6	18	18	11	7	0	0	0	0	0	0	0	0	0	0
6/4/1992	47	10	12	27	2	2	0	0	0	0	0	0	0	0	0	0
6/18/1992	0	0	0	66	17	16	1	0	0	0	0	0	0	0	0	0
5/17/1994	0	0	0	46	27	25	2	0	0	0	0	0	0	0	0	0
6/22/1994	0	0	0	23	24	48	5	0	0	0	0	0	0	0	0	0
5/16/1995	0	0	0	69	14	17	0	0	0	0	0	0	0	0	0	0
6/8/1995	37	6	9	18	9	19	2	0	0	0	0	0	0	0	0	0
6/19/1996	0	0	0	86	1	10	3	0	0	0	0	0	0	0	0	0
5/20/1997	33	7	16	14	18	11	1	0	0	0	0	0	0	0	0	0
6/24/1997	0	0	0	13	1	23	58	5	0	0	0	0	0	0	0	0
5/18/1998	41	6	8	16	18	10	1	0	0	0	0	0	0	0	0	0
4/7/1999	0	0	0	44	1	30	25	0	0	0	0	0	0	0	0	0
5/21/1999	23	4	10	44	16	2	1	0	0	0	0	0	0	0	0	0
4/7/2000	73	15	6	1	0	1	2	2	0	0	0	0	0	0	0	0
5/3/2000	0	0	0	55	13	18	14	0	0	0	0	0	0	0	0	0
4/21/2001	0	0	0	37	3	27	33	0	0	0	0	0	0	0	0	0
5/22/2001	58	8	9	15	6	3	1	0	0	0	0	0	0	0	0	0
6/20/2001	0	0	0	65	4	24	7	0	0	0	0	0	0	0	0	0
5/7/2002	0	0	0	0	1	18	70	8	1	1	1	0	0	0	0	0
4/3/2003	0	0	0	0	1	8	52	23	8	4	3	1	0	0	0	0
5/12/2003	0	0	0	95	1	3	1	0	0	0	0	0	0	0	0	0
6/6/2003	76	13	6	0	1	2	2	0	0	0	0	0	0	0	0	0
4/15/2004	53	8	7	8	2	16	6	0	0	0	0	0	0	0	0	0
5/24/2004	0	0	0	51	2	9	33	4	1	0	0	0	0	0	0	0

Table F.3 BORAMEP Input – bed material percent in range

Title	0.001 0.002 mm	0.002 0.004 mm	0.004 0.016 mm	0.016 0.0625 mm	0.0625 0.125 mm	0.125 0.25 mm	0.25 0.5 mm	0.5 1 mm	1 2 mm	2 4 mm	4 8 mm	8 16 mm	16 32 mm	32 64 mm	64 128 mm	128 256 mm
5/2/1990	0	0	0	1	13	68	18	0	0	0	0	0	0	0	0	0
6/9/1990	0	0	0	0	0	11	57	18	7	3	3	1	0	0	0	0
5/22/1991	0	3	0	18	32	35	10	2	0	0	0	0	0	0	0	0
6/17/1991	0	3	0	18	32	35	10	2	0	0	0	0	0	0	0	0
5/7/1992	0	0	0	35	0	7	10	9	3	2	2	4	1	27	0	0
5/21/1992	0	0	0	64	19	16	1	0	0	0	0	0	0	0	0	0
6/4/1992	0	0	0	40	40	19	1	0	0	0	0	0	0	0	0	0
6/18/1992	0	0	0	0	6	40	42	9	1	0	0	2	0	0	0	0
5/17/1994	0	0	0	0	2	36	48	14	0	0	0	0	0	0	0	0
6/22/1994	0	0	0	0	2	46	35	5	3	2	3	4	0	0	0	0
5/16/1995	0	0	0	4	0	68	26	0	0	0	1	1	0	0	0	0
6/8/1995	0	0	0	0	4	32	32	9	6	6	4	7	0	0	0	0
6/19/1996	0	0	0	1	1	25	49	5	1	1	3	9	5	0	0	0
5/20/1997	0	0	0	0	4	24	6	3	2	4	6	16	35	0	0	0
6/24/1997	0	0	0	1	4	37	46	7	0	1	1	3	0	0	0	0
5/18/1998	0	0	0	2	13	47	2	0	1	1	3	8	3	20	0	0
4/7/1999	0	0	0	0	0	2	51	33	8	4	0	2	0	0	0	0
5/21/1999	0	0	0	0	1	5	26	22	17	17	15	11	3	0	0	0
4/7/2000	0	0	0	0	0	3	33	39	15	6	3	1	0	0	0	0
5/3/2000	0	0	0	0	1	5	40	25	11	7	6	5	0	0	0	0
4/21/2001	0	0	0	0	0	6	42	21	6	5	6	8	6	0	0	0
5/22/2001	0	0	0	1	3	8	32	19	0	0	0	0	0	0	0	0
6/20/2001	0	0	0	0	1	8	42	23	11	6	5	4	0	0	0	0
5/7/2002	0	0	0	43	0	17	40	0	0	0	0	0	0	0	0	0
4/3/2003	0	0	0	88	1	6	5	0	0	0	0	0	0	0	0	0
5/12/2003	0	0	0	0	1	27	59	12	1	0	0	0	0	0	0	0
6/6/2003	0	0	0	0	2	7	62	22	5	2	0	0	0	0	0	0
4/15/2004	0	0	0	0	2	24	58	13	1	1	0	1	0	0	0	0
5/24/2004	0	0	0	0	0	4	40	33	10	6	4	3	0	0	0	0

Table F.4 BORAMEP Output

OUTPUT
5/21/1992

METHOD OF COMPUTATION MODIFIED EINSTEIN DATE OF COMPUTATION 7/18/2006
DATE OF SAMPLE 5/21/1992 TIME OF SAMPLE 1430 TEMPERATURE 68 SLOPE OF ENERGY GRADIENT 0.00011
D65 = 0.06 mm D35 = 0.01 mm
Velocity (ft/s) = 4.07 Width (ft) = 155 Depth (ft) = 5.1
Dn (ft) = 0.3 Ds (ft) = 4.8

SIZE FRACTION IN MILLIMETERS		PERCENT OF MATERIAL SUSPENDED BED	IBQB T/D	QPRIME SUBS(T/D)	Z-VALUES COMPUTED	FITTED	COMPUTATIONAL FACTORS F(J)	F(I)+1	COMPUTED TOTAL LOAD
0.001	0.002	40	0	-9999	4025.749	-9999	0.486	1.308	-9999	5264.013
0.002	0.004	6	0	-9999	603.862	-9999	0.534	1.365	-9999	824.481
0.004	0.016	18	0	-9999	1811.587	-9999	0.614	1.489	-9999	2697.952
0.016	0.0625	18	64	147.272	1811.587	-9999	0.739	1.773	84.692	3212.201
0.0625	0.125	11	19	72.537	1107.081	0.847	0.847	2.134	33.566	2362.325
0.125	0.25	7	16	84.345	704.506	0.916	0.916	2.415	21.178	1786.223
0.25	0.5	0	1	6.814	0	-9999	0.965	-9999	15.799	107.654
0.5	1	0	0	-9999	0	-9999	1.000	-9999	-9999	0
1	2	0	0	-9999	0	-9999	1.028	-9999	-9999	0
2	4	0	0	-9999	0	-9999	1.054	-9999	-9999	0
4	8	0	0	-9999	0	-9999	1.079	-9999	-9999	0
8	16	0	0	-9999	0	-9999	1.105	-9999	-9999	0
16	32	0	0	-9999	0	-9999	1.131	-9999	-9999	0
32	64	0	0	-9999	0	-9999	1.158	-9999	-9999	0
64	128	0	0	-9999	0	-9999	1.185	-9999	-9999	0
128	256	0	0	-9999	0	-9999	1.213	-9999	-9999	0
TOTAL										16254.848

6/4/1992,6/4/1992,-9999,FITTED Z-VALUES GENERATED NEGATIVE EXPONENT, NOT CONTINUING...

OUTPUT
6/18/1992

METHOD OF COMPUTATION MODIFIED EINSTEIN DATE OF COMPUTATION 7/18/2006
DATE OF SAMPLE 6/18/1992 TIME OF SAMPLE 1430 TEMPERATURE 71.6 SLOPE OF ENERGY GRADIENT 0.00011
D65 = 0.34 mm D35 = 0.21 mm
Velocity (ft/s) = 2.69 Width (ft) = 155 Depth (ft) = 4.9
Dn (ft) = 0.3 Ds (ft) = 4.8

SIZE FRACTION IN MILLIMETERS		PERCENT OF MATERIAL SUSPENDED BED	IBQB T/D	QPRIME SUBS(T/D)	Z-VALUES COMPUTED	FITTED	COMPUTATIONAL FACTORS F(J)	F(I)+1	COMPUTED TOTAL LOAD
0.001	0.002	0	0	-9999	0	-9999	0.007	-9999	-9999	0
0.002	0.004	0	0	-9999	0	-9999	0.014	-9999	-9999	0
0.004	0.016	0	0	-9999	0	-9999	0.043	-9999	-9999	0
0.016	0.0625	66	0	-9999	758.600	-9999	0.183	1.099	-9999	834.067
0.0625	0.125	17	6	1.193	195.397	0.543	0.529	1.343	248.782	262.424
0.125	0.25	16	40	22.494	183.903	0.906	0.968	2.647	14.909	486.852
0.25	0.5	1	42	66.805	11.494	1.514	1.455	10.802	3.761	251.258
0.5	1	0	9	20.718	0	-9999	1.907	-9999	2.434	50.419
1	2	0	1	0.780	0	-9999	2.364	-9999	2.019	1.576
2	4	0	0	-9999	0	-9999	2.872	-9999	-9999	0
4	8	0	0	-9999	0	-9999	3.465	-9999	-9999	0
8	16	0	2	0	0	-9999	4.169	-9999	1.550	0
16	32	0	0	-9999	0	-9999	5.011	-9999	-9999	0
32	64	0	0	-9999	0	-9999	6.022	-9999	-9999	0
64	128	0	0	-9999	0	-9999	7.236	-9999	-9999	0
128	256	0	0	-9999	0	-9999	8.695	-9999	-9999	0
TOTAL										1886.596

OUTPUT
5/17/1994

METHOD OF COMPUTATION MODIFIED EINSTEIN DATE OF COMPUTATION 7/18/2006
DATE OF SAMPLE 5/17/1994 TIME OF SAMPLE 1430 TEMPERATURE 60.8 SLOPE OF ENERGY GRADIENT 0.00011
D65 = 0.37 mm D35 = 0.24 mm
Velocity (ft/s) = 5.12 Width (ft) = 170 Depth (ft) = 6.3
Dn (ft) = 0.3 Ds (ft) = 4.8

SIZE FRACTION IN MILLIMETERS		PERCENT OF MATERIAL SUSPENDED BED	IBQB T/D	QPRIME SUBS(T/D)	Z-VALUES COMPUTED	FITTED	COMPUTATIONAL FACTORS F(J)	F(I)+1	COMPUTED TOTAL LOAD
0.001	0.002	0	0	-9999	0	-9999	0.001	-9999	-9999	0
0.002	0.004	0	0	-9999	0	-9999	0.002	-9999	-9999	0
0.004	0.016	0	0	-9999	0	-9999	0.011	-9999	-9999	0
0.016	0.0625	46	0	-9999	8397.694	-9999	0.074	1.066	-9999	8953.738
0.0625	0.125	27	2	2.347	4929.082	-9999	0.306	1.156	1707.124	5700.272
0.125	0.25	25	36	119.514	4563.964	0.706	0.706	1.640	63.631	7484.328
0.25	0.5	2	48	450.716	365.117	1.256	1.256	5.746	5.636	2540.435
0.5	1	0	14	305.812	0	-9999	1.830	-9999	2.540	776.638
1	2	0	0	-9999	0	-9999	2.451	-9999	-9999	0
2	4	0	0	-9999	0	-9999	3.182	-9999	-9999	0
4	8	0	0	-9999	0	-9999	4.087	-9999	-9999	0
8	16	0	0	-9999	0	-9999	5.228	-9999	-9999	0
16	32	0	0	-9999	0	-9999	6.680	-9999	-9999	0
32	64	0	0	-9999	0	-9999	8.530	-9999	-9999	0
64	128	0	0	-9999	0	-9999	10.890	-9999	-9999	0
128	256	0	0	-9999	0	-9999	13.903	-9999	-9999	0
TOTAL										25455.410

OUTPUT
6/22/1994

METHOD OF COMPUTATION MODIFIED EINSTEIN DATE OF COMPUTATION 7/18/2006
DATE OF SAMPLE 6/22/1994 TIME OF SAMPLE 1430 TEMPERATURE 77 SLOPE OF ENERGY GRADIENT 0.00011
D65 = 0.35 mm D35 = 0.21 mm
Velocity (ft/s) = 5.07 Width (ft) = 167 Depth (ft) = 5.3
Dn (ft) = 0.3 Ds (ft) = 4.8

SIZE FRACTION IN MILLIMETERS		PERCENT OF MATERIAL SUSPENDED BED	IBQB T/D	QPRIME SUBS(T/D)	Z-VALUES COMPUTED	FITTED	COMPUTATIONAL FACTORS F(J)	F(I)+1	COMPUTED TOTAL LOAD
0.001	0.002	0	0	-9999	0	-9999	0.002	-9999	-9999	0
0.002	0.004	0	0	-9999	0	-9999	0.004	-9999	-9999	0
0.004	0.016	0	0	-9999	0	-9999	0.016	-9999	-9999	0
0.016	0.0625	23	0	-9999	2312.175	-9999	0.095	1.071	-9999	2476.947
0.0625	0.125	24	2	2.689	2412.704	0.348	0.350	1.182	1042.177	2850.951
0.125	0.25	48	46	174.923	4825.409	0.740	0.729	1.688	51.516	8143.417
0.25	0.5	5	35	376.445	502.647	1.179	1.190	4.510	6.638	2498.696
0.5	1	0	5	107.396	0	-9999	1.652	-9999	3.028	325.174
1	2	0	3	67.833	0	-9999	2.149	-9999	2.205	149.548
2	4	0	2	28.582	0	-9999	2.731	-9999	1.856	53.044
4	8	0	3	12.290	0	-9999	3.442	-9999	1.653	20.317
8	16	0	4	0.380	0	-9999	4.326	-9999	1.514	0.576
16	32	0	0	-9999	0	-9999	5.430	-9999	-9999	0
32	64	0	0	-9999	0	-9999	6.814	-9999	-9999	0
64	128	0	0	-9999	0	-9999	8.550	-9999	-9999	0
128	256	0	0	-9999	0	-9999	10.728	-9999	-9999	0
TOTAL										16518.671

5/16/1995,5/16/1995,-9999,NOT ENOUGH OVERLAPPING BINS FOR MEP

OUTPUT
6/8/1995

METHOD OF COMPUTATION MODIFIED EINSTEIN DATE OF COMPUTATION 7/18/2006
DATE OF SAMPLE 6/8/1995 TIME OF SAMPLE 1430 TEMPERATURE 63.5 SLOPE OF ENERGY GRADIENT 0.00011
D65 = 0.47 mm D35 = 0.24 mm
Velocity (ft/s) = 4.63 Width (ft) = 165 Depth (ft) = 5.7
Dn (ft) = 0.3 Ds (ft) = 4.8

SIZE FRACTION IN MILLIMETERS		PERCENT OF MATERIAL SUSPENDED BED	IBQB T/D	QPRIME SUBS(T/D)	Z-VALUES COMPUTED	Z-VALUES FITTED	COMPUTATIONAL FACTORS F(J)	COMPUTATIONAL FACTORS F(I)+1	COMPUTED TOTAL LOAD
0.001	0.002	37	0	-9999	7760.628	-9999	0.007	1.050	-9999	8150.707
0.002	0.004	6	0	-9999	1258.48	-9999	0.014	1.052	-9999	1323.482
0.004	0.016	9	0	-9999	1887.72	-9999	0.038	1.057	-9999	1995.208
0.016	0.0625	18	0	-9999	3775.441	-9999	0.150	1.087	-9999	4104.349
0.0625	0.125	9	4	3.853	1887.72	0.420	0.407	1.220	671.140	2303.938
0.125	0.25	19	32	87.181	3985.187	0.673	0.728	1.677	51.747	6684.619
0.25	0.5	2	32	246.586	419.493	1.135	1.084	3.352	8.931	2202.312
0.5	1	0	9	159.856	0	-9999	1.408	-9999	4.121	658.744
1	2	0	6	103.898	0	-9999	1.727	-9999	2.894	300.654
2	4	0	6	56.915	0	-9999	2.075	-9999	2.367	134.741
4	8	0	4	8.725	0	-9999	2.473	-9999	2.066	18.024
8	16	0	7	0.068	0	-9999	2.941	-9999	1.861	0.127
16	32	0	0	-9999	0	-9999	3.494	-9999	-9999	0
32	64	0	0	-9999	0	-9999	4.150	-9999	-9999	0
64	128	0	0	-9999	0	-9999	4.927	-9999	-9999	0
128	256	0	0	-9999	0	-9999	5.851	-9999	-9999	0
TOTAL										27876.904

OUTPUT
6/19/1996

METHOD OF COMPUTATION MODIFIED EINSTEIN DATE OF COMPUTATION 7/18/2006
DATE OF SAMPLE 6/19/1996 TIME OF SAMPLE 1430 TEMPERATURE 73.94 SLOPE OF ENERGY GRADIENT 0.00011
D65 = 0.43 mm D35 = 0.28 mm
Velocity (ft/s) = 2.23 Width (ft) = 74 Depth (ft) = 1.4
Dn (ft) = 0.3 Ds (ft) = 4.8

SIZE FRACTION IN MILLIMETERS		PERCENT OF MATERIAL SUSPENDED BED	IBQB T/D	QPRIME SUBS(T/D)	Z-VALUES COMPUTED	Z-VALUES FITTED	COMPUTATIONAL FACTORS F(J)	COMPUTATIONAL FACTORS F(I)+1	COMPUTED TOTAL LOAD
0.001	0.002	0	0	-9999	0	-9999	0.001	-9999	-9999	0
0.002	0.004	0	0	-9999	0	-9999	0.002	-9999	-9999	0
0.004	0.016	0	0	-9999	0	-9999	0.009	-9999	-9999	0
0.016	0.0625	86	1	0.008	2372.709	-9999	0.060	1.059	8388.584	2513.052
0.0625	0.125	1	1	0.039	27.590	0.246	0.236	1.113	850.733	30.717
0.125	0.25	10	25	2.770	275.896	0.460	0.513	1.293	92.222	356.661
0.25	0.5	3	49	15.357	82.769	0.922	0.864	1.860	14.616	224.463
0.5	1	0	5	4.317	0	-9999	1.223	-9999	5.277	22.781
1	2	0	1	0.259	0	-9999	1.614	-9999	3.132	0.811
2	4	0	1	0.008	0	-9999	2.077	-9999	2.329	0.019
4	8	0	3	0.000	0	-9999	2.648	-9999	1.919	0.000
8	16	0	9	0	0	-9999	3.365	-9999	1.662	0
16	32	0	5	0	0	-9999	4.271	-9999	1.477	0
32	64	0	0	-9999	0	-9999	5.420	-9999	-9999	0
64	128	0	0	-9999	0	-9999	6.877	-9999	-9999	0
128	256	0	0	-9999	0	-9999	8.724	-9999	-9999	0
TOTAL										3148.503

OUTPUT
5/20/1997

METHOD OF COMPUTATION MODIFIED EINSTEIN DATE OF COMPUTATION 7/18/2006
DATE OF SAMPLE 5/20/1997 TIME OF SAMPLE 1430 TEMPERATURE 62.6 SLOPE OF ENERGY GRADIENT 0.00011
D65 = 16 mm D35 = 0.63 mm
Velocity (ft/s) = 4.59 Width (ft) = 162 Depth (ft) = 5.7
Dn (ft) = 0.3 Ds (ft) = 4.8

SIZE FRACTION IN MILLIMETERS		PERCENT OF MATERIAL SUSPENDED BED	IBQB T/D	QPRIME SUBS(T/D)	Z-VALUES COMPUTED	Z-VALUES FITTED	COMPUTATIONAL FACTORS F(J)	COMPUTATIONAL FACTORS F(I)+1	COMPUTED TOTAL LOAD
0.001	0.002	33	0	-9999	26998.76	-9999	0.003	1.040	-9999	28078.61
0.002	0.004	7	0	-9999	5727.011	-9999	0.006	1.041	-9999	5959.037
0.004	0.016	16	0	-9999	13090.31	-9999	0.019	1.043	-9999	13647.43
0.016	0.0625	14	0	-9999	11454.02	-9999	0.080	1.054	-9999	12070.86
0.0625	0.125	18	4	2.846	14726.6	-9999	0.233	1.094	1809.552	16110.14
0.125	0.25	11	24	48.298	8999.588	0.435	0.435	1.188	222.309	10688.7
0.25	0.5	1	6	34.152	818.144	0.668	0.668	1.401	34.560	1180.3
0.5	1	0	3	48.298	0	-9999	0.884	-9999	10.020	483.953
1	2	0	2	91.072	0	-9999	1.101	-9999	4.702	428.260
2	4	0	4	209.478	0	-9999	1.339	-9999	3.006	629.743
4	8	0	6	180.511	0	-9999	1.616	-9999	2.304	415.953
8	16	0	16	119.546	0	-9999	1.945	-9999	1.947	232.788
16	32	0	35	2.171	0	-9999	2.339	-9999	1.730	3.755
32	64	0	0	-9999	0	-9999	2.811	-9999	-9999	0
64	128	0	0	-9999	0	-9999	3.378	-9999	-9999	0
128	256	0	0	-9999	0	-9999	4.059	-9999	-9999	0
TOTAL										89929.530

OUTPUT
6/24/1997

METHOD OF COMPUTATION MODIFIED EINSTEIN DATE OF COMPUTATION 7/18/2006
DATE OF SAMPLE 6/24/1997 TIME OF SAMPLE 1430 TEMPERATURE 71.06 SLOPE OF ENERGY GRADIENT 0.00011
D65 = 0.35 mm D35 = 0.22 mm
Velocity (ft/s) = 2.85 Width (ft) = 114 Depth (ft) = 3
Dn (ft) = 0.3 Ds (ft) = 4.8

SIZE FRACTION IN MILLIMETERS		PERCENT OF MATERIAL SUSPENDED BED	IBQB T/D	QPRIME SUBS(T/D)	Z-VALUES COMPUTED	Z-VALUES FITTED	COMPUTATIONAL FACTORS F(J)	COMPUTATIONAL FACTORS F(I)+1	COMPUTED TOTAL LOAD
0.001	0.002	0	0	-9999	0	-9999	0.355	-9999	-9999	0
0.002	0.004	0	0	-9999	0	-9999	0.389	-9999	-9999	0
0.004	0.016	0	0	-9999	0	-9999	0.447	-9999	-9999	0
0.016	0.0625	13	1	0.043	587.731	-9999	0.538	1.348	283.081	792.346
0.0625	0.125	1	4	0.801	45.210	0.645	0.615	1.452	104.390	65.638
0.125	0.25	23	37	20.946	1039.831	0.628	0.664	1.525	60.011	1586.113
0.25	0.5	58	46	73.656	2622.183	0.640	0.699	1.571	39.638	4118.983
0.5	1	5	7	19.231	226.050	0.796	0.724	1.582	28.616	550.298
1	2	0	0	-9999	0	-9999	0.744	-9999	-9999	0
2	4	0	1	0.170	0	-9999	0.762	-9999	16.389	2.779
4	8	0	1	0.000	0	-9999	0.781	-9999	12.570	0.000
8	16	0	3	0	0	-9999	0.799	-9999	9.607	0
16	32	0	0	-9999	0	-9999	0.818	-9999	-9999	0
32	64	0	0	-9999	0	-9999	0.837	-9999	-9999	0
64	128	0	0	-9999	0	-9999	0.857	-9999	-9999	0
128	256	0	0	-9999	0	-9999	0.877	-9999	-9999	0
TOTAL										7116.158

OUTPUT
5/18/1998

METHOD OF COMPUTATION MODIFIED EINSTEIN DATE OF COMPUTATION 7/18/2006
DATE OF SAMPLE 5/18/1998 TIME OF SAMPLE 1430 TEMPERATURE 60.8 SLOPE OF ENERGY GRADIENT 0.00011
D65 = 2 mm D35 = 0.17 mm
velocity (ft/s) = 4.49 width (ft) = 160 Depth (ft) = 4.8
Dn (ft) = 0.3 Ds (ft) = 4.8

SIZE FRACTION IN MILLIMETERS		PERCENT OF MATERIAL SUSPENDED	IBQB BED	QPRIME T/D	SUBS(T/D)	Z-VALUES COMPUTED	FITTED	COMPUTATIONAL FACTORS F(J)	F(I)+1	COMPUTED TOTAL LOAD
0.001	0.002	41	0	-9999	3349.747	-9999	0.083	1.062	-9999	3558.289
0.002	0.004	6	0	-9999	490.207	-9999	0.117	1.071	-9999	524.995
0.004	0.016	8	0	-9999	653.609	-9999	0.198	1.096	-9999	716.218
0.016	0.0625	16	2	0.783	1307.218	-9999	0.397	1.194	978.833	1561.358
0.0625	0.125	18	13	23.772	1470.62	0.632	0.661	1.483	73.019	2181.099
0.125	0.25	10	47	243.093	817.011	0.998	0.892	2.065	15.698	1687.505
0.25	0.5	1	2	29.258	81.701	1.026	1.097	3.091	6.544	191.453
0.5	1	0	0	-9999	0	-9999	1.255	-9999	-9999	0
1	2	0	1	25.936	0	-9999	1.394	-9999	3.533	91.618
2	4	0	1	18.152	0	-9999	1.531	-9999	3.071	55.746
4	8	0	3	18.036	0	-9999	1.675	-9999	2.760	49.783
8	16	0	8	2.543	0	-9999	1.829	-9999	2.519	6.406
16	32	0	3	0.000	0	-9999	1.997	-9999	2.307	0.000
32	64	0	20	0	0	-9999	2.181	-9999	2.102	0
64	128	0	0	-9999	0	-9999	2.380	-9999	-9999	0
128	256	0	0	-9999	0	-9999	2.598	-9999	-9999	0
TOTAL										10624.470

OUTPUT
4/7/1999

METHOD OF COMPUTATION MODIFIED EINSTEIN DATE OF COMPUTATION 7/18/2006
DATE OF SAMPLE 4/7/1999 TIME OF SAMPLE 1430 TEMPERATURE 51.8 SLOPE OF ENERGY GRADIENT 0.00011
D65 = 0.64 mm D35 = 0.39 mm
velocity (ft/s) = 2.1 width (ft) = 106 Depth (ft) = 2
Dn (ft) = 0.3 Ds (ft) = 4.8

SIZE FRACTION IN MILLIMETERS		PERCENT OF MATERIAL SUSPENDED	IBQB BED	QPRIME T/D	SUBS(T/D)	Z-VALUES COMPUTED	FITTED	COMPUTATIONAL FACTORS F(J)	F(I)+1	COMPUTED TOTAL LOAD
0.001	0.002	0	0	-9999	0	-9999	0.000	-9999	-9999	0
0.002	0.004	0	0	-9999	0	-9999	0.000	-9999	-9999	0
0.004	0.016	0	0	-9999	0	-9999	0.000	-9999	-9999	0
0.016	0.0625	44	0	-9999	47.551	-9999	0.004	1.047	-9999	49.804
0.0625	0.125	1	0	-9999	1.081	-9999	0.056	1.058	-9999	1.144
0.125	0.25	30	2	0.085	32.421	0.295	0.295	1.139	436.860	36.938
0.25	0.5	25	51	6.112	27.017	0.963	0.963	2.237	10.879	66.496
0.5	1	0	33	11.187	0	-9999	2.067	-9999	2.080	23.272
1	2	0	8	1.863	0	-9999	3.685	-9999	1.444	2.690
2	4	0	4	0.010	0	-9999	6.135	-9999	1.252	0.012
4	8	0	0	-9999	0	-9999	9.969	-9999	-9999	0
8	16	0	2	0	0	-9999	16.060	-9999	1.101	0
16	32	0	0	-9999	0	-9999	25.793	-9999	-9999	0
32	64	0	0	-9999	0	-9999	41.382	-9999	-9999	0
64	128	0	0	-9999	0	-9999	66.366	-9999	-9999	0
128	256	0	0	-9999	0	-9999	106.421	-9999	-9999	0
TOTAL										180.355

OUTPUT
5/21/1999

METHOD OF COMPUTATION MODIFIED EINSTEIN DATE OF COMPUTATION 7/18/2006
DATE OF SAMPLE 5/21/1999 TIME OF SAMPLE 1430 TEMPERATURE 69.8 SLOPE OF ENERGY GRADIENT 0.00011
D65 = 1.57 mm D35 = 0.55 mm
velocity (ft/s) = 2.65 width (ft) = 162 Depth (ft) = 5.2
Dn (ft) = 0.3 Ds (ft) = 4.8

SIZE FRACTION IN MILLIMETERS		PERCENT OF MATERIAL SUSPENDED	IBQB BED	QPRIME T/D	SUBS(T/D)	Z-VALUES COMPUTED	FITTED	COMPUTATIONAL FACTORS F(J)	F(I)+1	COMPUTED TOTAL LOAD
0.001	0.002	23	0	-9999	1038.925	-9999	0.000	1.046	-9999	1086.742
0.002	0.004	4	0	-9999	180.683	-9999	0.000	1.046	-9999	189.010
0.004	0.016	10	0	-9999	451.706	-9999	0.003	1.047	-9999	472.721
0.016	0.0625	44	0	-9999	1987.509	-9999	0.030	1.052	-9999	2090.468
0.0625	0.125	16	1	0.033	722.730	-9999	0.170	1.088	3931.462	786.258
0.125	0.25	2	5	0.463	90.341	0.459	0.459	1.245	243.733	112.496
0.25	0.5	1	26	6.816	45.171	0.899	0.899	2.088	14.840	101.153
0.5	1	0	22	16.313	0	-9999	1.405	-9999	3.446	56.222
1	2	0	17	32.592	0	-9999	1.998	-9999	2.038	66.435
2	4	0	17	5.151	0	-9999	2.748	-9999	1.634	8.414
4	8	0	15	0.001	0	-9999	3.735	-9999	1.443	0.001
8	16	0	11	0	0	-9999	5.055	-9999	1.327	0
16	32	0	3	0	0	-9999	6.832	-9999	1.246	0
32	64	0	0	-9999	0	-9999	9.227	-9999	-9999	0
64	128	0	0	-9999	0	-9999	12.460	-9999	-9999	0
128	256	0	0	-9999	0	-9999	16.825	-9999	-9999	0
TOTAL										4969.917

OUTPUT
4/7/2000

METHOD OF COMPUTATION MODIFIED EINSTEIN DATE OF COMPUTATION 7/18/2006
DATE OF SAMPLE 4/7/2000 TIME OF SAMPLE 1430 TEMPERATURE 65 SLOPE OF ENERGY GRADIENT 0.00011
D65 = 0.84 mm D35 = 0.49 mm
velocity (ft/s) = 2.14 width (ft) = 104 Depth (ft) = 2
Dn (ft) = 0.3 Ds (ft) = 4.8

SIZE FRACTION IN MILLIMETERS		PERCENT OF MATERIAL SUSPENDED	IBQB BED	QPRIME T/D	SUBS(T/D)	Z-VALUES COMPUTED	FITTED	COMPUTATIONAL FACTORS F(J)	F(I)+1	COMPUTED TOTAL LOAD
0.001	0.002	73	0	-9999	1159.302	-9999	0.000	1.046	-9999	1212.579
0.002	0.004	15	0	-9999	238.213	-9999	0.001	1.046	-9999	249.193
0.004	0.016	6	0	-9999	95.285	-9999	0.005	1.047	-9999	99.751
0.016	0.0625	1	0	-9999	15.881	-9999	0.038	1.053	-9999	16.729
0.0625	0.125	0	0	-9999	0	-9999	0.167	-9999	-9999	0
0.125	0.25	1	3	0.078	15.881	0.377	0.390	1.191	222.688	18.907
0.25	0.5	2	33	2.421	31.762	0.761	0.698	1.517	29.591	48.170
0.5	1	2	39	8.093	31.762	0.973	1.024	2.285	7.996	64.712
1	2	0	15	5.077	0	-9999	1.382	-9999	3.871	19.655
2	4	0	6	0.054	0	-9999	1.809	-9999	2.590	0.139
4	8	0	3	0	0	-9999	2.343	-9999	2.031	0
8	16	0	1	0	0	-9999	3.023	-9999	1.720	0
16	32	0	0	-9999	0	-9999	3.895	-9999	-9999	0
32	64	0	0	-9999	0	-9999	5.017	-9999	-9999	0
64	128	0	0	-9999	0	-9999	6.461	-9999	-9999	0
128	256	0	0	-9999	0	-9999	8.319	-9999	-9999	0
TOTAL										1729.834

OUTPUT
5/3/2000

METHOD OF COMPUTATION MODIFIED EINSTEIN DATE OF COMPUTATION 7/18/2006
DATE OF SAMPLE 5/3/2000 TIME OF SAMPLE 1430 TEMPERATURE 77 SLOPE OF ENERGY GRADIENT 0.00011
D65 = 0.85 mm D35 = 0.41 mm
velocity (ft/s) = 1.92 Width (ft) = 109 Depth (ft) = 1.7
Dn (ft) = 0.3 Ds (ft) = 4.8

SIZE FRACTION IN MILLIMETERS		PERCENT OF MATERIAL SUSPENDED BED		IBQB T/D	QPRIME SUBS(T/D)	Z-VALUES COMPUTED	FITTED	COMPUTATIONAL FACTORS F(J)	F(I)+1	COMPUTED TOTAL LOAD
0.001	0.002	0	0	-9999	0	-9999	0.000	-9999	-9999	0
0.002	0.004	0	0	-9999	0	-9999	0.001	-9999	-9999	0
0.004	0.016	0	0	-9999	0	-9999	0.005	-9999	-9999	0
0.016	0.0625	55	0	-9999	37.886	-9999	0.042	1.054	-9999	39.917
0.0625	0.125	13	1	0.010	8.955	0.219	0.211	1.101	1100.593	9.857
0.125	0.25	18	5	0.135	12.399	0.477	0.523	1.295	88.391	16.053
0.25	0.5	14	40	3.054	9.644	1.012	0.957	2.143	10.041	30.666
0.5	1	0	25	5.399	0	-9999	1.435	-9999	3.451	18.629
1	2	0	11	1.776	0	-9999	1.985	-9999	2.206	3.918
2	4	0	7	0.004	0	-9999	2.668	-9999	1.763	0.006
4	8	0	6	0	0	-9999	3.550	-9999	1.535	0
8	16	0	5	0	0	-9999	4.705	-9999	1.390	0
16	32	0	0	-9999	0	-9999	6.230	-9999	-9999	0
32	64	0	0	-9999	0	-9999	8.244	-9999	-9999	0
64	128	0	0	-9999	0	-9999	10.908	-9999	-9999	0
128	256	0	0	-9999	0	-9999	14.433	-9999	-9999	0
TOTAL										119.047

OUTPUT
4/21/2001

METHOD OF COMPUTATION MODIFIED EINSTEIN DATE OF COMPUTATION 7/18/2006
DATE OF SAMPLE 4/21/2001 TIME OF SAMPLE 1430 TEMPERATURE 59.9 SLOPE OF ENERGY GRADIENT 0.00011
D65 = 0.71 mm D35 = 0.4 mm
velocity (ft/s) = 2.27 Width (ft) = 162 Depth (ft) = 1.9
Dn (ft) = 0.3 Ds (ft) = 4.8

SIZE FRACTION IN MILLIMETERS		PERCENT OF MATERIAL SUSPENDED BED		IBQB T/D	QPRIME SUBS(T/D)	Z-VALUES COMPUTED	FITTED	COMPUTATIONAL FACTORS F(J)	F(I)+1	COMPUTED TOTAL LOAD
0.001	0.002	0	0	-9999	0	-9999	0.000	-9999	-9999	0
0.002	0.004	0	0	-9999	0	-9999	0.001	-9999	-9999	0
0.004	0.016	0	0	-9999	0	-9999	0.003	-9999	-9999	0
0.016	0.0625	37	0	-9999	137.835	-9999	0.030	1.052	-9999	145.011
0.0625	0.125	3	0	-9999	11.176	-9999	0.157	1.084	-9999	12.116
0.125	0.25	27	6	0.655	100.582	0.417	0.417	1.210	186.818	121.732
0.25	0.5	33	42	12.971	122.934	0.820	0.820	1.767	17.750	230.225
0.5	1	0	21	18.343	0	-9999	1.276	-9999	4.641	85.131
1	2	0	6	4.557	0	-9999	1.796	-9999	2.574	11.732
2	4	0	5	0.200	0	-9999	2.437	-9999	1.934	0.387
4	8	0	6	0.000	0	-9999	3.264	-9999	1.632	0.000
8	16	0	8	0	0	-9999	4.353	-9999	1.451	0
16	32	0	6	0	0	-9999	5.795	-9999	1.324	0
32	64	0	0	-9999	0	-9999	7.711	-9999	-9999	0
64	128	0	0	-9999	0	-9999	10.258	-9999	-9999	0
128	256	0	0	-9999	0	-9999	13.645	-9999	-9999	0
TOTAL										606.335

OUTPUT
5/22/2001

METHOD OF COMPUTATION MODIFIED EINSTEIN DATE OF COMPUTATION 7/18/2006
DATE OF SAMPLE 5/22/2001 TIME OF SAMPLE 1430 TEMPERATURE 72.5 SLOPE OF ENERGY GRADIENT 0.00011
D65 = 1.17 mm D35 = 0.41 mm
velocity (ft/s) = 2.41 Width (ft) = 164 Depth (ft) = 3.6
Dn (ft) = 0.3 Ds (ft) = 4.8

SIZE FRACTION IN MILLIMETERS		PERCENT OF MATERIAL SUSPENDED BED		IBQB T/D	QPRIME SUBS(T/D)	Z-VALUES COMPUTED	FITTED	COMPUTATIONAL FACTORS F(J)	F(I)+1	COMPUTED TOTAL LOAD
0.001	0.002	58	0	-9999	1352.311	-9999	0.001	1.046	-9999	1414.764
0.002	0.004	8	0	-9999	186.526	-9999	0.002	1.046	-9999	195.191
0.004	0.016	9	0	-9999	209.841	-9999	0.010	1.048	-9999	219.897
0.016	0.0625	15	1	0.010	349.736	-9999	0.069	1.060	17895.94	370.806
0.0625	0.125	6	3	0.143	139.894	0.287	0.279	1.131	1174.85	158.197
0.125	0.25	3	8	1.081	69.947	0.582	0.620	1.423	70.895	99.565
0.25	0.5	1	32	12.226	23.316	1.099	1.059	2.818	7.842	95.868
0.5	1	0	19	20.531	0	-9999	1.512	-9999	3.041	62.445
1	2	0	0	-9999	0	-9999	2.007	-9999	-9999	0
2	4	0	0	-9999	0	-9999	2.594	-9999	-9999	0
4	8	0	0	-9999	0	-9999	3.323	-9999	-9999	0
8	16	0	0	-9999	0	-9999	4.243	-9999	-9999	0
16	32	0	0	-9999	0	-9999	5.411	-9999	-9999	0
32	64	0	0	-9999	0	-9999	6.897	-9999	-9999	0
64	128	0	0	-9999	0	-9999	8.790	-9999	-9999	0
128	256	0	0	-9999	0	-9999	11.203	-9999	-9999	0
TOTAL										2616.733

OUTPUT
6/20/2001

METHOD OF COMPUTATION MODIFIED EINSTEIN DATE OF COMPUTATION 7/18/2006
DATE OF SAMPLE 6/20/2001 TIME OF SAMPLE 1430 TEMPERATURE 51.44 SLOPE OF ENERGY GRADIENT 0.00011
D65 = 0.76 mm D35 = 0.38 mm
velocity (ft/s) = 1.78 Width (ft) = 92 Depth (ft) = 1.8
Dn (ft) = 0.3 Ds (ft) = 4.8

SIZE FRACTION IN MILLIMETERS		PERCENT OF MATERIAL SUSPENDED BED		IBQB T/D	QPRIME SUBS(T/D)	Z-VALUES COMPUTED	FITTED	COMPUTATIONAL FACTORS F(J)	F(I)+1	COMPUTED TOTAL LOAD
0.001	0.002	0	0	-9999	0	-9999	0.002	-9999	-9999	0
0.002	0.004	0	0	-9999	0	-9999	0.005	-9999	-9999	0
0.004	0.016	0	0	-9999	0	-9999	0.018	-9999	-9999	0
0.016	0.0625	65	0	-9999	45.125	-9999	0.086	1.064	-9999	48.035
0.0625	0.125	4	1	0.005	2.777	0.304	0.273	1.128	752.016	3.132
0.125	0.25	24	8	0.120	16.662	0.425	0.548	1.327	81.758	22.113
0.25	0.5	7	42	1.776	4.860	1.045	0.901	1.984	12.825	22.774
0.5	1	0	23	2.750	0	-9999	1.242	-9999	4.913	13.512
1	2	0	11	0.546	0	-9999	1.583	-9999	3.098	1.691
2	4	0	6	0.000	0	-9999	1.959	-9999	2.391	0.000
4	8	0	5	0	0	-9999	2.401	-9999	2.014	0
8	16	0	4	0	0	-9999	2.932	-9999	1.768	0
16	32	0	0	-9999	0	-9999	3.576	-9999	-9999	0
32	64	0	0	-9999	0	-9999	4.359	-9999	-9999	0
64	128	0	0	-9999	0	-9999	5.313	-9999	-9999	0
128	256	0	0	-9999	0	-9999	6.474	-9999	-9999	0
TOTAL										111.258

5/7/2002,5/7/2002,-9999,FITTED Z-VALUES GENERATED NEGATIVE EXPONENT, NOT CONTINUING...
4/3/2003,4/3/2003,-9999,FITTED Z-VALUES GENERATED NEGATIVE EXPONENT, NOT CONTINUING...

OUTPUT
5/12/2003

METHOD OF COMPUTATION MODIFIED EINSTEIN DATE OF COMPUTATION 7/18/2006
DATE OF SAMPLE 5/12/2003 TIME OF SAMPLE 1430 TEMPERATURE 73.4 SLOPE OF ENERGY GRADIENT 0.00011
D65 = 0.39 mm D35 = 0.27 mm
Velocity (ft/s) = 1.58 Width (ft) = 137 Depth (ft) = 0.99
Dn (ft) = 0.3 Ds (ft) = 4.8

SIZE FRACTION IN MILLIMETERS		PERCENT OF MATERIAL SUSPENDED	BED	IBQB T/D	QPRIME SUBS(T/D)	Z-VALUES COMPUTED	FITTED	COMPUTATIONAL FACTORS F(J)	F(I)+1	COMPUTED TOTAL LOAD
0.001	0.002	0	0	-9999	0	-9999	0.002	-9999	-9999	0
0.002	0.004	0	0	-9999	0	-9999	0.005	-9999	-9999	0
0.004	0.016	0	0	-9999	0	-9999	0.021	-9999	-9999	0
0.016	0.0625	95	0	-9999	123.249	-9999	0.124	1.075	-9999	132.449
0.0625	0.125	1	1	0.011	1.297	0.459	0.457	1.242	148.179	1.611
0.125	0.25	3	27	0.844	3.892	0.950	0.957	2.199	10.733	8.558
0.25	0.5	1	59	5.218	1.297	1.578	1.571	7.567	3.012	15.716
0.5	1	0	12	2.520	0	-9999	2.185	-9999	2.036	5.132
1	2	0	1	0.010	0	-9999	2.843	-9999	1.716	0.017
2	4	0	0	-9999	0	-9999	3.609	-9999	-9999	0
4	8	0	0	-9999	0	-9999	4.543	-9999	-9999	0
8	16	0	0	-9999	0	-9999	5.701	-9999	-9999	0
16	32	0	0	-9999	0	-9999	7.146	-9999	-9999	0
32	64	0	0	-9999	0	-9999	8.955	-9999	-9999	0
64	128	0	0	-9999	0	-9999	11.220	-9999	-9999	0
128	256	0	0	-9999	0	-9999	14.057	-9999	-9999	0
TOTAL										163.482

OUTPUT
6/6/2003

METHOD OF COMPUTATION MODIFIED EINSTEIN DATE OF COMPUTATION 7/18/2006
DATE OF SAMPLE 6/6/2003 TIME OF SAMPLE 1430 TEMPERATURE 64.4 SLOPE OF ENERGY GRADIENT 0.00011
D65 = 0.47 mm D35 = 0.33 mm
Velocity (ft/s) = 1.7 Width (ft) = 107 Depth (ft) = 1.3
Dn (ft) = 0.3 Ds (ft) = 4.8

SIZE FRACTION IN MILLIMETERS		PERCENT OF MATERIAL SUSPENDED	BED	IBQB T/D	QPRIME SUBS(T/D)	Z-VALUES COMPUTED	FITTED	COMPUTATIONAL FACTORS F(J)	F(I)+1	COMPUTED TOTAL LOAD
0.001	0.002	76	0	-9999	285.977	-9999	0.004	1.047	-9999	299.468
0.002	0.004	13	0	-9999	48.917	-9999	0.008	1.048	-9999	51.264
0.004	0.016	6	0	-9999	22.577	-9999	0.025	1.051	-9999	23.735
0.016	0.0625	0	0	-9999	0	-9999	0.111	-9999	-9999	0
0.0625	0.125	1	2	0.013	3.763	0.357	0.334	1.159	395.959	4.363
0.125	0.25	2	7	0.130	7.526	0.536	0.634	1.432	45.862	10.779
0.25	0.5	2	62	3.258	7.526	1.086	0.983	2.216	9.578	31.202
0.5	1	0	22	3.270	0	-9999	1.311	-9999	4.435	14.501
1	2	0	5	0.122	0	-9999	1.643	-9999	3.009	0.366
2	4	0	2	0.000	0	-9999	2.011	-9999	2.383	0.000
4	8	0	0	-9999	0	-9999	2.443	-9999	-9999	0
8	16	0	0	-9999	0	-9999	2.959	-9999	-9999	0
16	32	0	0	-9999	0	-9999	3.580	-9999	-9999	0
32	64	0	0	-9999	0	-9999	4.329	-9999	-9999	0
64	128	0	0	-9999	0	-9999	5.235	-9999	-9999	0
128	256	0	0	-9999	0	-9999	6.331	-9999	-9999	0
TOTAL										435.678

OUTPUT
4/15/2004

METHOD OF COMPUTATION MODIFIED EINSTEIN DATE OF COMPUTATION 7/18/2006
DATE OF SAMPLE 4/15/2004 TIME OF SAMPLE 1430 TEMPERATURE 62.6 SLOPE OF ENERGY GRADIENT 0.00011
D65 = 0.4 mm D35 = 0.28 mm
Velocity (ft/s) = 4.72 Width (ft) = 162 Depth (ft) = 2.5
Dn (ft) = 0.3 Ds (ft) = 4.8

SIZE FRACTION IN MILLIMETERS		PERCENT OF MATERIAL SUSPENDED	BED	IBQB T/D	QPRIME SUBS(T/D)	Z-VALUES COMPUTED	FITTED	COMPUTATIONAL FACTORS F(J)	F(I)+1	COMPUTED TOTAL LOAD
0.001	0.002	53	0	-9999	12773.28	-9999	0.013	1.050	-9999	13417.12
0.002	0.004	8	0	-9999	1928.042	-9999	0.023	1.053	-9999	2029.278
0.004	0.016	7	0	-9999	1687.037	-9999	0.056	1.060	-9999	1787.614
0.016	0.0625	8	0	-9999	1928.042	-9999	0.177	1.094	-9999	2109.378
0.0625	0.125	2	2	1.906	482.011	0.436	0.411	1.217	373.107	586.780
0.125	0.25	16	24	64.698	3856.085	0.586	0.674	1.529	50.898	5895.014
0.25	0.5	6	58	442.236	1446.032	1.028	0.946	2.248	12.725	5627.35
0.5	1	0	13	276.939	0	-9999	1.181	-9999	6.190	1714.341
1	2	0	1	22.625	0	-9999	1.404	-9999	4.161	94.149
2	4	0	1	14.554	0	-9999	1.640	-9999	3.227	46.972
4	8	0	0	-9999	0	-9999	1.903	-9999	-9999	0
8	16	0	1	0.117	0	-9999	2.204	-9999	2.317	0.270
16	32	0	0	-9999	0	-9999	2.549	-9999	-9999	0
32	64	0	0	-9999	0	-9999	2.949	-9999	-9999	0
64	128	0	0	-9999	0	-9999	3.410	-9999	-9999	0
128	256	0	0	-9999	0	-9999	3.943	-9999	-9999	0
TOTAL										33308.270

OUTPUT
5/24/2004

METHOD OF COMPUTATION MODIFIED EINSTEIN DATE OF COMPUTATION 7/18/2006
DATE OF SAMPLE 5/24/2004 TIME OF SAMPLE 1430 TEMPERATURE 68 SLOPE OF ENERGY GRADIENT 0.00011
D65 = 0.78 mm D35 = 0.43 mm
Velocity (ft/s) = 2.56 Width (ft) = 158 Depth (ft) = 4
Dn (ft) = 0.3 Ds (ft) = 4.8

SIZE FRACTION IN MILLIMETERS		PERCENT OF MATERIAL SUSPENDED	BED	IBQB T/D	QPRIME SUBS(T/D)	Z-VALUES COMPUTED	FITTED	COMPUTATIONAL FACTORS F(J)	F(I)+1	COMPUTED TOTAL LOAD
0.001	0.002	0	0	-9999	0	-9999	0.000	-9999	-9999	0
0.002	0.004	0	0	-9999	0	-9999	0.000	-9999	-9999	0
0.004	0.016	0	0	-9999	0	-9999	0.002	-9999	-9999	0
0.016	0.0625	51	0	-9999	2342.864	-9999	0.019	1.051	-9999	2462.485
0.0625	0.125	2	0	-9999	91.877	-9999	0.099	1.070	-9999	98.278
0.125	0.25	9	4	0.478	413.447	0.258	0.261	1.126	951.376	465.536
0.25	0.5	33	40	13.532	1515.971	0.475	0.502	1.289	121.236	1954.229
0.5	1	4	33	31.577	183.754	0.919	0.773	1.683	23.297	309.304
1	2	1	10	11.078	45.939	0.978	1.087	2.607	7.435	82.361
2	4	0	6	0.622	0	-9999	1.479	-9999	3.694	2.298
4	8	0	4	0.000	0	-9999	1.988	-9999	2.466	0.000
8	16	0	3	0	0	-9999	2.660	-9999	1.927	0
16	32	0	0	-9999	0	-9999	3.556	-9999	-9999	0
32	64	0	0	-9999	0	-9999	4.750	-9999	-9999	0
64	128	0	0	-9999	0	-9999	6.344	-9999	-9999	0
128	256	0	0	-9999	0	-9999	8.472	-9999	-9999	0
TOTAL										5374.492

Appendix G – HEC-RAS Sediment Transport Application Limits

The information presented in the pages below was taken from HEC-RAS v. 3.1.3 (USACE 2005).

Ackers-White (flume):

0.04 < d < 7 mm 1.0 < s < 2.7
0.07 < V < 7.1 fps 0.01 < D < 1.4 ft
0.00006 < S < 0.037 0.23 < W < 4.0 ft
46 < T < 89 degrees F

A total load function developed under the assumption that fine sediment transport is best related to the turbulent fluctuations in the water column and coarse sediment transport is best related to the net grain shear with the mean velocity used as the representative variable. The transport function was developed in terms of particle size, mobility and transport. A dimensionless size parameter is used to distinguish between the fine, transitionary, and coarse sediment sizes. Under typical conditions, fine sediments are silts less than 0.04 mm, and coarse sediments are sands greater than 2.5 mm. Since the relationships developed by Ackers-White are applicable only to non-cohesive sands, greater than 0.04 mm, only transitionary and coarse sediments apply. Experiments were conducted with coarse grains up to 4 mm. This function is based on over 1000 flume experiments using uniform or near-uniform sediments with flume depths of up to 1.4 m. A range of bed configurations was used, including plane, rippled, and dune forms, however the equations do not apply to upper phase transport (e.g. anti-dunes) with Froude numbers in excess of 0.8. A hiding adjustment factor was developed for the Ackers-White method by Profitt and Sutherland (1983), and is included in RAS as an option. The hiding factor is an adjustment to include the effects of a masking of the fluid properties felt by smaller particles due to shielding by larger particles. This is typically a factor when the gradation has a relatively large range of particle sizes and would tend to reduce the rate of sediment transport in the smaller grade classes.

Engelund-Hansen (flume):

0.19 < dm < 0.93 mm 0.65 < V < 6.34
0.19 < D < 1.33 fps 0.000055 < S < 0.019 ft
45 < T < 93 degrees F

A total load predictor, which gives adequate results for sandy rivers with substantial suspended load. It is based on flume data with sediment sizes between 0.19 and 0.93 mm. It has been extensively tested, and found to be fairly consistent with field data.

Laursen (Copeland) (field):

0.08 < dm < 0.7 mm 0.068 < V < 7.8 fps
0.67 < D < 54 ft 0.0000021 < S < 0.0018
63 < W < 3640 ft 32 < T < 93 degrees F

Laursen (Copeland) (flume):

0.011 < dm < 29 mm 0.7 < V < 9.4 fps
0.03 < D < 3.6 ft 0.00025 < S < 0.025
0.25 < W < 6.6 ft 46 < T < 83 degrees F

A total sediment load predictor, derived from a combination of qualitative analysis, original experiments and supplementary data. Transport of sediments is primarily defined based on the hydraulic characteristics of mean channel velocity, depth of flow and energy gradient, and on the sediment characteristics of gradation and fall velocity. Contributions by Copeland (Copeland, 1989) extend the range of applicability to gravel-sized sediments. The overall range of applicability is 0.011 to 29 mm.

MPM. Meyer-Peter Muller (flume):

0.4 < d < 29 mm 1.25 < s < 4.0
1.2 < V < 9.4 fps 0.03 < D < 3.9 ft
0.0004 < S < 0.02 0.5 < W < 6.6 ft

BED LOAD ONLY! A bed load transport function based primarily on experimental data. It has been extensively tested and used for rivers with relatively coarse sediment. The transport rate is proportional to the difference between the mean shear stress acting on the grain and the critical shear stress. Applicable particle sizes range from 0.4 to 29 mm with a sediment specific gravity range of 1.25 to in excess of 4.0. This method can be used for well-graded sediments and flow conditions that produce other-than-plane bed forms. The Darcy-Weisbach friction factor is used to define bed resistance. Results may be questionable near the threshold of incipient motion for sand bed channels as demonstrated by Amin and Murphy (1981).

Toffaleti (field):

0.062 < d < 4 mm 0.095 < dm < 0.76 mm
0.7 < V < 7.8 fps 0.07 < R < 56.7 ft
0.000002 < S < 0.0011 63 < W < 3640 ft
40 < T < 93 degrees F

Toffaleti (flume):

0.062 < d < 4 mm 0.45 < dm < 0.91 mm
0.7 < V < 6.3 fps 0.07 < R < 1.1 ft
0.00014 < S < 0.019 0.8 < W < 8 ft
32 < T < 94 degrees F

A modified-Einstein total load function that breaks the suspended load distribution into vertical zones, replicating two-dimensional sediment movement. Four zones are used to define the sediment distribution. They are the upper zone, the middle zone, the lower zone and the bed zone. Sediment transport is calculated independently for each zone and the summed to arrive at total sediment transport. This method was developed using an exhaustive collection of both flume and field data. The flume experiments used sediment particles with mean diameters ranging from 0.45 to 0.91 mm, however successful applications of the Toffaleti method suggests that mean particle diameters as low as 0.095 mm are acceptable.

Yang (field, sand):

0.15 < d < 1.7 mm 0.8 < V < 6.4 fps
0.04 < D < 50 ft 0.000043 < S < 0.028
0.44 < W < 1750 32 < T < 94 degrees F

A total load function developed under the premise that unit stream power is the dominant factor in the determination of total sediment concentration. The research is supported by data obtained in both flume experiments and field data under a wide range conditions found in alluvial channels. Principally, the sediment size range is between 0.062 and 7.0 mm with total sediment concentration ranging from 10 ppm to 585,000 ppm. Yang (1984) expanded the applicability of his function to include gravel-sized sediments.